Università degli Studi di Milano

DIPARTIMENTO DI PRODUZIONE VEGETALE
Scienze molecolari e biotecnologie agrarie, alimentari ed ambientali
Biologia vegetale e produttività della pianta coltivata ciclo XXIII

Tesi di Dottorato di Ricerca

Multifaceted investigation into apple to unravel texture physiology

AGR/07

Relatore & Co-relatore:
Prof. Ilaria Mignani

Candidato:
Sara Longhi

Fabrizio Costa

Coordinatore del dottorato:
Prof. Daniele Bassi

Anno Accademico 2010–2011

Contents

CHAPTER 1

Introduction

1.1 The myth of apple

"Snow White longed for the beautiful apple, and when she saw that the peddler woman was eating part of it, she could no longer resist, and she stuck her hand out and took the poisoned half. She barely had a bite in her mouth when she fell to the ground dead." Snow White and the Seven Dwarves is one of the numerous tale and ancient myth that tell about tempting and actractive apples that are the cause or the beginning of important or wretch events.

In the Holy Bible, Eva was convinced by the evil snake to eat the forbidden fruit, a tempting apple symbol of knowledge, provoking God's anger and the Fall from the Eden Garden. The story tells also that Adam's apple was caused by the forbidden fruit sticking in the throat of Adam as warning. In the holy book, however, there is not a specific and clear reference to the apple as the fruit of sin, but it was chosen by the collective imagination as the fruit par excellence thanks to its tempting appearance and good taste.

Several are also the examples in the ancient greek myths. Eris, the greek goddess of discord, became disgruntled after she was excluded from the wedding of Peleus and Thetis. In retaliation, she tossed a golden apple inscribed "for the most beautiful one", into the wedding party. Three goddesses claimed the apple: Hera, Athena, and Aphrodite. Paris of Troy was appointed to select the recipient. After being bribed by both Hera and Athena, Aphrodite tempted him with the most beautiful woman in the world, Helen of Sparta. He awarded the apple to Aphrodite, thus indirectly causing the Trojan War. Atalanta, also of Greek mythology, raced all her suitors in an attempt to avoid marriage. She outran all but Hippomenes (also known as Melanion, a name possibly derived from melon the Greek word for both "apple" and fruit in general), who defeated

her by cunning, not speed. Hippomenes knew that he could not win in a fair race, so he used three golden apples (gifts of Aphrodite, the goddess of love) to distract Atalanta. It took all three apples and all of his speed, but Hippomenes was finally successful, winning the race and Atalanta's hand. But after that Hippomenes had won his prize he was so happy that he forgot to thank Aphrodite. He went instead to the temple of Zeus to celebrate his victory with Atalanta. Aphrodite was furious and sent flaming desire coursing through Hippomene's and Atalanta's veins and they lay together right there in Zeus' holy temple.

The central thread of all these myths is that the appearance of prohibited of attractive apples tempted humans, enlightening the importance of this quality in the choice of the fruit. The English word of fruit comes from the latin verb "frui", meaning to enjoy, to delight [156], the very first quality factors that can describe apple are in fact refered to sensual pleasure.

The places where this work of thesis was realised are also connected by the apple fruit as a central thread. The main work was realised in Trentino Alto Adige (Italy), the region that accounts for the 70% of Italian apple production, then in the Washington State (USA), which national symbol is an apple and finally in the New York State. New York City is one of the most important city in the world for its relevance on the global economy and culture. This city is also knwon as "The Big Apple", entailing to this fruit a meaning of opportunities, progress and development.

1.2 Fruit quality factors

Fruit and food quality can be defined as the property to respond and satisfy consumer requirements, desire and expectations. Quality, in fact, is determined as the subjective comparison that customers make between their expectations (deriving by previous experiences) about a product and its perception. In particular custumer's requirements agree with fruits that have an appealing apperance, flavour and taste, that are fresh, with a good shelf life, and characterized by an appropriate texture.

Fruit quality is measured accomplishing four main points, also known as Principal Quality Factor:

1. **Appearance**, comprises colour, shape, size and gloss; its evaluated by optical sense

2. **Flavour**, comprises taste and odor, perceived on the tongue and in the olfactory center in the nose, respectively. It is the response of receptors in the oral and nasal cavities to chemical stimuli.

3. **Texture** is primarily the response of the tactile senses to the physical stimuli resulting from the contact between tactile receptors and the food.

4. **Nutrition** comprises major and minor nutrients affecting human health. Regarding this aspect we can mention the 19th century statement: "an apple a day keeps the doctor away". Nutraceutical properties are considered extremely important, but, because of their expensive laboratory analysis and the inability of consumer to perceive them directly by their senses, they are considered rather an added food value than a quality factor.

Nowadays, foods supply is no longer a crucial issue in developed countries, thus food/fruit quality became the driving properties affecting the choice of consumers. Other factors, such as cost, convenience and packaging are also important but are not considered as food quality factors.

1.3 Texture: definition and importance

Contrary to the other quality factors which are perceived by a single and specific sense such as view and taste for the evaluation of appearance and flavour respectively, it is not possible to define texture with a single characteristic and attribute. This trait is in fact a heterogeneous complex of properties having different peculiarities, with both mechanical and acoustic nature. For this reason the definition of texture, or "textural properties" which infers a group of related properties, requires particular attention and regard.

Literally, texture assumed different definitions according to people's culture, customs and education, as described by Szczesniak and Kleyn [211], Yoshikawa *et al.* [243] and Rohm [186]. It is possibile however to determine some common characteristics of food texture [25].

- it is a group of physical properties that derive from the structure of the food;
- it belongs under the mechanical or rheological subheading of physical properties;
- it consist in a group of properties, rather than a single attribute;
- texture is sensed primarily by the feeling of touch, usually in the mouth, even if other part of the body may be involved, hands for istance;
- it is not related to the tactile or olfactory sense.

On the light of these observations, texture can be defined as a multifaceted group of food properties with the following general definition: "the textural properties of a food are that group of physical characteristics that arise from the structural elements of the food, are sensed primarily by the feeling of touch, are related to the deformation and flow of the food under a force and are measured objectively by function of mass, time and distance" [25].

Various are the terms that can well describe or replace the word "texture"

1. *rheology*, a branch of physics that describes the physical properties of the food. Rheology is important in food technology because it has many applications in the three principal quality factors previously indicated. There is a small component of rehology in appearance and flavour. Some structural and mechanical properties of several foods, in fact, can be determined by appearance and also the ways the food breaks down in the mouth can affect the release of flavour compounds. Rehological properties are a major factor in the evaluation of food quality by the sense of touch and hearing. Foods are in fact holded in the hand, and from the sense of deformability and recovery after squeezing is possible to have an idea of their textural quality [25]. The sound of a food during the mechanical break is also an indication of its texture.

2. *haptaesthesis* (from the Greek words meaning sensation and touch), a branch of psychology that deals with the perception of the mechanical behaviour of materials.

3. *kinesthetics* (from the Greek word "kinen", the muscle sense to move, and "aesthesis", perception), those factors of quality that consumer evaluate with his sense of feel, expecially mouthfeel.

4. *body*, the quality of a food or beverage, relating to its consistency, compactness of texture, fullness, or richness.

Finally it is also important to take into accout the relevance that texture exerts with regards to people health. Because obesity has become a major health problem in the industrialised countries, the food industry devotes considerable effort to present low calorie foods on the market, in order to alleviate the overweight problem. It has been noticed that different foods have very different effects on energy production and satisfaction which is the feeling of fullness that arise from eating [106]. High satiety foods tended to have a bulky, cruncy, or fibrous texture which makes them relatively more difficult to chew and swallow, giving a long-lasting feeling of satiety, and hence reducing the total caloric intake.

1.3.1 Texture from a sensorial point of view and its role in breeding programs

Texture is the third quality factor but it plays a crucial role in consumer acceptability. Contrary to the other quality factors, appearance and flavour, which are commonly found to be the most important sensory factor responsible for the appreciation of many foods, texture is often cited by consumers as the reason for not liking certain foods. This is expecially true for food which texture may be observed as creating a lack of control in the mouth. These are for example foods with sticky, soggy or slimy texture, or for foods principally characterized

and chosen for their peculiar and unique texture, as potato chips or cornflakes [33]. Texture can be thus classified in three main groups based on its importance [25]:

1. *Critical*: Foods in which texture is the dominant quality characteristic, such as potato chips, cornflakes and celery.

2. *Important*: Foods in which texture makes a significant but not a dominant contribution to the overall quality, such as most of the fruits, vegetables, cheese, bread and candy.

3. *Minor*: Foods in which texture makes an imperceptible quality contribution like for instance soups or beverages.

According to this classification it is easy to understand the great importance and relevance that texture has for fruit appreciation and preference.

Within the heterogeneous fruit panorama, texture of apple is distinguished by a "crispy flesh type" respect to banana, orange, cherry, pear, kiwi fruit, persimmon or tomato. The group of apple varieties is however assorted and variable, and it is composed by different cultivars defined by very distinct textural attributes and peculiarities. Apple flesh can be in fact defined as mealy, crispy, juicy or firm. Nowaday consumers' appreciation is mainly addressed towards crispy apple, accounting for the 90% of the preference.

Fruit texture is to date a main priority in several breeding programs, not only for its sensorial impact but also for its importance in the post harvest maintenance. Differently from other fruits like cherries, strawberries or kiwi fruit, apples are constantly present on the fresh market over the twelve months, and not limited to precise period of the year. Because texture affects shelf life, storability and resistance to mechanical processing and damages, is a critical point for the selection of new varieties. Good textural performance in fact:

- allows product loss reduction during shipping;

- allows prolungated selling assuring the same quality over the time;

- improves post harvest mechanical and disease resistance;

- improves shelf-life quality maintainance;

The breeding and the market goals are mainly driven by texture. Modì, Honeycrisp or "WA 5", for istance, are Italian and North American new cultivars and accessions that are all described and promoted for their high textural performances, with particular regards for crispness and juiciness, considered a worldwide breeding priority more than any other traits [102].

1.4 Fruit texture

1.4.1 State of the art

Texture, derived from the latin word *textura* which means a "weave", and it was originally used to describe fabrics [189]. Starting from 1960s it was used to describe the "constitution, structure or substance of anything with regards to its constituents formative elements" as defined by the Oxford English Dictionary (1989).

Two scientists, both in England, enunciated two principles crucial for the texture measurements. Robert Hood in 1660 enunciate the principle of elastic deformation of solids which in simple terms says that strain is directly proportional to stress. In 1687 Isaac Newton enunciated the law governing the flow of simple liquids, giving rise to the term "Newtonian liquid" which is a fluid whose stress versus strain rate curve is linear and passes through the origin. Prior 1940, it was generally considered that sensory measurements of texture of fruit and food in general were purely subjective and as such generally unreliable. Variation in individuals as well as variability of any one person from day to day, seems to make sensory analysis of food an art without any scientific value.

Since one of the foundament of the scientific approach is reproducibility, researcher decided to rely on instrumental measurements carried out under standardized and reproducible conditions. Probably the first person to develop a specific instrument for food testing was Lipowitz (Germany 1861), who developed a simple puncture tester for measuring the firmness of jellies. The first authors mentioning the multifaced nature of texture were Goldthwaite in 1909, working on fruit jelly, and Washburn (1910), who tryed to define differences in texural properties distinguished between "body" and "texture" of ice cream. Attitude towards objective of sensory research, changed after the Second World War, in fact US army started to invest in developing food ratio for troops, discovering that the meal was not often appreciated. A research program was developed by the US Quartermaster Corps to look at issued of food acceptability, appropriateness and satisfactoriness.
Development of controlled sensory tests, and the advances in statistic approaches, helped to bring the conception of sensory testing into scientific respectability. In fact even if there exist a lot of instruments able to help to assess food texture, this is essentialy a human experience that arise from the interaction between the body and the food.
For this reason, food texture measurement are performed both with instruments but also by trained testers (panelists).

1.4.2 Texture measurement

The wide range in food types and their rheological and textural properties, together with the availability of suitable methods to measure these features,

made necessary to classify these methods into specific groups. Measurements can be defined according to the commodity that has to be tested, according to the food textural properties or the type of test adopted. This last strategy seems to be the most appropriate being focused more on the kind of test than on the food nature. In this way many tests are applicable to more than one type of food. Tests, as previously mentioned, can be divided in sensorial and objective [25]. Sensorial test are performed by panelist, usually trained, and are divided in oral (mechanical, geometrical and chemical) and non-oral (performed with fingers, hand and eyes). Objective tests are direct (fundamental, empirical and imitative) and indirect (optical, chemical and acoustical). Ideal objective tests collect all the favourable qualities of the mentioned tests; they are simple to perform, rapid and suitable for routine work, showing good correlation with sensorial methods and suitable to process large sample set.

A study realized on apple and pear [38] showed that for traits like crispness, hardness and fracturability, a correlation from strong to moderate was oberved between instrumental and sensory attributes. Other traits, like for example juiciness, were weakly correlated with instrumental determinations. Moreover, it was showed that the sensorial accuracy and instrumental measurements change according to the fruit texture itself [38], [100].
When apples are soft, the testers are more sensitive to texture differences than available instruments are, while when apples are firm, the ability of consumers to evaluate textural differences may decrease because of fatigue, making instrumental determination more reliable [38].

In food and fruit texture determination, instruments measuring force and distance are the most prefered. In the particular case of apple fruit, penetrometer has been largely employed to determine fruit firmness [27], [173], [99]. It consists in a cone and vertical shaft that is allowed to sink into a solid under the force of gravity for a standard time after which the depth of penetration is measured. This instrument alone, however, is limited to a single datapoint analysis and for this reason it is nowadays considered inappropriate to describe the fruit texture trait complexity [112].

1.4.3 Crispness

The contribution that texture has on the consumers' appreciation has been studied for nearly 50 years, and since the first studies, the importace of crispness on consumers' preferences was highlighted [190].
Crispness was assessed in different studies [119], [226], were products were ranked in the same order for crispness and consumers's preferences, emphasizing the significance of this trait in food acceptability. As for texture, also crispness is not easy to describe. Barret *et al.* [12] defined crispness as "the perceived horizontal force requested to separate the product into two or more distinct pieces during a single bite with incisors." According to Decreamont [52] is something "noisy at biting, aerated, light and crumble", while for Duizer *et al.*

[67] is a "combination of the noise produced and the breakdown of the product as it is bitten entirely through with the back molars".

Looking at the definitions, five aspects, some more emphasized that others, showed up [190] :

- **structure** of the intact product,
- **sounds** emitted at fraction,
- **force** needed to cruch the sample,
- **how** the product **collapses**,
- **how** the pieces **appear** after fracture.

Definitions focus on the ease of the fracturing in the mouth combined with the sound amplitude produced during the fracture. A relationship between crispness and emitted sound has been in fact hypothesized by many scientists [71],[224],[227],[65],[41]. Many factors may be responsible for the large variation in crisp perception: size, shape and orientation of the food in the mouth, the amount of contact surface between teeth and food, the degree to which the mouth is opened, variations within the food, the rate and force of biting, or the way the food breaks down [39]. For this reason it is necessary to identify standardized, reproducible and conventional methods for routine tests, in order to measure and record simultaneously the mechanical force exerted by the food and the sound produced during tissue fracturing [225]. A study realized on Royal Gala apple showed that correlation between average amplitude of bite or chew sounds and sensory crispness depended on the panelists and remained rather low [60], giving two important messages. The first is that a simple sensorial analysis is not sufficient to describe the trait with high detail, the second is that there is a correlation between the amplitude of sound produced and food crispness. From this point of view, the stimulus for crispness may be vibratory more than an auditory sensation [41]. In particular the measuring methods have to determine both mechanical and acoustic aspects. Mechanical features are described by the force-deformation pattern characterized by a series of sharp force peaks corrisponding to the rupture of individual cell walls. The acoustic characteristics are described by the sound amplitude, the acoustic frequecy vibration and the sound pression wave. In this way, the determination of a series of different parameters for correlation with sensory measurements will be possible.

In a crispy tissue during biting, it is possible that a high number of small fracture events suppress the development of a large rupture, competing in this way for energy and crispness sensation [144], [228]. In particular the requirement of a series of fractures entail a fundamental role of food morfology, the break involves, in fact, repetitive deformation and the fracture of subsequent layers in the tissue. A food defined as crispy is necessarily constituted by a brittle material, and for this reason the fraction surface will be relatively simple and

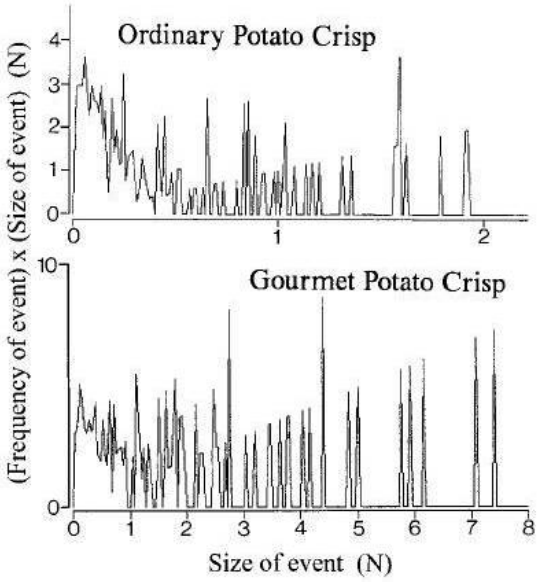

Figure 1.1: The picture reports two force spectrums of different kind of potato chips [228]

regular and the total energy absorbed on the fraction will be proportional to the crack length. Moreover, the fraction of a crispy food will produce pieces of a comparable size, requiring equal amounts of energy to chew these particles [228]. Crispness presents a correlation with the logarithm of the number of spacial ruptures [174], fitting with the vibro-tactile theory of crispness perception. From this point of view is possible to evaluate the trait on the basis of the number of ruptures detected at the first bite [51]. Figure 1.1 reports the force spectrum of two different kind of potato chips; showing that the crispier (gourmet potato) is described by an higher frequecies of events than the less crispy (ordinary chips).

Is also possible to assess the product crispness looking at the acoustic profile during the bite. In particular the frequecy of the sound emitted (defined as the rate at which the sound vibrate, measured in herz) and the amplitude of this sound allows a differentiation between crispy and not crispy foods.

The sound is generated during the cell breaking, while cell content expands. A sound pression wave, made of alternate regions of compression and rarefaction moving through the air, is then produced. The amplitude of this compression and rarefaction is directly proportional to the force applied to the sample, in a way that bigger is the force applied, bigger is the amplitude detected [66]. In particular, as mentioned before, crispy foods are described by frequencies that have an higher range (5-13 kHz) and a sound with an higher amplitude, if compared with not crispy products.
The Figure 1.2 reports the amplitude-time plot of different food: a) water-

soaked green pepper, b) fresh green pepper, c) Pringles potato chips and d) almond . It is worth noting that the higher the amplitude of the amplitude-plot, the crispier is the food analysed [228].

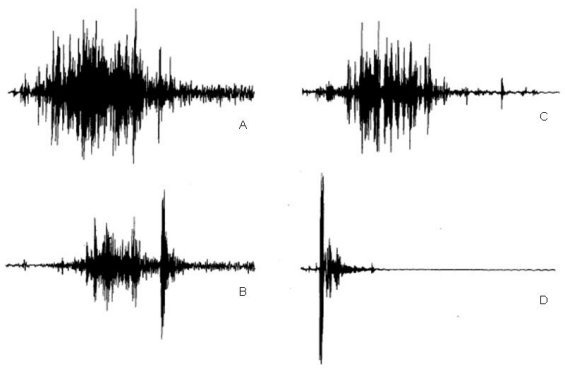

Figure 1.2: Amplitude-time plot of different foods. A: water soaked green pepper, B: fresh green pepper, C: Pringles potato chips, D: almond [227]

In conclusion, acoustic and mechanical data are therefore correlated and show information that are connected and complementary to each other. In fact the number and intensity of the acoustic profile depends on the change of energy released during the fracture [222]. For this reason both are usefull and necessary for the dissection of a complex trait, such as crispness.

1.5 Cell wall anatomy

Fruit maturation and ripening processes are the result of a complex series of events, determined by genetically programmed physiological and biochemical changes. These variations generally include pigment modifications (which affects appearance), conversion of starch into sugar and accumulation of flavour and aromatic volatiles (affecting fruit flavour), modifications of cell wall ultrastructure (affecting the final fruit texture) and syntesis of vitamins, minerals, antioxidant and fiber (affecting nutrition) [85],[29]. Among these, modifications of the cell wall architecture are crucial phenomena for texture dynamics during fruit ripening.

The primary cell wall is constituted by a large number of polymers that vary between species; however eight polymeric components are usually present: cellulose, three matrix glycans composed of neutral sugars (xyloglucan, galactoglucomannan, glucoronoarabinoxylan), three pectin rich in D-galacturonic acid (homogalacturonan, rhamnogalacturonan I and II) and structural proteins [29]. Cell wall is composed by a rigid and inextensible cellulose microfibrils, coated together by a crossed-linked matrix of glycans, of which the most adbundant is xyloglucan [155]. More in detail xyloglucan backbone is binded to cellulose

by hidrogen bonding, and xyloglucan molecules can span between adiacent microfibrils, linking them together. Also glucomannan and glucuronoarabinoxylan are cross-linked to microfibril. Spaces between the cellulose and the glycans matrix are filled by pectins; this final complex network may be locked together by covalent links between some xyloglucan molecules and pectins [218].

Other structural proteins may form an additional network, causing cell wall modifications; these proteins, all existing in multigene families, are extensin, Proline-Rich Protein (PRPs) and Glycine-Rich Protein (GRPs) [241]. The best-known structural wall proteins are the extensins. They are basic proteins able to interact with acidic pectic blocks in the cell wall, helping the wall reinforcement [120]. In cases where the cross linkages are labile, extensins provide a chemical basis for changes in cell wall plasticity which are necessary for extension of plant cells [132]. As extensins, PRPs are presumably insolubilized in the cell wall matrix [35]. They are mainly present in the xylem where they might be involved either in xylem differentiation or in lignification [35]. GRPs, mainly localized in the modified primary walls of protoxylem cells, are another class of structural wall proteins. They seem to play important roles in the development of vascular tissues, nodules, and flowers and during wound healing and freezing tolerance [35].

1.6 Cell wall gene regulation

1.6.1 Cell wall enzymes and their role in fruit ripening

The modification occurring in the cell wall polymers during ripening is a complex phenomena involving the co-ordinated and interdependent action of a range of cell wall-modifying enzymes and proteins like Polygalacturonase, Pectin methylesterase, β Galactosidase, Pectate lyase, Endo 1$\rightarrow$4 β-D-glucanase, Xyloglucan endotransglycosylase and Expansin. One family of cell-wall enzyme may mediate the activity of another, resulting in a co-ordinated wall modification process [187]. Cleavage of the matrix backbone of hemicellulose or pectins (made by endo-glucanases), remove for istance the side-chains allowing the interaction between polysacharide backbones (made by glycosidases) [88].

Pectin-degrading enzymes, PG, PME and PL are surely key players in fruit softening, as pectins are synthesized and deposited in the cell wall in a methylesterified form, and their main function is to cement plant cells together into tissue structures [185]. Their action exposes the wall to the action of other cell wall enzymes, initiating all the transformations typical of ripening. Polygalacturonase (PG) are enzymes that catalyse the hydrolytic cleavage of galacturonide linkages (PG substrate in the cell wall are mainly homogalacturonan) and can be of exo- or endo- acting types, even if the endo-acting enzymes more likely contribute to pectin depolymerization in ripening fruits. An increase in the activity of this enzyme has long been associated with fruit ripening, although the amount detected varies widely with species and during the different stage of

ripening. The degrading activity has been studied in different systems like avocado, cherry, tomato, peach, pepper, pear, grape, melon, strawberry and apple [2],[18],[89],[110],[168]. PG is responsible for a major component of polyuronide solubilization and depolymerization during ripening; its action however is necessary but not sufficient for fruit softening [88]. The accumulation is regulated by the ethylene, with low levels of hormone able to induce mRNA accumulation proportional to ethylene exposure [204]. During ripening, methyl-esterification of cell wall pectin declines sensibly from mature green fruit to red ripe fruit, accomplished by Pectin methylesterase (PME), which de-esterifies polyuridonides allowing their degradation by PG enzymes. De-esterification of homogalacturonans may also induce the formation of Ca^{2+} bonds among pectins, reinforcing thus the cell wall structure. Pectate Lyase (PL) catalyse the cleavage of de-esterified pectin [34]. β-Galactosidase catalyse one of the largest changes occurring in the cell wall of ripening fruits: the loss of galactosyl residues from wall polymers which increases the porosity of cell wall and allows the access of other hydrolase to pectic or glycan substrates and depolymerization of structural polysaccharides [29]. Endo 1$\rightarrow$4 β-D-glucanase (EGase), often referred as cellulase, are belived to contribute substantially to fruit softening, they hydrolyze internal linkages of 1$\rightarrow$4 β-D-linked glucan chains adjacent to unsubstituted residues. EGase substrates probably are xyloglucan, integral and peripheral regions of non-crystalline cellulose and glucomannan, where is present a sufficient number of consecutive 1$\rightarrow$4 β-D-linked glucan residues for substrate binding. These genes have been described in several species [29]. Hemicellulose modification is brought by enzymes such as EGase and Xyloglucan endotransglycosylase-hydrolase. Xyloglucan endotransglycosylase (Xet), enzymes that are specific for both donor as well as acceptor, catalyse the cleavage of internal linkage of 1$\rightarrow$4 β-D-glucan backbones of xyloglucan and transfer the newly formed reducing end to another xyloglucan polymer or oligosaccharide [29]. Xet is belived to be involved in different processes during plant development, like in cell wall loosening during growth and in the rearrangements or strengthen of cell wall by an incorporation of newly synthesized xyloglucan into the wall, having thus a maintenance role [30].

Not all cell wall modifying enzymes show hydrolase or transglycosylase activity or cause depolymerization of carboxymethylcellulose or cell wall matrix glycans or pectins [158]. Expansins (Exp) strongly bond to cellulose coated with matrix glycans, cause a reversible disruption of hydrogen bonding between cellulose microfibrils and polysaccharides matrix, particularly xyloglucan. This action brings to a cell wall relaxation without significat expansion, contributing along with an increased apoplastic solutes to the reduction in turgor and a turgor-driven slippage of close microfibrils. In particular, if xyloglucan is bound to cellulose, is not accessible to endo 1$\rightarrow$4 β-D-glucanase, but the presence of ripening-related Expansin could allow the loosening of glucan-xyloglucan hydrogen bonds and a sufficient separation between chains to permit the bind. More recently a non-enzymatic scission of polysaccharides has been suggested

to contribute to fruit softening during ripening. The release of ascorbate in the apoplast, due to membrane permeabilization, may in fact provoke apoplastic hydroxyl production whose radical is potentially involved in non-enzymatic scission of plant cell wall polysaccharides [68]. In tomato fruit, oxidative ions and changes in the activity of superosside dismutase, catalase and enzymes involved in ascorbate cycle during ripening, suggest that antioxidative system plays a role in ripening [115].

The final picture that emerges is a series of different enzymes, whose expression is regulated both in time and amount during maturation, acting in concert in an interdependent and synergyc way to control changes in softening and texture. These enzymes are controlled by a large number of genes, which have, in turn, to be regulated and expressed co-ordinately. The complexity of ripening physiology and fruit maturation have been confirmed by the recent discovery that in the genomes sequenced to date almost 10% of the entire gene inventory is devoted to cell wall metabolism [154].

1.6.2 Cell wall modifications during ripening

During ripening, cell wall architecture is progressively modified, determining the texture peculiar for every fruit [29]. General changes in polysacharides are: polyuronide depolymerisation, loss of galactan and arabinan, pectin solubilization and demethylesterification, cellulose and glycan matrix depolymerisation. Usually the first change observed during ripening is a biochemical dissolution of the middle lamella, the pectin-rich layer between cells, by a series of enzymes degrading polysaccharides [28],[29]. Difference in the middle lamella was observed by Ben-Arie *et al.* [19] in mature hard and soft tissue of both apple and pear fruits. In apple, cell wall from immature and hard fully ripe fruits was similar in structure, showing a packed fibrillar material in the wall of adjacent cells as well as in the middle lamella. In soft mealy fruits instead, some of the fibrillar material from the outer part of the wall had undergone dissolution and appeared to be dispersed and the disassembled middle lamella. Also in pear cell wall from hard mature and immature fruit was not different. It consisted in fact of tightly packed fibrillar material and a conspicuous middle lamella in between. Soft fruits, on the contrary, showed a reduced stainig of cell walls and sparce appearance of fibrils. The region occupied before by the middle lamella appered then reduced and empty, showing a difference also with apple soft fruits. Ben-Arie work showed also that the action of degrading enzymes do not affect the wall material surrounding the plasmodesmata and their persistence in the cell wall undergoing degradation in softening fruit. The breakdown of plant tissue, usually involves cell separation or cell breakage as mentioned above. In unripe fruits or uncooked vegetables cell adhesion is strong and tissue fraction involves rupture across cell walls, releasing cells content and making tissue texture juicy and crispy. On the contrary, in softened tissue like mealy fruits, middle lamella undergoes extensive dissolution and the cells are completely separated upon

compression, slipping one on the other [233].
Cherry crispy and soft fruit has been analysed by Batisse and collaborators [17] in order to see the difference in sugar content between the two textural different fruit. In particular they concluded that, during maturity, crispy fruits have more neutral sugars than mealy fruits and, consequentely, more possibility of associations between the different cell wall polymers. In contrast, for mealy fruit the situation was the opposit. Crispy fruits had an higher level of rahmnose, arabinose and hemicelloluse while, on the other hand, presented a descreased amout of galacturonic acid which is instead permanent in soft fruits. The rate of protein synthesis was instead greater for the soft fruits than the crispy ones. A similar situation observed for soft cherry, was discerned for apples stored 30 weeks [151], where arabinose and galactose content decreased with time. For apple, in particular, it has been suggested that softening is the result of two sequential cell wall modification, a loss of galactan which precedes or accompanies an increase in soluble polyuronide, derived from a pectic polysaccharide of relatively low neutral sugar content [128]. A very specific declines in cell wall galactose have also been reported for strawberries, pears and tomatoes ripening [4], [92]. Changes in normal ripening are similar to the two-stages pattern of wall modification observed in apple, with a galactose and arabinose reduction and an increase of soluble polyuronide content. From this description it is easy to understand that plant tissue mechanical properties depend on the contribution of different levels of structure, and how this levels interact to each other [233]. The lowest level is the polymers constitution of the cell wall, the way they connect and how they are arranged. The next level is constituted by cells, which can differ in shape, size and orientation, based on their function. Other important levels are how cells are organised in the tissue and the final organs's characteristics. It is important to note that every level of this hierachy involves properties of the cell wall (Figure 1.3).

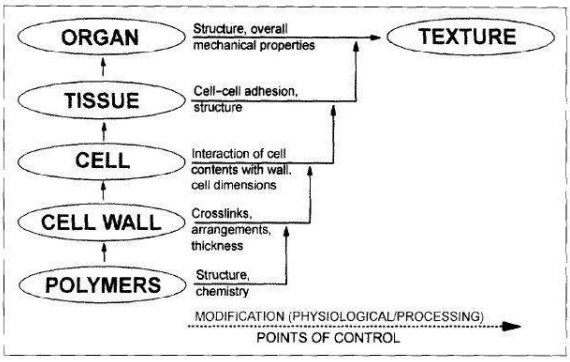

Figure 1.3: Schematic representation of the levels of structure contributing to the mechanical properties of plant tissue [233]

1.7 The hormone ethylene

1.7.1 Ethylene and fruit ripening

Fruits have been categorized in climacteric and non-climacteric type, depending on their enhanced ethylene production and associated increase in respiration rate at the onset of ripening. In climacteric fruits, such as tomato, apple, peach, and banana, ripening is in fact accompanied by a peak in respiration and a concomitant burst of ethylene required for fruit ripening. In non-climacteric fruits, such as citrus, grape, and strawberry, respiration shows no drammatic change and ethylene production remains at a basal level. These distinctions, however, are not absolute. Melon fruit in fact, can be both climacteric and non-climacteric, and both ethylene dependent and independent gene regulation pathways coexist in order to co-ordinate the different kind of fruits [6], [14]. To date, molecular factors influencing fruit maturation, and particularly ethylene perception, have been mainly described via mutant and gene cloning in *Arabidopsis*. *Arabidopsis* fruit is however classified as dry and dehiscent, not favorable for studying the physiological process occurring in fleshy fruits. For this reason tomato has been chosen as the model species to study fleshy fruit physiology and genetics. Tomato is the most genetically tractable plant system for studying fruit ripening because of its simple diploid genetics, relatively short generation time, small habit compared to fruit crop species, excellent genetics, facility of routine transformation and extended repertoire of genetic and genome information (http://www.sgn.cornell.edu/) [14]. Besides tomato, other plants have been used to study the ripening process. Strawberry for example, is a primary model for non-climacteric fruits but also apple, peach or citrus are becoming models for genomics analysis of fruit ripening in fruit crop species.

Hormonal involvement on plant development was discovered observing plant placed near artificial illumination. Coal carbon was an important source of light but its relevance was "illuminant" also for fruit ripening process [40]. In 1858 Fahnestock attributed the deterioration of a collection of plants in greenhouse to the presence of illumination gas, even if he was not able to identify the responsible component. Some years later, Giarardin verified that trees growing near places with leaking gas illumination showed senescence symptoms. In 1886 Neljubov discovered that the orizontal growth of etiolated pea seedlings was casused by ethylene, the biologically active component of illumination gas. Since that several observation were made on ethylene effects on plants and in 1930s most of the physiological effects had already been described. The chemical proof that plants naturally produce ethylene was provided by Gane in 1934 after a study on apple ripening, and later, in tomato, the production of this hormone was associated with a peak in the respiration rate. Elucidating that the mechanisms that are involved in the fruit ripening process are a crucial keys to understand fruit quality.

1.7.2 Ethylene biosynthesis

Ethylene pathway is well estabilished in higher plants and is synthesized from methionine in three fundamental steps [22] (Figure 1.4):

1. conversion of methionine to S-adenosyl-L-methionine (SAM) by the SAM synthetase enzyme,
2. formation of 1-aminocyclopropane-1-carboxylic acid (ACC) from SAM via ACC synthase (ACS),
3. conversion of ACC to ethylene, which is catalyzed by ACC oxidase (ACO).

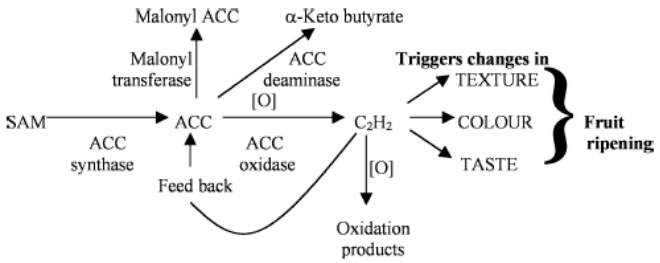

Figure 1.4: Pathway of the ethylene biosynthesis and metabolism [177]

The formation of ACC also leads to the production of 5'-methylthioadenosine (MTA), which is recycled via the methionine cycle to yield a new molecule of methionine [14]. This savage pathway preserves the methylation group through every revolution cycle at the cost of one molecule of ATP, in this way ethylene biosynthesis can be mantained even when the pool of free methionine is limited [6]. ACS and ACO are both encoded by a multigene families in all plant species studied and their expression is regulated according to plant developmental stage, environmental and hormonal signals [121]. Up to now *Arabidopsis* genome presents nine differently regulated ACS genes that encode eight functional and one non-functional ACS proteins [14]. In tomato plants, nine genes encoding ACS have been described to date, four of which are differentially expressed during fruit ripening; five ACO where instead identified, three of which are differentially expressed in fruit [32], [140]. In pre-climacteric tomato fruits, few members of the ACS and ACO gene families (namely, *Le*ACS1, *Le*ACS3, *Le*ACS6, *Le*ACO1 and *Le*ACO4) are active and responsible for System 1 basal ethylene biosynthesis. During ripening, the transition to System 2 is the result of *Le*ACS6 silencing and increased expression of *Le*ACS2, *Le*ACS4, *Le*ACO1 and *Le*ACO4 [6], [14]. ACS and ACO genes have been characterized in many other fruits like melon [240], apple [64], banana [142], kiwifruit [238], peach [192] and persimmon [166]. ACS was initially considered as the key regulatory enzyme in ethylene biosynthesis pathway since the rate-limiting reaction of ethylene biosynthesis pathway is the conversion of S-adenosylmethionine into ACC,

and ACO activity was thougth constitutuve; ACO role however become apparent in recent years. The rise of the activity of this enzyme precedes ACS activity in preclimacteric fruit response to ethylene, indicating that ACO is also important for controlling the hormone production [6]. In climacteric plants two systems of ethylene regulation have been proposed. System 1, which functions during normal growth and development and during stress responses, is regulated by an autoinhibitory feedback, such that exogenous ethylene inhibits the hormone synthesis. System 2, which operates during floral senescence and fruit ripening, is stimulated by ethylene and is therefore under an autocatalytic feedback regulation, and inhibitors of ethylene inhibit ethylene production [157].

1.7.3 Ethylene perception

Much of what is nowadays known regarding the steps involved in ethylene perception and signalling transduction, derived by studies carried out on the model plant species *Arabidopsis* (Figure 1.5).

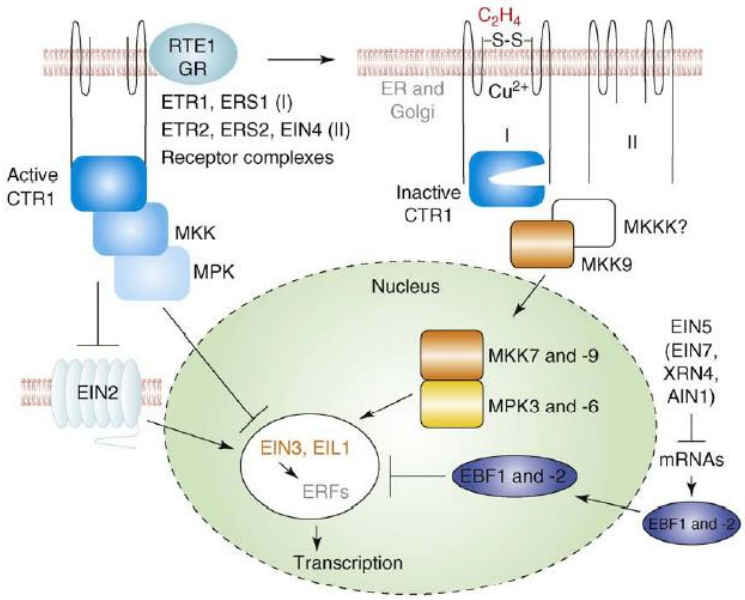

Figure 1.5: Current model for the ethylene signal transduction pathway [242]

Ethylene is sensed in *Arabidopsis* by a family of receptors which are related to bacterial two-component histidine kinase (HK) sensors that bind ethylene through their N-terminal domain, localized in the endoplasmic reticulum [170], [180]. In *Arabidopsis* there are five membrane receptors (ETR1, ETR2, ERS1, ERS2 and EIN4), while six are the receptors in tomato (*Le*ETR1, *Le*ETR2, *Le*ETR4, *Le*ETR5, *Le*ETR6 and NR). Analysis of ethylene receptor null mutations have led to the proposal of an inverse-agonist model for ethylene receptor

signaling. In absence of ethylene, for instance, the receptor is costitutively active, whereas when ethylene is bound, the receptor in switched off [242]. These receptors thus act as negative regulators through another negative regulator: the COSTITUTIVE TRIPLE RESPONSE1 (CTR1). Downstream this regulator, a membrane metal transporter-like, named EIN2, has a pivotal role in ethylene signaling. CTR1 seems to regulate the availability of the key transcriptor factor named EIN3, through an unknown mechanism. In response to ethylene, EIN3 is stabilized and accumulated in the nucleous activating hormone-inducible primary transcription [94], [242]. Without exogenous ethylene induction or application, EIN3 is degraded constantly through the 26S proteasome. Successively EIN3 and EIN3 like1 transcription factors activate ETHYLENE RESPONSE FACTOR1 (ERF1), which induce the expression of the secondary response gene in ethylene-dependent transcription cascades.

Many fundamental components in the ethylene signal transduction pathway are also controlled by ethylene, providing in this way, layers of negative or positive feedback loops for the correct tuning of response dynamics. ERS1, ERS2 and ETR2 transcripts increase in fact as primary response to ethylene [109]. The newly synthesized receptors that have not yet perceived ethylene might suppress the downstream ethylene signaling, diminishing the hormone response as negative feedback mechanism. By contrast, ethylene binding can initiate the proteasome-dependent degradation of *Arabidopsis* ETR2, and might increase the ethylene sensitivity in plant [242]. Upstream the ethylene regulatory cascade, is possible to identify different developmental transcription factors like for example MADS-box, CNR or NAC genes. The study of ripening mutant specific for this gene set, allowed to better understand their role in ripening regulation. Two well characterized phenotypes are *nor* (non-ripening) and *rin* (ripening inibitor) mutant. In tomato, *rin* mutant fails to exibit the typical ripening-associated increase in ethylene production, lacks in the pro-vitamin A and carotenoid accumulation and showes a reduced softening and flavour compounds production. *Rin* locus encodes a MADS box transcription factor, and phenotype has been interpreted to reflect a function in ripening control over climacteric ethylene synthesis, probably controlling genes envolved in ethylene biosynthesis pathway [86]. Neverthless, *rin* fruit do not ripen in response to exogenous ethylene, yet they display induction of at least some ethylene-responsive genes, indicating retention of fruit ethylene sensitivity. These results have been interpretated to mean that the RIN gene encodes a genetic regulatory component necessary to provoke climacteric respiration and ripening-related ethylene bio-synthesis, in addition to require factors whose regulation is not ethylene influenced. This picture shows that RIN acts upstream of both ethylene and non-ethylene mediated ripening control [242]. *Nor* mutation effect on tomato phenotype is similar to *rin*, except for the final fruit colour that is pale orange. These two mutantion affect the ability of fruits to produce autocatalytic ethylene, thus to ripen in response to exogenous ethylene [162].

As previously reported, in climacteric fruit, ripening is mainly controlled

by a signalling pathway and involves the hormone ethylene perception. This physiological mechanism has been used to develop strategies for the control of the climacteric fruit ripening. One of these strategies relies on the use of 1-methylcyclopropene (1-MCP), a cyclopropene derivative, which chemical structure is similar to natural ethylene, which binds permanently to the ethylene receptors present at the time of treatment, competing thus with ethylene binding. It has been demonstrated that any return of ethylene sensitivity is due to appearance of new binding sites [21]. The effect of this inhibitor is variable depending, on the temperature, growing region, the concentration at which 1-MCP is applied or delays between harvest and fruit treatment [236]. Relatively little information concerning commercial aspects of its use are available; one exception is apple, for which 1-MCP based technology is available throughout the world and for which many studies have been already realised [235], [236]. Apple varieties differ each other for ripening rates, harvest criteria, post harvest handling procedures and storage periods in controlled atmosphere; is therefore not surprising that these factors affect response to the inhibitor. These responses could be a combination of the effects of the internal ethylene concentration at the harvest point, the physiology of the cultivar and their abilities to develop new ethylene receptor sites. 1-MCP impact on fruit ripening science is double, on one side, in fact, is a compound that allows a longer shelf life of harvested fruit, on the other side, is a powerful tool for the scientific investigation on ethylene-dependent ripening and fruit senescence.

Ehtylene even having a key role in fruit ripening, is not the unique hormone able to influence plant biology; in fact hormones, including jasmonates, auxin, and brassinosteroids, have all been implicated, together with light and sugar, in the promotion of ripening in various species [14].

1.7.4 Ethylene impact on cell wall metabolism

Enzymatic dynamics, which act in concert in the cell wall modification, are, in climacteric fruit, for the most guided by the gaseous hormone ethylene. Ethylene, in fact, trigger and co-ordinates the gene activation and expression in genetically programmed sequence.

Accumulation of PG mRNA in tomato, for istance, is regulated by ethylene, with low levels of the hormone being sufficient for inducting the mRNA accumulation, which increased under ethylene exposure. Moreover, PG mRNA accumulation is ethylene regulated in a concentration and time dependent manner [204]. The mRNA adbundance of a tomato expansin, *LeExp1*, resulted to be positively and directly regulated by ethylene in ripening fruit. Its level is, in fact, strongly diminished after treatments with ethylene antagonists and in ripening plants mutant for ethylene syntesis [188]. β-galactosidase activity is also ethylene regulated; it was in fact observed that the total content of β-galactosidase was markedly reduced in non ripening tomato mutant when compared to the wild type. In these mutants the loss of cell wall galactose and the

increase of free galactose were strongly reduced, and the ripening-related induction of β-galactanase activity was not observed [91], [90],[29]. Accumulation of some endo 1$\rightarrow$4 β-D-glucanase mRNA in tomato is promoted during ripening by exogenous ethylene, and inhibited by an ethylene antagonist, suggesting an ethylene regulated expression pattern [133]. Also ripening-related Xet activity and mRNA adbundance are positively regulated by ethylene, both in kiwi and in tomato fruit. In tomato, *rin* mutants present a reduced activity of Xet gene compared to the wild type. Despite the fact that it has not yet confirmed, it seems likely that, in climacteric fruit, ripening-related Xet gene expression is positively regulated by ethylene [183],[146].

1.7.5 Genetic manipulation of ripening regulatory genes

By the picture described in this chapter, and underlined also by Figure 1.6, cell wall enzymes and genes involved in the ethylene biosynthesis pathway are valuable target for future genetic engineering stategy addressed to present on the market fruits with desirable flavour and colour and moreover texture attributes, avoiding the negative conseguences of over-ripening like oversoftening, decay, mechanical damages or post harvest desease.

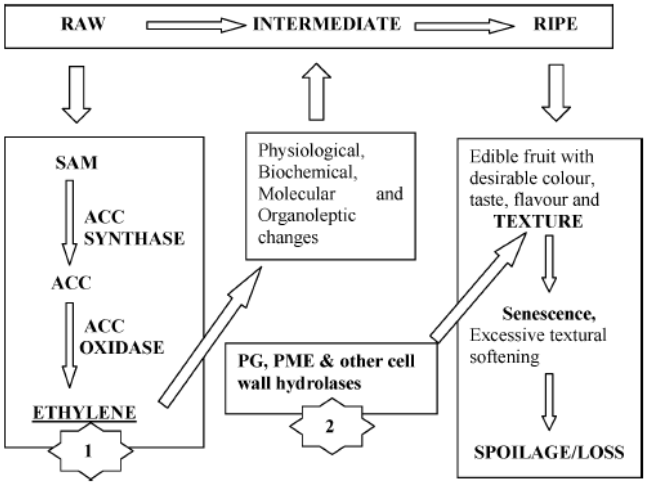

Figure 1.6: An overview of fruit ripening with particular emphasis on textural softening. Control points at ethylene (1) and post-ethylene (2) levels [177].

The study of the ripening dynamics is important in order to extend shelf life qualiy maintainance, post harvest mechanical and disease resistance and product loss. For this reason, many studies have been performed on model species. Being apple characterized by a relatively long shelf life, and a the market demand covers the 12 months period, it is important to identify which are the genes responsable of the control of this complex physiology. To date,

attempts to manipulate the expression of target genes during fruit ripening have been realised mainly in tomato and strawberry, to improve shelf life or nutrition [108],[123],[116]. Different experiments have shown that it is possible to "turn off" the expression of existing genes in transgenic plants by introducing a gene constructed to generate antisense RNA, useful to curtail the expression of ripening genes, enhancing the shelf life and reducing fruit senescence.

Smith and colleagues [205] performed in tomato an experiment where they used antisense RNA techniques to manipulate the polygalacturonase (one of the main gene involved in the in cell wall modification) gene expression. Similar experiments have been carried out also by Sheehy and collaborators [201], using a full-length eDNA. Transgenic plants, expressing the antisense gene showed a reduced levels of both PG mRNA and PG enzyme activity in the fruit at all ripening stages. Interestingly other aspects of ripening such as ethylene production and lycopene accumulation were not affected in the mutant plants. The cDNA for a fruit pectinesterase, a cell wall degrading enzyme, was used to construct an antisense gene controlled by a 35S promoter. Expression of this antisense gene in transgenic tomatoes greatly inhibited PE activity in fruit, but had no effect on enzyme activity in leaves or roots, suggesting this enzyme as a good candidate for fruit shelf life enhancing [96].
Antisense experiments were carried out also in strawberry, a soft fruit with a short post harvest life [116]. To control the strawberry fruit softening, a transgenic line was realised incorporating an antisense sequence of a strawberry pectate lyase gene, involved in the cell wall modification during fruit ripening. The post harvest softening of transgenic fruit was diminished together with an high increased fruit firmness, indicating that pectate lyase gene is an excellent candidate for biotechnological improvement of fruit softening in strawberry.

Transcritpional control has been applied at the *rin* mutation in tomato commercial lines in order to delay ripening and extend shelf-life [152]. This modification, however, results in inhibition of other traits like flavour or nutritional compound accumulation. This last example, enlightening the complexity of the ripening system, showed the indispensability of the identification of the right gene target useful for following transcriptional control and genetic engineering approaches. Candidate genes characterization can be accomplished through different strategies; forward genetics is one of them.

CHAPTER 2

Aim of the work

Fruits greatly differ in texture properties, and among them apple is distinguished by a "crispy type". The group of apple varieties is highly heterogeneous and represented by different cultivars defined by distinct textural attributes and peculiarities. Taking into account that crispness is the most appreciated characteristic by consumers as well as the driver trait in breeding programs, we started a pilot project aiming the identification of the genomic regions involved in the control of this complex trait, with the final task to set up a molecular tool kit to assist the traditional breeding in the selection process.

Aware of the great importance and attention that the scientific community is giving to phenomics, the first purpose of this work was the improvement of the apple texture variability dissection. Sensory evaluation is nowadays the most used approach to assess fruit texture, suffering, however, of some important limitations. For this reason, in *Chapter 3*, it was investigated whether a combined and simultaneous mechanical and acoustic evaluation of fruit texture could provide a helpful methodology for the description of all the aspects related to apple texture, providing also a valuable link with sensory attributes.

Successively this high resolution phenotyping strategy has been adopted for a Quantitative Trait Loci (QTL) analysis, carried out on two bi-parental crosses (*Chapter 4*), selected in order to represent a "broad spectrum" of the texture variability. The aim of the QTL study was to obtain an overview of the genomic regions possibly involved in the determination of the traits under investigation. The anchor on the Golden Delicious genome allowed the discovery of the gene set underlying the statistical QTL interval, putative new candidates involved in the texture control.

A fine mapping, described in *Chapter 5*, was afterwards accomplished employing a candidate gene based analysis. The aim of this approach was the

investigation on two specific hot spot regions, where a polygalacturonase and a xyloglucan endotransglycosilase genes were mapped, with the final purpose to design specific markers valuable for assisted selection.

Conscious that physiological informations are the bases and the starting point for association studies, a functional investigation was also performed with the final aim to obtain a more precise picture of the expression dynamics occurring during fruit ripening (*Chapter 6*). The transcription analysis allowed to confirm previous information about candidate genes and to investigate other possible elements in crispness determination. This would be also the starting point for the identification of new candidate genes having a putative impact on fruit texture and future association studies.

CHAPTER 3

Assessment of apple (*Malus x domestica* Borkh.) fruit texture by a combined mechanical-acoustic profiling strategy

[1]

3.1 Abstract

Texture of apple fruit originates from anatomic traits related to cell wall architecture and is one of its most important quality characteristics, thus there is the desire to better understand the different factors which contribute to apple texture. Here we present a novel approach based on the simultaneous profiling of the mechanical and acoustic response of the flesh tissue to compression, using a texture analyzer coupled with an acoustic device. The methodology was applied to a 86 different apple cultivars, measured after two months post harvest cold storage and characterised by 16 acoustic and mechanical parameters. Statistical treatment of the data with principal component analysis (PCA) allowed for the identification of three groups of variables, the mechanical ones being clearly distinguished from the acoustic ones. Moreover, the distribution of the apple cultivars in the multivariate PCA plot allowed characterisation of the cultivars according to their textural performance. Each cultivar was analyzed also with non-destructive vis/NIR spectroscopy in order to determine impartially the ripening stage. Sensory evaluation by panellists was performed on a selected group of cultivars and sensory data correlated with the acoustic-mechanical data. The results demonstrate the good performance of our combined acoustic-mechanical strategy in measuring apple crispness as it is perceived by human senses.

[1] Published on Postharvest Biology and Technology [46]

3.2 Introduction

Texture represents one of the four principal factors defining food/fruit quality, together with appearance, flavour and nutritional properties [25], and plays a key role in consumer acceptability and recognition of apples. In particular, textural characteristics of apples defined by "crispness", "juiciness", "hardness", "firmness" and "mealiness" are often key drivers of consumer preference [99]. Texture originates from several different physical properties rather than from a single trait, and depends on cellular structure and how this responds to applied forces [210]. In fruit and vegetables, crispness and crunchiness are mechanically expressed as a rapid decrease in force accompanied by a rapid textural fracture propagation. They normally represent the major traits contributing to general "food enjoyment" since both are considered by consumers as an indication of the freshness and healthy state of fruit [209], [80], [81].

In apple it has been shown that among the textural traits, crispness accounts for 90% of texture appreciation, and it has been largely recognised as the key attribute affecting consumer acceptability [97]. Microscopically, when the wall of a turgid cell is broken under mechanical pressure, a sound pressure wave is generated, resulting in the typical "sound" perceived as the crispy phenotype. Crispness events and sound pressure waves are strictly dependent on the breaking propagation toward adjacent cells, where the pressure exerted on the outer cell wall causes a catastrophic rupture [124]. In crispy apples, the cell breakage generates a sound wave which causes a vibration between molecules around their equilibrium, consequently propagating the pressure wave and thus producing the sound [66].

In contrast, low cell wall turgidity, due to a higher elastic tension of the wall, or by pectic polysaccharide solubilisation in the middle lamella, determine cell separation instead of cell wall fracturing [60], with a consequent rubbery texture typical of mealy apples [184], [167], [7]. Cell rupture (the event generating crispness) or separation (responsible for mealiness) have also a direct impact in the release or encapsulation of juice and aroma [124], [70]. Therefore, a crispy apple is generally preferred not only for texture characteristics, but also for an enhanced release of volatile compounds perceived by the receptors in the mouth space. To date, the most complete description of crispness is provided by sensory testing carried out by expert or trained panellists. However, there are fundamental limitations to this approach due to the difficulties in employing such a strategy for assessment of large cultivar collections and breeding material. To overcome these constraints, instrumental approaches dedicated to fruit/food textural quality analysis have been developed [190], and documented in several studies reporting textural analysis in apple performed with different techniques, such as compression [159], single-edged notched test [102], sound recording during mastication [190] and chewing sound measurements [59], [112]. However, the comparison between the sound amplitude recorded during the fruit biting and the corresponding crispness sensorially evaluated resulted

hardly reproducible and panellist dependent [60]. Other methodologies based on mechanical approaches focus on the physical response of the samples, such as deformation, fracturing and compression, the latter being probably the most widely used for its simplicity [190]. The use of the puncture test to predict consumer preference has been also reviewed and questioned [101].

Novel technological improvements in the direct measurement of fruit texture have been recently presented by Taniwaki *et al.* [213], based on the concept that the sensorially perceived crispness could be derived by the vibration produced during the fracturing (proposed by Christensen and Vickers, [41]). This device represented by a piezoelectric sensor able to detect the vibration caused by the sample's fracture has been used to quantify a texture index (TI) in several species, including apple [213], [215]. This equipment was also further coupled with non-destructive vibration methods (Laser Doppler Vibrometer- LDV) to measure the change of both elasticity and texture index during the ripening of persimmons [214] and pears [212]. It is likely that the combination of different methodologies may represent a further improvement for more efficient texture investigation, as already demonstrated in almonds, where a similar strategy was successfully applied and correlated with sensory evaluation [222]. Recently Zdunek *et al.* [245] reported crispness and crunchiness evaluation of three apple cultivars by measuring the contact acoustic emission together with the puncture test, and showed that the sensory attributes related to crispness and crunchiness correlated better with acoustic emission events rather than firmness. The purpose of our work was the improvement of the texture variability dissection, increasing the number of parameters acquired during the compression phase. We investigated whether mechanical and acoustic characterisation of a set of apple cultivars could provide a valuable methodology able to encompass all aspects related to apple texture, providing also a better link with sensory attributes.

3.3 Materials and methods

3.3.1 Plant materials

In this experiment we selected 86 apple cultivars harvested in 2009 in the experimental fields of two institutions: the Innovation and Research Centre of Edmund Mach Foundation in San Michele all'Adige (Trento), and the Research Institute Centre of Agriculture and Forestry Laimburg (Bolzano), both in the North of Italy (Trentino-Alto Adige region) and with similar climatic condition (Supplementary Table 8.1). All fruit were collected at commercial harvest, following the main parameters used to monitor the maturity and ripening evolution (standard practice), like fruit firmness, skin colour and total acid and sugar content. All harvested fruit were stored in a cold cellar at 2-4°C with a relative humidity of 95% for two months, and prior to start the instrumental analysis fruit were kept overnight at room temperature (20°C). For each cultivar only samples with similar size and without visible external damage were chosen.

3.3.2 Instrumental analysis: empirical methods and textural assessment

Fruit firmness was initially measured using a digital fruit firmness tester (TR Turoni srl, Forlì, Italy) with a 11mm probe (held on a stand) on five fruit samples for each cultivar. For each fruit, two puncture tests were performed on the two opposite peeled fruit sides. For each cultivar, ten measurements were obtained, analysing the maximum resistance required to enter the probe for 8mm. To perform a more comprehensive analysis of the fruit texture, we used a coupled acoustic-mechanical profile investigation of the use of a TA-XTplus Texture Analyzer equipped with an Acoustic Envelop Detector (AED) device (Stable MicroSystem Ltd., Godalming, UK). On the same fruit selected from the batch or cultivar, a cylindrical portion of cortex tissue was sampled with a flesh blade sampler along the vertical lengthwise plane perpendicular to the direction of the puncture test, avoiding the core portion with seeds. From each cylinder, four identical discs with a diameter of 1.70 cm and 1 cm thick (after removing the outer margins with peel) were cut with a home-made six-blade knife. Adopting this strategy, we avoided any possible influence of fruit size, as suggested by Duizer [66]. For each cultivar 20 discs, composed of four technical replications for five biological replicates, were tested. The force/displacement measurement was carried out using a 5 kg loading cell and a cylindrical flat head probe with a diameter of 4mm. The mechanical profile graph was based on two variables: force (N) and distance (strain, %). The force was measured with the following TA-XT*plus* settings: test speed of 300 mm/min, auto force trigger of 5 g and stop plot at target position. Distance was expressed in strain, compressing the sample disc until a deformation of 90%. Acoustic profiling, as a measure of sound recording, was operated simultaneously to the force assessment by the AED device. The sound generated during the sample compression was detected with a Brüel & Kjaer microphone (type 4955) positioned approximately 5 cm from the apple disc. The microphone was calibrated twice with a sound calibrator Brüel & Kjaer (type 4231), setting the sound pressure level calibrator (SPLC) initially at 114 dBs (known high level), and then it was repeated at 94 dBs (known lower sound pressure level). Both measurements were used to transform voltage signals into decibels. The envelop gain was set at 4 (on a 0 to 11 scale, with a gain of x6 dB) corresponding to 24 dB, in order to increase the sensitivity of the system to our environmental condition. The sound pressure signal, registered by the microphone, was automatically converted in dB units and plotted. With the settings chosen in this experiment the emitted sound fell in the range between 36 dB (background level) and 78 dB (maximum acoustic pressure registered during the experiment). The acoustic cut off selected by the envelop corner frequency was 3.125 KHz. The acoustic graph was based on two variables: sound pressure level (SPL in dB) and strain (%). For both profiles, data were acquired with a rate of 500 pps (points per second). From the combined mechanical/acoustic profile a total of 16 parameters were defined,

of which 12 were derived by the mechanical graph and 4 by the acoustic profile (Table 3.1).

The value of the parameters were calculated from the force displacement curve where four force values (related to the slope or yield point, maximum force, force at the end of the travel and mean value), number of force peaks, area (compression's work), force linear distance, number of peaks/distance, linear distance/distance and Young's module (or elasticity module) can be identified. From the mechanical profile we have also derived two parameters, namely force index and force difference, both linked to the mechanical curve directionality. These two indexes, being associated with physical proprieties of the underlying cell layers, provide information related to the adhesion and compression behaviour of the cells (indicating where the maximum force occurs) and the relative magnitude level. Moreover, we have targeted four parameters on the acoustic signature related to the acoustic peak number, maximum and mean acoustic pressure and acoustic linear distance.

3.3.3 Ripening stage evaluation

Prior to instrumental analysis, the ripening stage of each fruit used in the experiment was instrumentally assessed with a portable visible/near infrared (vis/NIR) spectroscopy ([249]; [47]; commercialized by TR Turoni srl, Forlì, Italy). This equipment was used in order to obtain a rapid, non destructive and objective characterization of ripening. This is necessary because the cultivars considered in this experiment were harvested at different times starting from mid July to the end of October.

3.3.4 Sensory evaluation by untrained expert panels

Sensory data on a subset of 21 cultivars (listed in Supplementary Table 8.1) were collected over 5 years at the Laimburg Research Centre for Agriculture and Forestry in a specific laboratory used for sensory testing. The panel, composed of a minimum of 12 to a maximum of 23 judges, was recruited from the Laimburg Research Centre staff expert in the field of apple breeding. For each evaluation day, six different samples (with 5 replicas/sample) were analyzed. Each sample was presented to the panellist as anonymous peeled apple slice and evaluated on a 1 to 9 scale, where 1 was used for low (soft, mealy and dry) and 9 for high (firm, crispy and juicy) values respectively. The three attributes evaluated were defined for firmness as the mechanical resistance exerted by the sample during chewing, crispness as the acoustic emission during the first bite and juiciness as the perceived release of juice in the mouth space during mastication.

3.3.5 Data analysis

Data acquisition of the combined acoustic-mechanical profiles was processed by the software Exponent v.4 (Stable MicroSystem) provided with the TA-XT*plus*

Mechanical Parameters	General description	Unit
Yield Force	Force measured at the yield point indicating the transition from the elastic to the plastic phase of the compressed sample	N
Max Force	Maximum force value recorded over the probe's travel	N
Final Force	Force measured at the end of the probe's travel	N
Mean Force	Mean force value over the entire mechanical profile	N
Force Peak	Number of counted force peaks	-
Area	Area underlying the mechanical profile	N%
Force Linear Distance	Computation of the force curve length	-
Young's Module	Elasticity module, computed as ratio between stress and strain	N%
Peaks/Distance	Number of Peaks/mm of probe's travel calculated as physical distance on the x axis	-
Linear Distance/Distance	Averaged length of linear distance /mm	-
ΔForce	Difference between F1 and F3, giving the direction of the force profile	N
Force Ratio	Ratio between F1 and F3, reporting the magnitude of the direction change	-
Acoustic Parameter	General description	Unit
Acoustic Peak	Number of the acoustic peaks calculated above the threshold of 10 dB	-
Max Acoustic Pressure	Highest acoustic peaks detected on the sound pressure wave	dB
Mean Acoustic Pressure	Mean value of the sound pressure recorded over the acoustic profile	dB
Acoustic Linear Distance	Computed length of the acoustic profile	-

Table 3.1: Description of the mechanical and acoustic parameters.

instrument. With the same software a macro instruction was also compiled to automate the parameter extraction from the force/sound curves. Basic descriptive statistical analysis, in particular boxplots, Pearson correlation analysis, principal component analysis (PCA), partial least squares (PLS) and dendrograms for cluster analysis (Manhattan distance and the complete linkage method; [8]) were carried out in R. Details on PCA and PLS can be found in Jolliffe (2002) [117] and Martens and Naes (1992) [150]. Root mean square error of cross validation (RMSECV) was used to quantify the quality of the prediction model [150].

3.4 Results and Discussion

3.4.1 Acoustic-mechanical combined profile analysis

The TA-XT*plus* texture analyzer equipped with the AED system allowed the simultaneous acquisition of two different types of source data, acoustic and mechanical, that are efficiently collected by the same instrument, as well as plotted and analyzed by the same software.

The mechanical profile obtained as a response to compression is mainly composed by two parts (Figure 3.1).

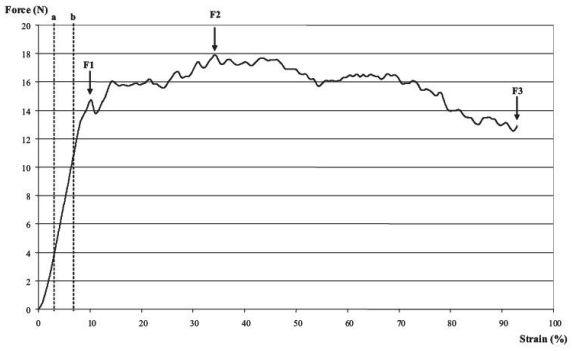

Figure 3.1: Force deformation profiled during the penetration of an apple disc. F1: yield force; F2: maximum force; and F3: final force. Anchors are indicated with a and b,

In the first step a compression slope is observed until the yield point (F1), which marks the transition from the elastic (reversible) to the plastic phase of the material (irreversible crushing). On the compression slope Hook's region the compiled macro computed the Young's module (or elasticity module), a parameter directly linked to the stiffness proprieties of the sample and positively correlated with the crispness sensorially evaluated, as suggested by Duizer [66]. After the yield point the probe breaks the tension of the outer tissue, starting the

travel through the apple disc. On the mechanical travel, two other points were identified: maximum force (F2) and final force (F3). Three main mechanical behaviours were identified after the yield point from the compression profile (Supplementary Figure 8.1): (i) descending resistance, where the yield point force value is higher than final point (F1>F3); (ii) equal resistance, when these two points are at a similar level (F1 = F3); (iii) increased resistance, exerted by the compressed layers, resulting in an increased compression resistance during the probe travel (F1<F3). The high heterogeneity of the fruit tissue creates a continuous series of brittle micro events leading to a jagged profile that generates the acoustic signal. Depending on the fruit flesh anatomic features, each variety responds with a distinct sound profile due to the acoustic emission generated during the probe travel (Supplementary Figure 8.2). As in the case of the force displacement, the sound curve was also recorded until a compression of 90%, resulting in a characteristic acoustic signature for each cultivar analyzed. The sound was recorded by a microphone directly positioned near the sample. Such a method is remarkably different from the employment of an operator for the sound recorded emitted during biting, where the bone-conducted sound is registered, often damped by mouth tissues [144].

Figure 3.2 shows the differences in the combined textural profiles of three selected cultivars. The first variety, Delearly (Figure 3.2 panel a), is distinguished for its lower general textural performance. The other two cultivars, Granny Smith and COOP39 (Crimson Crisp), respectively (Figure 3.2 panel b and c), both had a higher acoustic response, but with a clear difference in mechanical behaviour, being COOP39 much firmer than Granny Smith.

The 16 parameters identified here through the analysis of the combined acoustic-mechanical profile were extracted from the 86 cultivars showing a wide trait variation (Supplementary Figure 8.3), as a result of the different genetic control of the textural traits as well as different post harvest ripening performance during storage. Along with the data processed by TA-XT*plus*, we also included in the analysis the data obtained from the firmness measurements carried out by the fruit digital puncture test (penetrometer), which is still the most common instrument utilized in texture analysis [99]. The penetrometer alone is limited to a single data point/measurement, currently considered inappropriate to describe complex apple texture variability [112]. The use of the TA-XT*plus* coupled with the AED allowed us to target several parameters related to force displacement and acoustic response profiling, which can contribute to better define the apple fruit quality.

3.4.2 Clustering and principal component analysis (PCA)

Data related to the parameters computed here were standardized by means subtraction and rescaled by standard deviation, and dendrograms were constructed to display the clustering of the cultivars according to their textural properties (Supplementary Figure 8.4). Clustering based only on mechanical parameters

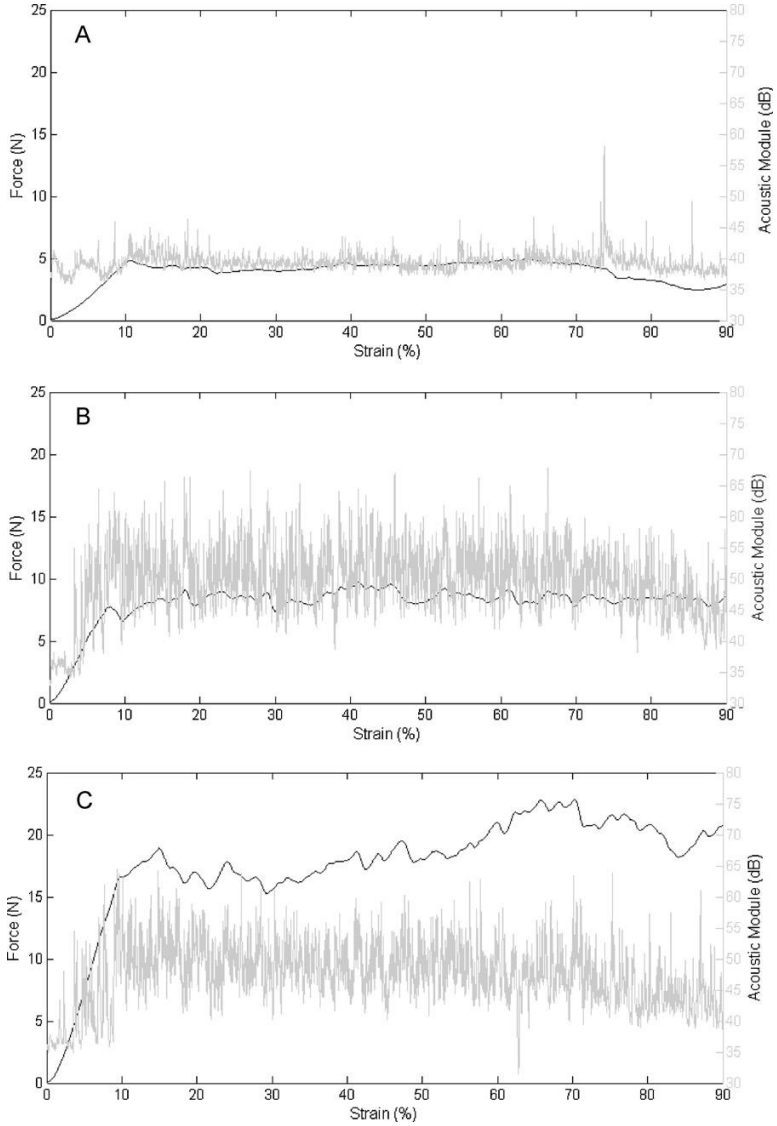

Figure 3.2: Combined mechanical and acoustic profile of three apple cultivars: Delearly (A), Granny Smith (B) and COOP39 (C). The black line refers to the force displacement.

results in some inconsistency. For instance, Granny Smith was positioned in a different group with respect to the cultivars with a similar crispy behaviour, such as Fuji and Cripps Pink, and grouped closer to Golden Delicious than the other two varieties. Previous reports have already published the distinct crispy properties of these cultivars, indicating Granny Smith, Fuji and Cripps Pink had superior crispness compared to Golden Delicious after a storage period [53], [113], [81]. Implementing the acoustic parameters in the computation, Fuji, Cripps Pink and Granny Smith were clustered together, while Golden Delicious was grouped with cultivars with mealy or low textural properties after storage, such as Renetta Canada, Elstar, Gloster and other old apple varieties. The observed change in cluster organization validates the implementation of acoustic parameters for a better characterization of textural proprieties.

Multivariate statistical techniques, such as principal component analysis (PCA), illustrate the main features regarding the cultivars investigated in a single bidimensional plot. Figure 3.3 shows the projection of the data on the first two principal components (PC1 and PC2) that explain 83.4% of the total variance (PC1: 71% and PC2: 12.4%).

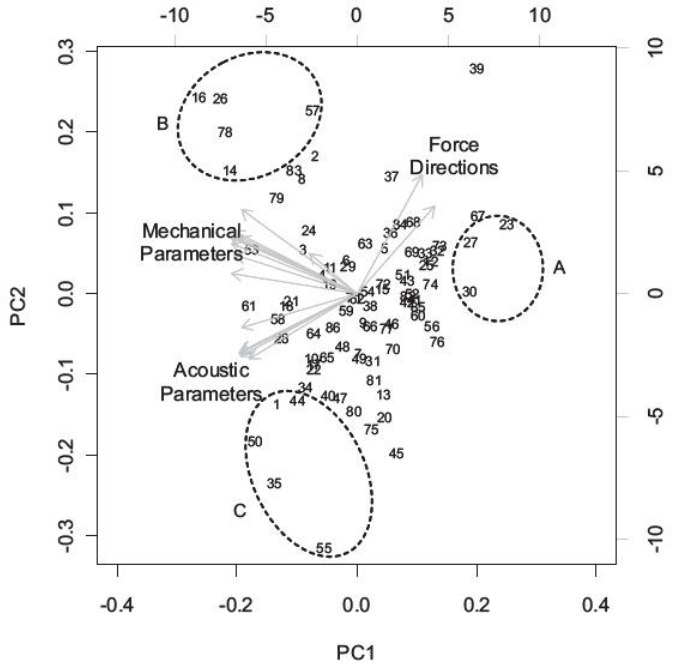

Figure 3.3: First two dimensions of PCA analysis of the texture data, calculated using all parameters extracted from the combined mechanic and acoustic analysis. Numbers indicate the apple cultivars as reported in Supplementary Table 8.1, arrows mark the parameters coordinates.

Each parameter is indicated by an arrow, and the entire set of variables is

clearly separated into three main groups: the first one related to the mechanical parameters, the second group joined together the acoustic parameters, while the third group comprises the two derived parameters (Δforce and force ratio), both describing the force direction change (named force direction). The three sets of variables highlighted by PCA represented the three types of information related to fruit texture. In addition it is important to note that the two mechanical parameters "number of force peaks" and "number of force peaks/distance" were grouped in the acoustic parameter set, suggesting that these parameters are suitable to describe the acoustic profile. This association could be explained considering that the crispness response is largely controlled by the rapid drop in force occurring during the mechanical compression, and thus associated with the fracturing progression, as described by Vincent [228]. On the PCA plot (Figure 3.3(the first axis describes the variability related to both acoustic and mechanical parameters, separating mealy apples (group A in Figure 3.3) such as Delearly (27),Dalla Rosa (23) and Early Gold (30), from both hard and crispy apples, on the positive and negative section of the plot, respectively. The second component describes the variability associated with the interplay of acoustic and mechanical parameters. Along the positive axes of the second component, apple cultivars COOP39 (16), Nevson (57), CIVG198 (14) Scifresh (78) and Delcoros (26) were characterized by a high level of firmness and acceptable crispness. In comparison, apple cultivars along the negative axes of PC2 are characterized by a higher acoustic signature and a lower firmness the variability related to both acoustic and mechanical parameters. Along the positive axes of the second component, apple cultivars COOP39 (16), Nevson (57), CIVG198 (14) Scifresh (78) and Delcoros (26) were characterized by a high level of firmness and acceptable crispness. In comparison, apple cultivars along the negative axes of PC2 are characterized by a higher acoustic signature and a lower firmness than the previous ones. It is worth noting that the cultivars considered to have the best fruit quality were included in this latter group (group C in Figure 3.3) such as Minnewashta (55), Ligol (50), Fuji (35), Granny Smith (44), Cripps Pink (18) and Ambrosia (1). The correlation matrix over the entire parameter set (Supplementary Figure 8.5) confirmed the indications of the PCA: the mechanical parameters were in fact significantly correlated, with values ranging between 0.81 and 0.99 ($p<10^{-4}$), apart from the number of force peaks (and consequently the number of peaks/distance), which are less correlated with the rest of the mechanical readings ($p<10^{-4}$) than with the acoustic data ($p<10^{-4}$). In the following we will refer to the mechanical parameters excluding "number of peaks" and "number of peaks/distance". Mechanical parameters exhibited a moderate correlation ($p<10^{-4}$) with the acoustic data, indicating the necessity of complementing textural analysis with acoustic data for a better dissection of general trait complexity. Indeed in our PCA plot we observed that some cultivars, represented by Ananas Renette (2), Tiroler Spitzlederer (83), Breaburn (8) and Nevson (57), despite their high average firmness values of 16.25, 17.62, 12 and 13 N, showed a limited number of acoustic peaks: 35, 31.7, 46.1 and

43.5; while Fuji and Granny Smith have acoustic peaks of 107.23 and 99.87, respectively. This result clearly suggested that the mechanical profile alone is not sufficient for a reliable texture analysis for the selection of a favourable crispy apple.

Similar conclusions were obtained with the fruit digital puncture test, which was more correlated with the mechanical (0.70-0.77; $p<10^{-4}$), than the acoustic parameters (0.50-0.57; $p<10^{-4}$).

3.4.3 Influence of ripening stage on apple textural properties

It is well known that physiological changes occurring during ripening are not identical for all the cultivars. This variation can be related, for instance, to the different levels of ethylene known to be regulated by the allelotypes of Md-ACS1 and Md-ACO1 [49]. Beside these two genes, others contribute to the regulation of the apple ripening, determining at the end, a wide harvesting season. In addition some old varieties, considered in this study, are also affected by the pre-harvest drop phenomenon, which forces early harvesting. To check whether the observed textural performance (mainly crispness) was related to the different ripening stage of each of the cultivars tested we assessed fruit ripening instrumentally with a portable vis/NIR spectrometer. As expected, the I_{AD} value measured by vis/NIR showed a detectable variability among the cultivars (Supplementary Figure 8.3), however, none of the textural parameters investigated here (both acoustic and mechanical) were statistically correlated with the I_{AD} value (from -0.21 to 0.17; $p>0.05$), suggesting that the observed effects are not related to differences in harvest time and ripening stage.

3.4.4 Sensory data and correlation with instrumental data

In addition and separately we modelled and predicted the relationships between sensory data and the instrumental data for crispness, firmness and juiciness using PLS analysis with standardised variables (both dependent and independent), predicting one single sensory attribute at a time. This correlation was performed using the instrumental and sensorial data collected from 21 cultivars representing the whole range of textural variability. For all sensory attributes the best models (minimum prediction errors) were obtained with only two components. For firmness and crispness a relatively good RMSECV lower than 0.5 was achieved, while for juiciness a 0.8 value indicates a poor performance of the model. This is summarised in Figure 3.4 where we plotted the cross-validated predicted values of the sensory attributes versus the true measured values.

This is a "true" cross validation, in the sense that every prediction is done with a model that was set without considering the predicted sample. PLS analysis also provides an indication about the importance of the variables in the prediction models. Figure 3.5 shows the first two loadings for the models of firmness and crispness. For better reading of the figure, the independent variables

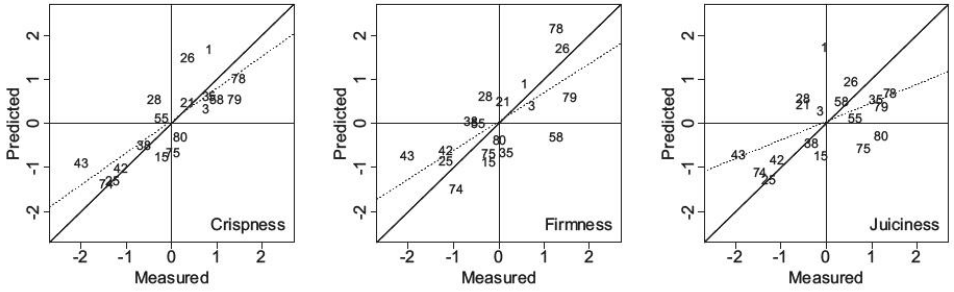

Figure 3.4: Cross validated prediction of standardised sensory attributes on the basis of all available instrumental parameters.

are listed according to a similitude quantification based on linear correlation. We note that the first component (explaining 70% of the total variability in both crispness and firmness) used all parameters besides the force direction for both sensory attributes, even if it seems to be more positively related to the firmness trait in the second loading. The second component (explaining 21% of the variability for crispness and 22% for firmness) gave instead an opposite and interesting indication: the acoustic parameters together with the number of force peaks and force peaks/distance were positively correlated to crispness and negatively to firmness, confirming the importance of acoustic parameters in the prediction of crispness, which is in fact a trait based on acoustic components.

These results confirmed two important aspects. The first, of physiological relevance, is that high crispness requires high firmness, while the opposite is not true, as it was also observed in the distribution of varieties over the PCA plot. This could be the reason since consumers cannot easily distinguish these two attributes when a sample presents excessive firmness. The second aspect is that the parameters involved in the acoustic signature of texture seem to be correlated with crispness, an acoustic driven sensory attribute, suggesting the proposed method as a promising tool for texture comprehension and dissection in apple.

3.5 Conclusion

In this study we developed a novel strategy based on a combined mechanical and acoustic profiling to better categorise textural properties of apple fruit. We applied it to the largest apple collection investigated to date for this purpose (86 cultivars). Furthermore, the instrumental data were compared with sensory evaluation. Multivariate data analysis allowed the identification of a clear separation of the mechanical set of parameters from the acoustic ones. Moreover, a good separation of the different cultivars was achieved. Analysis indicates that the mechanical parameters are able to separate firm from mealy fruit, however

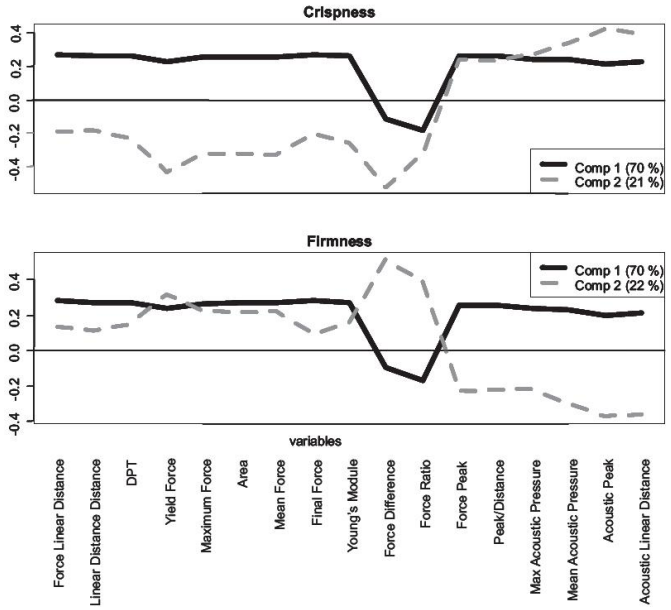

Figure 3.5: PLS analysis: first (black) and second (dashed grey) loading for the models of firmness and crispness sensorially evaluated. DPT: digital puncture test (penetrometer).

the finer separation on the basis of crispness takes advantage of the acoustic characterisation. From this we conclude that this novel strategy performs better than the mechanical ones in the fine characterisation of apple texture. It is noteworthy that the wide range in textural variations is seen as variability in the PCA. This actually describes the breeding success of the cultivars for different crispness: in fact positive and negative PC1 values (Figure 3.3) characterize cultivars based on their general texture performance, while PC2 components separate the cultivars according to their acoustic response between crisp and firm. A sensory analysis with a panel was carried out on a sub-set of 21 selected cultivars and complements the data analysis. It confirms the correct classification with our new acoustic-mechanical method. Vice versa, the results from the sensory panel justify the high priority that texture has in apple breeding programs. We envisage that applying our new strategy on an even wider apple collection will support precise QTL mapping. This would allow identification of the genomic regions involved in apple texture control. The final goal is the identification of markers for assisted selection of new varieties with optimum textural performance, in which our acoustic-mechanical strategy may prove useful.

CHAPTER 4

Comprehensive QTL mapping survey dissects the complex fruit texture physiology in apple (*Malus x domestica* Borkh.).

[1]

4.1 Abstract

Fruit ripening is a complex physiological process in plants whereby cell wall programmed changes occur mainly to promote seed dispersal. Cell wall modification also directly regulates the textural properties, a fundamental aspect of fruit quality. In this study two apple full-sib populations crossing 'Fuji', used as common maternal parent, with 'Delearly' and 'Pink Lady', were employed to comprehend the fruit texture control towards QTL mapping and *in silico* gene mining. Texture was dissected with a novel high resolution phenomics strategy, simultaneously profiling both mechanical and acoustic fruit texture components. In 'Fuji x Delearly' 9 linkage groups were associated with QTLs accounting from 15.6 to 49% of the total variance, and a high significant QTL cluster for both textural components was mapped on chromosome 10 and co-located with *Md-PG1*, a polygalacturonase gene that in apple is known to be involved in cell wall metabolism processes. In addition, other candidate genes related to *Md-NOR* and *Md-RIN* transcription factors, *Md-Pel* and *Md-ACS1* were mapped within statistical intervals. In 'Fuji x Pink Lady' we observed a smaller set of linkage groups associated to QTLs identified for fruit texture (15.9-34.6% variance). The analysis of the phenotypic variance over a two dimensional PCA plot highlighted a transgressive segregation for this progeny, revealing two QTL sets distinctively related to both mechanical and acoustic texture components.

[1] Accepted on Journal of Experimental Botany, doi 10.1093/jxb/err326

The mining of the apple genome allowed the discovery of the gene inventory underlying each QTL, and functional profile assessment unravelled specific gene expression patterns of these candidate genes.

4.2 Introduction

Fruit development and ripening is a programmed physiological process unique to plants that has been intensively studied by the scientific community because of the importance of fruit in the human diet [85]. Amongst all the biochemical and physiological evolution of traits occurring during ripening (colour, sugar, acid content, fibre, vitamins, volatile and antioxidant compounds) change in texture is one of the most evident variation [86].

Texture change is interdependently coordinated by a wide range of cell-wall enzymes acting on both middle lamella and primary cell wall, that together with the alteration of the turgor pressure cause the weakening of the cell wall structure leading to seed dispersal and the final conversion of unripe hard fruit into edible soft and crispy fruit [28], [194], [217]. The primary cell wall is composed mainly by a series of polysaccharides as well as structural proteins and phenolic compounds. The polysaccharides are degraded by several enzymes [29], which normally increase their activity during the maturation phase, such as: polygalacturonase (catalyzing the hydrolytic cleavage of galacturonids linkages); pectin methylesterase (removing methyl groups from the galacturonic acid residues); β-galactosidase (removing terminal non reducing galactosyl residues); Endo $1\rightarrow4$ β-D-glucanase (hydrolyzing internal linkage of glucan chain); xyloglucan endo-transglicosylase (reversebly endo-cleaving xyloglucans) and expansin (disrupting the hydrogen bounding between cellulose microfibrils and polysaccharides matrix).

Fruit texture is nowadays recognized as a combination of different features, all dependent on the anatomical properties of the primary cell wall. Force applied on the apple cortex breaks the chemical bonding of either the middle lamella or the cell wall, resulting in a mealy or crispy apple flesh texture characteristic, respectively.

The ripening physiology machinery has been already unravelled in tomato, the model species for fruit ripening studies [85], [86], [162]. Specific tomato mutants together with informative genomic tools have elucidated the gene cascade involved in the ripening processes [161], [5]. Cell wall disassembly has been described as a complex physiology due to the synergic action of several enzymes activated in a time specific fashion to degrade the cell wall polysaccharide network. The complexity of this physiology is further illustrated by the recent discovery that in the genomes sequenced to date almost 10% of the entire gene inventory is devoted to cell wall metabolism [154]. Functional surveys to profile cell wall gene dynamics over apple fruit maturation and ripening have been recently published employing different platforms, [206], [45]. The contri-

bution of each gene in the trait control can be quantitatively estimated by QTL mapping approach [43], [163], [9], [107], a forward genetic strategy also used to target novel elements in fruit development and ripening [85]. Specific genomic regions controlling fruit texture in apple have already been reported, targeting major QTLs positioned on linkage groups (LG) 1, 10 and 15, and co-localised with *Md-ACS1*, *Md-ACO1*, *Md-Exp7* and *Md-PG1* candidate genes [49], [48], [98], [50], [247]. Recently other three elements derived from the FRUITFULL and SHATTERPROOF of *Arabidopsis thaliana* orthologous have been mapped on other linkage groups, such as 6, 9 and 14 [36], further suggesting apple texture to be a complex trait. High resolution QTL mapping carried out with high marker density and high quality phenotypic data can represent a valuable tool for functional genomics. QTL targeting and cloning can in fact be employed to investigate the physiology of complex traits [163]. Fruit texture, besides its biological relevance, is also a fundamental aspect in the definition of general fruit quality, together with appearance, flavour and nutritional properties [25]. Fruit texture has in fact the capacity to influence the general consumer appreciation [99]. Excessive softening heavily limits shelf-life and storage, and promotes the development of infection by post harvest pathogens. From an anatomical point of view the propagation of the cell wall disruption, together with the internal turgor pressure, generates an expanding sound pressure wave perceived by the human senses as crispness [124]. This feature related to the integrity and rigidity of the cell wall is also physiologically associated with other important aspects of the fruit quality, such as the juice release and fruit freshness [97]. A major goal in modern breeding programs is the selection of a novel cultivar able to overcome rapid flesh decay [152]. To achieve these results a precise QTL mapping performed with a high resolution phenotyping may represent the key strategy to link the perceived quality with the physiological structure of the plant cell wall [232], as well as to target the genomic regions involved in the fruit texture control. In this work we describe a comprehensive QTL mapping for fruit texture in apple, distinguishing both mechanical and acoustic texture components. Based on our knowledge, crispness as acoustic response, has never been instrumentally characterized for QTL mapping purposes, and we are also not aware of any references regarding the identification of the genomic regions or candidate gene discovery involved in the control of the dissected texture subtraits. The anchoring of the QTL genomic intervals to the assembled genome [223] allowed the discovery of a novel gene set that could be exploited in the future to gain novel insight in the comprehension of the cell wall physiology in apple.

4.3 Materials and Methods

4.3.1 Plant material

Two full-sib progenies derived by crossing the high texture quality apple cv. 'Fuji' (common maternal parent) with cv. 'Delearly' (poor texture cultivar) and cv. 'Pink Lady' (high texture cultivar) had 94 seedlings each, were located in the same block at the experimental orchard of FEM (Foundation Edmund Mach, Trento, Italy), and maintained *in situ* following standard technical management. Each individual was grafted on M9 rootstock, and at the time of the first harvest the plants were 10 years old. Total genomic DNA was isolated from young leaf tissue using the Qiagen DNeasy Plant kit. DNA quantity and quality was measured spectrophotometrically with a Nanodrop ND-8000® (Thermo Scientific, USA).

4.3.2 Fruit texture assessment

The optimal harvest time for the two progenies, occurring from August to the beginning of November, was instrumentally determined through the use of a vis/NIR (near infrared spectrometer) DA-meter [47], collecting the samples within a IAD range of 1-1.4. After harvesting, fruit samples were stored at 2°C in a controlled temperature cellar for two months prior to assessment. High resolution phenotyping was carried out measuring the apple texture components in three consecutive years (2008, 2009 and 2010). For the first two years both populations were assessed, while for the last experimental season the phenotyping was carried out only for 'Fuji x Delearly' ('FjxDel'). 'Fuji', as known, is affected by biennial bearing, and because of that the yield of 2010 for 'Fuji x Pink Lady' ('FjxPL') was not sufficient for genetic investigation, thus we did not include this year of analysis in the study. Mechanical and acoustic signatures were detected and measured using a texture analyser TA-XT*plus* coupled with an AED - acoustic envelop device (Stable Micro System Ltd., Godalming, UK). Sample preparation, instrument setting and parameter characterization are fully described by Costa *et al.* [46]. Mechanical and acoustic assessments were performed in isolated room avoiding possible external noise interference. Texture profiles were analyzed with an *ad-hoc* compiled macro (operated with Exponent v.4 software, Stable Microsystems) which allowed the definition of three parameter categories: (i) mechanical: yield force (end of the initial slope), maximum force, final force, mean force, area, force linear distance, Young's module (elasticity) and number of force peaks; (ii) acoustic: acoustic linear distance, number of acoustic peaks, maximum and mean acoustic pressure; (iii) force direction: Δforce and force index (as difference and ratio, respectively, between the yield force and the final force). For each sample 20 measurements were performed, composed by 5 technical (samples obtained from the same fruit) and 4 biological replicates (samples obtained from different fruit). Each sample

represented by a cortex disc was compressed until the deformation of 90% (as described in [46]).

4.3.3 Molecular marker genotyping

To perform genetic mapping and QTL calculation two types of genetic markers were used: SSR and SNPs. The microsatellite markers used to anchor the two maps to the published data in literature [147],[137] were selected based on their chromosome position as showed in the HiDRAS web-site (www.hidras.unimi.it). SSR primers were assembled in new triplex (three primer pairs in multiplex; Supplementary Table 9.1 and labeled with three different fluorochromes 6-FAM, HEX and NED). PCR reactions were performed in a final volume of 20 μl with 5 ng DNA, 10X buffer, 0.25 mM dNTPs, 0.075 μM forward labelled and reverse primers and 0.625 U of Eppendorf® Taq polymerase. Amplification thermal condition started with a denaturation at 94°C for 2 min followed by 10 cycles of denaturation at 94°C for 30 sec, annealing at 58°C for 30 sec, extension at 72°C for 1 min; 15 cycles of denaturation at 94°C for 30 sec, annealing at 57°C for 30 sec, extension at 72°C for 1 min and a final round of 10 cycles of denaturation at 94°C for 30 sec, annealing at 56°C for 30 sec, extension at 72°C for 1 min finishing with a final extension at 72°C for 5 min. The three consecutive rounds of annealing temperatures allowed the amplification of all the triplex employing the same thermal setting, avoiding specific optimization for each set. Single SSR PCR mix contained 5 ng of DNA, 10X buffer, 0.25 mM dNTPs, 0.12 μM of forward labelled and reverse primers and 0.5 U of Eppendorf® Taq polymerase in a final volume of 12.5 μl. Amplification thermal setting started with 94°C for 2 min followed by 32 cycles of denaturation at 94°C for 30 sec, annealing at 58°C for 30 sec, extension at 72°C for 45 sec, and a final extension at 72°C for 5 min.

SSR-anchored to functional candidate genes were also positioned on both populations. Sequences used for SSR screening regarding the polygalacturonase (*Md-PG1*) and the alcohol acyltransferase (*Md-AAT6*) were retrieved from literature [48], [69], respectively). The other elements were derived by a combined homologous/heterologous investigation to analyze the common gene set differentially expressed during the apple and tomato ripening [45]. Sequences for *MADS-RIN* and *NOR* were obtained from the TED database (Tomato Expression Database, http://ted.bti.cornell.edu; [79]). These sequences were used to query the apple genome [223] via blastn algorithm. The SSR based on candidate genes were tested following the strategy of the labelled tail [199], where a M13, SP6 or T7 sequence (tail) was synthesized at the 5' of each forward primer, acting as annealing site for the fluorescent probe. PCR reactions mix for the tailed SSR were carried out in a final volume of 25 μl containing 5 ng of DNA, 10X buffer, 0.2 mM dNTPs, 0.2 μM reverse primers, 0.04 μM forward primers, 0.16 μM labelled primer and 0.75 U of Eppendorf® Taq polymerase.

Amplification condition was 94°C for 90 sec, 30 cycles of denaturation at

94°C for 30 sec, annealing at 58°C for 30 sec, extension at 72°C for 1 min, 10 cycles of denaturation at 94°C for 30 sec, annealing at 53°C for 30 sec, extension at 72°C for 1 min and a final extension at 72°C for 7 min. Fragments analysis was performed with an ABI PRISM® 3730 capillary sequencer (Applyed Biosystem by Life Technologies) in a final mix of 0.3 μl of PCR product, 9.67 μl formammide and 0.03 μl of 500-LIZ denaturated for 3 min at 95°C. Fragment sizing was operated with GeneMapper® software (Applied Biosystems, by Life Technologies). Both maps were saturated using SNP markers (Supplementary Table 9.2) high throughput genotyped with two genomic platforms: Golden Gate assay by Illumina (384 SNP chip), and SNPlex Technology by Applied Biosystem (as described in [176]) testing 9 SNPset of 48 SNPs/each. The SNPs were identified during an early assembly draft (4X sequencing depth) of the 'Golden Delicious' genome sequencing project [223], as described in detail by Micheletti *et al.* [160].

4.3.4 RNA isolation and transcription analysis

Total RNA was isolated from fruit collected at harvest of four cultivars,'Golden Delicious' (used as reference), 'Delearly', 'Fuji' and 'Pink Lady' using the Plant total RNA kit (Sigma) with a modified protocol. Total RNA was initially purified from gDNA with a Deoxyribonuclease I, Amplification Grade (Invitrogen®), then complementary DNA was synthesized by SuperScript® VILO cDNA Synthesis kit. In order to choose the best housekeeping, six different genes were tested: ubiquitin, two actin genes, cortex genes: 8283:1:a, 4592:1:a and Efα1 (primer sequences available in [24], [55], [135]). RT PCR was performed using an Applied Biosystem (AB) 7000 Sequence Detection System machine in a final volume of 12.5 μl containing 1 μl of properly diluted cDNA, 6.25 μl of Platinum SYBR green qPCR Super-Mix UDG, 0.25 μl of Rox Reference Dye and 0.2 μM of forward and reverse primer. Amplification conditions were 50°C for 2 min, 95°C for 2 min and 40 cycles of denaturation at 95°C for 15 sec, annealing and extension at 60°C for 1 min. To choose the best housekeeping genes and for real time data analysis geNorm [221] and LinRegPCR version 12.9.0 software were used. The transcript levels of 11 specific genes including: *Md-PG1*, *Md-PG5*, *Md-NOR*, *Md-RIN*, *Md-Pel*, *Md-ACS1*, *Md-ACO1*, *Md-Exp7*, *Md-XET*, *Md-XXT* and *Md-XEG* was investigated. Besides *Md-PG1*, where primers sequences were obtained from [48], the primer sequences for the other 10 genes were retrieved from the apple genome contigs [223] using Primer3 software (http://primer3.sourceforge.net/). Designed primers were then tested by performing an electronic PCR (http://www.ncbi.nlm.nih.gov/projects/e-pcr/) with the apple in silico predicted transcriptome (Table 9.3).

4.3.5 Ethylene Analysis

Ethylene production was monitored over post harvest ripening for a period of 15 days. Starting from harvest, ethylene was measured at day 1, 6, 10 and 15. For each measurement data point three fruit/cultivars were closed in a sealed glass of 5 L for 1h. From the headspace, 10 ml of air were sampled with a siring and injected in a gas chromatographer (Carlo Erba Instruments GC6000) equipped with a flame ionization detector (FID).

4.3.6 Statistic computation and data analysis

For both progenies separated parental and combined genetic maps were constructed using JoinMap® 4.0 [171]. A LOD of 5 and a recombination frequency of 0.45 were used in order to define linkage groups, and genetic distances between markers were calculated using the Kosambi mapping function. Linkage groups were visualized using MapChart® 2.1 (Voorips, 2002) and numbered from 1 to 17 (according to [147], [202] and www.hidras.unimi.it). QTL analysis carried out to detect genomic regions associated to textural components was performed using MapQTL® 6 [172]. Initially the genomic regions with potential QTL effects were identified employing the Interval Mapping (IM) algorithm. To take over the role of other QTLs and to minimize the residual variance, markers coincident with the highest LOD value were selected as cofactors and further implemented in the MQM computation. Threshold established after running 1000 permutation was set at LOD=3, defined as average of the I type error α=0.05 for all parameters across the 17 linkage groups for both mapping populations. QTL-LOD profiles are shown in a heatmap produced by Harry Plotter software, a stand-alone program written in Java. Harry Plotter has been developed internally at FEM as a new tool to visualize genome and genetic map features. Multivariate statistical Principal Component Analysis (PCA) was computed with STATISTICA software v7. Microsatellite motives were identified in the 'Golden Delicious' genomic assembled contigs through Sputnik, an algorithm for searching repeated nucleotide pattern (http://espressosoftware.com/sputnik/index.html). 'Golden Delicious' information related to gene ID and contigs is available at the FEM data warehouse (http://genomics.research.iasma.it) and GDR (Genomic Database for Rosaceae; http://rosaceae.org). Genes were annotated through the Uniprot database (http://www.uniprot.org) and further compared with the information available at the GDR database

4.4 Results and Discussion

4.4.1 Experimental design

Fruit from the two progenies were assessed after two months of cold storage, in order to study the contribution of the two different genetic backgrounds in the fruit texture control. Moreover, from previous reports it has been emphasized that after two months of cold storage the physiological ripening evolution is maximized [130], enhancing therefore the trait variability, a fundamental requirement for the QTL intervals resolution. For the three years of phenotypic assessments all the parameters investigated showed a Pearson correlation from 0.57 to 0.9, resulting in a consistent quantitative trait distribution.

4.4.2 Texture physiology dissection and combined acoustic and mechanical profiling

Fruit from both progenies were harvested at the same physiological ripening stage, objectively determined by a vis/NIR portable spectrometer (DA-meter). Complex texture phenotype was assessed employing the texture analyzer TA-XT*plus* which produced a different texture profile for the three parental cultivars as well as for the two progenies (Figure 4.1).

'Fuji' and 'Pink Lady' greatly differ from 'Delearly' in terms of general texture performance, as demonstrated by the different mean value for the maximum force: 11.95 N, 13.30 N and 6.14 N; number of force peak: 22.23, 22.05 and 6.11; number of acoustic peaks: 107.23, 71 and 5.83 and mean acoustic pressure: 49.7 dB, 45.7 dB and 39.65 dB, respectively. The overall variability of the texture sub-traits represented by the set of 14 parameters for the two populations is showed in the two dimensional PCA plot (Figure A 4.2).

The first principal component (PC1), describing 55.39% of the entire phenotypic variability, together with the second principal components (PC2), accounting for an additional 20.29%, discriminated the orientation of the mechanical component from the acoustic signature (Figure B 4.2), confirming the results previously obtained from a large apple collection [46]. The PCA plot for the two progenies showed a bimodal distribution, in fact the variability detected in 'Fuji x Delearly' ('FjxDel') was mainly distributed along the PC1, with the extreme values represented by the two parental cultivars. The scenario observed in 'Fuji x Pink Lady' ('FjxPL') was different, where the transgressive distribution observed for this progeny was oriented more towards the PC2, with the seedlings exceeding the values observed for the two parental cultivars.

4.4.3 Genetic mapping

To unravel the highly coordinated cell wall physiology leading to the textural properties of apple during the post harvest ripening toward QTL mapping

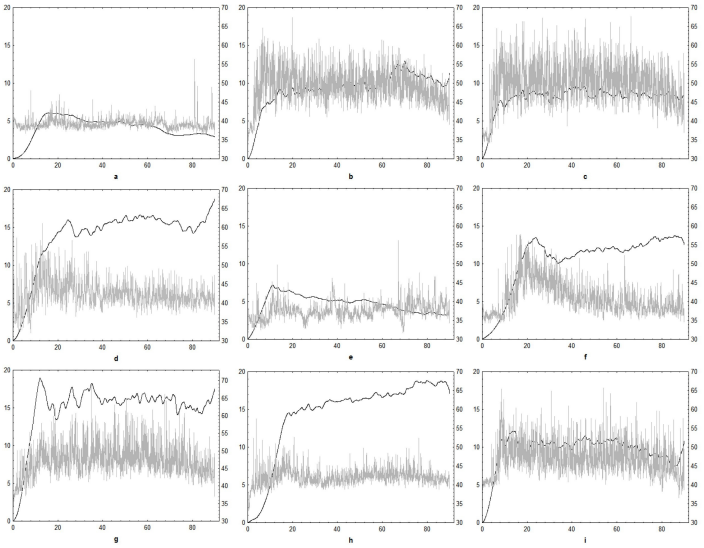

Figure 4.1: Combined acoustic-mechanical texture profiles. The nine panels represent: a- 'Delearly', b- 'Pink Lady', c- 'Fuji'; d, e and f three seedlings of the 'FjxDel' population; g, h and i-three seedlings of the 'FjxPL' population. For each graph the black line represents the mechanical force displacement profile scaled on the Y primary axis (Newton), while the grey line is the acoustic profile scaled on the Y secondary axis (dB). On the X axis is showed the 90% deformation (strain).

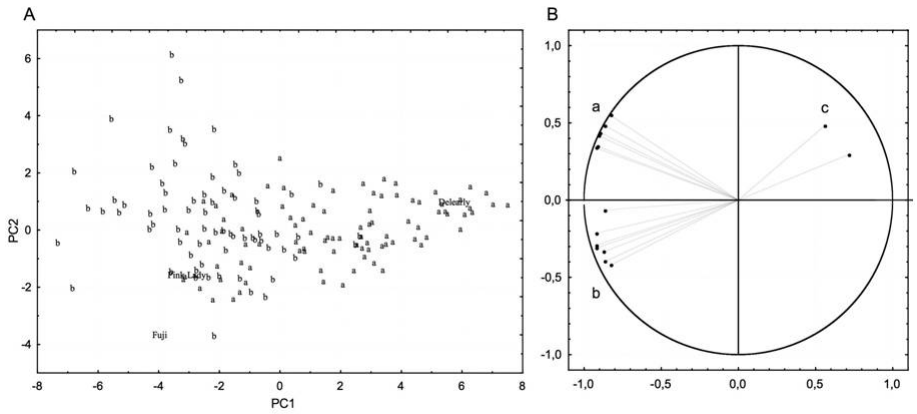

Figure 4.2: Principal component analysis plot showing the general texture variability of the two mapping populations explained by the first two components. In the figure a and b are for 'FjxDel' and 'FjxPL', respectively, while the three parental cultivars are indicated by full name.

approach, two genetic maps were *de-novo* developed and assembled. To construct the map scaffolds 734 markers were totally positioned (671 SNPs and 63 SSRs, Supplementary material Table 9.1, 9.2). The SNP transferability between the reference cv. 'Golden Delicious' and the parental varieties was of 38.97%, 50.38% and 50.95% for 'Fuji' 'Pink Lady' and 'Delarly' respectively, (in agreement with Micheletti *et al.* [160]). We anchored the saturated linkage maps with SNPs (newly identified during the early apple genome assembling) to the reference published maps with a set of 38 SSRs [137], [202] out of which 30 were assembled in novel triplex. Several multiplex have been published so far [175] requiring, however, several optimizations. The advantage of the set presented here is the common amplification protocol, which allowed a more standardized and efficient mapping. In both maps were also positioned new microsatellite markers identified into contigs where specific functional genes were tackled. Genes related to ethylene synthesis/perception, cell wall metabolism and transcription factors were selected from a heterologous microarray experiment designed to highlight a common set of differentially expressed genes during the ripening of both apple and tomato [45], [5]. The genetic maps for both populations were initially computed for single parental meiosis and then the assembled maps were further used for QTL mapping purposes. For the 'FjxDel' population the 494 segregating markers were assembled in 17 linkage groups (Supplementary Figure 9.1) with a final length of 1053.24 cM, and an averaged density of 2.28 cM between markers (range from 1.24 to 3.67 cM). In 'FjxPL' 487 markers were assembled in a map with a length of 1470.8 cM (Supplementary Figure 9.2) and an averaged density of 3.25 (1.61-6.96 cM). To test the synteny between the two genetic maps and the apple genome, we compared the genetic position of the 16 SSR anchored to candidate genes with their physical position on the apple genome (Supplementary Figure 9.3). The SSR-anchored to candidate genes were located in 8 chromosomes (2, 5, 8, 9, 10, 13, 14, 15 and 16), showing a consistent position beside three elements (*Md-ACS1* and two *MYB* TFs). This inconsistency is due to a low sequencing coverage of these genomic regions, leading to an erroneous genome assembling.

4.4.4 QTL detection and candidate gene mapping

Mechanical and acoustic data were used in a QTL analysis which allowed the identification of 22 total QTLs associated to texture sub-traits, 12 mapped in 'FjxDel' (Figure 4.3) and 10 in 'FjxPL' (Figure 4.4), respectively. QTL computed with IM algorithm and further validated by MQM reported a LOD values ranging from 3.11 to 10.86 and accounting for an explained variance from 10 up to 49%.

QTLs were detected based on a LOD threshold of 3, obtained after averaging the value corresponding to α=0.05 for all traits over the 17 LGs (Supplementary Figure 9.5). QTL mapping investigation carried out in the 'FjxDel' progeny enabled the detection of a QTL set related to textural components located in

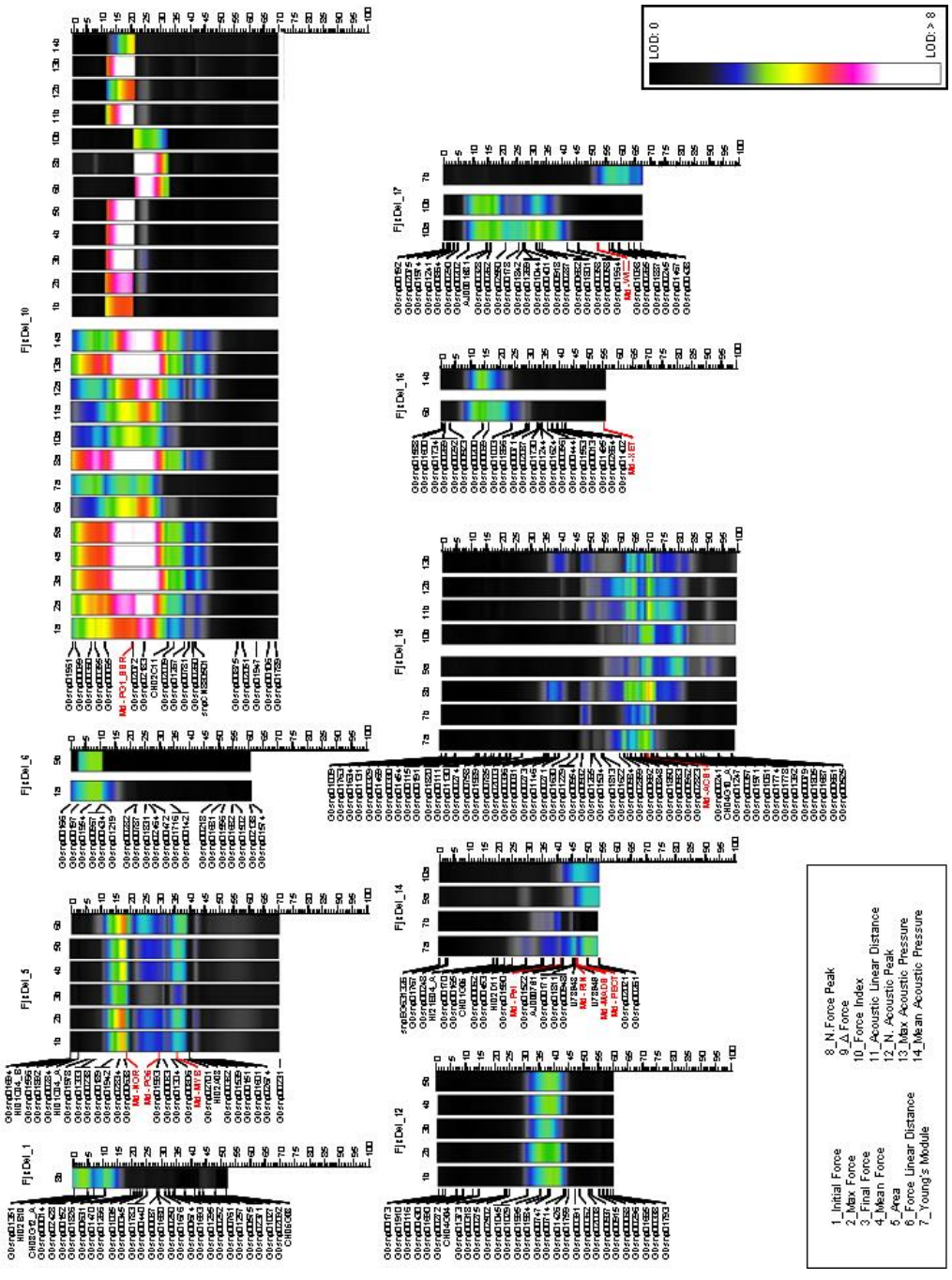

Figure 4.3: QTL-ATLAS for 'Fuji x Delearly' representing the heat-map QTL profiles detected in 9 linkage groups. Numbers above each heat-map bar refers to texture parameters (described in the box on the left side), while a and b are for Interval Mapping and MQM algorithm, respectively. In red text are indicated the markers linked to candidate genes. In the box on the right side is illustrated the Heatmap colours scale, going from black (LOD $= 0$) to white (LOD ≥ 8)

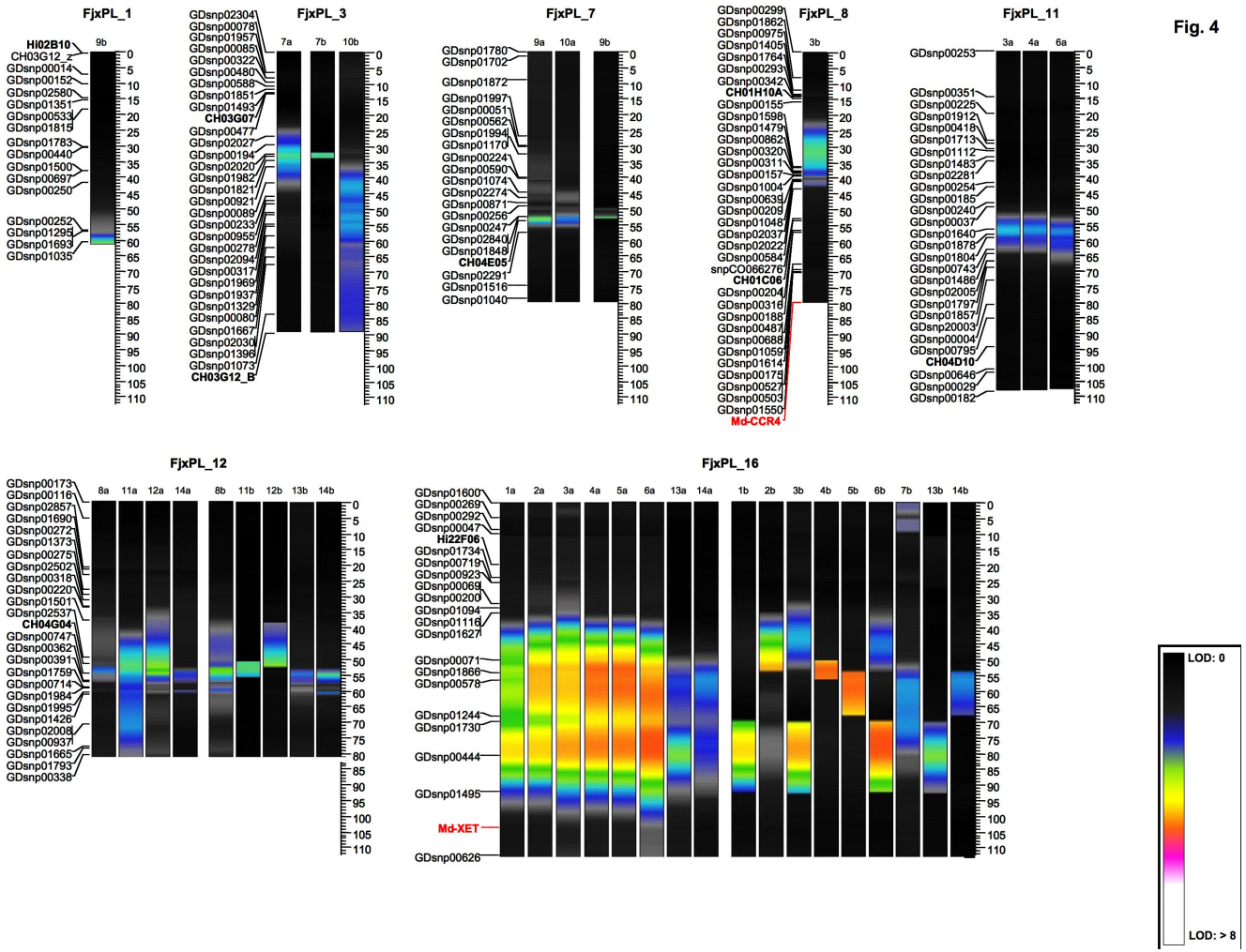

Fig. 4

Figure 4.4: QTL-ATLAS representing the heat-map QTL profile for 'Fuji x Pink Lady'. Letters and numbers are the same as for 'Fuji x Delearly' 4.3. Markers linked to candidate genes are visualized in red colour text.

9 linkage groups (1, 5, 6, 10, 12, 14, 15, 16 and 17, Figure 4.3). From the general QTL-ATLAS has emerged that LG10 represents a hot spot for texture control, being most of the QTLs computed for the three years associated to the texture parameters clustered in this chromosome (beside Δforce), with LOD values spanning from 4.35 to 10.97 and explaining from 20 to 49% of the total phenotypic variance (Table 4.1)

QTLs identified by IM were for the most confirmed also by MQM algorithm, exception made for force linear distance, mean force and Young's module (in 2009). This QTL cluster co-located with *Md-PG1* gene (mapped in this study as *Md-PG1*$_{SSR}$, a new microsatellite targeted approximately at 3 kb up-stream the starting codon (Supplementary Table 9.1); a candidate cell wall gene ethylene dependent [45] [48]. The *Md-PG1*-trait association in this region was consistent with the several works reporting QTLs mapped in this linkage group and associated with fruit firmness [148], [138], [122], [127] as well as vitamin C [58], that in tomato has been proposed to interact with the cell wall loosening process during cell expansion and fruit ripening [84]. The only parameter not associated with LG10 was Δforce, instead mapped on linkage group 6, 14 and 15. QTLs for force index were mapped on linkage groups 14, 15 and 10, but in the latter case it showed the lower statistical value. This observation is consistent with the projection of the parameters shown in the PCA (Figure B 4.2) where these two parameters are differentially oriented, suggesting therefore a different genetic control. On linkage group 14 two candidate genes were mapped in the QTL intervals associated to the two force directional parameters, *Md-RIN* (ortholog of the tomato *MADS-RIN* transcription factor, [229]) and the cell wall enzyme pectate lyase (*Md-Pel*), a gene known to be specifically over expressed during ripening and involved in the fruit softening process, as documented for strawberry [116], [149]. *Md-RIN* was interestingly associated to the Young's module (or elasticity module) for all the three years of assessments in 'FjxDel'. This result may suggest that this transcription factor plays an important physiological role also for apple, influencing the rigidity of the cell wall. From the functional assessment carried out on the three parental cultivars (plus 'Golden Delicious' used as reference) we observed a different transcript accumulation for *Md-Pel*, its transcript accumulation was in fact highly abundant in 'Delearly' with respect to the other cultivars, where low expression levels were detected (Figure 4.5).

This functional pattern was also consistent with the ethylene dynamics observed for this set of cultivars. 'Delearly', in fact, at harvest was already in the climacterium phase (producing 34.05 μlKg^{-1}h^{-1} of ethylene), and showed also the highest ethylene burst at the beginning of the post harvest ripening (8 days after harvest). 'Golden Delicious' is also a cultivar known to produce high amount of ethylene, but its burst was detected at the end of the observation period, thus at harvest (0.18 μlKg^{-1}h^{-1} of ethylene) the expression of *Md-Pel* is still at the minimum level. As additional proof of the tight ethylene dependent expression of *Md-Pel*, in 'Fuji' and 'Pink Lady' the transcript accumulation

Fj x Del

			IM			MQM		
Trait	**LG**	**marker**	**LOD max**	**LOD marker**	**%**	**LOD max**	**LOD marker**	**%**
Initial Force	5	GDsnp02834				5,50	5,48	18,70
	10	GDsnp02183	7,66	7,66	34,30			
	10	Md-PG1-SSR	7,66	6,00	28,00	6,37	6,00	28,00
	12	GDsnp00747				4,13	4,00	14,20
Forze Max	5	GDsnp02834				5,97	5,97	18,80
	10	GDsnp02183	9,25	9,25	39,80			
	10	Md-PG1-SSR	9,25	7,22	32,70	7,22	7,22	32,70
	12	GDsnp01984				4,51	4,51	14,70
Final Force	5	GDsnp02834				5,99	5,97	18,80
	10	GDsnp02183	10,86	10,86	44,90			
	10	Md-PG1-SSR	10,86	8,98	38,90	9,20	8,98	38,90
	12	GDsnp01984				4,51	4,51	14,70
Mean Force	5	GDsnp02834				5,14	5,12	18,80
	10	GDsnp02183	10,01	10,01	42,20			
	10	Md-PG1-SSR	10,01	8,03	35,60			
	12	GDsnp01984				4,09	4,09	12,90
Area	5	GDsnp02834				5,13	5,13	15,90
	10	GDsnp02183	9,91	9,91	41,90			
	10	Md-PG1-SSR	9,91	7,93	35,30	8,31	8,31	35,30
	12	GDsnp01984				3,97	3,97	12,70
Force Linear Distance	5	GDsnp02834				8,76	8,76	38,1
	10	GDsnp02183	8,76	8,76	38,10			
	10	Md-PG1-SSR	8,76	6,85	31,30			
	16	GDsnp00200				4,63	4,63	13,90
Young's module	10	GDsnp00355	4,35	4,35	20,20			
	10	Md-PG1-SSR	4,35	3,61	18,00			
	14	Md-Le-MADS	3,74	3,74	18,50			
	14	Md-PECT				3,11	2,86	10,00
	15	GDsnp002823	4,82	4,82	23,20	3,86	3,86	13,20
	17	GDsnp01098	3,74			3,74	3,74	12,80
n°Force Peak	1	Hi02b10				4,02	3,96	11,90
	10	GDsnp02183	9,05	9,32	39,10	9,32	9,05	39,10
	10	Md-PG1-SSR	9,05	8,87	38,50			
	15	GDsnp02823				5,54	5,54	16,00
	15	ACS 1				5,54	4,94	14,50
Pi-Pf	6	GDsnp00166	4,03	4,04	15,60	4,03	4,03	19,80
	14	Md-Le-MADS	3,29	3,29	16,50			
	15	Md-ACS1	3,80	3,80	18,88			
Pi Pf	10	Md-PG1-SSR	4,98	4,94	23,70	4,98	4,94	23,70
	14	Md-MADS/Md-PECT	3,54	3,55	17,70			
	15	ACS 1				4,17	4,16	15,60
	17	GDsnp00328	4,88	4,88	23,5	4,64	4,53	16,80
Acoustic Linear Distance	1	GDsnp00631	3,71	3,73	18,40			
	10	GDsnp02183	10,45	10,45	43,60			
	10	Md-PG1-SSR	10,45	8,97	38,80	8,97	9,87	38,80
	15	GDsnp02823				5,04	5,04	14,80
n°Acoustic Peak	1	GDsnp01027	3,98	3,98	20,70			
	10	GDsnp02183	7,97	7,97	37,20			
	10	Md-PG1-SSR	7,97	6,41	31,20	6,41	6,41	12,17
	15	GDsnp02823				4,81	4,81	16,80
max acoustic pressure	1	GDsnp01470	3,77	3,77	22,30			
	10	GDsnp02183	10,97	10,97	49,00			
	10	Md-PG1-SSR	10,97	9,79	45,20	9,85	9,79	45,20
	15	GDsnp02823				4,44	4,44	13,10
mean acoustic pressure	1	GDsnp01470	4,12	4,12	22,30			
	10	GDsnp02183	8,30	8,30	39,90			
	10	Md-PG1-SSR	8,30	7,91	38,50	5,31	5,31	21,60
	16	GDsnp00200				4,21	4,21	12,80

Table 4.1: In the Table are reported the traits, the linkage group on which the QTLs have been identified, the marker and the candidate gene closest to the LOD peak, the maximum LOD for the QTL, the LOD corresponding to the marker/candidate gene and the percentage of explained variability calculated with both IM and MQM.

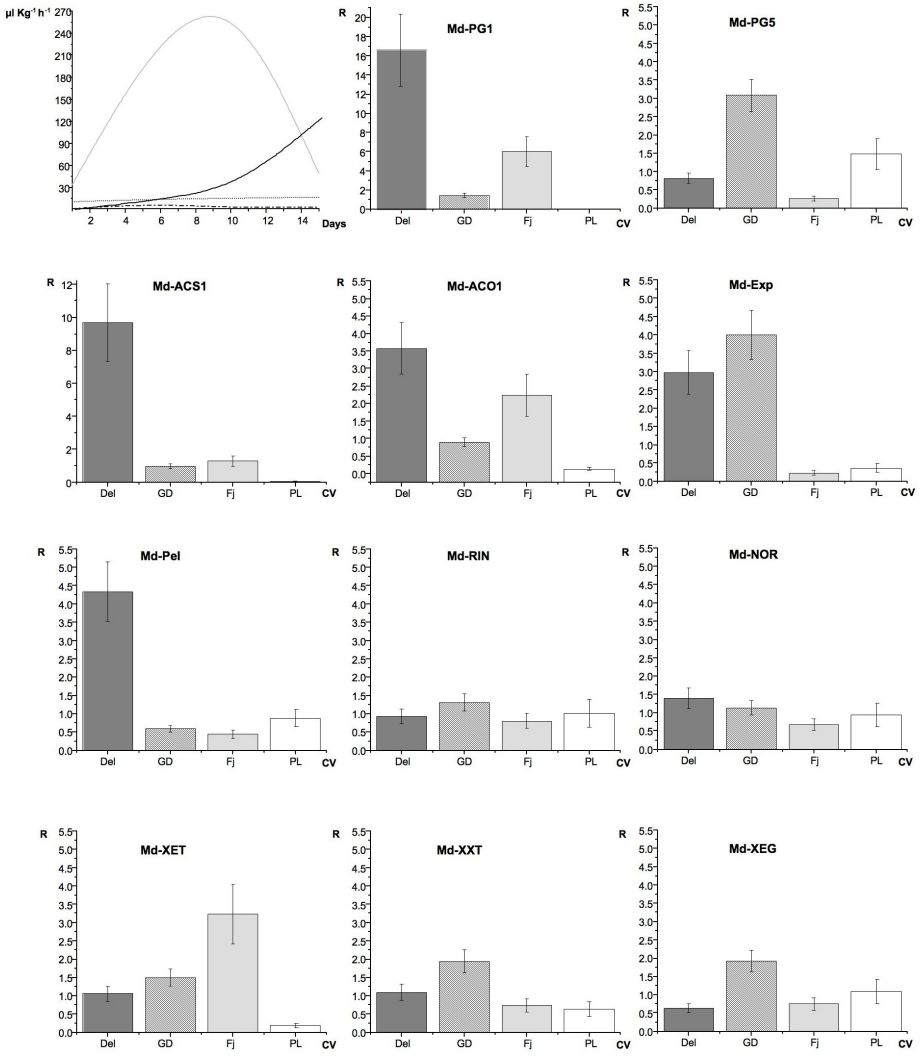

Figure 4.5: Ethylene dynamics and Real Time qPCR for three parental cultivars and 'Golden Delicious' (reference). Ethylene dynamics is expressed in μlKg^{-1}h^{-1} plotted on the Y axes, while on X axes are reported the days of measurements. Grey line is for 'Delearly', black line is for 'Golden Delicious', black dotted line is for 'Fuji' and black dashed line is 'Pink Lady'. Real Time histograms show the expression analysis of 11 genes: *Md-PG*1, *Md- PG5*, *Md-ACS1*, *Md-ACO1*, *Md-Exp*, *Md-Pel*, *Md-RIN*, *Md-NOR*, *Md-XET*, *Md-XXT* and *Md-XEG*. 'Delearly' is visualized in dark grey, 'Golden Delicious' in balck stripes, 'Fuji' in light grey and 'Pink Lady' in white. Bars mean standard error. X axes: cultivars (Del-'Delearly', GD-'Golden Delicious', Fj-'Fuji', PL-'Pink Lady'). Y axes: Relative expression level.

FJxPL			IM			MQM		
Trait	LG	marker	LOD max	LOD marker	%	LOD max	LOD marker	%
Initial Force	16	GDsnp00444	5,29	5,25	31,1	5,29	5,25	31,1
Forze Max	16	GDsnp01866	5,61	5,54	32,5			
	16	GDsnp00071				5,61	5,07	30,2
Final Force	8	GDsnp01598				3,75	3,41	14,5
	11	GDsnp01640	3,49	3,49	21,9			
	16	GDsnp00444	5,68	5,58	32,60	6,68	5,58	32,60
Mean Force	11	GCsnp01640	3,37	3,37	21,2			
	16	GDsnp01866	6,01	5,92	34,3	6,01	5,92	34,30
Area	16	GDsnp01866	6,04	5,95	34,40	5,98	5,95	34,40
Force Linear Distance	11	GDsnp01640	3,31	3,26	20,60			
	16	GDsnp00444	6,26	6,00	34,60	6,26	6,00	34,60
Young's module	3	GDsnp01982	3,78	3,78	23,50	3,78	3,78	23,50
n°Force Peak	12	GDsnp00747	3,30	2,45	15,90	4,67	3,56	18,20
Pi-Pf	1	GDsnp01035				3,96	3,96	18,40
	7	GDsnp00247	4,01	4,01	24,7	4,01	4,01	24,70
Pi Pf	3	GDsnp01937	3,40	3,37	21,30			
	7	GDsnp00247	3,30	3,30	20,90			
Acoustic Linear Distance	12	CH04G04	3,77	3,75	23,40	3,77	3,75	23,30
n°Acoustic Peak	12	CH04G04	4,48	3,95	24,40			
	12	GDsnp02537				3,83	3,83	23,80
max acoustic pressure	12	GDsnp00747				3,27	2,81	13,60
	16	GDsnp00578	3,94	3,10	19,70			
	16	GDsnp00444				3,94	3,94	24,40
mean acoustic pressure	12	GDsnp00747	3,11	2,93	18,7	3,74	3,39	16,9
	16	GDsnp00578	3,32	3,32	20,9	3,32	3,32	20,9

Table 4.2: Table 2 is organized as Table 4.1.

of this gene was at the minimum level, consistent with the low ethylene level detected (1.36 and 10.82 μlKg^{-1}h^{-1}, respectively). The main gene involved in the ethylene pathway, *Md-ACS1*, was mapped on the LG15 as already reported in other works [49]. For this gene, as well as for *Md-ACO1*, the transcript accumulation was consistent with the different ethylene accumulation measured amongst the cultivars. Delearly, which presented the faster ripening physiology and the highest ethylene production at the time of the assessment, showed in fact the highest expression for these two genes. The different magnitude level between these two members highlights, moreover, the role of *Md-ACS1* as a limiting factor in the ethylene pathway.

Traits such as Young's module and acoustic related parameters resulted associated with QTL on the linkage group 15 with a LOD range between 3.8 and 5.5 (13.10-16.8% of explained variance), however, the last passed the threshold only after MQM computation, hypothesizing possible epistatic effects. For force index was also identified another QTL (LOD of 4.88 and 16.8% of variance) located on the linkage group 17, further confirmed by MQM. On this linkage group MQM found also evidence for the presence of a QTL for Young's module trait, in the proximity of a candidate gene mapped and related to a *WIZZ* transcription factor. A specific set of parameters particularly related to the mechanical displacement profile were significantly associated to the linkage group 5, with a LOD value ranging from 5.14 and 8.76 (15.9-38.10% of expressed variance). The QTL cluster associated with these traits (identified only after MQM) resulted closely mapped to *Md-NO*R gene, a NAC trasnscription factor ortholog of *nor* (*non-ripening*), a tomato mutant that fails to ripe normally [86].

Among the cultivars tested *Md-RIN* (mapped on LG14) and *Md-NOR* (mapped on LG5) did not show any differential expression. The similar functional pattern of these two genes suggest that the different ripening physiology observed in the set of varieties depend mainly by gene acting in the final steps of the ripening pathway. For this class of parameters a possible second QTL was located further in the chromosome, but with a lower significant value. This second QTL was also closely mapped with other two candidate genes, a MYB transcription factor and the homoeologous PG gene of *Md-PG1* (here named *Md-PG5* and sharing 86% of sequence identity with *Md-PG1*). The different association observed for these two genes can be explained by the duplicated nature of the apple genome [223], which has led the formation of several chromosome doublets, of which 5-10 (where these two genes are located) is one of the most evident case of chromosome homology. It is worth noting that *Md-PG5* is much less associated with fruit texture than *Md-PG1*, suggesting that during the genome duplication event this gene has lost its functionality, as suggested also by the qPCR assessment. The comparison of the expression related to these two genes showed a clear different pattern. *Md-PG1* is in fact overxpressed in 'Delearly', consistent with the texture performance and ethylene production observed in this study at the harvest time (Figure 4.5). No significant functional variation was instead observed among the cultivars for *Md-PG5*. This hypothesis is also supported by the fact that during polyploidization events a large portion of duplicated genes (up to 50%) can be lost or functionally diverged [230]. In apple a previous work has already reported that almost 82% of young paralogs showed an uncorrelated expression profile, leading to subfunctionalisation and acquisition of novel gene expression pattern [196]. The same set of parameters (except the force linear distance) was also associated with QTLs identified on LG12, with a LOD of 3.97-4.51 and expressed variance between 12.7 and 14.2%. By MQM computation a QTL was mapped on the LG16 related to the mean acoustic pressure with a LOD of 4.63 and 13.9% of variance.

A different scenario was thereafter offered by the second population 'FjxPL' that, with respect to 'FjxDel', showed a transgressive segregation along the PC2 which explained 20% of the total texture variability. According to the different variable orientation showed by the PCA (Figure B 4.2), the phenotypic variability observed in 'FjxPL' determined the identification of a smaller number of chromosomes associated to textural parameters. In fact, in 'FjxPL' the QTLs were detected on a total number of 7 linkage groups (1, 3, 7, 8, 11, 12 and 16; Table 4.2). The main difference observed between the two QTL-ATLAS profiles is that on 'FjxPL' (Figure 4.4) most of the QTLs were mapped on LG16 rather than LG10, where no QTL was detected in this case. On linkage group 16, for both algorithms, were mainly detected QTLs associated to all mechanical plus two acoustic parameters (max and mean acoustic pressure) with a LOD interval between 3.32 and 6.68, and explaining up to 34.6% of the total variance. However the QTLs identified were more significantly associated to mechanical parameters rather than acoustic. All the textural parameters related to the

acoustic signature, together with the number of force peaks (that according to [46] is more correlated to the acoustic phenomena), were associated with a QTL identified on the LG12 (LOD: 3.11-4.48 and 13.6-24.4% of variance). A quite clear separation between the two components in 'FjxPL' was observed in the data obtained in 2009 (LG16 more specific for mechanical and LG12 for acoustic parameters, respectively) and found consistency with the variable projection showed in the PCA plot, where the PC2 separates and distinguishes the mechanical from the acoustic components. This result hypothesize a possible texture dissection also at the molecular level, identifying two putative genomic regions distinctively associated to the two main texture components not observed in the 'FjxDel' population. QTL mapping on linkage group 10 showed up already in previous works focused on texture fruit quality [127], [148], [138], [122]. QTLs mapped on linkage group 12 were identified only in Liebhard *et al.* [138], while LG16 was reported only in Kenis *et al.* [122]. QTLs were simultaneously found for these three linkage groups in [127], [126], where additional texture subtraits were considered. These results are fully consistent with our computations not only for the common set of linkage groups identified as associated to QTLs related to texture, but also for the LOD magnitude. It is worth noting that from the analysis of the estimated mean of the quantitative trait distribution associated with the genotypes of both populations resulted a specific genetic control of the texture phenotype (Supplementary Figure 9.5). In the 'FjxDel' population was clear the role of one allele of 'Delearly' in the control of the texture subtraits distribution (Supplementary Figure 9.5 a and b). For the second population, 'FjxPL', it seems to be present a more distinct and specific effect regarding the two components. For mechanical traits one allele of 'Fuji' was responsible for most of the quantitative distribution, while acoustic parameters appears to be more controlled by a specific combination of two alleles, one from 'Fuji' and one from 'Pink Lady', respectively. From the analysis of the two QTL-ATLAS profiles it is clear that fruit texture is one of the most quantitatively inherited traits in apple, due by a time-specific activation of a high number of genes. This comprehensive texture dissection, at both phenotypic and molecular level, allowed the identification of the major regions controlling texture, that can be further exploited for advanced genetic and functional investigation addressed to unravel the fruit texture machinery and to create new markers valuable for advanced breeding selection. The re-sequencing of the *Md-XET* gene (2276 bp) among the three parental cultivars enabled the identification of a set of 40 SNPs (Supplementary Table 9.6). The segreagation of this polymorphisms within the 'FjxPL' progeny can be involved in the genetic control of the acoustic traits. These SNPs might be novel interesting markers useful for apple breeding, and further validation steps will be required in order to validate their possible real association with texture phenotype.

4.4.5 Gene mining

To date there is a large body of evidence reporting that specific gene function can also be unravelled by QTL mapping approach, emphasized by the colocation of candidate genes involved in biochemical pathways related to the trait of interest into the QTL intervals, as reported by Stevens *et al.* [208]. Keeping this concept into consideration, we exploited the apple genome for a post-genomic *in silico* positional discovery of the gene set underlying the QTL intervals here identified (listed in Table 9.4 and 9.5 for the two populations, respectively). For the two major LGs targeted in the two mapping populations (LG10 for 'FjxDel' and LG16 for 'FjxPL') significant gene categories have been annotated, identifying elements involved in cell wall metabolism (xyloglucan galactosyltransferase, cellulose synthase, xyloglucan endo-glucanase and polygalacturonase), ethylene synthesis and signalling pathway (ACO, ethylene regulated transcript and ERF), as expected due to the tight relationship existing between the level of ethylene produced and the rate of cell wall modification in apple [85],[49],[98],[231],[114]. Beside these two classes, several transcription factors have also been tackled within the QTL intervals (AP2, MADS, MYB and NAC), validating the results proposed [237],[16],[45] that cell wall metabolism is a physiological process controlled by a complex regulatory network. This theory was also supported by the finding of *Md-RIN* and *Md-Pel* in a QTL related to texture traits and mapped on linkage group 14. In tomato it is well known the effect that the rin allele has on the normal ripening. Based on this result we can also hypothesize that this gene conserved a common regulatory action across species belonging to different botanical families, theory supported also by the study of Vrebalov *et al.* [229] and Seymour *et al.* [200] showing the effect of rin in the ripening of strawberry .

It is also interesting to note that comparing the gene inventory annotated among these three linkage groups we identified both common and specific gene families. Genes encoding for pectinesterases were commonly present in all the QTLs targeted in linkage groups 10, 12 and 16. Xyloglucan endotransglycosylase and polygalacturonase were mainly present in LG 10 and 12. Cell wall enzymes such as pectate lyase, pectin acetylesterase and xyloglucan xylosyltransferase were specifically identified on LG 10, 12 and 16 respectively (Supplementary Table 9.4, 9.5). A cluster of α expansin was discovered only in LG12. This class of genes are thought to cause a reversible disruption of the hydrogen bounding between cellulose microfibrils and polysaccharides matrix, which may be one of the initial step of the cell wall loosening process [44]. The functional activation and ethylene relationship of the expansin gene was also confirmed here. A gene of this cluster resulted in fact highly accumulated in 'Delearly' and 'Golden Delicious' (characterized by high ethylene level and strong firmness decay during ripening) than 'Fuji' and 'Pink Lady' (showing low ethylene production and low softening). The early activation of this gene is clearly represented by 'Golden Delicious' which showed the maximum expression at harvest that for this cul-

tivar coincides with the beginning of the climacteric phase, the stage where all the ripening changes occur. All these cell wall modifying proteins, together with the water loss regulation, are thought to act in concert in influencing the fruit softening process [194],[29]. Two major associated phenomena are depolymerization of the pectin network through a hydrolytic cleavage of homogalacturonan (a major component of the middle lamella) by polygalacturonase action, and the endocleavage of the hemicellulosic glycan matrices (of which xyloglucan is the most abundant in dicots) by the action of the hemicellulases [30],[29],[28]. While still poorly understood, it seems that depolymerization of xyloglucan may act as major contributor in the reduction of the cell wall turgidity [187],[195]. This theory find consistency with the results showed in the QTL-ATLAS reported for the two populations (Figure 4.3 and Figure 4.4). In 'FjxDel' progeny the high texture variability resulted in a major QTL cluster located in the linkage group 10, coinciding with the position of *Md-PG1* gene. This gene acting on the middle lamella can be the causal factor determining the difference between the mealy and the high texture apple. However this is not sufficient to discriminate mechanical and acoustic behaviour, *Md-PG1* is in fact indistinctively associated to all the parameters defined and related to the different textural components. Sequencing of the genomic region harbouring *Md-PG1*$_{SNP}$ highlighted that 'Pink Lady' shares the same allelotype of 'Fuji' (T/T), while 'Delearly' showed a heterozygous state (G/T) as 'Mondial Gala', where the "G" was described as the causal allele for the loss of firmness [48]. The homozygousity of the "T" allele for both parents of the second population may be the reason that a QTL was not identified on the linkage group 10 in the 'FjxPL' population. Two relevant QTLs were instead detected in this progeny, one associated to mechanical components (LG16) and one specific for the acoustic signature (LG12), where a xyloglucan transglycosylase was annotated. In this scenario the enzymatic action on the middle lamella could be less evident because of the absence of the *Md-PG1*$_{SNP-G}$ allele, enabling the possible action of *Md-XET* in reducing the rigidity of the cell wall. The hypothesis that solubilisation and depolymerisation of pectic and hemicellulosic polymers caused by these two enzymes may act in concert during the fruit softening process found consistency in the study of Hiwasa and collegues [104] carried out on three different cultivars of pear such as "La-France", showing a climacteric melting ripening with fruit undergoing a dramatic softening, "Nijisseiki", with a non-climacteric behaviour showing a limited change in firmness during ripening, and "Yali", which shows a massive climacteric ethylene production but flesh remains crispy even in late ripening. The distinct physiology observed in these cultivars was associated to a specific gene expression patterns. In "La-France", in fact, the transcript abundance of *Pc-PG1* and *Pc-PG2* was high and the expression of *Pc-XET1* slightly increased during ripening, resulting in a remarkable softening and melting texture. In "Nijisseki" the gradual decrease in fruit firmness and mealy texture was attributed to the low and absent expression of *Pc-PG2* and *Pc-PG1*, respectively, and to a constitutive expression of *Pc-XET1*. In "Yali", the small change in firmness

and the crispy phenotype was explained by the observed lack of a detectable endo-PG activity and the constitutive expression of *Pc-XET1*. The effect of *XET* in regulating texture change in fruit was also supported by the functional assessment that was carried out for xyloglucan endotransglycosilase (*Md-XET*), xyloglucan-6-xyloxyltransferase (*Md-XXT*) and xyloglucan endoglucanase (*Md-XEG*). Amongst these only *Md-XET* showed a distinct expression pattern, with its major transcript accumulation in 'Fuji' (crispy type of apple). The role of this gene may be the causal event of the acoustic segregation observed in the 'FjxPL' population, detectable for the absence of *Md-PG1* expression. The interplay between polygalacturonase and xyloglucan endotransglycosylase may regulate the differential weakening of the binding in the middle lamella and cell wall, respectively, event putatively responsible for the crispy and mealy phenotype [28]. Nowadays crispness is a priority in worldwide breeding programs, thus functional markers based on these two candidate genes may be fundamental for a marker assisted breeding towards the selection of new superior cultivars.

4.4.6 Conclusion

Fruit texture is a feature composed of several sub-traits determined by the activity of different enzymes encoded by multi-gene families and regulated by a transcriptional network. This complex physiology and genetic control is showed in this work by the high number of significant QTLs targeted in the two mapping populations, co-located with several cell wall structural and regulatory genes.

The employment of a high sophisticated texture analyzer (TA-XT*plus*) furnished with an acoustic envelop device (AED) allowed a comprehensive phenotypic dissection of the textural components. Thanks to this advanced phenomics tool we have discovered and mapped the highest number of texture QTLs reported till now, unravelling new genomic regions and genes with possible important effects in the texture control. The choice of the two mapping populations characterized by a divergent but very distinct textural behaviour enabled assessment of a wide textural variability. In 'FjxDel' we have identified several QTLs located on 9 linkage groups, with the major located on chromosome 10 and coincident with *Md-PG1*, explaining from 28 to 45.2% of total variance and indistinctly related to all the textural parameters.

The new SSR-anchored to this gene can be used as a valuable and efficient marker to improve fruit texture in apple. Moreover, in this experimental design the use of 'FjxPL' population was of great value, where its transgressive segregation (essential for breeding) has shed light on other loci, specifically involved in the control of either the mechanical or acoustic component.

The knowledge of the genetic loci controlling texture traits together with the annotation of the genes underlying the QTL intervals, allowed by the availability of the apple genome, can gain insight to better understand the complex physiology regulating the fruit texture dynamic during apple ripening. Future candidate genes association studies will further validate this finding in order to

fine mapping these potential markers valuable for assisted breeding.

CHAPTER 5

Fine mapping and association analysis of a fruit texture QTL in apple (*Malus x domestica* Borkh.)

[1]

5.1 Abstract

Apple is one of the most cultivated fruit crops, due to its quality properties and extended storability. These qualities mainly depend on the degradation process occurring in both fruit cell wall and middle lamella, which are regulated by an enzymatic network generally encoded by large gene families. Among them, the polygalacturonase gene (*Md-PG1*), and a gene encoding for a Endo Xyloglucan Transferase (*Md-Xet*) were mapped on chromosome 10 and 12 respectively, within a QTL cluster associated to several texture dissected sub-phenotypes. In this work, a fine mapping of these genes was carried out in order to validate the association with the texture variability in a collection of apple cultivars, with the final aim to target marker alleles and haplotypes as valuable markers suitable for assisted breeding programs. A new set of SNP markers were used for fine mapping the QTL discovered around the *Md-PG1* and the *Md-Xet* genes, using association analysis approach and novel high resolution phenomic strategy. A total of 495 markers were genotyped, out of which 44 were located in the *Md-PG1* region, and 83 on LG12. After the association analysis, just the markers mapped within the region of *Md-PG1* resulted to be statistically associated to the phenotypic traits under investigation. Among them, 12 markers, showing a MAF>0.05, and four specific haplotypes were statistically associated with several texture components. It is worth noting that haplotyes 3 and 10, associated

[1] Submitted

to favourable texture properties, lack the allele "3" of the microsatellite marker *Md-PG1*$_{SSR}$_10kd, which showed an allelic dosage effect with the general apple fruit texture distribution, as illustrated by the principal component analysis. In this study we emphasize that prior QTL mapping data and basic knowledge on the gene's role can successfully lead to candidate-gene association mapping program, to resolve complex trait variation also in apple. In linkage disequilibrium with the SNPs identified within PG gene, a novel microsatellite marker was also targeted and statistically associated to the texture dissected sub-phenotypes. The allele *Md-PG1*$_{SSR}$_10kd_3, together with the four haplotype, can be thus considered as a novel and reliable marker tool to be promptly used in advanced breeding programs, towards the selection of new apple ideotypes characterized by high fruit texture quality behaviour.

5.2 Background

In a society where food is largely available, consumers' appreciation has become one of the main criteria in food preference, together with food healthiness and nutritional values [190]. General food quality is determined by four principal factors: appearance, flavour, texture and nutritional properties [25]. The present study is focused on apple texture, in particular fruit crispness which accounts for more than 90% of general texture fruit quality [97]. Crispness is physically determined by the tissue fracturing combined with the sound amplitude produced during the crushing propagation [124], and it is described by both kinesthesic and auditory components [190]. The fruit-ripening process involves a large number of enzymes, acting in concert to modify both cell wall and middle lamella. These processes are regulated by a complex network, involving cell wall, ethylene related and transcription factor genes [16], [45] leading to the final fruit softening, a physiological process originally programmed for seed dispersing [85]. These physiological processes can be thought as quantitative traits, which inheritance is normally regulated by the action of several genes, their interaction plus the environmental impact [77].

Fruit texture is nowadays considered a trait controlled by a wide gene set [154], and QTL mapping can be considered a valuable strategy to dissect the genetic basis of complex traits [153],[63],[145],[105]. The QTL mapping approach, generally carried out on bi-parental crosses, has been already extensively used in fruit texture assessment in apple. Several reports have already identified major genomic loci putatively involved in fruit firmness and softening control [148],[127],[126],[122],[49],[50],[48], with the largest texture QTL survey described by Longhi *et al.* [143].

However, QTL mapping carried out using full-sib progenies presents important limitations due to the number of alleles that can be simultaneously analysed which, in the case of apple, are a maximum of four/locus. Linkage analysis, moreover, requires the design of a new segregating population for the traits of

interest, making this procedure laborious and time consuming. In addition, in this type of material the number of recombination events per chromosome is generally low, limiting the genetic mapping resolution [82],[57],[165]. Thus, the number of genes included in the QTL statistical interval can vary from hundreds till thousand [63]. To overcome these limitations, association mapping rapidly became the main strategy for the dissection of complex genetic architecture in plants [73],[72],[87],[111]. Association mapping analysis is in fact realized on large population (or germplasm collection) with unknown relatedness and with recombination events that have occurred over evolutionary history, thus increasing the number of alleles [165]. Association mapping can be performed following two main approaches: whole genome association (GWAS) and candidate gene association mapping (CG). The choice between the two methods largely depends on the extent of linkage disequilibrium (LD). If LD decays rapidly, a high marker density will be required in order to identify the allelic variants associated to the trait, and mapping resolution will be high. Where LD is extensive, a relatively modest number of markers is needed for a whole genome investigation, but with no possibility of resolution at the single gene level [181]. In species with short LD blocks and large genome, association mapping can be feasibly performed at the CG resolution level, but in this case prior knowledge about the genes regulating the biochemical pathway is essential to select the right candidates [103]. In this scenario, CG association mapping can take advantage of prior genetic knowledge, for instance QTL position on a bi-parental mapping population [182],[239]. This type of association analysis have been already employed to target statistic association between allele variants and phenotypic variance in different crops, such as lettuce [203], maize [239] and rice [61]. Recently, this approach has also been used in perennial trees to study drought stress response in pine [87] and Muscat flavour control in grapevine [74]. Association based on a candidate gene has also been recently published for apple [69], where specific SNPs and haplotypes related to the *Md-AAT1* gene (involved in the pathway of ester) were associated with the overall ester content. In this work, association mapping of a candidate gene is conducted to validate and fine map QTLs previously identified on LG10 and LG12 [48],[143]. For this study a high resolution phenomic strategy [46] was employed in order to improve the phenotypic data quality, to date considered the major bottleneck limiting the association statistical power [182]. Application of marker assisted strategy can greatly improve the trait selection efficiency, specially for quality traits in fruit crop species, due to the long unproductive juvenility phase. The aims of this study were 1) fine mapping of the *Md-PG1* and *Md-Xet* regions, 2) test for associations between individual polymorphisms and texture dissected sub-phenotypes and 3) haplotype characterization. Finally we also present the discovery and validation of a new valuable microsatellite marker, suitable for a simple selection of novel individuals defined by a superior fruit texture.

5.3 Materials and Methods

5.3.1 Plant material

A panel of 77 individuals, including both modern and old apple cultivars (Table 5.1), was chosen from two germplasm: the Research and Innovation Centre of the Edmund Mach Foundation, in San Michele all'Adige (Trento), and the Laimburg Research Centre for Agriculture and Forestry (Bolzano). Both institutes are located in the North of Italy (Trentino-Alto Adige region) and have similar climatic conditions. All the cultivars were planted in triplicates on M9 rootstock and maintained following standard technical management. Apple fruit were collected at the commercial harvest stage defined by standard pomological parameters, such as skin and seed colour, brix value (total sugar content), cortex firmness value assessed on site and starch conversion index. Total genomic DNA was isolated from young leaf tissue, using the Qiagen Dnasy Plant kit. DNA quantity and quality was measured spectrophotometrically with the Nanodrop ND-8000 ® (Thermo Scientific, USA).

5.3.2 Texture phenomic assessment

Fruit samples after harvest were stored in a controlled temperature cellar at 2°C for two months, and high resolution phenotyping was carried out in years 2009 and 2010. Apples were maintained overnight at room temperature (20°C) prior the analysis, in order to avoid any effect of low temperature on the fruit cortex physiological properties. Fruit texture was assessed simultaneously profiling both mechanical and acoustic signatures, dissected into specific sub-phenotypes by using a texture analyser TA-XT*plus* (Stable Micro System Ltd., Godalming, UK). Sample preparation, instrument setting and parameter characterization are fully described in [46]. The phenotyping assessment was performed in a specific isolated room, avoiding thus any possible external noise interference. Texture profiles were analysed with an *ad-hoc* compiled macro (Exponent v.4, Stable Microsystems), which allowed to distinguish the parameters in three categories, i_mechanical: yield force (end of the initial slope), maximum force, final force, mean force, area, force linear distance, Young's module (elasticity module) and number of force peaks; ii_acoustic: acoustic linear distance, number of acoustic peak, maximum and mean acoustic pressure; iii_force direction: Δforce and force index (as difference and ratio between yield and final force, respectively). Twenty measurements for each cultivar were performed, represented by 5 technical (discs obtained from the same apple) and 4 biological (discs isolated from different apples belonging to the same cultivar) replicates. Each flesh disc was compressed until the deformation of 90%, during which the two profiles, mechanical and acoustic, were simultaneously acquired and digitally analyzed by the software provided with the instrument. General texture variability, expressed by the 14 defined parameters (see [46] for more details), was illustrated by mul-

n°	cultivar	a	b	c	type	n°	cultivar	a	b	c	type
1	Ambrosia	x			E	40	La Flamboyante (Mairac)	x	x	x	E
2	Ananas Renette	x	x	x	O	41	Ligol	x	x	x	E
3	Ariane (Les Naturiannes)	x	x	x	E	42	Limoncini	x	x		O
4	Ariwa	x	x	x	E	43	Magre	x	x	x	O
5	Baumans Renette		x	x	O	44	Maigold	x	x	x	E
6	Bellida	x	x	x	E	45	Milwa (Junami)	x	x	x	E
7	Berner Rosen		x	x	O	46	Minnewashta (Zestar)	x	x	x	E
8	Boujade	x	x	x	E	47	Napoleone	x	x	x	O
9	Breaburn	x	x	x	E	48	Nevson (Sonya)	x	x	x	E
10	Brina	x	x	x	E	49	Nicogreen (Greenstar)	x	x	x	E
11	Brookfield	x	x	x	E	50	Nicoter (Kanzi)	x	x	x	E
12	Calamari	x			O	51	Permain Dorato	x	x	x	O
13	Calvilla	x	x	x	O	52	Pilot	x	x	x	E
14	Caudle	x	x	x	E	53	Pinova	x			E
15	CIVG198 (Modi)	x	x	x	E	54	Red chief	x	x	x	E
16	Civni (Rubens)	x			E	55	Red Elstar	x	x	x	E
17	Coop 39 (Crimson Crisp)	x	x	x	E	56	Red Field	x	x	x	E
18	Crimson Snow	x	x	x	E	57	Rome Beauty	x			E
19	Cripps Pink (Pink Lady)	x	x	x	E	58	Rosmarina Bianca	x	x	x	O
20	Cripps Red	x	x	x	E	59	Royal Gala	x	x	x	E
21	Croncels	x	x	x	O	60	Rubinola	x	x	x	O
22	Dalinette (Choupette)	x	x	x	E	61	Sansa	x			E
23	Dalla Rosa	x	x	x	O	62	Santana	x	x	x	E
24	Delblush (Tentation)	x	x	x	E	63	Saturn	x	x	x	E
25	Delcorf (Delbarestivale)	x	x	x	E	64	Scarlet	x	x	x	E
26	Delearly	x	x	x	E	65	Schifresh (Jazz)	x	x	x	E
27	Delfloki	x			E	66	Schinano Gold	x	x	x	E
28	Delorina (Harmonie)	x			E	67	Schniga	x	x	x	E
29	Early Gold	x	x	x	E	68	Scilate (Envy)	x	x	x	E
30	Florina	x	x	x	E	69	Summerfree	x	x	x	E
31	Fuji	x	x	x	E	70	Tiroler Spitzlederer	x			O
32	Galmac	x	x	x	E	71	Topaz	x			E
33	Gelber Edelapfel	x	x	x	O	72	Weisser Wintertaffen	x	x	x	O
34	Gewurtzluiken	x			O	73	Tavola bianca		x	x	O
35	Gloster	x	x	x	E	74	San Lugano		x	x	O
36	Golden Delicious	x	x	x	E	75	Renetta Champagne		x	x	O
37	Golden Orange	x	x	x	E	76	Coop 38		x	x	E
38	Granny Smith	x	x	x	E	77	Gold chief		x	x	E
39	Red Delicious (Hapke Delicious)	x			E						

Table 5.1: Cultivar collection. Varieties listed by name and trade mark, between brackets when available. The phenotyping assessments are indicated with the letters: “a” and “b” for postharvest of 2009 and 2010, respectively, and “c” for harvest of 2010 . With “type” is indicated if the variety is considered as old (O) or elite (E, new) cultivar.

tivariate techniques, such as principal component analysis (Statistica software v7). PCA was employed to plot the data in a reduced hyperspace defined by the first two principal components.

5.3.3 Population structure

The genetic population structure of the apple collection was initially investigated with a set of 17 SSR markers (one per each chromosome, Supplementary Table 10.1). Each marker was selected according to the map position, amplification efficiency, allele size and multilocus properties as shown in the HiDRAS website (www.hidras.unimi.it). Population structure was inferred using the admixture model of the software package STRUCTURE 2.3.3 [178], assuming correlation of allele frequencies among subgroups and independent segregation of alleles [78]. Q matrix was estimated with a burn-in length of 100,000 and a run of 100,000 steps. Three independent runs with K ranging from 2 to 8 were performed, and the smallest K, after having reached a plateau of the "LnP(D)" value, was chosen to capture the major structure in the data set, following the criterion suggested by Pritchard and Donnelly [178]. Because old apple cultivars are affected by pre-harvest drop and biannual bearing, not all the cultivars included in the apple collection produced enough fruit to be evaluated for the two consecutive years. As a consequence, 70, 65 and 64 cultivars were included in the association study for 2009 and 2010 at post harvest and 2010 at harvest, respectively, calculating the population structure independently for the two years of analysis. Coloured images representing the population structures were obtained with Excel software, while genetic distance among the cultivars was estimated using NTSYS v2.0, employing the SIMQUAL module with simple match (SM) coefficient. The similarity matrix was used for cluster analysis, visualized as a dendrogram designed by the unweighted pair clustering group methods (UPGMA), and implemented in the Sequential and Hierarchical Numeric algorithm (SHAN).

5.3.4 Md-PG1 gene cloning

In this study a region of 6 Kb harbouring the *Md-PG1* region was investigated. In particular, 2,395 bp (gene full length) and two regions of 800 bp each located approximately at 1 kb up and downstream from the START and STOP codon respectively, were cloned and sequenced among a reference set of 8 cultivars (Golden Delicious, Delearly, Granny Smith, Braeburn, Cripps Pink, Scarlet, Royal Gala and Fuji). The cloning was performed in order to design specific primers able to distinguish *Md-PG1* from its homoeologous *Md-PG5*. The characterization between these two members allowed the design of the specific primers further used in the GBS (genotyping by sequencing) phase. For cloning the following primers were used: PG_full, PG_1ku and PG_1kd (Supplementary Table 10.2). Fragment amplification for the subsequent *Md-PG1* cloning was

performed for the 1 kb up and downstream regions in a final volume of 25 μl with 10 ng DNA, 10X buffer, 0.25 mM dNTPs, 0.1 μM reverse and forward primers and 0.625 U of Eppendorf ® Taq polymerase. Amplification thermal condition started with a denaturation at 94°C for 2 min, followed by 32 cycles of denaturation at 94°C for 30 sec, annealing at 56°C for 30 sec, extension at 72°C for 1 min and a final extension at 72°C for 7 min. The *Md-PG1* gene was amplified in a final volume of 50 μl, with 10 ng DNA, 10X Advantage 2 PCR Buffer, 0.2 mM dNTPs, 0.4 μM reverse and forward primers and 50X Clonthech® Advantage 2 Polymerase Mix. Amplification started with a denaturation at 95°C for 1 min followed by 30 cycles of denaturation at 94°C for 30 sec, annealing and extension at 68°C for 3 min and 30 sec, and a final extension at 68°C for 3 min. Ten amplicons/PCR fragment were cloned using TOPO® XL PCR Cloning Kit (Invitrogen®), following manufacturer's instructions. Plasmid DNA was then extracted using QIAprep Spin Miniprep Kit (Qiagen®). SNPs found in the *Md-PG1* region were genotyped by sequencing the apple collection. The two SNP identified in the 1kb upstream were instead genotyped using the artificial mismatch strategy (as described by Costa *et al.* [48]) in a final volume of 20 μl, with 10 ng DNA, 5X GoTaq® Buffer, 0.3 mM dNTPs, 0.4 μM reverse and forward primers and 2.5U GoTaq® DNA polymerase. Amplification condition started with a denaturation at 94°C for 2 min, followed by 35 cycles of denaturation at 94°C for 30 sec, annealing at 56°C for 30 sec, extension at 72°C for 45 sec, and a final extension at 72°C for 5 min. PCR fragments were scored on a 5% polyacrylamide gel.

5.3.5 Genotyping scheme

To find association with texture sub-phenotypes, markers distributed over the chromosome 10 and 12 were genotyped at two scale levels, here named "macro" and "micro allelotyping".

For *Md-PG1* the genotyping carried out at the macro scale was performed using SSR markers already available in literature (www.hidras.unimi.it) and distributed in a region spanning from 5 to 25 cM up and downstream with respect to *Md-PG1* gene. For LG12 we *de-novo* developed one SSR for every conting indentified within the QTL interval, determined in a previous QTL analysis [143] on the chromosome under investigation (Supplementary Table 10.2). The strategy to investigate the entire QTL interval was chonsen because of the poor information about QTLs on LG12 and Xet role in apple fruit ripening. The PG micro-allelotyping was performed in order to have a more dense marker coverage in the candidate gene region (10 kb up-down stream), by using SSR and SNP markers *de-novo* developed by the availability of the apple genome [223]. Microsatellite markers were identified within the contig sequences with Sputnik, a software for searching microsatellite motives (http://espressosoftware.com/sputnik/index.html). In the analysis $Md-PG1_{SSR}$, a microsatellite marker previously identified at 3 kb upstream from

the *Md-PG1* start codon [143], was also included. *Md-Xet* full length SNPs were identified by sequencing 2,286 bp of the gene; while PG SNPs were identified by sequencing 2,396 bp of the gene, plus 800 bp at about 1 kb up and downstream the START and STOP codon, respectively. The sequencing was performed using an ABI PRISM 3730xl DNA sequencer (Applyed Biosystems, by Life Technologies). Resulting data were analysed using Pregap4 software version 1.3 (Staden Package optional). PCR reaction for SSR marker genotyping was performed in a final volume of 20 μl with 5 ng DNA, 10X buffer, 0.25 mM dNTPs, 0.075 μM reverse and forward labelled primers and 0.625 U of Eppendorf® Taq polymerase. Amplification started with a denaturation at 94°C for 2 min, followed by 32 cycles of denaturation at 94°C for 30 sec, annealing at 58°C for 30 sec, extension at 72°C for 45 sec and a final extension at 72°C for 5 min. Fragment size was called by GeneMapper® software (Applied Biosystems, by Life Technologies). Candidate gene full length PCR amplification was performed following the protocol as reported for gene cloning. An amount from one to two ng of amplified DNA/100 bp of sequence length was used in the sequencing process in both forward and reverse direction. PCR products were purified with 1.5 μl of ExoSapIT (Amersham Pharmacia Biotech, Uppsala, Sweden) in a final volume of 6.5 μl. Further sequencing was performed with the BigDye® Terminator v3.1 Cycle Sequencing Kit (Applied Biosystems) using 3.2 μM of specific forward or reverse primer (PG_1, PG_2, PG_3, PG_4, Xet_1, Xet_2 and Xet_3 for primer pairs; Supplementary Table 10.2) according to the manufacturer's instructions. Sequences were assembled and analysed with Pregap4. A second SNP genotyping survey was also performed with a 384 SNP chip (Golden Gate assay by Illumina), exploited for a wide genome coverage and to enrich the SNP collection in the micro and macro haplotyping regions (SNP details are available at http://genomics.research.iasma.it).

5.3.6 Linkage Disequilibrium and Association analysis

The linkage disequilibrium level among the markers identified within the *Md-PG1* region was calculated and illustrated by Haploview 4.2, a software package designed for linkage disequilibrium statistics and haplotype block inference from genotype data [13]). Association mapping analysis was initially carried out with the software package PLINK release 1.07 ([179] http://pngu.mgh.harvard.edu/~purcell/PLINK/). The General Linear Model (GLM) was used to test for association between dissected texture sub-phenotypes and both single SNP and haplotypes. Genome-wide empirical *P*-values were computed performing 1,000 permutations. The Q-matrix for population structure (computed with STRUCTURE), describing the percent of each cultivar into the subpopulation parentage, was used as a covariate in the model. To increase the statistical power of this analysis, phenotype data of both years were combined into a single data file for the 77 apple cultivars, computing the LS (least square) means for each trait. To account for population structure and genetic relatedness, PCA values

(computed with Statistica software v7), used as covariates, and kinship matrix, used as random factor, were included in the Mixed Linear Model (MLM) implemented in TASSEL [26]. For both PCA (structure) and K (kinship) matrix 368 SNPs were used. PCA was preferred to STRUCTURE because it is faster and less computationally intensive [165]. To select the appropriate number of principal components, six runs were performed (from 5 to 30, with a step of 5). Twenty significant PCs were finally selected, explaining 52% of the total variance, with a contribution ranging from 4.2 (1^{st} PC) to 1.76% (20^{th} PC), mean of 2.47% and st.dev. of 0.66. This PC set was set as the minimal number of components representing most of the expressed variance without affecting the final association results. For haplotype association only significant SNP markers showing a MAF (minor allele frequency) higher than 0.05 were used. The different haplotypes present in the population structure were determined by FastPHASE algorithm [198].

5.4 Results and Discussion

5.4.1 Texture physiology dissection and combined acoustic and mechanical profiling

The apple collection fruit texture variability, represented by the set of 14 parameters, was illustrated over two years of phenotyping assessments by the two dimensional PCA plot (Figure 5.1). The first principal component (PC1), describing at post harvest 74.14% and 70.95% of the entire phenotypic variability for years 2009 and 2010, respectively, together with the second principal component (PC2), accounting for an additional 12.44% (in 2009) and 12.95% (in 2010) (Supplementary Figure 10.1), discriminated the orientation of the mechanical from the acoustic signature, suggesting a possible different genetic control between these two components . The projection of the variables (parameters) clearly shows, for the data at post harvest, the distinct characterization between mechanical and acoustic components, confirming the results presented by *Costa et al.* [46] about the proof of concept of the strategy. The general Pearson correlation reported by the authors, in fact, showed as variables were much more correlated within each group rather than between the two categories. The data consistency between the two years confirms this novel phenomic strategy as a robust and reliable method to dissect texture complexity. In both years, the data distribution clearly and consistently distinguished mealy cultivars (such as Delearly, Golden Delicious, Gelber Edelapfel, plotted on the positive PC1 values) from known firm and crispy varieties (such as COOP39, Granny Smith, Fuji and Cripps Pink) plotted on the negative PC1 values area of the plot (Figure 5.1). Different was the situation for the data collected at harvest during 2010. In this case the first and the second principal component described the 44.6% and the 32.59% of the variability respectively (Supplementary Figure 10.1), and the clear separation among the three variables' projection was not present. More-

over cultivars having different textural characteristics were grouped near in the graph, suggesting this period as not usefull for the traits discrimination and variability dissection (Figure 5.1 panel E and F).

5.4.2 Population structure analysis

When phenotypic traits are correlated with population structure, loci that are not related to the trait under investigation may nonetheless be statistically associated [111]. In order to avoid this false positive effect, population structure was included in the model. With our sample data, the best population subdivision was obtained with K=6 in 2009 (70 cultivars, Supplementary Figure 10.2) and K=4 for 2010 (65 and 64 cultivars, Supplementary Figure 10.3). For each of the two years, the means of the population assignments obtained by the different independent runs were used as covariates (Q matrix) in the association analyses. The difference in the two K values here reported can be explained by the fact that to increase the statistical computation power only genotypes with available phenotypes were considered, in order to avoid missing data. Between the two years, 24.7% of the individuals (19 cultivars) were assessed for only one season. These accession are for the most represented by old and local varieties (accounting for the 30% of the entire apple collection), which are normally affected by biannual bearing and pre-harvest drop. These old varieties are also more genetically unrelated with the rest of the collection, represented by elite cultivars. A variation in this subgroup of the dataset can thus contribute to important modifications in the population structure.

5.4.3 Md-PG1 cloning and Md-Xet and Md-PG1 sequence diversity

The apple genome underwent a recent duplication [223]. *Md-PG1*, the candidate gene that has been investigated in this work and mapped on chromosome 10, shows a similarity of 86% with its homoeologous gene *Md-PG5* mapped on chromosome 5 [143]. To enable the characterization of the specific sequence for *Md-PG1*, the sequences of the two genes were initially retrieved from the Golden Delicious genome and aligned, defining the specific site for *Md-PG1*. The gene sequencing (2,395 bp), carried out within the entire apple collection, identified 22 SNPs with an average frequency of 1 SNP/108.9 bases. Among them, 10 were located in exons (total length of 1,380 bp) with a frequency of 1 SNP/138 bp, and 12 SNPs in introns (total length of 1,015 bp) with a frequency of 1 SNP/84.5 bp (Figure 5.2). These frequencies are consistent with the previous observation made for apple of about 1 SNP/149 bp [37] as well as in other outcrossing plant species, such as pine with 1 SNP/102 bp [56], but lower than white clover 1/59 bp [42] and grapevine 1/64 bp [139]. SNP found in non-conding regions were two fold more frequent than coding, as reported also by Kulheim *et al.* [131], Kolkman *et al.* [129], and Simko [203].

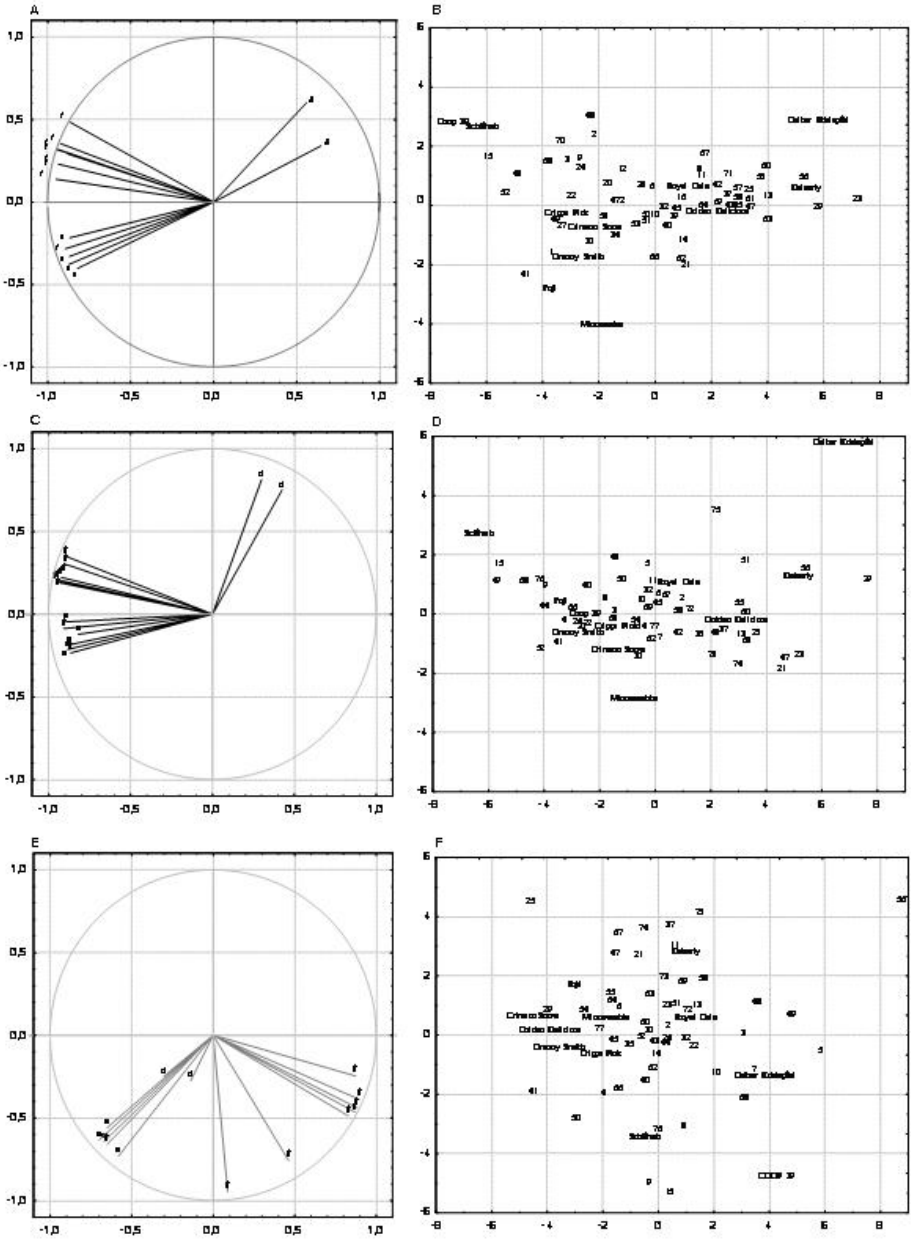

Figure 5.1: PCA plot (first two dimensions) distribution of the varieties assessed with the novel texture phenomics strategy for the two years, 2009 (B) and 2010 (D for post harvest and F for harvest), respectively. On the variables' projection (panel A for post harvest 2009 and , C and E for post harvest and harvest 2010 respectively) "a" and "f" means acoustic and force parameters, while "d" is for force direction. Numbers: variety code as reported in Table 5.1.

Non-coding (targeted in introns and UTR), synonymous and non-synonymous SNPs are important for mapping/association purpose, but the latter are arguably more suitable to define correlations between genotypes and phenotypes in a CG approach, since amino acid changes more likely have a direct impact on the plant phenotype expression [125]. Within the *Md-PG1* predicted gene (which intron/exon structure is consistent with Bird *et al.* [20], Atkinson and Gardiner [11] and Atkinson [10]) 25 SNP were finally genotyped, and their location and functional annotation is present in Table 5.2 and Supplementary Figure 10.4.

SNP	location	type	aa change	bp after ATG
1	exon 1	ns	F/V	196
2	intron	nc	-	355
3	intron	nc	-	387
4	intron	nc	-	466
5	intron	nc	-	469
6	exon 2	ns	R/Q	703
7	intron	nc		824
8	exon 3	ns	F/I	944
9	exon 4	s	T/T	1146
10	exon 5	ns	R/C	1358
11	exon 5	ns	S/Stop	1143
12	intron	nc	-	1478
13	intron	nc	-	1507
14	intron	nc	-	1508
15	intron	nc	-	1776
16	intron	nc	-	1780
17	exon 7	s	I/I	1877
18	exon 7	ns	V/A	1999
19	intron	nc	-	2133
20	intron	nc	-	2180
21	exon 8	s	V/V	2208
22	exon8	s	G/G	2259
23	UTR	nc	-	2527
24	UTR	nc	-	2531
25	UTR	nc	-	2543

Table 5.2: SNP organization within the *Md-PG1* gene. For each SNP used in the association analysis are reported the location respect the gene structure (location), type of aminoacid substitution (type; nc: non-coding, ns: non-synonymous, s: synonymous), change of aminoacid and physical position in bp after the start codon (ATG).

Md-Xet gene sequencing (2,286 bp), carried out within the entire apple

SNP	location	type	aa change	bp after ATG	SNP	location	type	aa change	bp after ATG
1	exon 1	s	Y/Y	72	32	intron	nc	-	986
2	exon 1	s	P/P	138	33	intron	nc	-	1000
3	exon 1	ns	R/S	184	34	intron	nc	-	1001
4	intron	nc	-	201	35	intron	nc	-	1006
5	exon 2	s	F/F	311	36	intron	nc	-	1011
6	intron	nc	-	418	37	intron	nc	-	1084
7	intron	nc	-	461	38	intron	nc	-	1099
8	intron	nc	-	474	39	intron	nc	-	1101
9	intron	nc	-	481	40	intron	nc	-	1107
10	intron	nc	-	486	41	intron	nc	-	1119
11	intron	nc	-	487	42	intron	nc	-	1146
12	intron	nc	-	488	43	intron	nc	-	1170
13	intron	nc	-	489	44	intron	nc	-	1234
14	intron	nc	-	490	45	intron	nc	-	1246
15	intron	nc	-	491	46	intron	nc	-	1274
16	intron	nc	-	492	47	intron	nc	-	1301
17	intron	nc	-	493	48	intron	nc	-	1326
18	intron	nc	-	494	49	intron	nc	-	1335
19	intron	nc	-	495	50	intron	nc	-	1376
20	intron	nc	-	545	51	intron	nc	-	1401
21	intron	nc	-	569	52	intron	nc	-	1478
22	intron	nc	-	586	53	intron	nc	-	1492
23	intron	nc	-	591	54	intron	nc	-	1546
24	intron	nc	-	601	55	intron	nc	-	1559
25	intron	nc	-	612	56	intron	nc	-	1774
26	intron	nc	-	631	57	intron	nc	-	1779
27	intron	nc	-	651	58	intron	nc	-	1809
28	exon 3	s	V/V	762	59	intron	nc	-	1844
29	exon 3	s	Y/Y	798	60	intron	nc	-	1902
30	exon 3	s	R/R	858					
31	intron	nc	-	962					

Table 5.3: SNP organization within the Md-Xet gene. For each SNP used in the association analysis are reported the location respect the gene structure (location), type of aminoacid substitution (type; nc: non-coding, ns: non-synonymous, s: synonymous), change of aminoacid and physical position in bp after the start codon (ATG).

collection, identified 50 SNPs and a small insertion of 10 bp with an average frequency of 1 SNP/45.7 bases. Among them, 6 SNPs were tagged in exons (with a total length of 879 bp) with a frequency of 1 SNP/146.5 bp, and 44 SNPs plus the insertion in the introns (with a total length of 1,407 bp) showing a frequency of 1 SNP/32 bp (Figure 5.3). Within the *Md-Xet* predicted gene 60 SNP were finally genotyped, and their location and functional annotation is present in Table 5.3 and Supplementary Figure 10.5

5.4.4 Macro and micro allelotyping

While a genome-wide LD study has not been yet reported for apple, LD usually decays rapidly in outcrossing species [95], therefore a genotyping at two scale

>MDP0000326734_Md-PG1

ATGGCTTTAAAAACACAGTTGTTGTGGTCATTTGTTGTTGTTTTTGTTGTTTCCTTCAGTACAACTTCATGTTCTGGTAG
TAGTTTCCAGGAGGTCAACGCGCTTCATAGTTACGTTGACCATGTTGATGATAAAGAGTCCGGCTATAATTCTAGGGCTT
ATCCTTCATACACGGACACCATAGAARGTTTAAAGKTCATGGAATTGATCAGGCCAAGAACTCAGCTCTTCAGTTCAAGG
AAGCTCAACACAATCACCGGTGGGATAGCAACATCATCAGCTCCGGCCAAAACCATTAGCGTCGACGATTTTGGAGCTAA
AGGGAATGGTGCTGATGACACACAGGTAAACAACMGATGATGGACTCATAGGCTTAATAATATTAGWATATTAGAATATT
CATATGGTGATGCTAACTATAACAACATTTCTGGTCACATTTCTGTTTTATGAAAGATGTGTCCAYAAYGTTTGGTACAA
ATTAATAGTACTATTATTATTTGGACCGAACTCATTATTATTTATTGAGTAAATGTGATACAAATAACATTACTTAAGCG
TTTAATTTGGTTGAACCAAAAGTTTAAAGTTTATGTATGAATATAATATTGTTTAATTTTTTGTATGTGTTGGTTTAGGC
ATTTGTGAAGGCATGGAAGGCAGCTTGTTCTTCCAGTGGAGCTATGGTTCTTGTGGTACCACRGAAGAACTATCTTGTTA
GGCCGATTGAATTCTCAGGCCCATGCAAATCTCAACTTACACTGCAGGTAATAATTAATTCGGATCATCTATGTAATTAT
CTTTAAATGTAATTCCGGACTATWAACTTTGACGATTATATAATAATTAATATTGCTTAATATTTGGAAAAATTCAGATT
TATGGAACCATAGAAGCATCAGAAGACCGATCAATCTACAAAGACATAGACCACTGGCTCATCWTTGACAATGTCCAAAA
CTTGCTAGTTGTTGGTCCTGGAACCATCAATGGCAATGGAAACATCTGGTGGAAAAACTCATGCAAAATAAAACCTCAGG
TACGTTCTAATTAAACAAATAATTAGCTCTCACTAATACTAACCCTGTACTAATTACAATCTCTTTCATTGATTTACAGC
CCCCTTGCGGTACATACGCCCCCACRGTACGTGTACATACGTACTCTAATCTGAATATGTATGTGCATTTTAATTAATTA
AGCACCATTATTTCTGGAACTAATTAAAATTTGTACATGTAATGTGCAGGCTGTGACCTTCAACAGGTGCAATAACTTGG
TGGTGAAGAATCTGAATATCCAAGACGCACAACAAATCCATGTCATATTCCAAAACTGCATCAACGTTCAAGCTTCCYGT
CTCACGGTAACTGCACCAGAGGACAGCCCTAATACGGACGGAATTCATGTGACAAATACCCAGAACATCACTATCTCGAG
CTMGGTTATAGGAACAGGTGTGACAAATAGTTCATGAYGCTTTCAAAAGTCATCATTTTGGTCTCTYRCGTTTGATAAAT
ACATATGATCGATCAAACACATTAAGATAAAAAAACTAAACCATATTATGCATAAAATTAACAATCTTATGGTTTCTAAT
TTGTATTGTGAAGGTGATGACTGTATTTCTATTGTGAGTGGGTCCCAAAGAGTTCAAGCCACAGACATTACTTGTGGACC
AGGCCATGGAATCAGGTAATTTCCAACCCTAGTCTCCAAATTGTTCGACAAATCATCCTAAATTCCTCTTGTCAACATAT
TATTAATGTTTTTTAYGTCRAGAAAAGTGCGGGATGACTTTTTATAGTGTCAATAACAGCTGATTAGTAAATATACCAAT
ATATATTAACGGCTGTTTTAATTTTGTGATCAGTATYGGTAGCTTGGGAGAAGACGGCTCAGAAGATCATGTTTCAGGAG
TATTTGTGAATGGAGCTAAGCTTTCAGGAACCTCCAATGGACTCCGGATCAAGACGTGGAAGGGAGGCTCAGGCAGTGYA
ACCAACATTGTTTTCCAGAATGTGCAAATGAACGATGTCACCAACCCCATCATCATCGACCAGAACTACTGTGACCACAA
AACCAAAGATTGCAAACAACAGGTAATTAATTAATTTAACTAGTTCTTACGCRTTTCGTTAATTAGTCCCCAGACAAACC
TTAATCACTTCTTGATCGTYTATTTCGTTATGGCAGAAATCGGCGGTYCAAGTGAAAAATGTGTTGTACCAAAACATAAG
AGGAACGAGTGCTTCCGGYGACGCGATAACGTTGAACTGCAGCCAAAGTGTTCCTTGTCAGGGGATCGTGCTGCAAAGTG
TTCAACTGCAGAATGGAAGAGCTGAATGCAACAATGTTCAGCCTGCTTACAAAGGAGTTGTCTCCCCTAGATGTT

Figure 5.2: *Md-PG1* full length sequence characterization. In grey are shown the predicted exons as for the Golden Delicious sequenced genome. Bold green colour is for SNP associated to texture sub-traits. Bold underlined green colour is for SNP associated to texture sub-traits causing a non-synonymous variation in the predicted aminoacid sequence. Red text is for SNP identified by resequencing the other 7 cultivars, but not present in Golden Delicious. Bold red text is for SNP associated to texture sub-traits but not detected within the Golden Delicious heterozygous genome. Underlined red text is for SNP associated to texture sub-traits, not detected in Golden Delicious and with a MAF$<$0.05.

>MDP0000180043_XET
ATGGCTATCTTCCTGTTCCTCCTGATTCTTTTAGTCCCTGCAACCAATGCTGACTGGCCACCATCACCTGGSTACTGGCC
AAGCTCTAAGTTCAGGTCTATGAGCTTTTATAAAGGATTCAAAACTCTCTGGGGTCCWCAGCATCAAAGCTTAGACCAAA
ATGCATTAACAGTCTGGCTTGATMGCACCACAGGTCTCACWCCCACTTTTACTTCATATTTTACTGCTTCCTGAATTAGC
AGGGCACCTATTGAATTTGTTTATAATTTTGTCTAAATTCTTGTCCATTTTACTGAACAGGAAGTGGGTTYAAATCAGTT
CGTCCATTTAGATCCGGTTACTTTGGTGCCTCCATTAAGCTTCAAACTGGTTACACAGCAGGAGTCATAACAGCTTTCTA
TGTGAGAAAATTTAAAGWACTCAAACATGCATGCAGATGGGCATATTTTCTGCCATTTAARGAATTGAAGCTTKGTTATG
YCATTTgactaagacaGTGTATCCTACCCTTTGCACGCATTTCGAATCCTCCTTTTATATATTASAGTAGTTTAGAATAT
CATTTTATMAAAAAAACCAATTGCAYCCCAYTTGAATCCTKCTCCTATTTAYTAACGTAGTTTCGAATATWTGTTAGAAT
GGTTTTACAARTTCTAAGCAAAATTGGGTGTTCTAGATTAAGTAAATGCCTGGTGAATTGATCAAATAGTATTATTGCAG
CTTTCAAACAGTGAAGCTCATCCAGGATACCATGATGAAGTRGACATTGAGTTTCTTGGGACAACATTTGGGAAGCCWTA
TACTTTGCAGACCAATGTTTACATCAGAGGAAGTGGGGATGGAAGAATTATTGGCAGRGAGATGAAGTTTCACTTGTGGT
TTGATCCCACTAAGAATTTCCATCACTATGCTATATTATGGAGTCCCAAGGAGATAATGTAAGTTTTCTAACTTGAAATC
ARAGAGTAAGAATTGTTAATCGGAASAAACTTGAAATCAMRGAATRACTTRGAATTGTTAATCTGAATAAACTTTTACCA
GAAAATTCAGGAAAGAAGCCTTCTGTAATTAAGGGCAGGGTTCRTATTCATCATATTAYAYTGAAARGCTTTAATGATRA
TTTTAAAGTTGAAACAATAATATGAYTATGCCAAATCATTTCTTACTTTWTCTCTAAAATTAAGGAAAATCCAAGTGATT
TGACAGCAGTAAATATAAATTATAAAAAGAGACYAATATGCATGTRCAAACTTGTAAGCAACGTAAGAAGTAAKACCCGA
TCAGTTAACCTAGTTGATCARTTAGCGTGGACTTTTTCTTGTTCTYAAGTTCAAWTTTTTATCATTGTTGGTATATATAC
AATCTTAAGAGTAAARCTTTTATGTAACTGTTGTATATCAYTTTTGTGTATGTTGTTCTCTTGTCATGTGATAAATAAGT
TATTCGTTATCCTCAATTATGTTAGTTTGAAGGCCCCRTATTCAAATATGTWAAGTACCGTGAAAGGGATGTCATTGGCG
AAAGAAAAAGTTTCCTCCAATTTTARTCTTTATAAAAAMTTTGACAAAAAAAAGTGAAGGAAAAAAAAAACTAATGAAAT
RAGTTAACKWTAAAKWYAAAATAAAGGGTAAAATAAATAATACCAGGATTGACTTTTTARTGTAAAAATATGATTTTTMR
TTAAAGTRAAYMGTACCGGWAGCTTTTCGTTAAAGTTAAAAAAAAAAAAAAAAAARAAACTAAATCTAATAGTACAAAGCC
ATTGGTTCCTCTTRCTGGYCACTAATTAAGCTAATAATAAAATATATTYGGAATAGTAATTAACAGTCATATTATTCCAA
ACARGAACTGTGATGTTACCTTGTTGCTGGGTTTAATTATCTTATGTTTAAGTTAATACCARATTAATTTTTGGTACAGA
TTTTTGGTTGATGATGTGCCCATAAGGAGGTATGCTAGGAAAAGTGTTGCAACATTTCCCTTAAGGCCAATGTGGGTTTA
TGGTTCAATTTGGGATGCCTCATCTTGGGCAACTGAAGATGGAAAATACAAGGCAGATTACAGATATCAACCATTTGTTG
CCAAGTATACCAATTTCAAAGCCAGCGGTTGCTCCGCCTATTCCCCGGCATGGTGCCGCCCAGTGTCCGCCTCTCCCTTT
CGGTCCGGCGGGCTGACCCGACAGCAGTACAGGACCATGAGATGGGTTCAAACCAACCATTTGGTATATGACTATTGCAG
GGACCCCAAGAGGGACCATTCCAAAACACCTGAGTGTTGGGGCTAA

Figure 5.3: Md-Xet full length sequence characterization. In yellow the SNPs used in th association study and present in Golden Delicious. In red the SNPs used in the association but not detected in the Golden Delicious heterozygous genome

levels was performed, here named macro and micro allelotyping, to investigate the different level of LD between markers around the candidate genes. For PG the macro-allelotyping aim was to study the association with alleles in a region from 5 to 25 cM upstream and downstream the PG coding region, while the micro-allelotyping investigated a region in a window of 10 kb up and downstream from the START and the STOP codon respectively, with SNP and SSRs *de-novo* developed. For *Md-Xet* a different strategy has been chosen; less information about the gene involvement in apple texture were in fact available. A wider investigation interval was for this reason considered. In particular on LG12 the attention has been focus within the QTL interval identified in a previous work [143]. To perform the association analysis, a total of 495 markers were employed. Among them, 368 were scattered over the genome tested by a 384 Illumina platform Golden Gate assay, available from previous study [143]; and were used to evaluate population structure and kinship matrix. On LG10 four were SSR markers chosen for the macro-allelotyping scale (HiDRAS series), 2 were SSR markers used for the micro-allelotyping, of which one was retrieved from [143] (*Md-PG1*$_{SSR}$), and one (*Md-PG1*$_{SSR}$_10kd) was *de-novo* designed. Finally, a set of 38 SNPs were genotyped by sequencing in the region spanning 6 kb up and downstream the *Md-PG1* gene. On LG12 twenty-two were the *de-novo* designed SSR markers chosen for the macro-allelotyping scale, while for the micro-allelotyping a set of 60 SNPs were genotyped by sequencing *Md-Xet* full length. Within the set of 384 SNPs, 16 failed, and a possible explanation could be the fact that the probes were originally designed on the Golden Delicious genome, thus other additional polymorphisms present in other cultivars of the collection might have inhibited the correct annealing. The marker selected for the macro-allelotyping and all the markers selected for LG12 did not show any relevant association with the texture sub-traits, and for this reason they are no longer discussed. Also the analysis performed during harvest time did not show any significant association, suggesting physiological differences with post harvest, which strongly impact the final trait variance.

5.4.5 Association mapping based on the Md-PG1 candidate gene

In apple a rapid LD decay was expected, thus a candidate gene association mapping was chosen as the best strategy to genetically dissect apple fruit texture complexity, finding relationships between causal alleles and phenotypic variation [247],[95]. LD analysis, performed in order to estimate the non-random association among the 40 markers employed in the *Md-PG1* micro-allelotyping design, was computed by HaploView using the statistic r^2 (Figure 5.4). Four haplotype blocks were identified, defined by markers showing a r^2 between 0.19 and 0.85.

The first block includes two SNPs positioned in two adjacent exons, the second comprises SNPs in both exons and introns, while the other two blocks contains markers identified after the *Md-PG1* STOP codon. The third haploblock, in fact, contains two SNPs identified in the 3'UTR region and 1 kb

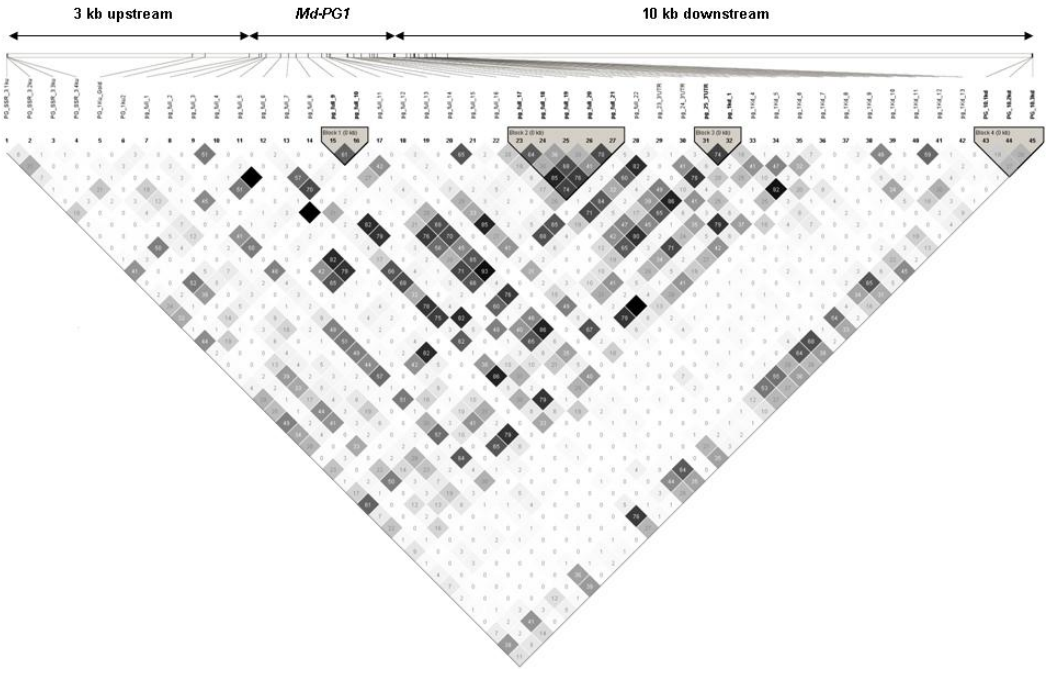

Figure 5.4: Figure 3 LD plot and haploblock of *Md-PG1* region. The LD image is based on r^2 values, the darker the colour of the box the higher is the r^2 value. In the upper part of the plot are indicated the number of polymorphic site and the marker considered into the computation. The four haploblocks are highlighted in grey. On the top are also illustrated the positions of the markers on the *Md-PG1* contig on which are distinguished the three main portion: 3 Kb upstream, gene full length and the 10 Kb downstream. Markers in bold are those included in the haploblocks. The *Md-PG1*$_{SSR}$ microsatellite alleles are indicated as *Md-PG1*$_{SSR}$_3.1Ku, *Md-PG1*$_{SSR}$_3.2Ku and *Md-PG1*$_{SSR}$_3.3Ku. The *Md-PG1*$_{SSR}$_10Kd alleles are indicated as *Md-PG1*$_{SSR}$_10Kd_1, *Md-PG1*$_{SSR}$_10Kd_2 and *Md-PG1*$_{SSR}$_10Kd_3.

	2009		2010	
	PC 1	PC 2	PC 1	PC 2
PG full 1	0,004995**	1	0,004995**	0,5255
PG full 6	0,01299**	1	0,002997**	0,988
PG full 10	0,004995**	1	0,000999**	0,9441
PG full 12	0,092910	1	0,008991**	1
PG full 18	0,03097**	1	0,002997**	0,8362
PG full 19	0,126900	1	0,008991**	1
PG full 20	0,575400	1	0,04096**	1
PG full 21	0,004995**	1	0,000999**	0,9401
PG full 23	0,005994**	1	0,01199**	0,7672
PG 1kd 1	0,520500	1	0,02498**	1
PG 1kd 5	0,330700	1	0,00999**	1
PG 1kd 7	0,01598**	1	0,000999**	0,991
$Md-PG1_{SSR}$_10kd_2	0,705300	1	0,03297**	0,977
$Md-PG1_{SSR}$_10kd_3	0,000999**	1	0,000999**	0,3986

Table 5.4: SNP association with the first two principal components (PC1 and PC2). **significative statistic association at *P-value*$\leq$0.05. "-": data not significative for both principal components.

downstream, respectively, the fourth is instead characterized by the presence of a SSR identified at 10 kb downstream the *Md-PG1* STOP codon, and here named *Md-PG1*$_{SSR}$_10kd. Fruit texture has been characterized by fourteen parameters, clustered in two fundamental categories (named mechanical and acoustic components), as illustrated by the PCA projection and defined by the first two phenotypic principal components (explaining, at the post harvest stage, 86.58 and 83.9% for the two years respectively Supplementary Figure 10.1). A preliminary association was carried out using the two phenotypic PCs, as traits, and a total number of 412 markers (368 genome-wide SNPs and 44 on LG10). Among them 14 alleles, included in the micro-allelotyping core set, resulted associated with the PC1 values for the two years of phenotypic assessments. PC1 computed over the phenotypic data distribution for 2010 resulted with a higher number of markers associated respect 2009 (Table 5.4). No association were found using PC2, possibly due to the lower percentage of variability expressed by this component.

This hypothesized that other genes may be involved in the control of the specific dissection between mechanical and acoustic components. The identification of new elements together with the use of a more wide cultivar collection able to improve the quote of variability explained by the PC2 (increased statistical power for the dissection of the mechanical-acoustic component), will be required to define novel markers suitable for the selection of the acoustic phe-

notype. To fine map the *Md-PG1* region (previously identified as a major QTL for fruit firmness and softening [143]) 40 markers were employed, out of which fifteen SNPs had a MAF$<$0.05. This set, however, was initially included in the association analysis performed between single SNP alleles and texture sub-traits (Supplementary Table 10.3) because discovered in four cultivars characterized by a high texture performance (CIVG198, COOP39, Minnewashta and Ligol). The collection here assembled does not represent the entire genetic diversity and phenotypic variability, thus a future implementation with additional novel crispy flesh type cultivars may increase their frequency, making their use relevant for further association studies. These SNPs were finally excluded in the following haplotype-texture sub-traits association analysis. In the association analysis all the 14 parameters, characterizing the texture sub-phenotypes, were considered. However, four texture sub-traits (Young module, force linear distance, Δforce and force index) did not present a significant association with any of the selected markers, suggesting that these traits are controlled by other genes not yet identified (thus they are no longer described). For the data collected at post harvest, twenty-one alleles resulted associated with the texture sub-traits (Supplementary Table 10.3), with the higher number (20) significant for the five acoustic components (acoustic linear distance, maximum and mean linear distance, number of acoustic peaks and number of force peaks; the latter more associated to acoustic response, according to [46]), and only 8 alleles associated with the five mechanical parameters (yield, maximum, mean and final force and area). Among the SNP set associated with acoustic sub-traits, six were significant (for the same texture sub-traits) for both years. Out of these six, three (PG_full 10, 21 and 23) were correlated, showing a LD value of r^2=0.76 and 0.93, while the other three (PG_10Kd_1, *Md-PG1*$_{SSR\_}$ 10kd_3 and GDsnp02072) were independent. GDsnp02072 is a SNP not included in the set used for the *Md-PG1* fine mapping, but still located on chromosome 10, at 0.3 and 0.5 cM apart from the *Md-PG1* gene based on FjxDel and FjxPL populations, respectively [143]. In addition to the marker located on chromosome 10, other two SNPs resulted associated with texture sub-traits (Supplementary Table 10.3), GDsnp02371 and GDsnp01634. These two markers are located on chromosomes known to contain QTLs and candidate genes involved in fruit ripening metabolism [49], [143]. These regions can be exploited for future candidate gene based association studies. In addition to the association analysis carried out with trait data by individual years, a second investigation was performed joining all the post harvest data from both years into a single dataset containing all the 77 apple cultivars (see Methods). For this analysis we employed the MLM module implemented in TASSEL, which corrects for kinship relatedness [244]. Effect of population structure and genetic relatedness, leading to false positive, was illustrated by the -log quantile-quantile (Q-Q plot) *P-value* distribution (Supplementary Figure 10.6). The association data obtained by MLM (with Q+K matrix defined with 368 SNPs, which resulted the superior model; Supplementary Table 10.3 column C) are quite consistent with the computation made

initially by PLINK (GLM model + Q matrix defined by 17 SSRs), beside minor exceptions. In some cases MLM did not confirm the results obtained by PLINK, and this can be attributed to possible false positive association, further adjusted by the Q+K matrix. In other cases, TASSEL highlighted new associations, and this can be interpreted as results ignored by PLINK (false negative) or by the different stringency of the two softwares. Finally, to model more accurately the frequency of relevant SNPs and to improve the power of the association analysis, adjacent markers were considered estimating the association of marker haplotypes with the texture sub-traits. For this purpose, haplotypes were constructed with the software FastPHASE, and only markers with a MAF$>$0.05 and a *P-value*$\leq$0.05 were considered. Twelve allele were finally selected and included into the analysis: PG_full 1-6-10-12-18-19-20-21, 23_3' UTR, 1kd_1, 1kd_7 and *Md-PG1*$_{SSR}$_10kd_3, defining a total of 16 haplotypes. Out of these, 10 haplotypes were shared between the two years of association, while three were unique for each year. Among the 16 total haplotypes identified, four were statistically associated to the different texture dissected subtraits collected during post harvest (haplotypes 1, 3, 9 and 10, Table 5.5). These haplotypes resulted statistically associated to the mechanical components, with haplotype 1 and 3 more associated to the variability expressed in the second year, and haplotype 9 and 10 to the first one, with *P*-value ranging from 0.047 to 0.004, a frequency range of 2.6%-26% and an effect size of r^2=1.04-27.93. For the acoustic subtraits, haplotypes 1 and 3 resulted more significantly associated in the analysis carried out in the second year, while haplotype 10 was more associated with the data collected in the first year of assessment. For the two texture components, such as acoustic linear distance and number of acoustic peaks, the association was consistent across years. Haplotype 3 and 10 were discovered in varieties known for their superior texture performance, such as Cripps Pink, Fuji and Granny Smith characterized by haplotype 3, and CIVG198, COOP39, Minnewastha and Ligol characterized by haplotype 10 (Supplementary Table 10.4). Haplotype 1 was shared by cultivars plotted in both positive and negative PCA areas, such as Ambrosia, Braeburn, Golden Delicious, Royal Gala and Gelber Edelapfel, while haplotype 9 was presents in particular in the cultivars plotted in the positive PC1 area of the PCA graph, thus characterized by an extremely poor textural behaviour (Brina, Gelber Edelapfel, Rome Beauty, Rubinola and Topaz). These findings suggest that both haplotypes 3 and 10, as well as *Md-PG1*$_{SSR}$_10kd can be considered as a valuable tool for marker assisted breeding programs.

5.4.6 Allelic dosage of Md-PG1$_{SSR}$_10kd_3

The microsatellite *Md-PG1*$_{SSR}$_10kd was tagged in a contig overlapping the genomic scaffold containing *Md-PG1* region, which resulted to be in LD with the SNPs targeted within the *Md-PG1* coding portion. We have emphasized this marker since it resulted highly significant with the texture phenotype in

N.	Haplotype	%	size effect	Yield Force		Final Force		Force Peaks		Max Force		Mean Force	
				A	B	A	B	A	B	A	B	A	B
1	GATTCGTCTCAG	26,0	9,95-27,93	0,1608	0,1039	0,1808	0,0119**	0,3027	0,0329**	0,0999	0,0209**	0,1109	0,0279**
3	TGCCTACTGTGA	17,0	5,36-22,04	0,2458	0,1908	0,0989	0,1908	0,3526	0,0219**	0,1379	0,1369	0,1858	0,0819
9	GATCCATCTCAG	3,9	3,18-13,16	0,4675	0,999	0,0219**	0,2178	0,1239	0,5355	0,3397	0,99	0,2438	0,9351
10	TGCCTATTGTGA	2,6	1,04-22,22	0,1359	0,999	0,0389**	0,8262	0,0339**	0,1199	0,0509	0,8881	0,0549	0,9141

N.	Haplotype	%	size effect	Area		Acoustic Linear Distance		Acoustic Peaks		Max Acoustic Pressure		Mean Acoustic Pressure	
				A	B	A	B	A	B	A	B	A	B
1	GATTCGTCTCAG	26,0	9,95-27,93	0,0849	0,0239	0,2378	0,0039**	0,3077	0,0029**	0,1588	0,0039**	0,7333	0,0049**
3	TGCCTACTGTGA	17,0	5,36-22,04	0,1409	0,0769	0,08192	0,0009**	0,07792	0,0019**	0,3057	0,0029**	0,6913	0,0019**
9	GATCCATCTCAG	3,9	3,18-13,16	0,2018	0,959	0,3926	0,4585	0,6653	0,6533	0,6484	0,9301	0,05395	0,4935
10	TGCCTATTGTGA	2,6	1,04-22,22	0,0439**	0,9261	0,0009**	0,0359**	0,0009**	0,0149**	0,0009**	0,1239	0,0029**	0,0989

Table 5.5: Association between the four significant haplotypes and texture sub-phenotypes for the two years of phenotypic assessments (A 2009, B 2010). **significative statistic association at $P\text{-}value \leq 0.05$. % is for haplotype frequency.

all the analysis performed in this work. Texture assessed for the two years at post harvest, showed a consistent cultivar distribution, as demonstrated by the PCA graphs in Figure 5.1 and the association results carried out using the first two PCs (Table 5.4). It is worth noting that apple cultivars presenting a homozygote allelic state for *Md-PG1*$_{SSR}$_10kd_3 (Supplementary Figure 10.7) were distributed in the positive PC1 values area of the PCA plot characterizing the general low texture performance (Supplementary Figure 10.8). Opposite was the scenario in case this allele was absent, with all the cultivars generally distinguished by PC1 values from 0 to -8, thus with a superior texture properties. Apple cultivars characterized by a heterozygous state for the "3" allele showed an intermediate texture distribution, being spread over the PCA plot and comprehended between the other two categories. The consistent distribution across the two years (as illustrated in Supplementary Figure 10.8) hypothesized a dosage effect for the "3" allele. On the PCA plot the only exception is represented by Ambrosia (1) that, even if it shows a homozygous allelotype for this allele, is plotted in the negative PC1 area of the texture distribution. Also the haplotype association with the texture traits reflected the allele dosage observation. The four significant haplotypes can in fact be divided in two different groups, according to the presence/absence of the allele *Md-PG1*$_{SSR}$_10kd_3, as well as the position on the PCA plot. Haplotype 1 and 9, presenting the *Md-PG1*$_{SSR}$_10kd_3 allele in homozygous state, characterized those cultivar showing a general low texture performance, such as Gelber Edelapfel, Dalla Rosa, Early Gold, Croncels, Rubinola and Delearly. Haplotype 3 and 10, which lack this allele, are shared by cultivars such as CIVG198, COOP39 and Ligol, and it is worth noting that the cultivars positioned in the PCA graph defined by negative value of both principal components (thus with the best acoustic resolution), showed only the haplotype 10. To date great technological progress have been made in marker high throughput genotyping, which has elected SNP as the most suitable marker for genetic study, especially for high density and time effective genome wide scanning. However, microsatellites still remain a useful tool for assisted selection programs, because of their higher allele diversity and easiness of transferability across species and laboratories [93]. For this reason, in addition to the haplotypes, we also propose this SSR marker *Md-PG1*$_{SSR}$_10kd as a valuable marker for assisted breeding programs towards the selection of high texture performing apple cultivars.

5.5 Conclusion

Fruit texture is one of the main principal quality factors as well as a world wide main priority in modern apple breeding programs. To date texture has been phenotyped with too poor and empirical methods, reducing its complexity to a simple and not always exhaustive flesh firmness assessment. Many works have been already presented to the scientific community, but all are related to a QTL

survey focused on bi-parental map, thus with alleles involved in the genetic control restricted to the genetic background of the parental cultivars. In this study, for the first time, we fine mapped the *Md-PG1* region with a set of new SNP and SSR markers discovered mining the apple genome contig sequences. LD mapping analysis defined a set of 12 SNPs in linkage, with a MAF value$>$0.05 and characterizing 16 haplotypes. SNPs and haplotypes, together with the texture components dissected with a novel texture analyzer equipment coupled with an acoustic device, were used for a candidate gene association mapping investigation. Haplotypes 3 and 10 resulted significantly associated to the high texture behaviour in particular with the acoustic component, the most preferred features by consumers. It is also interesting to note that these two haplotypes lack the allele *Md-PG*1$_{SSR}$_10kd_3, that showed an allelic dosage correlated with the texture variability illustrated by the PCA, where its homozigousity corresponded with the cultivars characterized by the most extreme low texture performance. Here, we finally report the characterization and the validation in a large apple collection of two haplotypes, as well as a microsatellite as a novel tool kit for the selection of high texture fruit quality apple accessions.

CHAPTER 6

Transcription profiling by microarray approach unravel the apple climacteric fruit ripening physiology

6.1 Abstract

Final apple fruit texture is the result of a complex series of physiological and biochemical changes occurring during the ripening process. In apple, in fact, these processes are triggered and regulated by the gassous hormone ethylene. The different texture observed in the several apple cultivars is the result of a complex gene expression dynamics occurring during fruit development and ripening. The aim of this study was the investigation of a gene functional profiling performed in two main apple varieties, in order to unravel gene dynamics over fruit development and climacteric ripening, from flower to post harvest stage. Transcriptional changes between 7 different stages in two apple cultivars, was investigated by using the Combimatrix microarray platform. On the chip were synthesized 3800 oligos *ad-hoc* designed from the Golden Delicious genome annotation, and containing the genes underlying the QTL intervals discovered in a precedent work [143]. According to their annotation, 75% of the gene-set is involved in the ripening process, while 25% is related to regulatory and fundamental biological processes, such as carbohydrates metabolism, biological and regulatory processes, cellular components, signal transduction or aminoacid and energy pathways. Within the genes ripening specific 34% were transcription factors, 17% were genes involved in the secondary metabolism, 15% were genetic elements involved in the cell wall metabolism and 10% in plant hormone regulation. To unravel the ethylene impact on gene expression dynamics, the ethylene inhibitor 1-Methylcyclopropene was used. The comparison between the transcripts profiles in normal ripening samples (control) and treated samples shed light on the ethylene dependent and independent gene functional pattern. In

Golden Delicious, which is considered the reference cultivar, the overall genes expression was grouped in 70 categories according to their common profile determined based on SOTA clustering algorithm. Particular attention was given to the gene clusters both positively and negatively regulated in two specific developmental stages; breaker and ripening. Preliminary analysis revealed that the breaker stage represent a border line, distinguishing the developmental stages from the full ripening physiology. Other important expression profile changes were detected at harvest, in coincidence with the initiation of the ethylene burst.

6.2 Background

Fruit is an organ extremely various and heterogeneous among the different species. In fact, it ranges from simple dry dehiscent or indehiscent fruit (like silique in Arabidopsis or achenes) to fleshy fruit with expanded ovaries (tomato fruit) and vary complex fruit organs, such as apple [75]. Fruit ripening can be distinguished as climacteric and non-climacteric, depending on the capacity of the fruit to increase the respiration rate during the last stages of ripening, which occurs in combination with an increase of ethylene biosynthesis (ethylene burst); a gas hormone known to be involved in climacteric fruit ripening [6],[15]. Fruit development, maturation and ripening are complex physiological processes, characterized by unique and distinctive steps, described by important changes in colour, flavour, aroma and texture. All these characters are controlled by both external signals, such as temperature, water and light interception, and endogenous hormonal and genetic regulators [16]. In particular, during the first stages of growth, fruit undergoes several rounds of cell division, followed by cell expansion. During these stages, metabolites and energy are stored and a series of biochemical changes, making fruit attractive, occurs. All these changes are required to allow the fruit to develop all the characteristics that defines its final quality, beside rendering the fruit itself suitable for seed dispersing [85]. Fruit quality is measured accomplishing four main principal factors which are appearance, flavour, texture and nutrition. Fruit texture, in particular for apple, is an important factor for quality. It is, in fact, considered a reason for not liking a particular food, and directly impact its marketability. For this reason texture is now considered a worldwide breeding priority for apple fresh market. Fruit texture is the result of a complex enzymatic machinery degrading the middle lamella and the primary cell wall, usually encoded by multi-gene families. The complex regulation of this phenomena has been also confirmed by the recent finding that within the genomes sequenced to date, almost 10% of the entire gene inventory is committed to cell wall metabolism [154]. The physiological and biochemical changes occurring during fruit development, starting from the early stages, are regulated by the transcriptional regulation of many genetic elements. This modulation can be elucidated by high throughtput genomic technologies like microarrays. Gene expression studies have already been employed on numerous

ripening species like tomato [5], strawberry [3],[62], peach [220],[23], nectarine [248], pear [83] and grape [246], identifying genes involved in flavour and aroma, and associated with different stages of fruit development. Apple ripenig process, has been investigated by several microarray studies [45],[114],[197],[134] which described the dynamics occurring during maturation. In this work, the microarray technology has been chosen to define the functional profile of a specific gene set *ad-hoc* selected in different apple development and ripening stages, from the flower to post harvest. The latter stage, in particular, was exploited in a comparison with 1-Methylcyclopropene (1-MCP) treatment. 1-MCP is an ethylene inhibitor which binds irreversibly the ethylene receptors, preventig thus the hormone binding and the activation of the downstream cascade involved in ethylene response pathway. This treatment has been employed to investigate and elucidate transcriptome variation in response to ethylene, in different fruit species [45],[248],[136]. Transcriptome analysis was performed investigating the functional kinetics of about 3800 genes during fruit development and ripening of two cultivars differing for their textural characteristics. Golden Delicious is in fact characterized by middle textural performances, while Granny Smith possesses high textural performances. The genes set hybridized on the chip, derived from the gene annotation of the Golden Delicious genome, included genetic elements mapped within the QTL intervals targeted in the previous linkage analysis study [143]. The aim was to determine the genetic modulation of the elements defined within the QTLs. The array represents 1/15 of the apple genome, putatively involved in texture determination and ethylene biosynthesis and perception. The analysis realised initially on Golden Delicious allowed the survey of the genes specifically expressed in a normal climacteric condition, enabling the successive identification of the gene-set differentially expressed between the two cultivars. The understanding of the molecular events and the genetic dynamics associated with fruit development could be a starting point to obtain valuable information for the identification of candidate genes useful in following marker assisted selection programs.

6.3 Materials and Methods

6.3.1 RNA isolation and microarray hybridization

Cortex tissue of Golden Delicious and Granny Smith cultivars were collected at seven different stages, and stored at -80°C until the RNA isolation step. The time-series included different stages indicated as i) F_flower chosen as reference point on which all the functional dynamics has been anchored (selected when 80% of the flower on the tree were opened), ii) L_fruitlet (flower starts to swell and pollinated flowers are recognizable from not pollinated), iii) G_green (fruit with a diameter of 3 cm), iv) MG_mature green (fruit with a diameter of 6 cm or more, but still with a green colour) in these two stages the rate of cell expansion increased, while cell division has ceased [114], v) B_breaker (expan-

sion still increased and skin colour initiated its colour transition), vi) H_harvest (defined by commercial harvest time and defined by standard fruit quality parameters) and vii) P_post harvest (one week after harvest time). Sample at post harvest were divided in two different sub-groups. Both PC (for control) and PM (for 1-MCP treated) were maintained for a week at shelf life (20°C), but the treated one was incubated in a sealed and ventilated container with 1 ppm of 1-MCP for 12 h at room temperature after harvest. Total RNA was isolated in triplicate, grinding the cortex pool in presence of liquid nitrogen, using a Sigma-Aldrich extraction kit. RNA quantity and quality were checked spectrophotometrically with a Nanodrop ND-8000® (Thermo Scientific, USA) and an Agilent 2100 Bioanalyser (AGILENT, Palo Alto, CA.). Total RNA (2 μg) was amplified and labeled using the RNA ampULSe: Amplification and Labeling Kit (with Cy5 for CombiMatrix arrays, GEA-022; Kreatech). The purified labeled aRNA was quantified by spectrophotometer and 4 μg were hybridized to the Combimatrix array according to the manufacturer's directions. Prehybridization, hybridization, washing and imaging were performed according to the manufacturer's protocols (http://www.combimatrix.com). After hybridization and washing, the microarray slides were dipped in imaging solution, covered with LifterSlip™, and then scanned using a Axon GenePix 4400A (Molecular Devices). Densitometric analysis were performed with GenePix Pro 7 software (Molecular Devices). Probe signals higher than negative control values plus twice the standard deviation were considered as 'present'. Data were normalized by quantile normalization and differentially expressed genes were identified using Linear Models Microarray Analysis (LIMMA) with a False Discovery Rate (FDR)<5%.

6.3.2 Texture phenomic assessment

Texture profile over the samples collected during the time course was assessed simultaneously profiling mechanical and acoustic signatures, dissecting different sub-traits, by a texture analyser TA-XT*plus* (Stable Micro System Ltd., Godalming, UK). Mechanical measurements were performed with a 4 mm flat probe, speed of 100 mm/min and auto-force trigger at 5g. Distance was expressed as % of compression (strain). Acoustic envelop device (AED) allowed the additional and simultaneous collection of the pressure released during the sample's fracturing. Sample preparation, instrument setting and parameter explanations are described in Costa *et al.* [46].

6.3.3 Ethylene determination via PTR-ToF-MS and spectra analysis

Apple measurements were performed with a commercial PTR-ToF-MS 8000 instrument (Ionicon Analytik GmbH, Innsbruck, Austria), following the procedure described for other food samples [76],[207]. A whole apple fruit was placed in

a glass vessel (5 L, Bormioli, Srl, Italy), provided with silicone septa on the opposite sides, and incubated at 30°C for 40 min. Three replicates were performed per sample and 20 cycles were realized for each measurement, resulting in analysis time of 20 s per sample. All measurements were carried out under the following drift tube conditions: drift voltage, 600 V, drift pressure of 2.25 mbar, temperature 110 °C, corresponding to an E/N value of 140 Td (Td = Townsend; 10^{-17}cm^{-2}V^{-1}s^{-1}). Ethylene concentration, was expressed in ppbv (part per billion by volume) and has been calculated from peak areas according to the formula described by [141]. Peak identification and area extraction followed the procedure described in details in [31].

6.3.4 Scanning electron microscope observation

Small apple slices of Granny Smith and Golden Delicious at different developmental stages (G-B-H-PC) were cutted and initially fixed for 2 hours at 4°C in a 0.1 M phosphate tampon (Na_2HPO_4 and NaH_2PO_4) at pH 7, mixed with 5% formaldehyde. Successively, the samples were washed over night at 4°C in a 0.1 M phosphate tampon at pH 7. Samples dehydration was performed by washing the slices for 15-20 min, with ethanol solution at increasing concentration; 40%-60%-75%-85%-90%-95%-100%. An Emscope 750 (Emitech, Ashford, Kent) was then used to performe the critical point drying, in order to substitute ethanol with CO_2. Samples were finally coated with gold using a SC 500 gold sputter coater (Bio-Rad Micro-science division) and analysed at the scanning electron microscope (S.E.M. Hitachi S-2300, Hitachi, Tokyo, Japan).

6.3.5 Chip design and synthesis

Chip design, oligo synthesis and transcriptomic analysis were performed on a 2x40K Combimatrix Array. Microarrays were synthesized at the Plant Functional Genomics Center of the University of Verona (http://ddlab.sci.univr.it/ FunctionalGenomics/). CombiMatrix technology combines phosphoramidite chemistry and semiconductors for the digital control of probe synthesis on the chip surface. The 2x40K array contained 40,000 siliceous electrodes (features), supporting 7693 unique 35-40 mer DNA oligonucleotide probes synthesized in situ. For each gene, copies and replicates of the probe were designed. Copies indicate identical probes designed in the same gene region. Replicates are different probes designed in different position of the gene. Up to four replicates/probe were designed in order to improve the statistical power of the expression analysis. Each probe was repeated four times (copies) and randomly distributed over the array for an internal variability control. To target single transcripts from the Apple genome (http://genomics.research.iasma.it), probe were designed with OligoArray 2.1 [191]. When the design of the probes was not possible, according to thermodynamics requirements, the sequence was discarded. Oligonucleotide based on bacterial sequences were also used as negative internal controls.

6.3.6 Data Analysis

Statistical analysis, data normalization and quality control were realised using LIMMA library (R package). All values were log transformed (base 2) and genes with an absolute fold change log2$\geq$1 and a *P-value*$\leq$0.05 were considered differentially expressed between two different samples. In order to obtain a more consistent expression result, media value was considered from the data deriving from probes designed in different areas of the gene (replicates), while the median value was computed for the probe copies. Differentially expression statistics was visualized using Venn diagrams, drawn with Venny [169], allowing inter and intra developmental and ripening comparison among the different stages of one cultivar and between the two cultivars. Data were clustered according to SOTA (Self-Organizing Tree Algorithm) algorithm, and visualized by MultiExperiment Viewer [193].

6.4 Results and Discussion

6.4.1 Texture physiology dissection

Microarray slides were designed to identify differentially expressed genes in apple fruit over a time-course based experiment. Seven time points were selected to study the physiology related to fruit development and ripening. Seven different time point were chosen as described previously, starting from flower to post harvest. Successively, apple physiology was characterized analysing the ethylene bio-synthesis and texture profile in the two different cultivars. The ethylene production, for the two cultivars, was assessed employing a PTR-ToF-MS over a period of 30 days starting from harvest, comparing the normal physiology with the distorted one by 1-MCP. The ethylene burst occurred within 10 days after harvest, confirming the data reported by Costa *et al.* [49]. The comparison between the two cultivars showed substantial differences in hormone production, Golden Delicious, in fact, produced 1120,5 ppbv of ethylene 7 days after harvest, while Granny Smith, in the same period, produced only 35.9 ppbv (Figure 6.1). The second cultivar reached the highest amount of ethylene 19 days after harvest, producing 121.6 ppbv of hormone (almost ten time less than Golden Delicious). In both cultivars the ethylene production was affected by 1-MCP treatment. In the treated samples at the 7^{th} day of the post harvest ripening the ethylene level was 3 and 5 ppvb in Granny Smith and Golden Delicious respectively, and constantly remained at a basal level for almost 20 days. After this point the ethylene concentration slowly increased in Golden Delicious (Figure 6.1). This result find consistency with the analysis carried out in Golden Delicious by Dal Cin and collegues [54], where they observed an increased ethylene level of apple treated with 1-MCP 24 days after harvest. In Granny Smith, instead, the ethylene concentration after the treatment remained at basal level for all the analysed period (Figure 6.1).

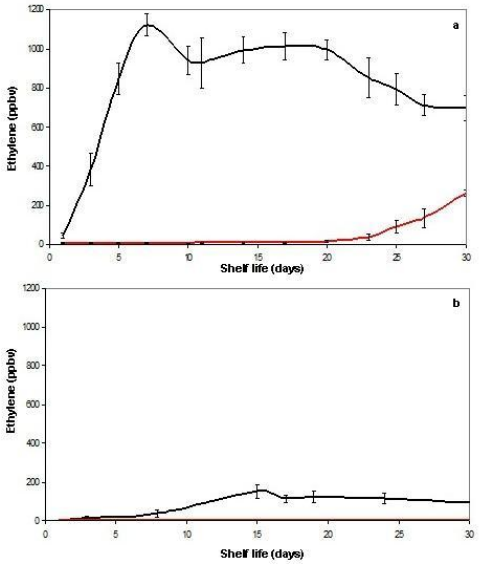

Figure 6.1: Ethylene bio-synthesis evolution for Golden Delicious (a) and Granny Smith (b). On the x axis the number of days after harvest is reported. Y axis is for ethylene concentration, measured in part per billion by volume (ppbv)

In apple is known that ethylene has a direct impact on texture, being several cell wall enzymes hormone dependent. Texture dynamics was profiled over the time course using a texture analyser equipment, distinctively characterizing the mechanical and acoustic texture profiles (Figure 6.2) [46]. The figure clearly showed as the mechanical component has a distinct kinetics respect the acoustic profile. In both cultivars the mechanical profile decreased continuously over the stages, while the acoustic response increased until the harvest stage for both cultivars, than it showed a specific trend variety dependent. In Golden Delicious, the acoustic profile decreased towards the post harvest stage, while in Granny Smith it remained almost unmodified, validating the different texture behaviour existing between the two cultivars. Ethylene regulation of the last ripening stages, has been also suggested by the dissection of the textural profile after the 1-MCP treatment. As showed in Figure 6.2, the mechanical profile for the treated samples, in both the cultivars, presented a trend which was similar to the profile described at the harvest point, indicating a possible slowdown of the physiological dynamics due to 1-MCP. The treatment heavily effected the acustic profile of Golden Delicious, which showed results closer to harvest. Granny Smith, instead, did not show any particular change between the samples analysed during the three last ripening stages: harvest, post harvest control and treated. Table 6.1 summarized the number of the acoustic and mechanical peaks during the time course, enlightening the differences occurring in the profiles between the varieties and texture ethylene dependency.

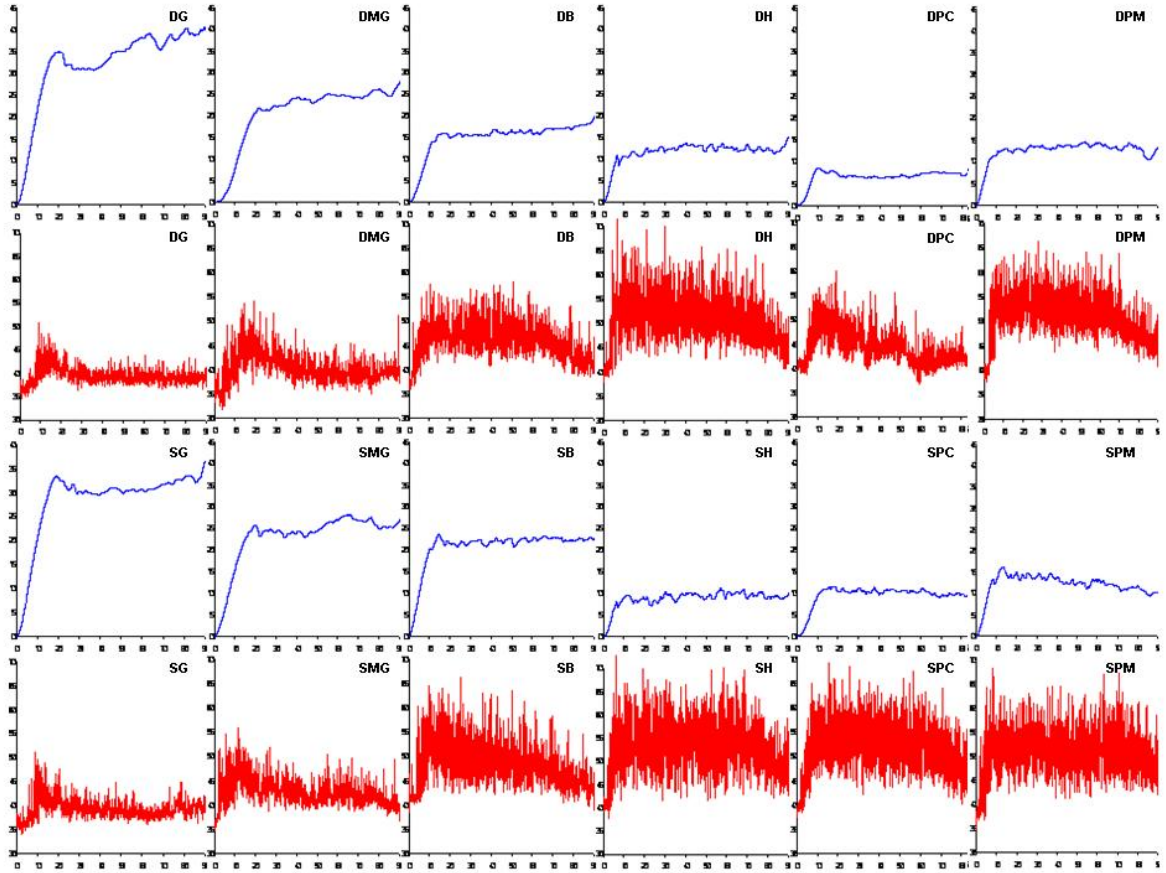

Figure 6.2: Mechanical and acoustic profiles for the two cultivars. Abbreviations: D, Golden Delicious; S, Granny Smith; G, green; MG, mature green; B, breaker; H, harvest; PC, post harvest control; PM, post harvest treated.

cultivar	Green		Mature Green		Breaker	
	F peaks	A peaks	F peaks	A peaks	F peaks	A peaks
Golden Delicious	10	3,5	12	16	16	60
Granny Smith	11	5	13	34	18	58

cultivar	Harvest		Post harvest Control		Post harvest treated	
	F peaks	A peaks	F peaks	A peaks	F peaks	A peaks
Golden Delicious	24	84	7	29	14	84
Granny Smith	17	128	23	87	22	88

Table 6.1: The table reports the number of the force peaks (F peaks) and the acoustic peaks (A peaks) for all the fruit stages analysed in the two cultivars.

Also the observation performed with the electronic microscope, supported the ethylene impact of fruit texture. Samples fixed at the green and breaker stages were similar for both cultivars, confirming the data collected with the texture analyser (Figure 6.3). Starting from harvest, the differences between varieties were more evident (Figure 6.4). At the harvest stage, Granny Smith cells were completely broken. In Golden Delcious, instead, most of the cell remain intact, but with a more collapsed shape. The situation was emphasized at the post harvest stage, where the differences occurring between the cultivars' cells was higher. Granny Smith cells appeared similar to the cells fixed at the harvest time, supporting the texture assessment. In Golden Delicious, instead, the cells were completely separated but intact. These results were consistent with the data reported by Waldron *et al.* [233]. In this work it was presented that in crispy fruit cell adhesion is strong and tissue fraction involves rupture across cell walls, releasing cells content and lendig to the characteristic crispness. On the contrary, in mealy fruits, middle lamella undergoes extensive dissolution and the cells are completely separated upon compression, slipping one on the other. This miscoscopic investigation confirmed also the previously measured differences occurring in the cultivars in both the ethylene bio-synthesis profile and texture parameters dynamics.

6.4.2 Data analysis and gene clustering

The reproducibility of the replicates and the accuracy of the hybridizations were confirmed by Pearson correlation and PCA analysis. A graphical overview of the correlation was showed by the two-dimensional heatmap plot of the 8 different conditions for Golden Delicious and Granny Smith (Figure 6.5). The PCA plot showed that the three replicates/sample were more closely clustered respect the seven samples of the time course, which showed a developmentally time progression. The samples treated with the ethylene inhibitor 1-MCP were specifically grouped closer to the harvest stage samples respect to the post harvest control stage, suggesting as the treatment delayed the overall ripening physiology at a functional level. In order to investigate gene expression and patters in the

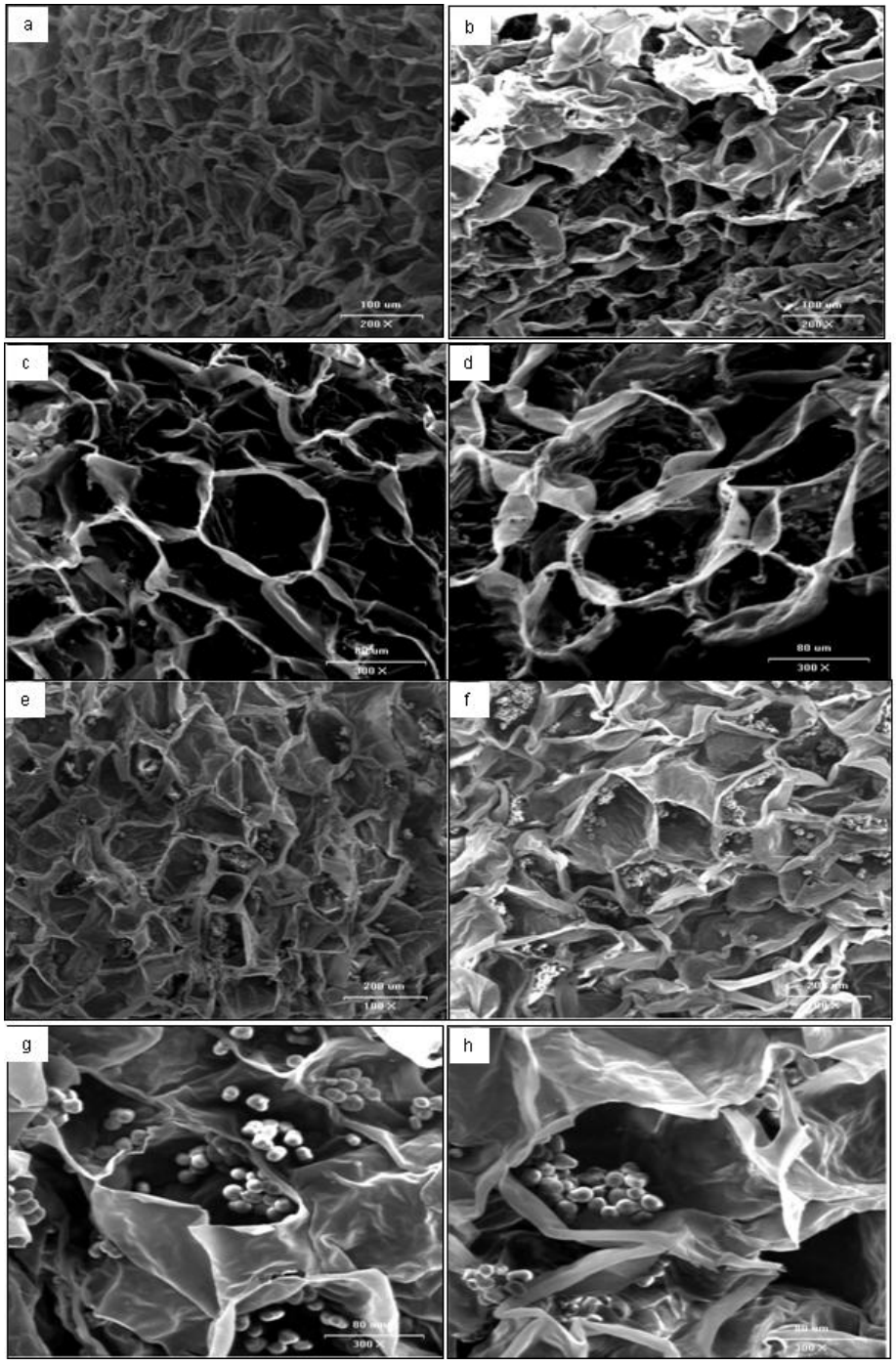

Figure 6.3: S.E.M. image analysis of Golden Delcious (a, c green stage and e, g breaker stage) and Granny Smith (b,d green stage and f, h breaker stage).

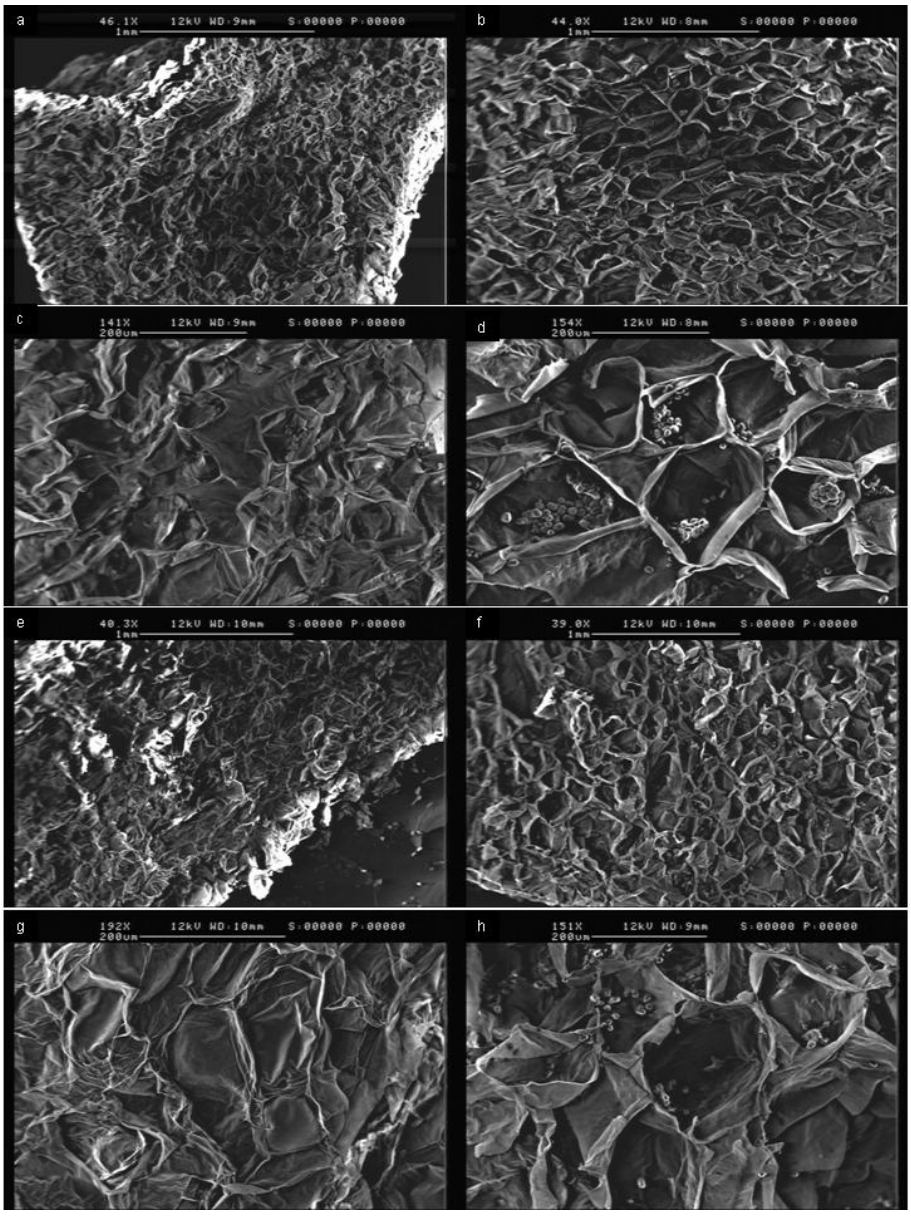

Figure 6.4: Figure microsopio: S.E.M. image analysis of Golden Delcious (a, c harvest time and e, g post harvest) and Granny Smith (b,d harvest and f, h post harvets).

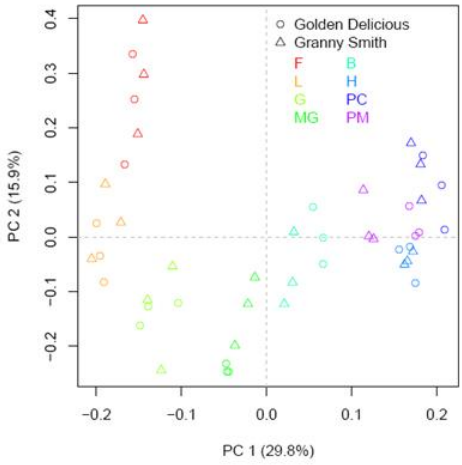

Figure 6.5: Two-dimensional graphical overview of the correlations existing among the expression values and the samples during the time course.

two different time course, a set of 3810 genes, subdivided in eleven classes, were represented on a Combimatrix Microarray gene categories (Figure 6.6). These classes were identified as: aminoacid pathways, biological processes, carbohydrate metabolism, cell wall metabolism, cellular component, energy pathway, plant hormone, polysaccharide metabolism, regulatory processes, secondary metabolism and transcription factor (Figure 6.6).

Specific gene classes, representing 1/15 of the total gene number in the apple genome, have been selected in order to capture and investigate a limited, but ripening specific, physiological dynamics, excluding supplemental information that a wide genome investigation would have given. The 75% of the selected genetic elements were genes involved in ripening processes like transcription factors (34% of the genes synthesized on the chip), secondary metabolism (16%), cell wall metabolism (15%) and plant hormone regulation (10%). The remaining 25% comprehended genes involved in carbohydrates metabolism (10%), biological or regulatory processes (1% each), cellular components (10%), signal transduction or aminoacid and energy pathways (0.07 and 4% respectively). The gene-set selection started from the annotation, based on the UNIPROT database, of all the genetic elements targeted in a previous QTL analysis study [143]. The annotated genes were successively blasted against the Apple Genome database, identifying all the genetic elements belonging to the gene-families. A total of 3404 genes passed the standard quality control and were finally considered for the expression data analysis. These genes were

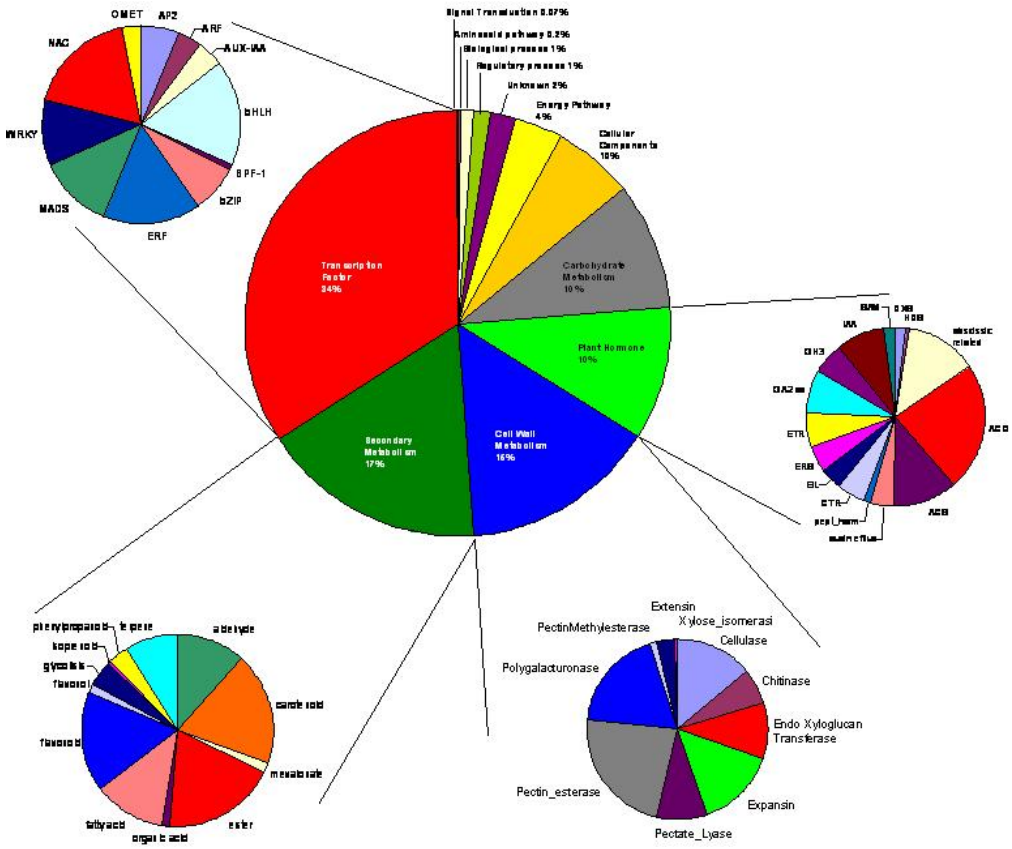

Figure 6.6: Pie chart summarizing the percentage of the gene-classes hybridized on the Combimatrix microarray chip.

grouped together according to their expression profile analysed by a SOTA clustering algorithm (MeV software). In Golden Delicious, chosen to represent the normal climacteric ripening dynamics, seventy clusters, each describing a specific trend, were identified. Two clusters showed an increasing dynamics after the flowering time and a decreasing sharp profile after the fruitlet stage (Figure a, b 6.7). The two main gene groups classified in these stages were transcription factors (22.6%) and genes involved in the cell wall metabolism (32.1 %). The classes less represented were genes involved in biological process (1.9 %), while were not identified genes involved in the aminoacidic pathays, regulatory processes or polysaccharides metabolism. The transition from flower to fruitlet was characterized by a complete change in shape and morfology. It is therefore reasonable that the genes mainly involved in this processes were mainly represented by transcription factors, which are devoted to initiate new developmental programs, and genes involved in the cell wall metabolism, which re-organize the polysaccharide structure to allow cell enlargement and division. Five clusters showed an initial up-regulation after the flowering time, and a following decrease after breaker stages towards the end of the time course (Figure c, d, e, f, g 6.7). The two main gene classes expressed in these stages were transcription factors (16.9 %) and genes involved in secondary metabolism (22.9 %). The class less represented comprehend genes involved in regulatory processes (0.48 %), while were not present genes involved in the polysaccharides metabolism. The genes here clustered were probably not involved in the final ripening, but mainly in fruit initial development and growth. In these clusters, genes involved in the ethylene bio-synthetic pathway were also identified. In particular 4 genes belonging to the Aminocyclopropane-1-Carboxylate Ossidase (ACO) family, 3 elements member of the Aminocyclopropane-1-Carboxylate Synthase (ACS) family and 2 S-adenosyl-l-methionine synthetase (SAM) were identified. These genes could be involved in the synthesis of the basal ethylene levels, but not in the ripening process, since they were not identified in the clusters having an increasing dynamics at the onset of ripening.

A endo-xyloglucantransferase (Xet), presented in previous QTLs analysis as putatively involved in the determination of the acoustic component of apple texture, was also grouped in this set of clusters, suggesting its role in the cell wall metabolism and mantainance [143]. This gene has been the target of a candidate gene association study (chapter 5). The association performed with phenotypic data collected at the post harvest stage was not statisticaly significant. This might be explained by the observation obtained after this expression study, where it was showed an involvement of the gene expecially during the initial-mid stages of fruit development and maturation, and not during the late ripening stages. Expression studies, describing genes dynamics, can therefore be a useful tool in the determination of the best developmental stage for phenotypic data collection and following genetic analysis. Two were the clusters that presented a slight decrease after the flowering stage, followed by an increase at breaker and reaching the highest value at the harvest point (Figure

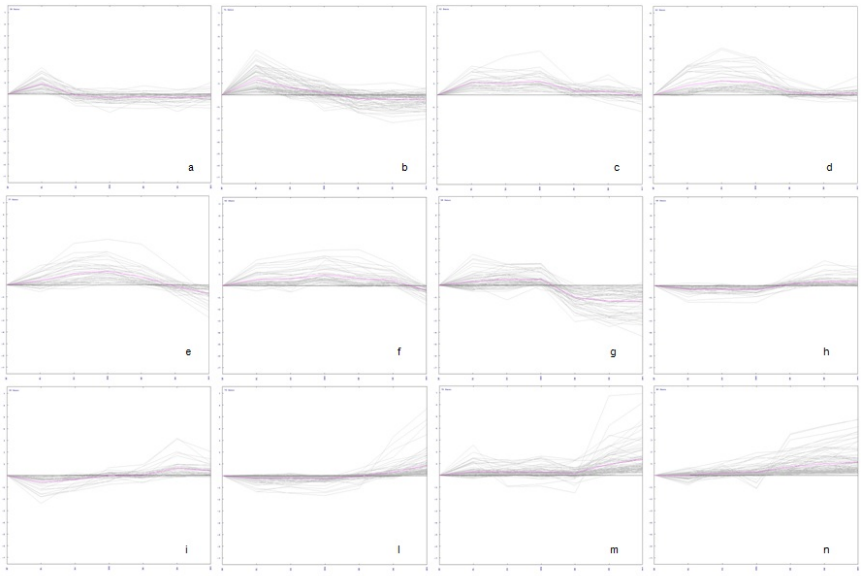

Figure 6.7: 12 specific clusters investigated for their particular dynamics along the time course.

h,i 6.7). Within this clusters, the gene categories more represented were plant hormone (20.5%) and transcription factors (22.9%). Genes involved in biological and regulatory processes and in the polysaccharide metabolism were, instead, not expressed. Fruit ripening is characterized by a dramatic change in softening, occurring in concomitance with the initiation of the ethylene burst. This observation can explain the high percentage of genes regulating phytohormones and transcription pathways. Finally, three clusters grouped together the genes putatively involved in the ripening process and senescence, showing a sharp up-regulation after breaker stage towards the post harvest (Figure l, m, n 6.7). The two main gene classes expressed in these clusters were related to secondary metabolism (20.3%) and transcription factors (26.9%). The gene categories less represented were aminoacid pathways, biological processes and polysaccharide metabolism (0.43% each). Some of the genes clustered in this final group were already known to be involved in apple climacteric ripening process, such as *Md-ACO1* and *Md-ACS1* which are genes involved in the ethylene biosynthetic pathway, ethylene receptors, expansin and polygalacturonase (*Md-PG1*), involved in the cell wall modification. The role of these genes in the determination of apple texture has been already investigate in different studies [49],[247],[50],[143]. Differently from the ACS and ACO genes underlined in the previous groups, the elements identified in these clusters (*Md-ACO1* and *Md-ACS1*) are involved in the ethylene burst occurring during ripening, suggesting two different observations. The first is that elements belonging to the same gene family are transcribed in very precise and genetically determinated

steps of fruit growth, the second is that the dynamics presented here for apple, are similar to those identified for tomato fruit suggesting putative conserved orthologous maturation and ripening related genes [5],[49].

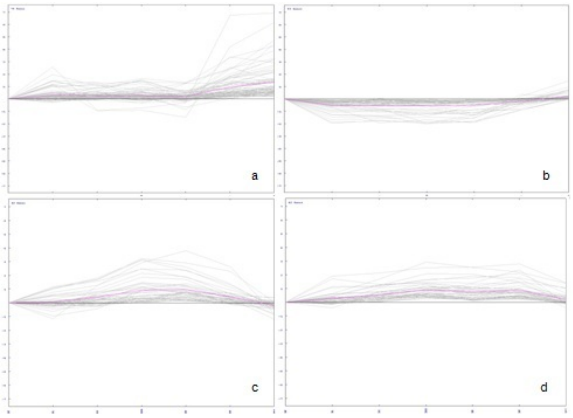

Figure 6.8: 4 specific clusters having distinctive dynamics during mauration and harvest.

Among the 70 classified clusters, four were selected for their distinctive profile during maturation and ripening (Figure 6.8). In particular, clusters presenting both positive and negative dynamics at the breaker and harvest stage were choosen . Within this four groups, 79 and 53 genes grouped in the breaker and harvest cluster respectiely, showed an up-regulation (Figure a,b 6.8). Within these set, genes involved in plant hormonal metabolism, such as ACS, gibberellins acid oxidase (GA2 ox), indole-3-acetic acid amidohydrolase (IAA or auxin) were included, underlying the important role of different hormonal signalling pathways in both maturation and ripening stages. Genes involved in the secondary metabolism like lipoxigenases (LOX) or pyruvate decarboxylase and cell wall enzymes like expansins, were also present in both these two stages, but not in the clusters presenting a down-regulation dynamics (Figure c, d 6.8). Within the group of genes upregulated only at the breaker stage, some elements belonging to the ACO family were found, suggesting their activation in a precise and exact time point during maturation. In climacteric fruits, the ethylene biosynthesis is characetrized by two distinct systems [157]. System 1 is proposed to be responsible for the basal level of ethylene production, while the transition to system 2 was proper of the ethylene burst [15]. System 1 continues throughout fruit development until the competence to ripen is obtained and system 2 starts. Different ACS and ACO genes have in apple critical functions in the two systems [234], sustaining the profile observed in the array. As mentioned above, in fact, different genes belonging to ACS and ACO family accumulated their transcripts in different developmental stages suggesting also their involvement in the two different ethylene synthesis systems. *Md-ACS3a* has, for example, a critical function in regulating the transition from system 1 to system 2, while

Md-ACS1 and *Md-ACO1* are involved in the ethylene bio-synthesis during the ethylene burst occurring at the late ripening stage [234]. In particular, these two enzymes, *Md-ACO1* and *Md-ACS1*, were both grouped in the cluster having an increasing trend at breaker. This observation suggested that, despite the fact that the ethylene accumulation starts to increase after harvest, their transcript accumulation initiated earlier, already at the breaker stage. This gap between the gene activation and the corresponding physiological response can hypothesize a relatively slow feedback in the activation of the ethylene machinery. Other genes involved in different plant hormonal pathways presented a positive regulation at breaker. These were mainly represented by ethylene receptors, like ETR and ERS, and auxin response promoter (GH3). Transcription factors such as WRKY or AP2 (APETALA2) were also unique of this cluster (among the four selected). It has been noticed, moreover, that the number of NAC and MADS-box transcription factor in this cluster was the highest respect to the other three. All these evidences suggested that the breaker stage represent a critical step, during which the majority of the functional changes occurs, suggesting this step as the transition from the maturation to the full ripening phase. These two stages are in fact regulated by a general modification of the functional dynamics. Also cell wall enzymes like pectate lyase, pectin methyl esterase (PME), pectin acetyl-esterase were present only in this cluster. Recently AP2a, a putative tomato ortholog of AP2 transcritpion factor, showed an involvement in fruit ripening and in gene regulation [118]. Relative real time expression profile, showed that, in tomato, this ortolog gene increase highly its expression starting from breaker stage. It was presented that AP2a may activate genes like LOX, expansins or PME that are normally induced during ripening, and it has been defined as a positive ripening regulatory element [118]. This picture is similar to the data here presented for apple, where at the breaker stage several AP2, PME, LOX and expansin genes were up-regulated.

Polygalacturonase are enzymes that catalyse the hydrolytic cleavage of galacturonide linkages in the cell wall, contributing to pectin depolymerization in ripening fruits [88]. PGs were detected in the cluster presenting an increasing dynamics at the harvest stage, confirming a high cell wall modification during ripening. During this stage, in fact, all the processes that determine fruit senescence, and the consecutive seed dispersal, initiate. Other groups of genes were instead distinctive of the cluster having a decreasing trend during breaker and ripening (42 genes each), (Figure c, d 6.8). These clusters shared enzymes like the cellular component actin. In plants actin filaments are presumed to play essential roles in many important processes including cell division, cell elongation, establishment of cytoplasmic organization, pathogen response, tropisms, and pollen tube growth. During the end of the maturation and ripening process, cells do not divide or elongate anymore. It is thus reasonable and expected a decrease of the amount of actin transcripts, during the fruit ripening and the consecutive senescence. Auxin transcription factors and auxin efflux carrier protein family were included in the cluster of genes with a decreasing trend during

breaker, suggesting also a decreasing role of this hormone at the end of maturation. These results were also confirmed by previous works carried out on apple [164], where the Indolyl-3-acetic acid concentration showed a 3-4 fold increase prior to the rapid rise in ethylene concentration; and a following descrease to about its original level as ethylene rise occurred. Cellulase were instead present within the cluster presenting a decreasing dynamics after harvest, suggesting a role of these enzymes during the mature/early ripening stages rather than during the late ripening. A previous study, drived by Abeles and collaborators on developing apple fruit, determined that cellulase was present in young expanding fruit and decreased in activity as the it reached the full size and ripening [1]. This observation confirmed the identification of cellulase in the cluster presenting a decreasing dynamics after the harvest point (Figure d 6.8).

6.4.3 Transcriptome variation within the cultivars

The general differential expression investigated with the array allowed the discovery of a specific gene pattern for the two cultivars. The difference in transcript accumulation between the two varieties was depicted through the Venn diagram, which revealed as the number of genes differentially expressed (DEGs) between the two cultivars at the same stage were lower than the variation detected, for the singular cultivar, over the time course (Figure 6.9). For both cultivars, considering the complete time course analysed comparing two consecutive stages by the time, 925 and 654 were the non-redundant genes differentially expressed in Golden Delicious and Granny Smith, respectively. The Venn diagram (Figure b, c 6.9 and Table 6.2) reported the number of genes differentially expressed during the physiological ripening evolution. The transitions from flower to fruitlet, from mature green to breaker and breaker to harvest, were characterized by the highest number of DEGs highlighting these transitions as the most critical over the entire fruit maturation and ripening physiological process. During these stages, in fact, cells undergoes physiological and biochemical changes; requiring, hence, the activation of an important gene machinery.

To unravel the ethylene impact on the general fruit climacteric ripening, the normal ripening was compared with the one affected by the 1-MCP treatment. 1-MCP is an antagonist of the ethylene action, providing an opportunity to gain insight into the physiological mechanisms of fruit ripening. The effects of 1-MCP on the expression dynamics were detected comparing the genes differentially expressed between the control and the treated samples at the post harvest stage (Table 6.2 and Figure b, c 6.9). Is worth noting that, for both cultivars, the number of differentially expressed elements, between the harvest and post harvest control, and between the control and the treated samples was similar, suggesting a common physiological control (Table 6.2). Genes involved in the cell wall metabolism, secondary metabolism, plant hormone and transcription factors were influenced by the 1-MCP application. Within the genes involved in the ethylene synthesis and signalling, SAMs, ACOs, ACSs, EILs (ethylene

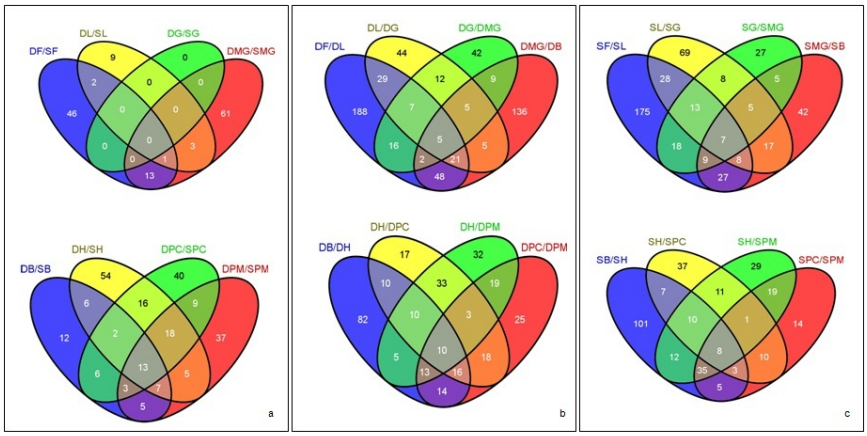

Figure 6.9: Gene differentially expressed visualized by a Venn diagram. Panel a reports the number of differentially expressed genes between cultivars, panel b within the same cultivar. Abbreviations: D, Golden Delicious; S, Granny Smith; G, green; MG, mature green; B, breaker; H, harvest; PC, post harvest control; PM, post harvest treated.

stages	Golden Delicious		Granny Smith	
	nr	r	nr	r
F-L	188	316	175	285
L-G	44	128	69	155
G-MG	42	98	27	92
MG-B	136	231	42	120
B-H	82	160	101	181
H-PC	32	117	37	87
PC-PM	25	118	14	95

Table 6.2: Number of the genes differentially expressed in the comparison between two subsequent stages of the two cultivars. The number of redundant (r) and non redundant (nr) genes is indicated.

insensitive like protein), ERFs (ethylene response factor), ETRs (ethylene receptors) and ERSs (ethylene response sensor) were down-regulated by 1-MCP. In particular genes belonging to the EILs and ERSs families, were differentially expressed in Golden Delicious only, while the other genes presented a decrease of their transcript accumulation in both cultivars. The general functional down-regulation of genes ethylene related is in agreement with the different ethylene dynamics assessed by PTR-ToF-MS at the postharvest stage, between the control and the treated condition. 1-MCP treatment of apple fruits resulted also in the down-regulation of several genes involved in cell wall degradation, such as cellulase, polygalacturonase, pectin esterase and pectin acetyl esterase. These genes modifying both middle lamella and cell wall, affect the final fruit texture. The obtained results are consistent with the data presented in a large trascriptome analysis carried out with μPEACH1.0 microarray platform on nectarine fruit treated with 1-MCP [248], and on tomato [219]. The treatment with 1-MCP had also an effect on cell walls, as demonstrated by the analysis performed with the texture analyser on the fruit at post harvest stage (Figure 6.2). Both acoustic and mechanical profiles presented differences in their dynamics when compared with the control samples. This imply a direct involvement of ethylene in the regulation of cell wall enzymes, and a delay of the cell wall and middle lamella disassembly after harvest by 1-MCP. Light harvesting chlorophyll A/B binding protein (members of the cellular component class), were up-regulated in both cultivars after the treatment, with an higher number of differentially expressed genes in Granny Smith. The increased accumulation for these transcripts, caused by the inhibitors, proposed a retardation of the expression dynamics occurring during the time course and a delay in the ripening process. Also the class of transcriptor factors was influenced by 1-MCP, confirming previous data reported in apple performed with a heterologous cDNA microarray [45]. In both studies the application negatively affected the expression of genes belonging to the bZIP, showing an ethylene dependent regulation. Other elements like MADS-box, NAC, and AP2, on the contrary, were stimulated by the inhibitor, suggesting negative regulation by the hormone. This regulation suggests an effort of the fruit to re-activate the functional machinery, in order to restore the normal physiology. The classes not influenced by the inhbitor, in both varieties, were genes belonging to the aminoacidic and carbohydrates pathways. Biological processes were not affected in Granny Smith and regulatory processes and energy pathway in Golden Delicious. The observations suggested that these processes are more time development regulated.

6.4.4 Transcriptome variation between cultivars

In order to enlight the gene activation dependent by the different genetic background, a transcription investigation was also performed between the same stage of the two cultivars. The pairwise comparison identified 259 non redundant genes (Figure 6.9). At the flower stage 62 genes were differentially expressed

between the two cultivars (Table 6.3). In particular Golden Delicious presented an higher espression of bHLH transcription factor, several genes belonging to the ACO multigene family, chitinases, LOX and Xet. In Granny Smith genes as expansins and pectate lyase were more expressed respect to the other cultivar. At fruitlet and green stage, 15 genes resulted differentially expressed in the first stage, while no difference was observed in the second (Table 6.3 and Figure a 6.9). This suggested that at the initial stages of fruit development and maturation, the different cultivars could be regulated by a common gene network, which became more specific with the progress of ripening.

stages	GD vs GS
F	62
L	15
G	0
MG	78
B	54
H	121
PC	107
PM	97

Table 6.3: Number of the differentially expressed genes between the same stage of the two cultivars. Abbreviations: D, Golden Delicious; S, Granny Smith.

From the mature green stage, the two varieties were more distinct. Among 78 genes differentially espressed between the cultivars, 18 of them presented an higher expression in Granny Smith (Table 6.3 and Figure a 6.9). These were cell wall proteins and ethylene genes related as extensins, expansins and ERF transcription factor genes. In Golden Delicious 60 genes were more expressed, belonging to transcription factors (bHLH and MADS box proteins), genes involved in the secondary metabolism like chalcone isomerase, chalcone syntase, AAT, LOX and cell wall genes (pectin acetyl esterase and cellulase). From this functional picture resulted that mature green stage can be considered as a "turning point", as the differences in transcript accumulation between the cultivars started to be more evident. At the breaker stage 54 genes were differentially expressed between the cultivars (Table 6.3 and Figure a 6.9). Among them, all the ACO genes presenting a differential transcript accumulation at this stage, were more expressed in Golden Delicious, as well as SAM and Xet members (exept for one). The same pattern of gene expression was also presents at the harvest point, where 121 genes resulted differentially expressed (Table 6.3 and Figure a 6.9). Golden Delicious presented an higher expression for most of the ACO, ACS, ETR, expansin, Xet and ERF, genes mainly involved in the hormone metabolic pathway and perception. The observation of their lower expression in Granny Smith is in agreement with the lower ethylene production measured during the ripening of this cultivar (Figure 6.1). The different functional dy-

namics of genes ripening specific, supported by the distinct ethylene production assessed, suggests as an anticipated and high expression of this gene set might also control the different harvest time. These two cultivars were, in fact, harvested with 26 days of difference. Transcription factors such as MADS box and NAC were instead more expressed in Granny Smith. The late functional transcript accumulation of this set of transcription factors in Granny Smith at this stage (compared to Golden Delicious) suggest that this cultivar has a delayed ripening initiation, hypothesis also supported by the lack of an evident ethylene burst. A differential mode of activation in this gene-set might be the causal effect of the different ripening between these two cultivars. 107 genes resulted differentially expressed at the post harvest stage (Table 6.3 and Figure a 6.9), with ACS, ACO and SAM genes more expressed in Golden Delicious, confirming the different ripening physiology between these two varieties. *Md-PG1*, a gene known to be involved in the cell wall modification and, consecutively, in texture determination, is also more expressed in Golden Delicious than Granny Smith. This results confirms the previous QTL survey and candidate genes association study ([143], and chapter 5), which proposed this gene as a relevant genetic element for the genetic control of the apple textural attributes. The differences in the transcripts accumulation between the two cultivars finds consistency with the two different texture behaviours (Figure 6.2), in particular with the acoustic profile. Two are the main differences in the acoustic response of the two varieties. The first is that, while in Golden Delicious the acoustic response increase until harvest, and the decrease towards the post harvest, in Granny Smith the profile remained almost unmodified after harvest until the end of the time course. The second was that in Granny Smith, at post harvest stage, the number of the acoustic peak was noticeably higher than in Golden Delicious; having the cultivars 87 and 29 peaks respectively (Table 6.1). However, there were differences also at the mechanical profile. The number of the peak force were for Granny Smith 23 and 7 for Golden Delicious, evidencing thus a similar mechanic profile dynamics between the two cultivars, but with different properties. This different physical response was also biologically enlightened by the analysis performed with the S.E.M., at the post harvest stage (Figure 6.4). Post harvest samples treated with 1-MCP showed an anatomical structure similar to the harvest. In this stage 97 genes were differentially expressed between the two cultivars (Table 6.3 and Figure a 6.9), with ACO, ACS, expansins and pectate lyase more expressed in Golden Delicius, while MADS box and NAC transcription factors more expressed in Granny Smith. The application of 1-MCP, competing with the ethylene perception, delayed the general ripening physiology. However, a similar functional pattern to harvest of the treated samples, suggest a reactivation of the functional machinery , in order to restore the normal ripening physiology.

6.4.5 Candidate genes dynamics

This microarray platform was used to highlights the gene dynamics of a particular set of genes specifically involved in the fruit ripening process, such as cell wall enzymes and plant hormone metabolism. To enlight the functional impact of these genes on the final ripening, the accumulation trend was analysed in correlation with the evaluation of the texture and ethylene physiology. *PG* are pectin-degrading enzymes that catalyse the hydrolytic cleavage of galacturonide linkages in the middle lamella, contributing to its modification. An increase in the activity of this enzyme has long been associated with fruit ripening in many studies although the amount detected varies widely during the different ripening stages of different species [88],[2] . The main *PG* involved in the apple ripening, indicated as *Md-PG1* (MDP0000326734) was mapped on LG10 co-locating with important QLTs associated with several texture sub-traits [48],[143]. In this study, *Md-PG1* showed a low accumulation during the initial stages of fruit development, and started to increase after breaker towards the end of the time course, where it reached the highest level. This profile underlined the involvement of this gene in the fruit ripening, validating its role in the final texture determination (Figure 6.10). For this gene was detected an increased expression of 4.4 and 4.7 fold between breaker and harvest in Golden Delicious and Granny Smith respectively. *Md-PG1* increased in the gene expression of 2.4 fold between harvest and post harvest in Golden Delicious, while no differential expression has been detected for the same stages in Granny Smith. The difference between the two cultivars at post harvest was, in fact, 1.6 fold. The differential expression between the cultivars at the post harvest stage, reflected the textural profiles, especially the acoustic trend (Figure 6.2). For both cultivars, at harvest, this gene showed a consistant functional profile, suggesting an initial common regulation (Figure 6.2). During the late ripening stage a more specific functional expression was observed, suggesting a specific gene activation cultivar dependent. The functional dynamics of *Md-PG1* between the two cultivars was in agreement with the acoustic profile evolution. In Golden Delicious, in fact, *Md-PG1* expression increased, while the acoustic profile decreased. In Granny Smith, on the contrary, the unchanged acoustic profile was supported by an un-modified transcription accumulation of this gene (Table 6.3). While, in fact, during harvest the number of acoustic and force peaks for the cultivars were similar, the differences were considerable more evident during the post harvest stage. This validated the different texture behaviour existing between the two cultivars, which, at post harvest was more evident than in other stages. After 1-MCP treatment, the *Md-PG1* level decreased considerably in both cultivars, reaching the same level as detected at the breaker stage, confirming the ethylene regulation of this gene [29]. A comparison between the control/treated post harvest samples, showed a reduction of transcript accumulation of 7 and 5.7 fold change in Golden Delicious and Granny Smith respectively. Also this result finds consistency with the texture profiles assessed.

Textural profiles (acoustic and mechanical) of the treated post harvest stage was similar as the one registered during the harvest (Table 6.3). The higher fold change measured for *Md-PG1* was detected for Golden Delicious in the comparison between normal and 1-MCP treated post harvest stage. This difference is functionally aligned with the ethylene reduction caused by the treatment, highlighting as this gene is included in the downstream ethylene related pathways. Considering the strict relationship existing between PG1 and ethylene [204], the clear reduction on the gene expression indicated that ethylene action is markely inhibited by 1-MCP. In the apple ethylene bio-synthetic pathway, the major gene is represented by *Md-ACS1* (MDP0000370791), which catalise the conversion of SAM to 1-aminocyclopropane-1-carboxylic acid (*ACC*) the ethylene precursor. *Md-ACS1* transcripts accumulation increased of 3.2 and 2.4 fold in Golden Delicious and Granny Smith respectively, between harvest and post harvest control stages (Figure 6.10). Also for this gene the application of 1-MCP caused a reduction of 3.2 fold change between the post harvest control and the post harvest treated samples in Golden Delicious, showing a transcript accumulation level similar to the amount registered during harvest. No differences were instead detected for Granny Smith. The *Md-ACS1* accumulation suppression in apple, after 1-MCP treatment, has been reported also in previous works [54],[216], indicating that this gene might represent a crucial factor in the hormone synthesis and fruit ripening. The last enzyme involved in the ethylene biosynthetic pathway is ACO. This enzyme catalyse the final conversion of ACC to ethylene. *Md-ACO1* functional profile was similar for both cultivars, showing an increased gene expression along the time course, reaching the highest level at the harvest point (Figure 6.10). In Golden Delicious and Granny Smith an increase of 7 and 6.8 fold times between breaker and harvest was detected. The fold change of this gene in Golden Delicious is the highest functional variation detected in this transcriptional investigation. For *Md-ACO1* no significant differential expression was detected from harvest to post harvest, as well as after the treatment, for both cultivars. Among the genes involved in the ethylene synthesis, *Md-ASC1* in Golden Delicious was highly down-regulated (3.2 fold) after the action of 1-MCP. These results were consistent with the data presented for the same cultivar by Dal Cin *at el.* [54], which detected a reduction of *ACS* transcript accumulation after the treatment. Also the results obtained analysing the transcript accumulation of *Md-ACO1* after the treatment are confirmed by a previous study realysed on two different apple cultivars; Orin and Fuji [216]. In this work Tatsuki and collegues determined that *Md-ACO1* expression did not decrease in 1-MCP-treated Orin fruit, and it decreased very slowly in 1-MCP-treated Fuji fruit respect to control samples. In the work of Dal Cin and collegues [54], a parallel between apple and peach, both climacteric fruit, after 1-MCP treatment was presented, showing as the two species reacted differently to the inhibition of the ethylene synthesis. In opposite with the data presented in this study for apple, in peach, the enzymes involved in the ethylene synthesis seemed to be slightly affected by the inhibitor. The authors hypotized that

the different response to 1-MCP might be related to differences in terms of expression pattern or turn-over of the ethylene receptors. The different ripening and shelf-life physiology between apple and peach can be thus controlled by a distinct functional ethylene production and perception mechanism. A possible different ethylene sensitivity might be the cause of the different fruit texture and storability between the two species. Among the genetic elements analysed with the array, also ethylene receptors were investigated. Among the element belonging to this family, two genes, ETR and ETR2 (MDP0000393617, and MDP0000195916 respetively; both mapped on LG5), presented a similar trend of differential expression during the last stages of fruit ripening (Figure 6.10). The transcript for both genes was up-regulated from breaker to harvest. The two ETR genes presented a hormone dependent regulation, being the expression level reduced significantly in post harvest treated samples in respect to the control in both cultivars (1.4 and 1.8 fold for ETR in Granny Smith and Golden Delicious respectively and 1.7 and 1.9 for ETR2, in Granny Smith and Golden Delicious respectively). The specific expression of these two elements can be involved in the transition from the system 1 (pre-climacterium) to the system 2 (full climacterium phase) of the ethylene pathway. Other elements belonging to the ETR family, did not show any particular regulation over the time course, suggesting the co-existance of dependent and independent ethylene gene regulation. Cell wall degradation is a physiological process regulated by a coordinated action of several genes. Among them, expansin have been proposed as one of the major enzymatic agent in cell-wall modification [44]. In this study the expression of the expansin gene family resulted quite consistent between the two cultivars.

Two genes (exp_a, MDP0000431696 and exp_b, MDP0000772420; both mapped on LG1), however, showed a significant increased expression at the mature green stage in Golden Delicious, reaching the highest accumulation at the post harvest (Figure 6.11). During the evolution from breaker to harvest, their expression increase of 2.1 and 1.7 times respectively. Exp_a showed also an increased expression (1.3 fold) from harvest to post harvest. Contrary to Golden Delicious, the expression level of these two expansin in Granny Smith was very low during the entire time course, without showing any differential expression. At the harvest point, the expression of exp_a was 2.4 times higher in Golden Delicious respect to Granny Smith, while exp_b was 2.1 times higher. At post harvest the expression of the exp_a was 2.8 times higher in Golden Delicious respect to Granny Smith, while exp_b, was 3.4 times higher in Golden Delicious than in Granny Smith. These indications, together with the identification in previous studies of QTLs associated to texture traits in the linkage group 1, support their involvement as important candidate in the texture control [50]. The reduced expression of the two elements in Golden Delicious after the 1-MCP treatment (of 2.9 for exp_a and 1.8 for exp_b), confirmed their ethylene dependent regulation, as initially proposed in tomato [188]. Another expansin gene (exp_c, MDP0000292477) was detected as differentially expressed, but with a higher

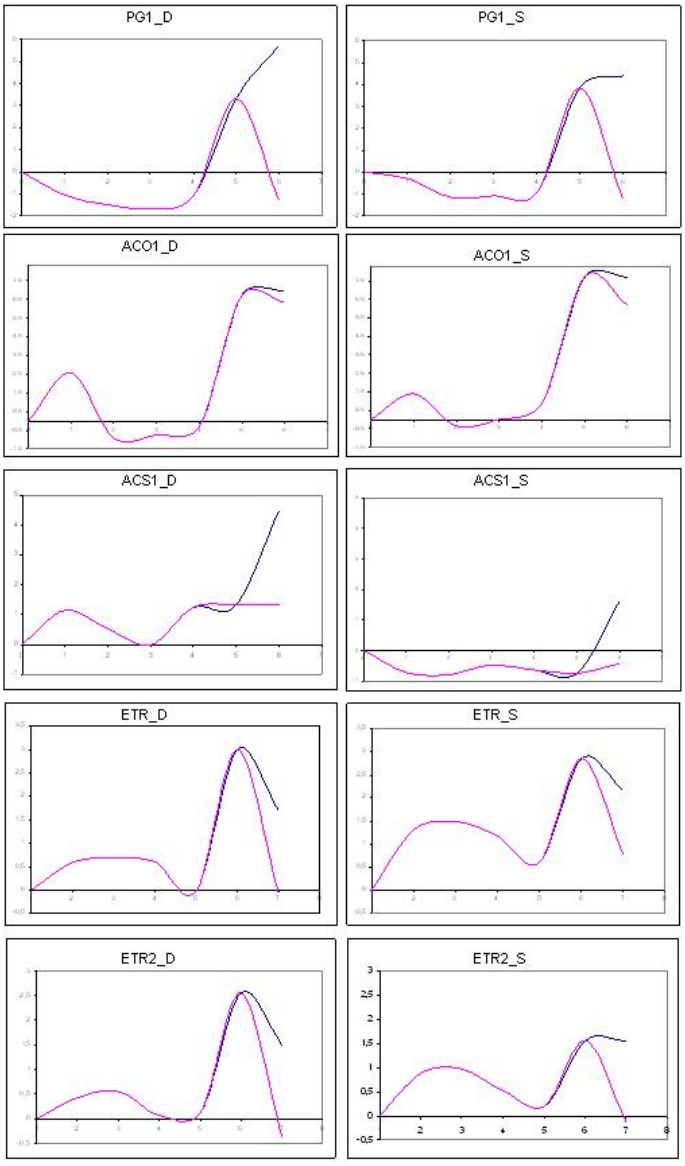

Figure 6.10: Expression pattern for the a set of genes involved in ethylene and cell wall metabolism. The blu line indicates the control samples, the red line indicates the samples treated with 1-Methylcyclopropene. Abbreviations: D, Golden Delicious; S, Granny Smith; PG1, polygalacturonase; ACO1, aminocyclopropane-1-carboxylate ossidase; ACS1 aminocyclopropane-1-carboxylate synthase; ETR, ethylene receptors

accumulation in Granny Smith respect to Golden Delicious [143],[36](Figure 6.11). During harvest and post harvest, this expansin was 1.9 and 1.6 times higher in Granny Smith than in Golden Delicious, respectively. In Granny Smith the dynamics increased 2.4 times from breaker to harvest and reached its highest value at the post harvest. The expression of this expansin resulted also functionally controlled by ethylene, since decreased 2 times between the control and the treated Granny Smith samples. In Golden Delicious there was no differentially espression among any considered stages for the expansin, suggesting a possible differential expression based on genetic background. Another gene that showed an up regulation over the Golden Delicious ripening stages is the pectin esterase gene (MDP0000251256). Its expression increased of 2.4 fold from breaker to harvest, and 1.3 fold from harvest to post harvest (Figure 6.11), showing an ethylene-related dynamics. The direct ethylene regulation on the expression of this gene was proved by 1-MCP, which down regulated its accumulation by 4.2 fold. The expression of this cell wall gene did not present any significant differential expression in Granny Smith for any of the pairwise comparison carried out among the considered stages, confirming its activation ethylene dependent. The two cultivars presented significant differences of the expression level of this gene, both at harvest and post harvest. At harvest, Golden Delicious showed an expression of the pectin esterase 2.3 times higher than Granny Smith, while the value was 2.6 higher during post harvest. The functional profile investigated in this survey, highlighted as ripening in apple is characterized by both developmentally and climacteric ripening dependent mechanisms. The last stages resulted also controlled by few specific genetic elements belonging to the principal gene families involved in the ripening process. This gene-set might be considered as a novel set of candidates for the design of new association mapping study to improve the dissection of important trait related to apple fruit quality.

6.5 Conclusion

The aim of this work was the functional dynamics investigation of a specific set of genes during the major ripening physiological changes (mainly fruit texture and ethylene). The assembling of the gene-set started from the identification of the genomic intervals detected in the QTL mapping survey, oriented to genetically dissect the fruit texture complexity. Due to the fact that this gene-set was initially selected because statistically associated to the phenotype detected only after two month of cold storage, additional understanding were necessary to better define their involvement in fruit climacteric ripening control. The genomic approach presented here, based on a custom microarray platform, provided a picture of a sub-set of molecular events occurring during apple fruit development, maturation and ripening. This investigation also contributed to gain knowledge about the complex regulatory machinery of these physiological events. The analysis of the transcription profiles over the time course in two

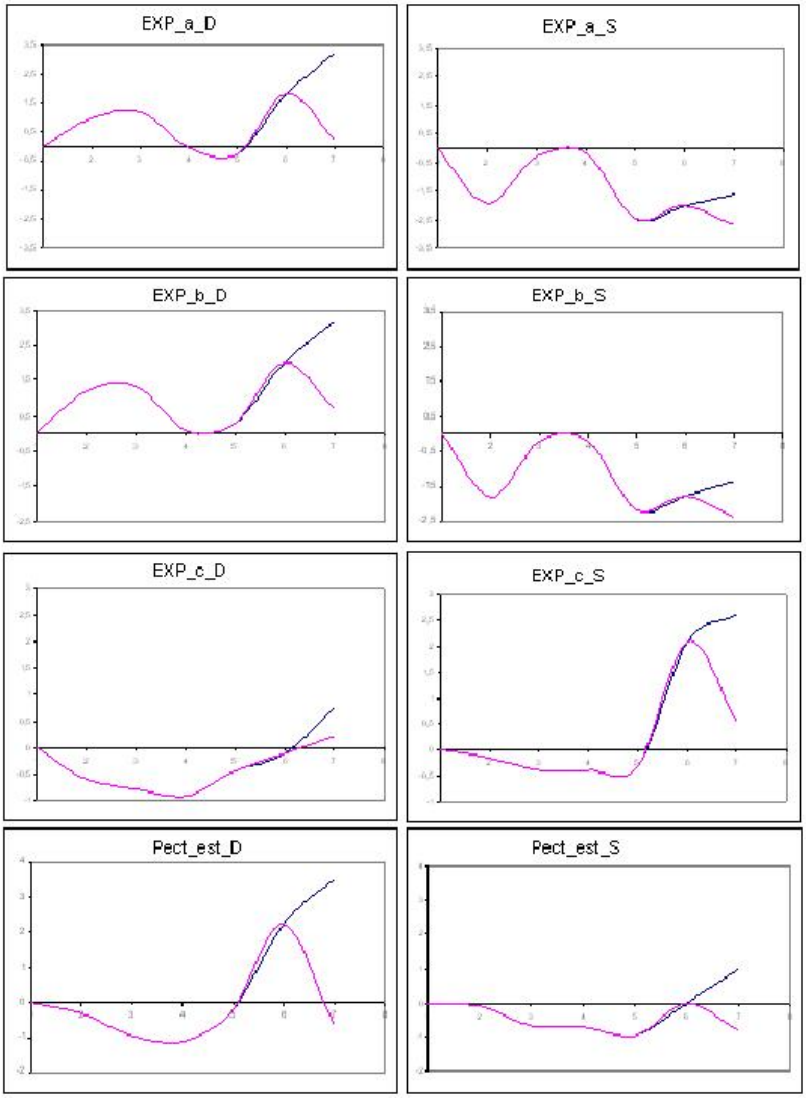

Figure 6.11: Expression pattern of cell wall genes. The blu line indicates the control samples, the red line indicates the samples treated with 1-Methylcyclopropene. Abbreviations: D, Golden Delicious; S, Granny Smith; Exp, expansin; Pect_est, pectin esterase

apple cultivars, characterized by a different ripening behaviours, allowed the identification of the stages for which the most evident functional variation occurred. These stages might be though as a crucial steps in the complex changes acting to turn the hard fruit into soft and edible. Among the several stages composing the ripening time course here defined, the last one, proper of the post harvest shelf-life ripening, represented the fundamental stage. Ethylene, the hormone coordinating the physiological events leading to the final fruit quality, is in fact produced after harvest, and its accumulation directly control other processes, such as fruit texture. In this view, it is important to define the functional pattern to highlight the genes specifically involved in the late ripening stage. However, ethylene dependent and independent responsive pathways are known to co-exist in different species. To dissect this functional interplay and to shed light on the regulatory processes underlying the ripening changes, the ethylene competitor 1-MCP was employed in addition to the cultivar comparison. The parallel between Golden Delicious and Granny Smith emphasized putative candidate genes with exclusive dynamics for genetic background and ethylene relationship, which could be considered as new target for texture complexity dissection. The results here obtained can be exploited in future works aiming to define the specific gene-set involved in the control of both mechanical and acoustic texture components. This will improve the knowledge to date available about the cell wall disassembly, as well as the definition of a novel set of candidate gene to exploit for the design of new functional makers suitable for assisted breeding programs toward the creation of ideotypes with superior fruit quality.

CHAPTER 7

Conclusions and future prospects

Fruit quality is measured accomplishing four main principal factors, among which texture is one of them. Texture, for apple in particular, is a fundamental trait accounting for most of the consumers appreciation. It is directly perceived by human senses, therefore it allows the distinguishing of a particular food or fruit and drive the preference towards an apple variety respect to another. Texture has also the capacity to influence directly the general fruit quality, regulating the maintenance during shipping and shelf life. Considering the importance of fruit texture on the quality of fresh apple, many research groups initiated, in the last decade, programs aimed to investigate the genes controlling the dynamics of this trait. Breeding, in fact, can take advantage of biotechnological applications, such as molecular markers, providing prediction power associated to a specific trait of interest. Technological improvement in genotyping techniques, and the following decrease in cost analysis, made the high-throughput genotyping feasible and economically affordable. However, despite this great improvement, phenotyping investigation is nevertheless much more limited. The study of a specific trait, in fact, is still affected by too individual investigations, inadequate instrumentations or insufficient technologies for the dissection of complex phenotypes on large sample sets. Most of the phenotyping are still based on estimation rather than analytical measures, consequently reducing the quote of variability necessary to increase the statistical power of the association studies programs, designed to target new elements involved in the control of important agronomical traits. Currently apple texture measurements and phenotypic observations are both instrumentally and sensorially performed. This, however, is not sufficient for a complete and accurate phenotyping investigation of all the peculiarities describing apple texture in a time-efficient fashion.

To improve the texture comprehension and sub-traits dissection, a new high

resolution phenomics strategy has been adopted and employed. In order to prove the concept of this combined methodology, data were collected within the most large assembled apple collection to date analyzed. This approach allowed to measure simultaneously both mechanical and acoustic parameters, focusing the interest in particular on apple crispness. Unlike other instrumental evaluation that measure single data point, this strategy dissected the apple texture measuring simultaneously 14 different parameters, which can represent new potential quality descriptors. These parameters have been further used to characterize the texture behaviour of two bi-parental populations, *ad-hoc* chosen to capture most of the texture variability.

The combination of the texture dissected parameters with the set of SSR and SNP markers, high throughput genotyped, allowed to performe a comprehensive QTL mapping analysis related to fruit texture. A wide number of QTLs specific for mechanical and acoustic components have been identified. The major QTL hot spots identified in the two populations co-located with candidate genes involved in the fruit texture control, such as polygalacturonase on LG10, xyloglucan endo-transglycosylase on LG12 and xyloglucan-xylosyltransferase on LG16. The observation in the two population, of three hot-spots on different linkage groups, could suggest a possible interplay and a physiological epistatic effect between candidate genes. In particular, PG enzyme, which acts on the middle lamella, controls almost 50% of texture variation, characterizing crispy and mealy apple fruit. From the genetic picture observed, it has been hypothesized that when PG is not active other genes involved in the degradation of cell wall polysaccharides structure may take important roles, previously masked by the action of PG.

The QTL analysis and the identification of specific regions involved in the texture definition, provided the starting point for a candidate gene association study in order to pinpoint the alleles effectively associated with the rate of phenotypic variability. Two genomic elements underlyined by the QTL analysis (PG on LG10 and a Xet on LG12), were then fine mapped through an association analysis, chosen to overcome the linkage analysis limitations. Due to the relative percentage of variability explained by the PG and Xet genes, which confirms the complex nature of this phenotype, and the possible low linkage disequilibrium present in apple, candidate gene driven association mapping seemed to be a valuable strategy to pinpoint molecular markers useful in assisted breeding programs. Beside the four haplotypes associated with a set of traits investigated, the use of the Golden Delicious genome allowed the identification of a SSR marker targeted in the PG region, showing significant and consistent association with both acoustic and mechanical traits. For this marker was moreover observed an allelic dosage effect on the fruit texture distribution, suggesting this allele as a valuable marker for assisted breeding towards the selection of new superior varieties.

Aware of the important results obtained with the CG approach, together with the incomplete percentage of variability explanied by the PG allele marker on

the trait, additional studies aimed to identify new genes involved in the texture determination have been performed. Knowledge on candidate gene function and mode of activation is, in fact, a fundamental requisite to target novel elements involved in the physiological pathways of interest. For this reason, a functional profiling on two main apple cultivars was performed in order to capture gene dynamics over the fruit development and ripening. To performe this functional investigation a Combimatrix platform was chosen, on which genes involved in the cell wall modification, secondary metabolism, hormone pathway and transcription factor oligos were synthesized. In order to study the transcription profile correlated with the cell wall modification and texture, and their connections with ethylene biosynthesis, the hormone competitor 1-MCP was applied to compete with the normal climacteric physiology. This treatment allowed the identification of different gene classes which expression was affected by the hormone. Cluster analysis allowed the identification of the gene kinetics occurring at the onset of the climacterium, grouping together gene categories having the same functional trend, thus possibly related by the same physiological mechanism. Further analysis will be performed to define the set of genes specifically related to mechanical and acoustic profiling, which can be exploited in future association mapping works to improve the genetic picture currently defined.

Fruit texture is a multifaceted and complex trait. This Ph.D. step forward in the comprehension of this complex physiology, enlightening some fundamental genetic elements responsible for fruit texture control. These genes can represent the basic knowledge for future association mapping studies, aimed to improve the marker efficiency towards the assisted selection of novel apple accessions characterized by valuable texture quality.

CHAPTER 8

Supplementary material of chapter 3

N.	Cultivar	Location	Sensorially tested	Harvest Date
1	Ambrosia	TN	S	08-Sept
2	Ananas Renette	BZ		27-Aug
3	Ariane (Les Naturiannes)	BZ	S	28-Aug
4	Ariwa	TN		18-Sept
5	Baujade	TN		29-Sept
6	Bellida	BZ		17-Aug
7	Boskoop	TN		31-Aug
8	Braeburn	TN	S	30-Sept
9	Brina	BZ		31-Aug
10	Brixner Plattling	BZ		10-Sept
11	Calamari	TN		25-Aug
12	Caudle (Cameo)	TN		1-Oct
13	Calvilla	TN		25-Sept
14	CIVG198 (Modi)	TN		8-Sept
15	Civni (Rubens)	TN	S	31-Aug
16	Coop39 (Crimson Crisp)	TN	S	17-Aug
17	Crimson Snow	BZ		20-Oct
18	Cripps Pink (Pink Lady)	TN		28-Oct
19	Cripps Red (Sundowner)	TN		15-Oct
20	Croncels	BZ		03-Aug
21	Dalinette (Choupette)	BZ	S	5-Oct
22	Dalitron	BZ		2-Sept
23	Dalla Rosa	TN		25-Aug
24	Delblush (Tentation)	TN		22-Sept
25	Delcorf (Delbarestivale)	BZ	S	17-July
26	Delcoros (Autento)	BZ	S	28-Aug
27	Delearly	TN		4-Aug
28	Delfloki	BZ	S	21-Sept
29	Delorina (Harmonie)	TN		30-Sept

30	Early Gold	TN		25-Aug
31	Edelböhmer	TN		11-Sept
32	Elstar	TN		31-Aug
33	Fiamma	TN		25-Aug
34	Florina	BZ		11-Sept
35	Fuji	TN	S	6-Oct
36	Gala (Brookfield)	TN		26-Aug
37	Gala (Schniga)	TN		26-Aug
38	Galmac	BZ	S	17-July
39	Gelber Edelapfel	BZ		17-Aug
40	Gewürzluiken	BZ		23-Aug
41	Gloster	TN		18-Sept
42	Golden Delicious	TN	S	16-Sept
43	Golden Orange	TN	S	30-Sept
44	Granny Smith	TN		29-Sept
45	Gravensteiner	BZ		30-July
46	Idared	TN		29-Sept
47	Jonagold	BZ		28-Aug
48	Kronprinz Rudolf	BZ		17-Sept
49	La Flamboyante (Mairac)	BZ		9-Sept
50	Ligol	BZ		21-Aug
51	Limoncini	TN		25-Aug
52	Magre'	TN		22-Sept
53	Maigold	BZ		21-Sept
54	Milwa (Junami)	BZ		11-Sept
55	Minnewashta (Zestar)	BZ	S	23-July
56	Napoleone	TN		31-Aug
57	Nevson (Sonya)	BZ	S	26-Aug
58	Nicogreen (Greenstar)	BZ	S	2-Sept
59	Nicoter (Kanzi)	BZ		9-Sept
60	Permain dorato	TN		26-Aug
61	Pilot	TN		8-Sept
62	Piova	TN		18-Sept
63	Rafzubin (Rubinette)	BZ		24-Aug
64	Red Delicious (Red Chief)	TN		8-Sept
65	Red Delicious (Red Chief 4047)	TN		8-Sept
66	Red Delicious (Hapke Delicious)	TN		8-Sept
67	Red Field	TN		26-Aug
68	Renetta Canada	TN		8-Sept
69	Rome Beauty	BZ		29-Sept
70	Rosa di Caldano	TN		11-Sept
71	Rosa Doppia	TN		11-Sept
72	Royal Gala	TN		17-Aug
73	Rubinola	TN		26-Aug
74	Sansa	BZ	S	6-Aug
75	Santana	BZ	S	17-Aug
76	Saturn	TN		31-Aug
77	Scarlet	TN		10-Sept
78	Scifresh (Jazz)	BZ	S	9-Sept

79	Scilate (Envy)	BZ	S	29-Sept
80	Shinano Gold	BZ	S	11-Sept
81	Stayman Red	TN		1-Oct
82	Summerfree	TN		26-Aug
83	Tiroler Spitzlederer	BZ		15-Oct
84	Topaz	TN		10-Sept
85	Weisser Rosmarin	BZ		25-Sept
86	Weisser Wintertaffet	BZ		7-Sept

Table 8.1: List of the 86 cultivars, with harvest date for 2009.Supplementary material Table 1. Brackets report the trade mark (when available), "S" points the varieties used in the sensorial evaluation. N: code number for each cultivar as reported in the PCA plot. In the location column, TN and BZ are for Trento (FEM) and Bolzano (Laimburg) respectively.

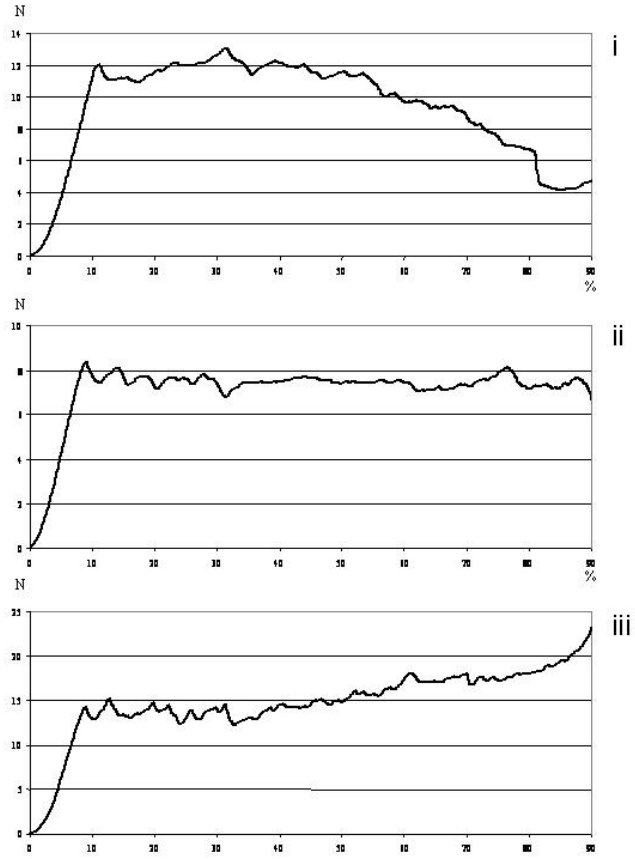

Figure 8.1: Three different type of mechanical profiles. In the three panels is plotted the dynamics of the force direction, where the yield point is at a higher (i), similar (ii) and lower (iii) level respect the final point.

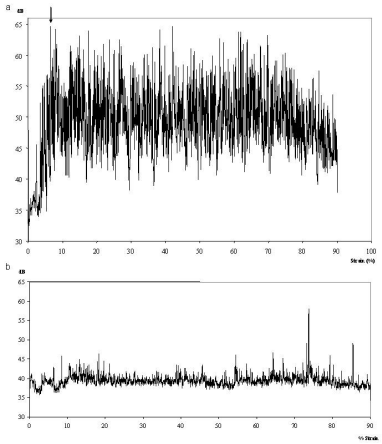

Figure 8.2: Sound pressure profiles generated during the mechanical penetration registered by the microphone and converted in dB. In the panel a is reported the acoustic profile of an apple characterized by a high sound pressure wave. Arrow points the main peak registered over the acoustic profile. In figure b is showed a profile of a sample characterized by a mealy texture

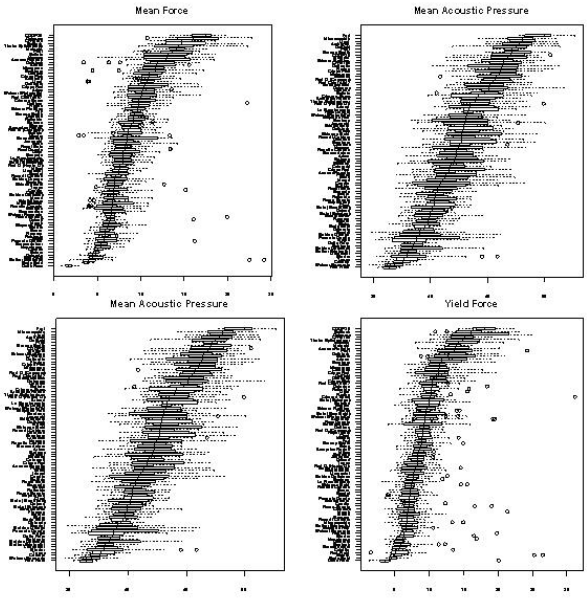

Figure 8.3: Box plot of the textural parameters measured for the 86 apple cultivars. Black line within each box represent the median, the width of the box is the data interquartile, dashed lines show the standard deviation and dots point the outliers.

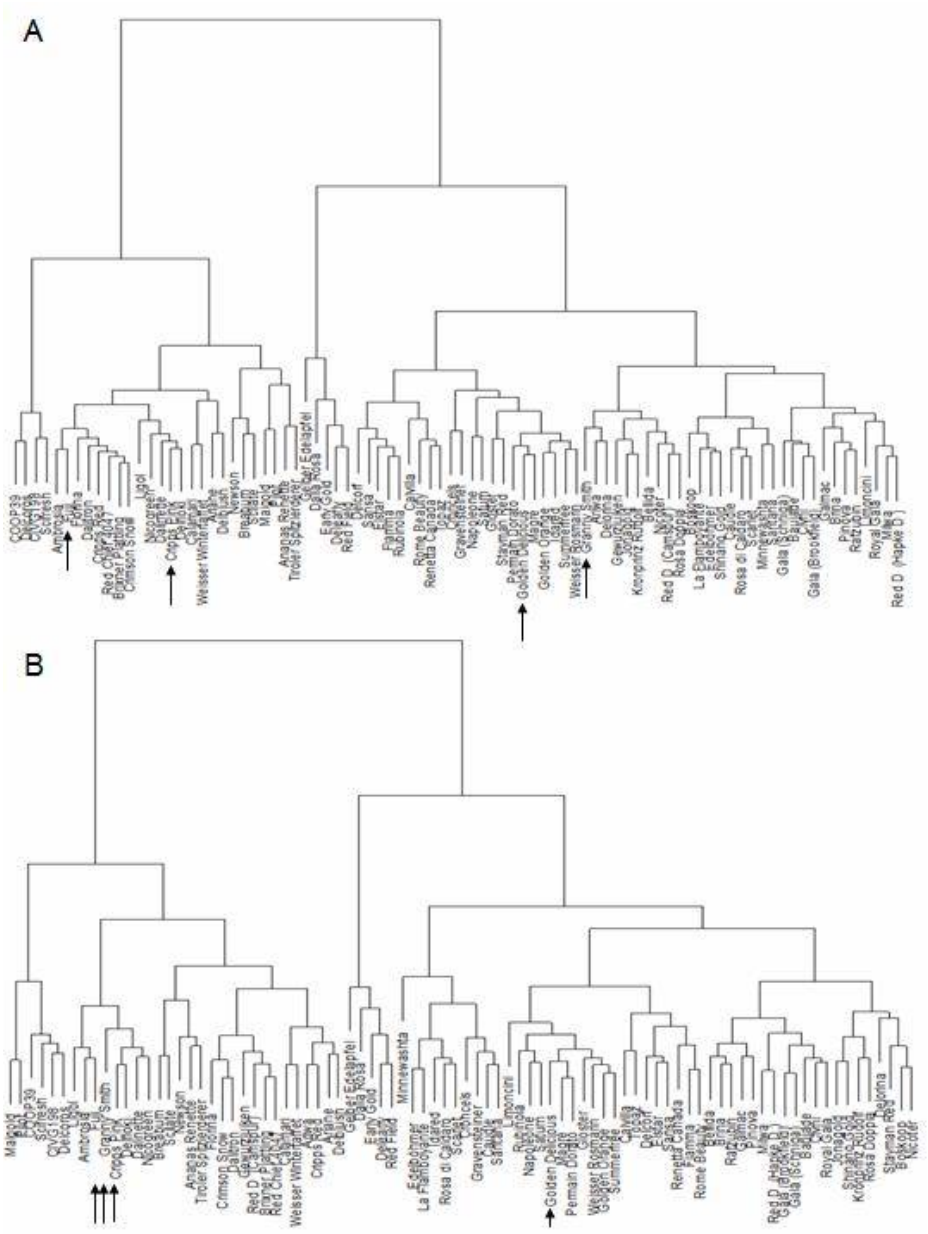

Figure 8.4: Similarity dendrogram computed for the 86 apple cultivars considering: a) mechanical parameters, b) mechanical and acoustical parameters. Arrows indicate Fuji, Cripps Pink, Granny Smith and Golden Delicious.

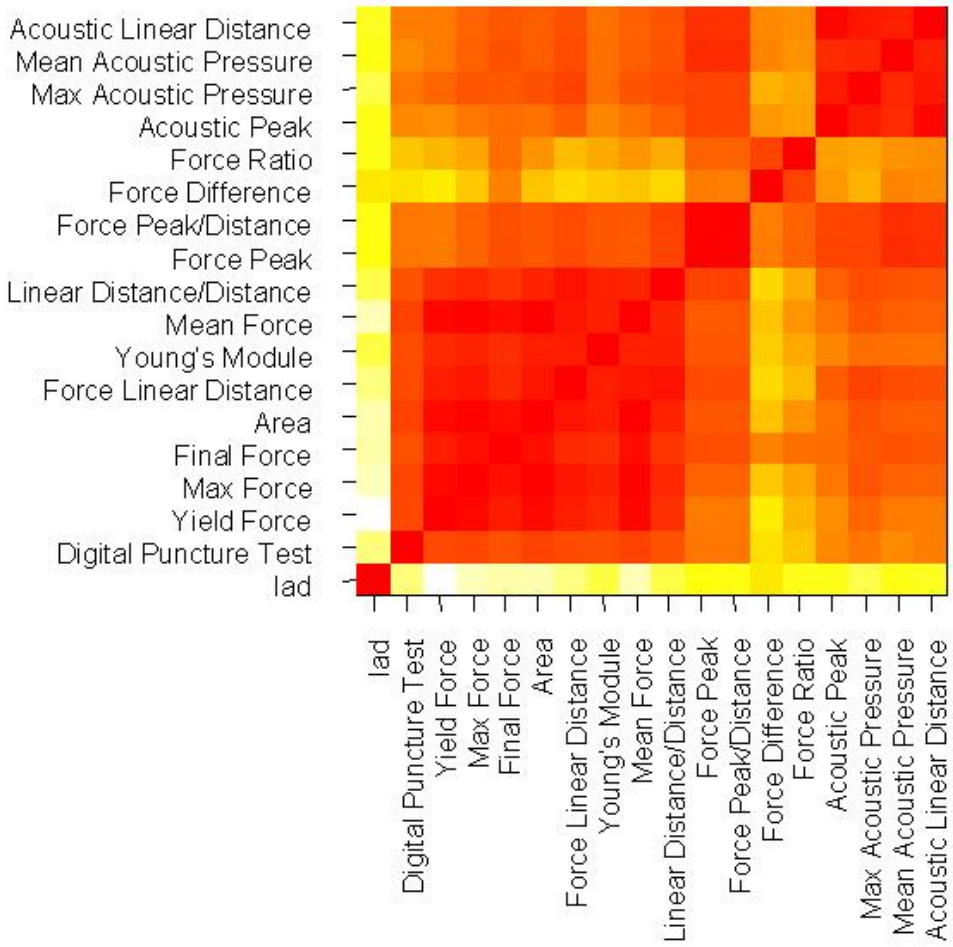

Figure 8.5: General Pearson correlation matrix visualized by a heat map plot calculated among all the parameters identified for mechanical and acoustic profiles. In the computation were also included also the IDA index for the ripening stage assessment and the fruit digital puncture test.

CHAPTER 9

Supplementary material of chapter 4

SNP	LG	FJ	PL	DEL
CONS12	–	p	np	–
CONS14	3	np	np	p
CONS17	2	np	p	p
CONS22	11	p	np	np
CONS40	2	np	p	p
CONS48	14	p	p	np
CONS49	–	p	np	p
CONS52	10	np	p	p
CONS78	8	np	p	p
GD SNP00004	11	np	p	np
GD SNP00013	16	np	–	p
GD SNP00014	1	np	p	p
GD SNP00022	2	p	p	p
GD SNP00029	11	np	p	np
GD SNP00031	15	p	–	np
GD SNP00033	9	np	np	np
GD SNP00034	11	np	np	np
GD SNP00035	2	p	–	np
GD SNP00037	11	np	p	np
GD SNP00042	4	np	–	p
GD SNP00045	9	p	p	p
GD SNP00047	16	p	p	–
GD SNP00048	14	p	np	np
GD SNP00051	7	p	np	p

GD SNP00053	9	p	p	p
GD SNP00058	17	p	p	p
GD SNP00060	13	np	p	np
GD SNP00061	–	np	np	np
GD SNP00062	14	p	p	np
GD SNP00063	4	np	np	np
GD SNP00065	10	np	p	p
GD SNP00066	1	np	np	np
GD SNP00067	13	np	p	p
GD SNP00068	12	np	–	p
GD SNP00069	16	p	np	np
GD SNP00071	16	p	p	np
GD SNP00074	1	np	np	np
GD SNP00078	3	p	np	p
GD SNP00079	15	p	p	p
GD SNP00080	3	p	np	–
GD SNP00083	5	p	np	p
GD SNP00085	3	p	p	p
GD SNP00086	8	np	np	p
GD SNP00087	1	np	np	p
GD SNP00088	17	np	np	np
GD SNP00089	3	np	p	np
GD SNP00091	17	np	np	np
GD SNP00096	9	np	–	np
GD SNP00098	13	p	np	p
GD SNP00099	10	np	np	p
GD SNP00100	5	np	np	np
GD SNP00101	13	np	np	np
GD SNP00103	3	np	np	np
GD SNP00106	10	p	np	np
GD SNP00110	13	np	np	p
GD SNP00111	15	p	p	np
GD SNP00113	11	np	np	np
GD SNP00115	15	p	p	np
GD SNP00116	12	p	np	p
GD SNP00120	2	np	np	np
GD SNP00123	11	np	np	p
GD SNP00124	3	np	np	p
GD SNP00136	4	np	p	np
GD SNP00140	13	np	–	p
GD SNP00142	6	np	p	p

GD SNP00146	2	p	np	p
GD SNP00148	4	np	np	p
GD SNP00150	7	–	–	–
GD SNP00151	5	p	p	np
GD SNP00152	1	np	p	p
GD SNP00155	8	np	p	–
GD SNP00157	8	p	p	p
GD SNP00158	2	np	np	p
GD SNP00159	2	np	np	p
GD SNP00164	13	np	np	np
GD SNP00165	14	p	p	np
GD SNP00166	6	np	p	p
GD SNP00167	2	np	p	–
GD SNP00168	3	np	np	p
GD SNP00170	14	p	p	p
GD SNP00171	14	np	np	p
GD SNP00173	12	p	np	np
GD SNP00174	2	np	p	np
GD SNP00175	8	p	np	np
GD SNP00177	4	np	p	p
GD SNP00178	17	p	np	p
GD SNP00182	11	np	p	p
GD SNP00184	13	np	p	np
GD SNP00185	11	p	np	p
GD SNP00188	8	p	np	p
GD SNP00189	5	np	p	p
GD SNP00190	–	np	–	np
GD SNP00191	15	np	p	p
GD SNP00192	17	np	np	p
GD SNP00193	12	np	np	np
GD SNP00194	3	np	p	p
GD SNP00195	13	p	–	p
GD SNP00196	16	np	–	np
GD SNP00197	6	p	np	np
GD SNP00200	16	p	np	p
GD SNP00202	17	p	np	p
GD SNP00203	2	p	np	p
GD SNP00204	8	p	np	p
GD SNP00205	9	p	p	p
GD SNP00207	14	np	np	np
GD SNP00209	8	np	p	p

GD SNP00211	14	np	np	np
GD SNP00212	11	np	np	np
GD SNP00213	14	np	np	np
GD SNP00214	2	p	np	p
GD SNP00218	6	p	np	np
GD SNP00220	12	np	p	np
GD SNP00221	4	np	–	p
GD SNP00222	2	p	p	np
GD SNP00224	7	p	np	p
GD SNP00225	11	np	p	np
GD SNP00226	4	np	p	p
GD SNP00228	2	np	np	np
GD SNP00231	5	p	np	np
GD SNP00232	4	np	p	p
GD SNP00233	3	np	p	p
GD SNP00237	4	p	np	p
GD SNP00238	5	p	np	p
GD SNP00239	5	np	np	np
GD SNP00240	11	p	p	p
GD SNP00241	15	np	p	p
GD SNP00243	2	np	np	p
GD SNP00244	5	p	p	–
GD SNP00245	17	p	–	p
GD SNP00246	8	np	np	np
GD SNP00247	7	np	p	p
GD SNP00248	14	p	p	np
GD SNP00250	1	p	np	p
GD SNP00252	1	p	np	p
GD SNP00253	11	np	p	p
GD SNP00254	11	np	p	–
GD SNP00256	7	p	p	np
GD SNP00260	10	p	np	p
GD SNP00261	14	p	p	np
GD SNP00262	17	np	p	p
GD SNP00264	5	np	p	np
GD SNP00265	17	p	np	np
GD SNP00267	2	np	p	np
GD SNP00268	17	np	np	np
GD SNP00269	16	p	np	np
GD SNP00271	15	p	p	np
GD SNP00272	12	p	np	np

GD SNP00273	15	np	np	p
GD SNP00274	15	np	p	p
GD SNP00275	12	p	–	p
GD SNP00276	3	np	np	p
GD SNP00277	4	p	p	np
GD SNP00278	3	p	p	np
GD SNP00280	9	p	p	np
GD SNP00282	6	np	p	p
GD SNP00284	5	p	p	p
GD SNP00287	17	p	np	p
GD SNP00289	2	np	np	p
GD SNP00290	17	np	p	p
GD SNP00292	16	p	p	np
GD SNP00293	8	p	np	np
GD SNP00296	12	np	np	p
GD SNP00298	9	np	np	–
GD SNP00299	8	np	p	np
GD SNP00302	4	np	p	p
GD SNP00303	10	np	np	np
GD SNP00306	5	np	np	np
GD SNP00307	10	np	p	np
GD SNP00308	2	p	np	p
GD SNP00311	8	p	np	–
GD SNP00316	8	p	np	p
GD SNP00317	3	p	p	np
GD SNP00318	12	p	p	p
GD SNP00319	3	np	np	np
GD SNP00320	8	p	np	p
GD SNP00321	4	np	np	p
GD SNP00322	3	p	p	np
GD SNP00324	4	p	–	np
GD SNP00328	17	p	p	np
GD SNP00329	15	np	p	p
GD SNP00330	15	np	p	p
GD SNP00331	9	np	p	np
GD SNP00333	2	np	np	np
GD SNP00334	12	p	p	np
GD SNP00336	15	np	p	p
GD SNP00337	9	p	p	np
GD SNP00338	12	p	p	np
GD SNP00340	13	np	np	np

GD SNP00341	17	np	–	–
GD SNP00342	8	p	np	np
GD SNP00343	9	np	–	p
GD SNP00344	8	np	–	np
GD SNP00345	1	p	np	np
GD SNP00347	6	np	p	np
GD SNP00348	2	np	p	p
GD SNP00349	15	np	p	np
GD SNP00350	13	p	p	p
GD SNP00351	11	np	p	p
GD SNP00352	9	np	np	p
GD SNP00354	8	np	np	p
GD SNP00355	10	np	np	p
GD SNP00356	16	p	–	p
GD SNP00357	15	np	p	p
GD SNP00358	17	p	p	p
GD SNP00360	10	np	np	p
GD SNP00361	1	np	np	np
GD SNP00362	12	np	p	p
GD SNP00363	4	np	p	p
GD SNP00364	4	np	p	–
GD SNP00366	2	np	np	p
GD SNP00382	5	p	np	np
GD SNP00391	12	np	p	p
GD SNP00400	9	np	p	p
GD SNP00401	17	p	np	p
GD SNP00405	10	np	np	np
GD SNP00408	2	np	p	p
GD SNP00418	11	np	p	np
GD SNP00419	8	np	np	–
GD SNP00425	2	np	p	np
GD SNP00430	12	np	p	np
GD SNP00434	6	np	p	p
GD SNP00438	17	np	p	p
GD SNP00440	1	p	np	p
GD SNP00444	16	p	p	p
GD SNP00452	9	p	p	p
GD SNP00452	9	p	p	p
GD SNP00453	14	p	p	np
GD SNP00464	12	np	np	–
GD SNP00471	2	np	np	np

GD SNP00472	6	np	p	p
GD SNP00477	3	p	p	np
GD SNP00480	3	p	p	np
GD SNP00483	2	np	p	np
GD SNP00487	8	p	np	np
GD SNP00495	1	np	p	–
GD SNP00503	8	p	np	np
GD SNP00505	2	np	np	p
GD SNP00514	9	p	p	np
GD SNP00522	14	p	p	np
GD SNP00525	15	np	np	p
GD SNP00527	8	p	np	p
GD SNP00531	13	–	np	p
GD SNP00532	13	p	p	np
GD SNP00533	1	np	p	np
GD SNP00538	–	np	np	–
GD SNP00559	5	np	np	np
GD SNP00562	7	p	np	p
GD SNP00575	1	np	p	p
GD SNP00578	16	p	np	–
GD SNP00581	13	np	np	np
GD SNP00584	8	np	p	np
GD SNP00588	3	p	p	p
GD SNP00590	7	p	np	–
GD SNP00604	10	np	np	np
GD SNP00611	5	np	np	np
GD SNP00619	4	np	np	np
GD SNP00626	16	np	p	np
GD SNP00627	8	np	np	p
GD SNP00629	2	np	p	np
GD SNP00631	1	np	np	p
GD SNP00632	5	np	np	np
GD SNP00633	2	p	np	p
GD SNP00638	5	np	np	p
GD SNP00639	8	p	p	np
GD SNP00640	15	np	p	np
GD SNP00646	11	np	p	np
GD SNP00655	2	np	np	p
GD SNP00661	15	np	np	p
GD SNP00664	3	np	np	p
GD SNP00674	1	p	–	p

GD SNP00682	17	np	p	p
GD SNP00685	12	np	np	np
GD SNP00688	8	np	np	np
GD SNP00692	15	p	np	p
GD SNP00697	1	np	p	–
GD SNP00714	12	p	p	np
GD SNP00719	16	np	p	np
GD SNP00723	–	np	–	np
GD SNP00727	4	np	p	p
GD SNP00735	11	p	–	np
GD SNP00737	5	np	–	np
GD SNP00743	11	p	np	np
GD SNP00744	13	np	np	np
GD SNP00747	12	p	p	np
GD SNP00748	13	p	p	np
GD SNP00758	15	np	p	–
GD SNP00761	1	np	p	p
GD SNP00762	12	np	np	np
GD SNP00766	9	np	np	p
GD SNP00768	4	p	p	–
GD SNP00770	13	np	np	np
GD SNP00781	10	p	np	np
GD SNP00782	1	np	np	np
GD SNP00785	15	p	p	np
GD SNP00787	6	np	p	p
GD SNP00795	11	p	np	np
GD SNP00799	2	p	np	p
GD SNP00803	9	p	p	np
GD SNP00806	5	np	p	p
GD SNP00816	17	np	np	np
GD SNP00818	17	p	p	–
GD SNP00819	8	np	np	np
GD SNP00833	2	np	p	p
GD SNP00848	15	np	–	p
GD SNP00862	8	p	p	np
GD SNP00864	17	np	np	p
GD SNP00867	5	np	np	np
GD SNP00871	7	p	p	np
GD SNP00875	10	p	p	np
GD SNP00881	4	p	p	p
GD SNP00883	12	np	np	–

GD SNP00886	9	p	p	p
GD SNP00890	13	p	np	np
GD SNP00893	9	p	p	np
GD SNP00904	15	np	np	p
GD SNP00915	12	p	–	np
GD SNP00918	17	p	np	p
GD SNP00921	3	np	p	np
GD SNP00922	13	np	p	p
GD SNP00923	16	p	np	p
GD SNP00928	4	p	np	np
GD SNP00932	15	np	np	p
GD SNP00934	2	np	p	np
GD SNP00937	12	np	p	p
GD SNP00948	14	np	np	p
GD SNP00954	15	np	np	p
GD SNP00955	3	np	p	np
GD SNP00958	9	np	p	np
GD SNP00962	15	np	p	p
GD SNP00963	17	np	np	np
GD SNP00967	6	np	p	p
GD SNP00975	8	p	p	np
GD SNP00983	15	np	p	p
GD SNP00984	15	np	p	p
GD SNP00985	2	np	np	–
GD SNP01003	16	np	np	p
GD SNP01004	8	p	np	p
GD SNP01009	15	np	p	p
GD SNP01013	14	np	np	np
GD SNP01026	4	np	p	p
GD SNP01027	1	np	p	p
GD SNP01029	12	np	np	p
GD SNP01035	1	p	np	np
GD SNP01040	7	p	p	np
GD SNP01044	17	np	p	p
GD SNP01045	12	np	np	p
GD SNP01048	8	np	p	p
GD SNP01051	12	np	np	–
GD SNP01059	8	np	p	p
GD SNP01061	15	np	p	p
GD SNP01070	12	np	p	np
GD SNP01073	3	np	p	p

GD SNP01074	7	p	np	np
GD SNP01077	15	p	np	p
GD SNP01090	2	np	p	np
GD SNP01094	16	np	p	np
GD SNP01098	17	p	np	np
GD SNP01112	11	np	p	np
GD SNP01116	16	p	np	–
GD SNP01130	15	np	p	p
GD SNP01131	15	p	p	np
GD SNP01134	2	p	p	p
GD SNP01140	11	np	np	p
GD SNP01146	15	p	p	np
GD SNP01162	2	np	np	p
GD SNP01170	7	p	np	p
GD SNP01172	7	np	–	np
GD SNP01181	2	–	–	p
GD SNP01186	16	np	np	–
GD SNP01189	9	p	np	p
GD SNP01190	13	np	p	np
GD SNP01195	4	np	np	p
GD SNP01199	13	np	np	np
GD SNP01206	15	np	p	–
GD SNP01219	6	np	p	p
GD SNP01223	2	p	np	p
GD SNP01229	15	p	p	np
GD SNP01241	17	p	np	np
GD SNP01244	16	np	p	p
GD SNP01247	15	np	p	p
GD SNP01251	2	np	p	np
GD SNP01257	1	np	np	p
GD SNP01265	15	p	p	p
GD SNP01266	1	p	p	np
GD SNP01267	10	p	–	p
GD SNP01269	17	np	p	p
GD SNP01277	9	np	np	p
GD SNP01292	4	p	p	np
GD SNP01295	1	p	np	p
GD SNP01298	17	np	np	–
GD SNP01304	5	np	p	p
GD SNP01322	2	p	np	p
GD SNP01329	3	p	np	p

GD SNP01333	5	p	np	p
GD SNP01334	13	p	np	p
GD SNP01336	4	np	p	p
GD SNP01339	9	np	–	p
GD SNP01351	1	p	p	p
GD SNP01373	12	p	np	p
GD SNP01386	9	p	np	p
GD SNP01390	4	np	np	p
GD SNP01392	15	p	np	p
GD SNP01396	3	p	p	np
GD SNP01402	16	np	np	p
GD SNP01405	8	np	p	np
GD SNP01426	12	np	p	p
GD SNP01454	15	np	np	p
GD SNP01465	11	np	np	np
GD SNP01467	17	np	np	p
GD SNP01469	15	np	p	p
GD SNP01470	1	np	np	p
GD SNP01471	4	np	p	–
GD SNP01476	2	np	–	np
GD SNP01479	8	p	p	np
GD SNP01481	4	np	p	p
GD SNP01483	11	np	p	p
GD SNP01485	4	np	p	p
GD SNP01486	11	p	np	p
GD SNP01487	3	np	np	np
GD SNP01488	15	np	p	np
GD SNP01493	3	p	np	p
GD SNP01495	16	np	p	p
GD SNP01498	2	p	np	p
GD SNP01500	1	np	p	np
GD SNP01501	12	np	p	np
GD SNP01502	6	np	p	p
GD SNP01505	5	np	p	np
GD SNP01507	13	np	p	p
GD SNP01516	7	p	p	np
GD SNP01522	14	np	p	p
GD SNP01523	12	np	np	np
GD SNP01524	9	np	np	p
GD SNP01526	–	–	np	–
GD SNP01532	2	p	np	p

GD SNP01534	15	p	p	np
GD SNP01536	13	p	np	np
GD SNP01539	5	p	np	p
GD SNP01550	8	np	p	p
GD SNP01551	15	–	–	–
GD SNP01556	6	p	np	np
GD SNP01563	16	np	np	p
GD SNP01565	2	p	p	p
GD SNP01566	5	p	np	p
GD SNP01570	10	–	–	–
GD SNP01574	6	np	p	p
GD SNP01577	2	np	p	np
GD SNP01582	8	np	np	np
GD SNP01584	17	np	np	np
GD SNP01588	16	p	p	np
GD SNP01590	14	np	np	p
GD SNP01596	9	np	np	p
GD SNP01598	8	np	p	p
GD SNP01600	16	p	np	p
GD SNP01601	5	p	p	np
GD SNP01604	3	np	np	p
GD SNP01614	8	np	p	p
GD SNP01619	10	np	np	np
GD SNP01620	5	np	p	np
GD SNP01622	15	p	p	p
GD SNP01624	16	np	np	p
GD SNP01626	17	np	np	np
GD SNP01627	16	np	p	np
GD SNP01628	4	np	np	np
GD SNP01630	15	p	p	np
GD SNP01634	15	np	p	p
GD SNP01640	11	p	p	np
GD SNP01641	2	p	np	p
GD SNP01644	–	np	np	np
GD SNP01646	9	p	p	np
GD SNP01648	9	np	p	p
GD SNP01650	14	np	np	np
GD SNP01651	5	np	np	np
GD SNP01654	13	np	np	np
GD SNP01655	13	np	np	np
GD SNP01656	4	p	p	p

GD SNP01663	2	p	np	p
GD SNP01665	12	p	p	p
GD SNP01667	3	p	p	p
GD SNP01676	1	np	np	p
GD SNP01678	1	np	np	np
GD SNP01680	15	np	p	np
GD SNP01681	6	np	p	p
GD SNP01682	6	p	p	p
GD SNP01687	15	np	p	p
GD SNP01690	12	p	np	p
GD SNP01693	1	p	np	np
GD SNP01694	5	np	np	p
GD SNP01694	5	np	np	p
GD SNP01702	7	np	p	np
GD SNP01704	13	np	np	np
GD SNP01706	9	p	p	np
GD SNP01710	10	np	np	np
GD SNP01713	11	p	p	p
GD SNP01714	–	np	np	np
GD SNP01716	6	np	np	p
GD SNP01718	–	np	np	np
GD SNP01730	16	p	p	p
GD SNP01734	16	p	np	np
GD SNP01735	2	p	p	p
GD SNP01742	13	p	p	p
GD SNP01749	3	np	np	p
GD SNP01759	12	p	p	np
GD SNP01760	12	np	np	np
GD SNP01761	10	np	np	np
GD SNP01763	15	np	–	p
GD SNP01764	8	p	p	np
GD SNP01766	4	np	np	np
GD SNP01767	14	p	p	np
GD SNP01769	12	np	np	np
GD SNP01769	12	np	–	np
GD SNP01771	9	np	np	np
GD SNP01772	1	np	np	np
GD SNP01774	15	p	p	np
GD SNP01776	13	np	np	np
GD SNP01777	4	np	np	np
GD SNP01778	15	p	p	np

GD SNP01780	7	np	p	np
GD SNP01783	1	p	np	p
GD SNP01786	13	np	np	np
GD SNP01789	10	p	np	np
GD SNP01793	12	p	p	np
GD SNP01797	11	np	p	np
GD SNP01801	17	np	p	p
GD SNP01804	11	np	p	np
GD SNP01805	15	np	np	p
GD SNP01807	8	np	np	np
GD SNP01809	–	np	np	np
GD SNP01810	10	np	p	np
GD SNP01811	14	np	np	p
GD SNP01813	15	p	np	np
GD SNP01815	1	np	p	np
GD SNP01820	15	np	p	p
GD SNP01821	3	p	p	np
GD SNP01826	1	np	np	p
GD SNP01829	2	np	p	p
GD SNP01830	5	np	np	np
GD SNP01831	6	np	p	p
GD SNP01840	2	np	p	–
GD SNP01842	17	p	p	p
GD SNP01844	13	np	np	p
GD SNP01846	14	np	p	np
GD SNP01848	7	p	np	np
GD SNP01850	15	np	–	p
GD SNP01851	3	p	p	p
GD SNP01855	12	–	–	–
GD SNP01857	11	p	np	np
GD SNP01859	5	np	np	np
GD SNP01862	8	p	p	p
GD SNP01866	16	p	p	np
GD SNP01867	10	p	np	np
GD SNP01872	7	p	p	p
GD SNP01875	15	np	p	np
GD SNP01878	11	p	np	np
GD SNP01880	9	np	np	p
GD SNP01886	4	np	np	np
GD SNP01887	17	p	p	p
GD SNP01888	14	np	p	np

GD SNP01891	9	p	np	p
GD SNP01892	5	p	np	p
GD SNP01899	13	np	np	np
GD SNP01910	12	np	np	p
GD SNP01911	9	np	p	np
GD SNP01912	11	p	p	p
GD SNP01914	3	–	np	p
GD SNP01915	–	p	p	p
GD SNP01917	13	p	p	np
GD SNP01919	7	–	np	–
GD SNP01935	11	np	np	np
GD SNP01937	3	p	p	np
GD SNP01942	5	np	p	p
GD SNP01945	2	p	np	np
GD SNP01947	10	np	np	p
GD SNP01954	6	np	p	p
GD SNP01955	3	np	–	np
GD SNP01956	5	np	np	np
GD SNP01957	3	np	p	np
GD SNP01961	10	np	p	p
GD SNP01962	14	np	np	np
GD SNP01964	17	np	–	p
GD SNP01965	4	p	p	np
GD SNP01967	9	p	np	p
GD SNP01969	3	p	np	p
GD SNP01971	15	p	np	np
GD SNP01974	17	p	np	np
GD SNP01978	5	p	np	np
GD SNP01982	3	p	p	p
GD SNP01984	12	np	p	p
GD SNP01989	15	np	p	p
GD SNP01990	3	np	np	np
GD SNP01993	5	np	p	p
GD SNP01994	7	np	np	np
GD SNP01995	12	p	np	np
GD SNP01996	6	np	p	np
GD SNP01997	7	p	p	np
GD SNP02001	6	np	p	np
GD SNP02002	13	p	p	p
GD SNP02003	15	np	p	p
GD SNP02005	11	np	p	np

GD SNP02008	12	np	p	p
GD SNP02009	10	p	p	p
GD SNP02013	9	p	np	p
GD SNP02014	9	p	p	np
GD SNP02018	13	np	p	np
GD SNP02020	3	p	p	p
GD SNP02021	14	np	p	p
GD SNP02022	8	p	p	np
GD SNP02025	4	np	–	p
GD SNP02027	3	p	p	p
GD SNP02028	13	np	np	–
GD SNP02029	15	np	np	np
GD SNP02030	3	p	p	np
GD SNP02033	3	np	np	np
GD SNP02037	8	p	np	p
GD SNP02046	9	np	p	np
GD SNP02049	17	np	np	np
GD SNP02051	10	p	np	p
GD SNP02055	2	np	np	np
GD SNP02058	–	np	np	np
GD SNP02063	13	np	p	–
GD SNP02069	13	np	–	np
GD SNP02071	9	p	p	np
GD SNP02072	10	np	p	p
GD SNP02075	17	np	np	p
GD SNP02076	2	np	p	np
GD SNP02083	17	np	np	np
GD SNP02087	16	np	–	p
GD SNP02091	7	np	np	np
GD SNP02092	1	np	p	p
GD SNP02093	2	np	p	p
GD SNP02094	3	np	p	p
GD SNP02138	6	p	np	p
GD SNP02144	2	np	p	np
GD SNP02183	10	np	p	p
GD SNP02201	9	p	p	p
GD SNP02274	7	p	np	np
GD SNP02281	11	p	np	np
GD SNP02291	7	p	p	np
GD SNP02296	4	np	np	np
GD SNP02304	3	np	p	np

GD SNP02326	12	np	np	np
GD SNP02371	1	np	p	p
GD SNP02428	1	np	np	p
GD SNP02436	7	np	np	np
GD SNP02437	9	p	p	p
GD SNP02452	13	np	np	np
GD SNP02460	9	np	p	p
GD SNP02464	6	p	np	np
GD SNP02482	9	p	p	p
GD SNP02502	12	np	p	p
GD SNP02535	2	np	np	np
GD SNP02537	12	np	p	np
GD SNP02543	14	np	np	np
GD SNP02550	17	p	p	p
GD SNP02580	1	np	p	np
GD SNP02581	9	p	p	np
GD SNP02646	4	np	p	p
GD SNP02655	13	np	np	p
GD SNP02657	7	np	np	np
GD SNP02664	16	np	–	p
GD SNP02674	5	p	p	np
GD SNP02701	5	np	p	p
GD SNP02703	17	np	np	np
GD SNP02706	14	np	np	np
GD SNP02823	15	p	np	p
GD SNP02834	5	p	np	–
GD SNP02838	11	np	np	np
GD SNP02840	7	p	np	np
GD SNP02845	9	np	p	p
GD SNP02857	12	np	np	np
GD SNP02859	15	np	p	p

Table 9.2: In the SNP table are listed all the SNP markers tested with both technologies (Golden Gate and SNPlex). For each marker is reported the LG and the polymorphism on each parental cultivar (where 'p' means polymorphic, 'np' non polymorphic and '-' not determined).

FjxDel			
Trait	**LG**	**Gene ID**	**Gene**
N°force peaks	1	MDP0000025650	ACO
	1	MDP0000633218	AP2/ERF
	1	MDP0000401140	AP2/ERF
	1	MDP0000199078	CCR4
	1	MDP0000159587	MADS
	1	MDP0000588331	Pectinesterase
	1	MDP0000588332	Pectinesterase
	1	MDP0000156045	Xylan 1,4-beta-xylosidase
Initial force	3	MDP0000202829	Pectinesterase
	3	MDP0000184620	Polygalacturonase
	3	MDP0000267641	Xyloglucan 6-xylosyltransferase
	3	MDP0000646125	β-1,3-glucanase
	3	MDP0000275455	βa-galactosidase
	3	MDP0000300393	NAC-domain
	3	MDP0000222045	NAC-domain
	5	MDP0000217947	β-1,3-glucanase
	5	MDP0000189637	β-1,3-glucanase
	5	MDP0000140016	β-glucosidase
	5	MDP0000165135	β-glucosidase
	5	MDP0000134558	CCCH type zinc finger
	5	MDP0000193664	Hydrolase
	5	MDP0000696333	MADS
	5	MDP0000234073	MADS
	5	MDP0000215760	MYB
	5	MDP0000118810	WRKY
Max force	5	MDP0000217947	β-1,3-glucanase
	5	MDP0000189637	β-1,3-glucanase
	5	MDP0000140016	β-glucosidase
	5	MDP0000165135	β-glucosidase
	5	MDP0000134558	CCCH type zinc finger
	5	MDP0000193664	Hydrolase
	5	MDP0000215760	MYB
	5	MDP0000118810	WRKY
	5	MDP0000696333	MADS
	5	MDP0000234073	MADS
	8	MDP0000211931	AP2
	8	MDP0000149337	β-glucosidase
	8	MDP0000273450	Expansin
	8	MDP0000232313	MADS
	8	MDP0000221319	Pectinacetylesterase
	8	MDP0000200867	Pectinacetylesterase
	8	MDP0000211931	AP2
	8	MDP0000149337	Beta-glucosidase
	8	MDP0000273450	Expansin
	8	MDP0000232313	MADS
	8	MDP0000200867	Pectinacetylesterase

Final force	10	MDP0000510383	ACO
	10	MDP0000286915	AP2/ERF
	10	MDP0000326734	Polygalacturonase
	10	MDP0000934866	bHLH
	10	MDP0000684989	bHLH
	10	MDP0000219146	bHLH
	10	MDP0000285151	Cellulose synthase
	10	MDP0000155026	Cellulose synthase
	10	MDP0000697030	NAC domain
	10	MDP0000130686	NAC domain
Force index	10	MDP0000687812	CCAAT
	10	MDP0000878773	Chitinase
	10	MDP0000131702	EIL
	10	MDP0000224275	Ethylene receptor
	10	MDP0000510383	GATA
	10	MDP0000586400	Glucan endo-1,3-β-glucosidase
	10	MDP0000128964	Glucan endo-1,3-β-glucosidase
	10	MDP0000246388	Glucan endo-1,3-β-glucosidase,
	10	MDP0000136027	GRAS
	10	MDP0000168650	GRAS
	10	MDP0000269126	GRAS
	10	MDP0000220092	MADS
	10	MDP0000266968	MYB
	10	MDP0000166020	NAC domain
	10	MDP0000191925	NAC domain
	10	MDP0000897594	Pectinesterase
	10	MDP0000938309	Pectinesterase
	10	MDP0000226667	Pectinesterase
	10	MDP0000697030	Pectinesterase
	10	MDP0000626215	Pectinesterase
	10	MDP0000130686	WRKY
	10	MDP0000190788	Xyloglucan galactosyltransferase
	10	MDP0000326734	Xyloglucan galactosyltransferase
	10	MDP0000168287	ACO
	10	MDP0000281965	ACO
	10	MDP0000320017	ACO
Initial force	10	MDP0000510383	ACO
	10	MDP0000286915	AP2/ERF
	10	MDP0000934866	bHLH
	10	MDP0000684989	bHLH
	10	MDP0000219146	bHLH
	10	MDP0000285151	Cellulose synthase
	10	MDP0000155026	Cellulose synthase
	10	MDP0000697030	NAC domain
	10	MDP0000130686	NAC domain
	10	MDP0000326734	Polygalacturonase
Max acoustic pressure	10	MDP0000457509	AP2/ERF
	10	MDP0000286915	AP2/ERF
	10	MDP0000934866	bHLH

	10	MDP0000791364	bHLH
	10	MDP0000285151	Cellulose synthase
	10	MDP0000155026	Cellulose synthase
	10	MDP0000269126	Endo-1,4-β-glucanase
	10	MDP0000307619	GRAS
	10	MDP0000326734	Polygalacturonase
	10	MDP0000206034	SAM
	10	MDP0000566005	WRKY
	10	MDP0000320017	Xyloglucan endotransglucosylase
Max force	10	MDP0000510383	ACO
	10	MDP0000286915	AP2/ERF
	10	MDP0000326734	Polygalacturonase
	10	MDP0000219146	bHLH
	10	MDP0000934866	bHLH
	10	MDP0000684989	bHLH
Mean acoustic pressure	10	MDP0000457509	AP2/ERF
	10	MDP0000286915	AP2/ERF
	10	MDP0000934866	bHLH
	10	MDP0000791364	bHLH
	10	MDP0000285151	Cellulose synthase
	10	MDP0000155026	Cellulose synthase
	10	MDP0000269126	Endo-1,4-β-glucanase
	10	MDP0000307619	GRAS
	10	MDP0000326734	Polygalacturonase
	10	MDP0000206034	SAM
	10	MDP0000566005	WRKY
	10	MDP0000320017	Xyloglucan endotransglucosylase
N°acoustic peaks	10	MDP0000510383	ACO
	10	MDP0000286915	AP2/ERF
	10	MDP0000934866	bHLH
	10	MDP0000684989	bHLH
	10	MDP0000219146	bHLH
	10	MDP0000285151	Cellulose synthase
	10	MDP0000155026	Cellulose synthase
	10	MDP0000697030	NAC domain
	10	MDP0000130686	NAC domain
	10	MDP0000326734	Polygalacturonase
N°force peak	10	MDP0000235663	Beta-1,3-glucanase
	10	MDP0000146967	Beta-1,3-glucanase
	10	MDP0000205113	bHLH
	10	MDP0000137050	bZIP
	10	MDP0000679946	NAC domain
	10	MDP0000302503	Pectate Lyase
	10	MDP0000188160	Xyloglucan galactosyltransferase
	10	MDP0000669665	Xyloglucan galactosyltransferase
	10	MDP0000475945	Xyloglucan galactosyltransferase
Area	10	MDP0000687812	ACO
	10	MDP0000878773	ACO
	10	MDP0000131702	ACO

	10	MDP0000224275	ACO
	10	MDP0000510383	ACO
	10	MDP0000586400	alpha-mannosidase
	10	MDP0000934866	bHLH
	10	MDP0000246388	AP2/ERF
	10	MDP0000187369	AP2/ERF
	10	MDP0000286915	AP2/ERF
	10	MDP0000457509	AP2/ERF
	10	MDP0000266968	Ethylene-regulated transcript
	10	MDP0000166020	Ethylene-regulated transcript
	10	MDP0000136027	Endo-1,3-βa-glucanase
	10	MDP0000168650	Endo-1,3-β-glucanase
	10	MDP0000269126	Endo-1,4-β-glucanase
	10	MDP0000220092	Endo-1,4-β-glucanase
	10	MDP0000307619	GRAS
	10	MDP0000326734	Polygalacturonase
	10	MDP0000281965	WRKY
	10	MDP0000320017	Xyloglucan endotransglucosylase
	10	MDP0000897594	MYB
	10	MDP0000938309	MYB
	10	MDP0000226667	MYB
	10	MDP0000697030	NAC domain
	10	MDP0000139773	NAC domain
	10	MDP0000626215	NAC domain
	10	MDP0000130686	NAC domain
	10	MDP0000190788	NAC domain
	10	MDP0000151113	ACO
	10	MDP0000187687	Beta-glucosidase-like
	10	MDP0000122965	bZIP
	10	MDP0000155956	Endo-1,3-beta-glucanase
Force index	14	MDP0000326390	MADS
	14	MDP0000289836	MADS
	14	MDP0000905135	BZIP transcription factor
	14	MDP0000157628	AP2/ERF
	14	MDP0000197375	AP2/ERF
	14	MDP0000261735	BZIP-like protein
	14	MDP0000853568	MYB transcription factor
	14	MDP0000119204	AP2/ERF
	14	MDP0000130785	NAC domain protein
	14	MDP0000779358	Putative bZIPtranscription factor
	14	MDP0000160026	Endo-1,4-β-glucanase
	14	MDP0000313820	Endo-1,4-β-glucancase
	14	MDP0000234846	MYB transcription factor
	14	MDP0000184989	MYB transcription factor
	14	MDP0000620281	MYB transcription factor
	14	MDP0000402013	Myb transcription factor
	14	MDP0000478453	R2R3 MYB transcription factor
	14	MDP0000231274	BZIP transcriptional repressor
	14	MDP0000319851	GRAS family transcription factor

	14	MDP0000171602	GRAS
	14	MDP0000840369	GRAS
	14	MDP0000265114	MYB transcription factor
	14	MDP0000656112	MYB transcription factor
	14	MDP0000656113	NAC domain protein
N°acoustic peak	15	MDP0000146933	AP2-ERF
	15	MDP0000650702	AP2-ERF
	15	MDP0000144922	AP2-ERF
	15	MDP0000557234	AP2-ERF
	15	MDP0000263391	Pectinesterase
	15	MDP0000171994	Alpha-expansin 13
	15	MDP0000163398	Alpha-expansin 13
	15	MDP0000159387	Ethylene responsive transcription
	15	MDP0000295058	Ethylene responsive transcription
	15	MDP0000187914	NAC domain
	15	MDP0000241137	WRKY transcription factor
	15	MDP0000188349	ACO
	15	MDP0000629440	ACO
	15	MDP0000843889	ACO
	15	MDP0000258530	ACO
	15	MDP0000392859	ACO
	15	MDP0000753730	Alpha-mannosidase
	15	MDP0000556230	mannose-6-phosphate isomerase
	15	MDP0000123530	AP2/ERF
	15	MDP0000446321	Endo-1,3-β-glucanase
	15	MDP0000188610	Endo-1,3-β-glucanase
	15	MDP0000133266	Endo-1,4-β-glucanase
	15	MDP0000630192	Endo-1,4-β-glucanase
Young's module	15	MDP0000902970	Ethylene regulated transcript
	15	MDP0000505151	Ethylene regulated transcript
	15	MDP0000297684	Jumonji domain
	15	MDP0000654314	MYB transcription factor
	15	MDP0000179962	MYB transcription factor
	15	MDP0000182455	MYB transcription factor
	15	MDP0000289385	NAC domain
	15	MDP0000392859	NAC domain
Force index	15	MDP0000683515	1,3-β-glucan synthase
	15	MDP0000654314	AP2
	15	MDP0000182455	AP2
	15	MDP0000289385	AP2
	15	MDP0000453797	AP2
	15	MDP0000283350	AP2
	15	MDP0000503275	β-glucanase
	15	MDP0000277999	bZIP
	15	MDP0000171308	Endo-1,3-1,4-β-d-glucanase
	15	MDP0000750914	Extensin
	15	MDP0000263391	GATA
	15	MDP0000245023	Glucan endo-1,3-β-glucosidase
	15	MDP0000241137	GRAS

	15	MDP0000846004	MADS
	15	MDP0000759612	NAC domain
	15	MDP0000181608	Pectate lyase
	15	MDP0000225437	Polygalacturonase
	17	MDP0000551969	AP2/ERF
	17	MDP0000945267	AP2/ERF
	17	MDP0000863909	bZIP
	17	MDP0000280712	MADS
	17	MDP0000366022	MADS
	17	MDP0000144744	MYB
	17	MDP0000126343	MYB
	17	MDP0000842702	NAC domain
	17	MDP0000501518	NAC domain
	17	MDP0000128464	WRKY
Young's module	17	MDP0000132870	Glucan endo-1,3-β-glucosidase
	17	MDP0000123429	GRAS
	17	MDP0000296007	MADS
	17	MDP0000619897	NAC domain
	17	MDP0000520807	Pectate lyase
	17	MDP0000657441	Polygalacturonase

Table 9.4: For both populations and for each trait are reported the genes identified and annotated within each QTL intervals belonging to ethylene biosynthesis/perception, cell wall metabolism and transcription factors. For each gene is also reported, the LG, the gene ID (according to [223] and the annotation.)

FjxPL			
Trait	**LG**	**Prediction**	**Gene**
Young's module	3	MDP0000595295	NAC domain
	3	MDP0000130797	NAC domain
	3	MDP0000133636	NAC domain
	3	MDP0000759504	NAC domain
Force index	3	MDP0000324718	AP2/ERF
	3	MDP0000255676	β-1,2-xylosyltransferase
	3	MDP0000106455	β-1,3-galactosyltransferase
	3	MDP0000134936	BZIP
	3	MDP0000308685	BZIP-like protein
	3	MDP0000212702	C2H2
	3	MDP0000289626	Endo-1,4-β-glucanase
	3	MDP0000243113	Ethylene responsive transcription factor
	3	MDP0000306058	Expansin
	3	MDP0000793615	GRAS
	3	MDP0000205622	GRAS
	3	MDP0000722954	MYB transcription factor
	3	MDP0000890154	MYB transcription factor
	3	MDP0000183451	MYB transcription factor
	3	MDP0000144751	Myb-related protein
	3	MDP0000180343	NAC domain protein

	3	MDP0000868419	NAC domain protein
	3	MDP0000262032	NAC domain protein
	3	MDP0000135860	NAC domain protein
	3	MDP0000315947	NAC transcription facto
	3	MDP0000263272	Polygalacturonase
	3	MDP0000946614	WRKY transcription factor
	7	MDP0000184706	NAC domain protein
	7	MDP0000399816	MADS
	7	MDP0000904420	MADS
	7	MDP0000148857	MADS
	7	MDP0000269607	WRKY transcription factor
	7	MDP0000783966	MADS
	7	MDP0000435100	ACS
	7	MDP0000228328	WRKY transcription factor
	7	MDP0000119031	WRKY transcription factor
	7	MDP0000909869	WRKY transcription factor
	7	MDP0000587614	WRKY transcription factor
	7	MDP0000705889	Ethylene receptor
	7	MDP0000247896	WRKY transcription factor
	7	MDP0000123248	ACS
	7	MDP0000282906	MYB transcription factor
	7	MDP0000214002	MYB transcription factor
	7	MDP0000127521	MYB transcription factor
	7	MDP0000133485	AP2/ERF
	7	MDP0000194206	AP2/ERF
	7	MDP0000915330	MYB transcription factor
	7	MDP0000575835	NAC domain protein
	7	MDP0000214515	NAC domain protein
	7	MDP0000215564	NAC domain protein
	7	MDP0000294573	NAC domain protein
	7	MDP0000231843	NAC domain protein
	7	MDP0000231845	NAC domain protein
	7	MDP0000835180	NAC domain protein
	7	MDP0000303041	NAC domain protein
	7	MDP0000126141	NAC domain protein
	7	MDP0000249947	NAC domain protein
	7	MDP0000243205	Ethylene receptor
	7	MDP0000130802	AP2
	7	MDP0000563165	NAC domain protein
	7	MDP0000226497	MYB transcription factor
	7	MDP0000173809	Beta-1,4-endoglycanohydrolase
	7	MDP0000203780	BZIP transcription factor
	7	MDP0000179206	Glucan endo-1,3-β-glucosidase
	7	MDP0000318598	Polygalacturonase
N°acoustic peaks	12	MDP0000871361	AP2/ERF
	12	MDP0000703626	AP2/ERF
	12	MDP0000313984	AP2/ERF
	12	MDP0000162363	AP2/ERF
	12	MDP0000308444	β-galactosidase

	12	MDP0000225360	β-galactosidase
	12	MDP0000413041	MYB
	12	MDP0000468411	NAC domain
	12	MDP0000168416	Polygalacturonase
	12	MDP0000220329	Polygalacturonase
	12	MDP0000147902	Polygalacturonase
Mean acoustic pressure	12	MDP0000157370	α-expansin
	12	MDP0000313984	AP2
	12	MDP0000169669	AP2
	12	MDP0000211581	AP2
	12	MDP0000871361	AP2/ERF
	12	MDP0000703626	AP2/ERF
	12	MDP0000162363	AP2/ERF
	12	MDP0000223609	AP2/ERF
	12	MDP0000250924	AP2/ERF
	12	MDP0000139446	AP2/ERF
	12	MDP0000250927	AP2/ERF
	12	MDP0000319736	AP2/ERF
	12	MDP0000880312	AP2/ERF
	12	MDP0000814798	AP2-EREBP
	12	MDP0000308444	β-galactosidase
	12	MDP0000225360	β-galactosidase
	12	MDP0000123905	β-galactosidase
	12	MDP0000899966	β-galactosidase
	12	MDP0000456076	bHLH
	12	MDP0000869137	bHLH
	12	MDP0000292881	Cellulose synthase
	12	MDP0000832632	β-beta-mannanase
	12	MDP0000302747	Ethylene insensitive
	12	MDP0000908969	Ethylene receptor ERS1b
	12	MDP0000634630	Ethylene responsive transcription factor
	12	MDP0000255883	Ethylene-overproduction protein
	12	MDP0000451242	Ethylene-overproduction protein
	12	MDP0000715154	Expansin
	12	MDP0000123864	Expansin
	12	MDP0000370956	Expansin
	12	MDP0000370957	Expansin
	12	MDP0000238208	Expansin
	12	MDP0000192434	Expansin
	12	MDP0000156815	Expansin
	12	MDP0000743239	Expansin
	12	MDP0000765613	Expansin
	12	MDP0000119093	GRAS
	12	MDP0000884524	GRAS
	12	MDP0000148294	GRAS
	12	MDP0000926466	GRAS
	12	MDP0000666991	GRAS
	12	MDP0000397638	GRAS
	12	MDP0000228437	MADS

	12	MDP0000307605	MADS
	12	MDP0000599449	MADS
	12	MDP0000162855	Mannosyl-transferase
	12	MDP0000413041	MYB
	12	MDP0000221801	MYB
	12	MDP0000186860	MYB
	12	MDP0000282792	MYB
	12	MDP0000276060	MYB
	12	MDP0000478512	MYB
	12	MDP0000219581	MYB
	12	MDP0000131797	MYB
	12	MDP0000288687	MYB
	12	MDP0000601420	MYB
	12	MDP0000468411	NAC domain
	12	MDP0000598303	NAC domain
	12	MDP0000718993	NAC domain
	12	MDP0000634006	NAC domain
	12	MDP0000286498	Pectinacetylesterase
	12	MDP0000186817	Pectinacetylesterase
	12	MDP0000186818	Pectinacetylesterase
	12	MDP0000212077	Pectinacetylesterase
	12	MDP0000202156	Pectinacetylesterase
	12	MDP0000870113	Pectinesterase
	12	MDP0000278118	Pectinesterase
	12	MDP0000278119	Pectinesterase
	12	MDP0000296741	Pectinesterase
	12	MDP0000200340	Pectinesterase
	12	MDP0000168416	Polygalacturonase
	12	MDP0000461741	Polygalacturonase
	12	MDP0000147902	Polygalacturonase
	12	MDP0000600336	Polygalacturonase
	12	MDP0000432773	Polygalacturonase
	12	MDP0000524522	Polygalacturonase
	12	MDP0000902285	Polygalacturonase
	12	MDP0000181053	S-adenosylmethionine synthetase
	12	MDP0000268364	WRKY
	12	MDP0000201945	WRKY
	12	MDP0000598428	WRKY
	12	MDP0000205962	WRKY
	12	MDP0000296025	WRKY
	12	MDP0000824128	WRKY
	12	MDP0000737757	WRKY
	12	MDP0000736483	WRKY
	12	MDP0000754989	WRKY
	12	MDP0000754992	WRKY
	12	MDP0000180043	Xyloglucan endotransglucosylase
	12	MDP0000119223	Xyloglucan endotransglucosylase
	12	MDP0000219509	Xyloglucan endotransglucosylase
N°force peaks	12	MDP0000169669	AP2

	12	MDP0000211581	AP2
	12	MDP0000871361	AP2/ERF
	12	MDP0000162363	AP2/ERF
	12	MDP0000250924	AP2/ERF
	12	MDP0000140003	bHLH
	12	MDP0000232803	CCAAT
	12	MDP0000157370	Expansin
	12	MDP0000167304	L-galactono-1,4-lactone dehydrogenase
	12	MDP0000304239	L-galactono-1,4-lactone dehydrogenase
	12	MDP0000819856	MYB
	12	MDP0000788644	MYB
	12	MDP0000598303	NAC domain
	12	MDP0000180043	Xyloglucan endotransglucosylase
	12	MDP0000119223	Xyloglucan endotransglucosylase
Young's module	14	MDP0000147080	NAC domain
	14	MDP0000807087	NAC domain
	16	MDP0000247270	Pectinesterase
	16	MDP0000413387	AP2-ERF
	16	MDP0000467753	AP2-ERF
	16	MDP0000130123	NAC domain
	16	MDP0000195096	Pectinesterase
	16	MDP0000123888	WRKY
	16	MDP0000628100	Xyloglucan 6-xylosyltransferase
	16	MDP0000213291	Xyloglucan 6-xylosyltransferase
	16	MDP0000512420	Xyloglucan 6-xylosyltransferase
Max force	16	MDP0000681724	Expansin
	16	MDP0000204699	MYB
	16	MDP0000140493	NAC domain
Final force	16	MDP0000413387	AP2/ERF
	16	MDP0000175514	Endo-1,3-1,4-β-d-glucanase
	16	MDP0000284599	Endo-1,3-1,4-β-d-glucanase
	16	MDP0000230225	Endo-1,3-1,4-β-d-glucanase
	16	MDP0000224701	Endo-1,3-1,4-β-d-glucanase
	16	MDP0000389286	Myb
	16	MDP0000167950	MYB
	16	MDP0000181940	squamosa
	16	MDP0000193659	Squamosa
	16	MDP0000628100	Xyloglucan 6-xylosyltransferase
	16	MDP0000213291	Xyloglucan 6-xylosyltransferase
	16	MDP0000512420	Xyloglucan 6-xylosyltransferase
	16	MDP0000281823	Xyloglucan endoglucanase
	16	MDP0000176500	Xyloglucan endoglucanase
	16	MDP0000299209	Xyloglucan endoglucanase
Initial force	16	MDP0000413387	AP2/ERF
	16	MDP0000467753	AP2/ERF
	16	MDP0000230225	Endo-1,3-1,4-β-d-glucanase
	16	MDP0000278072	Endo-1,3-1,4-β-d-glucanase
	16	MDP0000260097	Endo-1,3-1,4-βa-d-glucanase
	16	MDP0000284599	Endo-1,3-1,4-β-d-glucanase

	16	MDP0000230225	Endo-1,3-1,4-β-d-glucanase
	16	MDP0000181940	Squamosa binding protein
	16	MDP0000176500	Xyloglucanase-specific endoglucanase
	16	MDP0000299209	Xyloglucan-specific endoglucanase
	16	MDP0000628100	Xyloglucan 6-xylosyltransferase
	16	MDP0000213291	Xyloglucan 6-xylosyltransferase
	16	MDP0000512420	Xyloglucan 6-xylosyltransferase
Area	16	MDP0000151113	ACO
	16	MDP0000187687	β-glucosidase-like
	16	MDP0000122965	bZIP
	16	MDP0000155956	Endo-1,3-β-glucanase
	16	MDP0000220008	MADS
	16	MDP0000616402	MADS
	16	MDP0000812154	MYB
	16	MDP0000219846	MYB
	16	MDP0000910638	MYB
	16	MDP0000130123	NAC domain
	16	MDP0000233614	NAC domain
	16	MDP0000195096	Pectinesterase
	16	MDP0000137792	Polygalacturonase
	16	MDP0000249364	Squamosa
	16	MDP0000123888	WRKY transcription factor
	16	MDP0000256514	WRKY transcription factor
Max acoustic pressure	16	MDP0000196961	β-amylase
	16	MDP0000187687	β-glycosidase
	16	MDP0000413387	Ethylene response factor
	16	MDP0000600286	MYB transcription factor
	16	MDP0000130123	NAC domain
	16	MDP0000195096	Pectinesterase
	16	MDP0000792747	Polygalacturonase,
	16	MDP0000181940	Squamosa binding protein
	16	MDP0000123888	WRKY transcription factor

Table 9.5: For both populations and for each trait are reported the genes identified and annotated within each QTL intervals belonging to ethylene biosynthesis/perception, cell wall metabolism and transcription factors. For each gene is also reported, the LG, the gene ID (according to [223] and the annotation.)

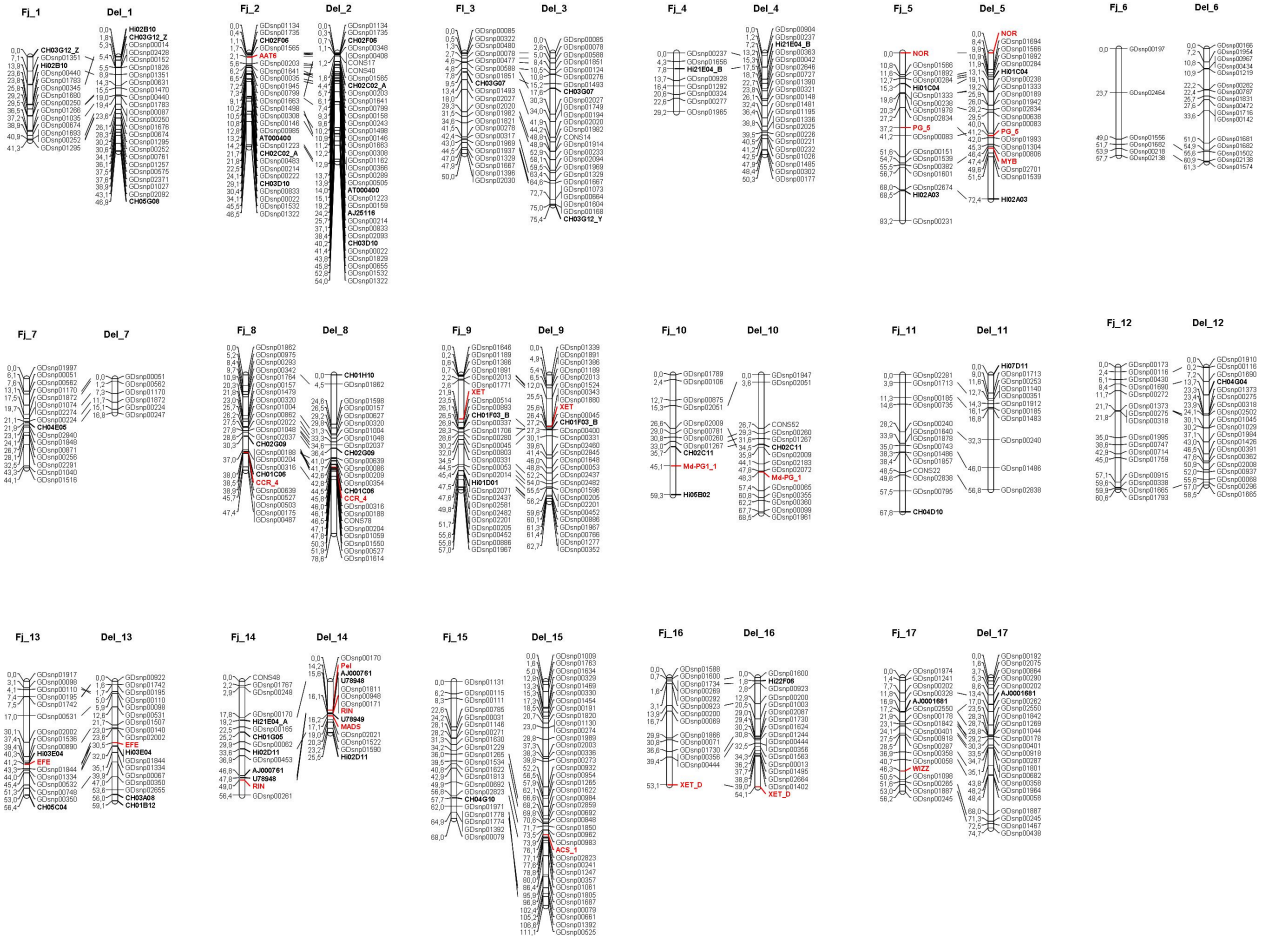

Figure 9.1: All the 17 linkage groups are shown separately for the two parental maps. Microsatellite used to anchor the linkage groups to the reference maps are highlighted in bold, marker related to candidate genes are in red.

Figure 9.2: The 17 chromosome are visualized distinctively for each parental map, where for each homologous chromosome pairs are highlighted the common markers. The linkage group 2 of 'Pink Lady' is split in two sub-groups due to a lack of markers in this region. Microsatellite used to anchor the maps are in bold, and in red are showed the SSR associated to candidate genes.

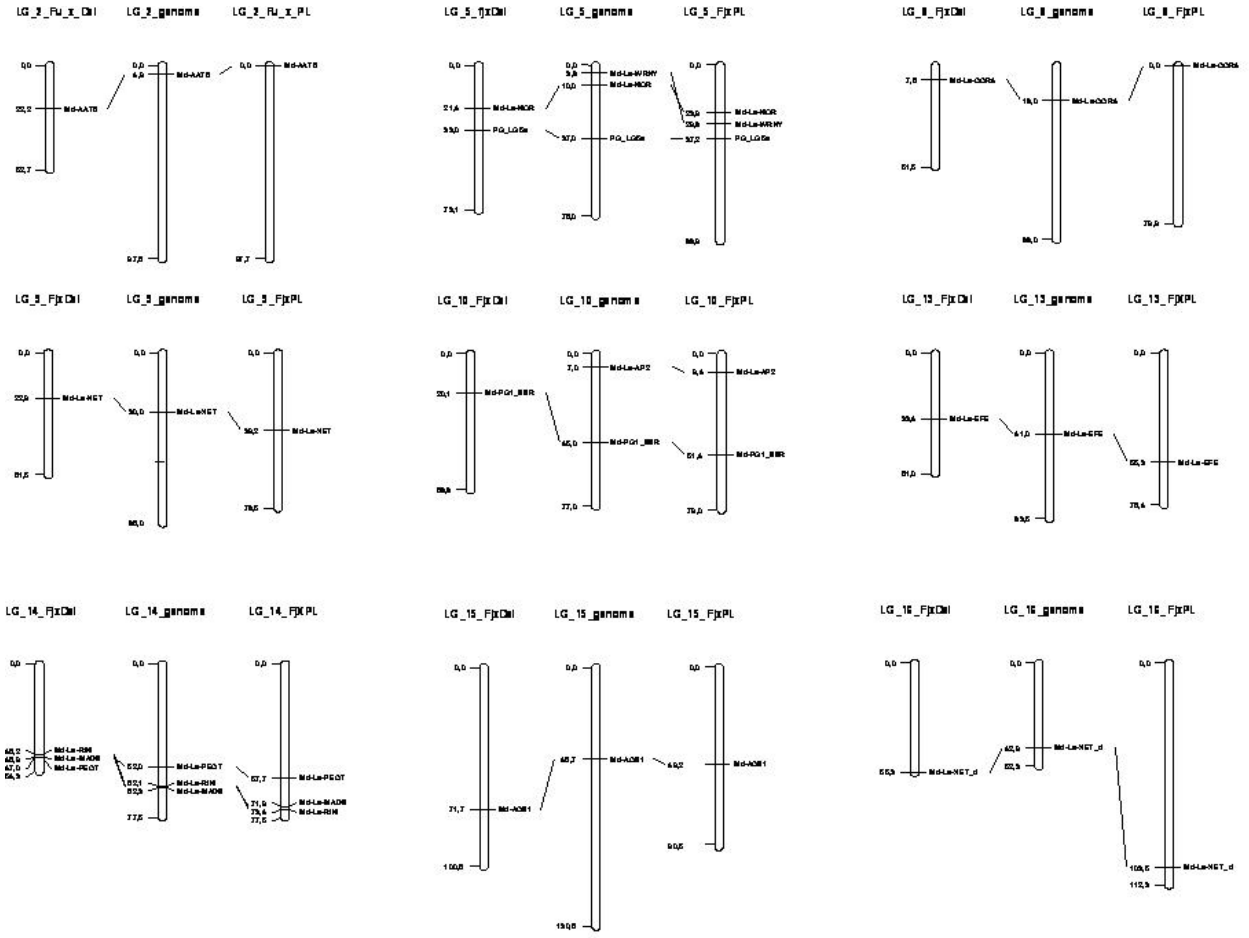

Figure 9.3: The genetic distancees are showed in computed cM for the two genetic maps ('FjxDel' and 'FjxPL') and in estimated cM for the physical map, considering that 1 cM correspond to 400 kb.

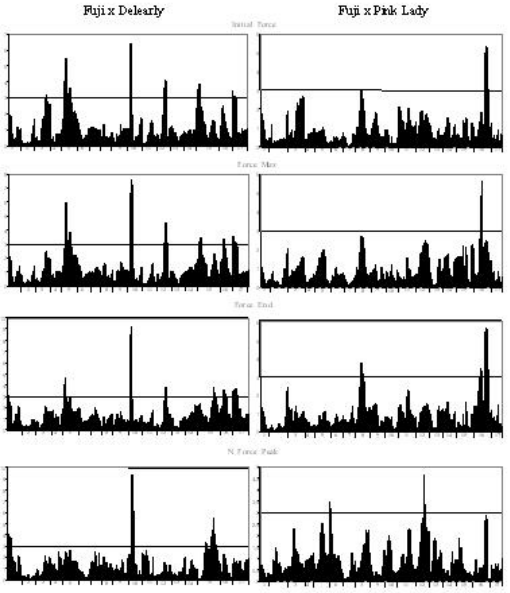
Fuji x Delearly
Fuji x Pink Lady

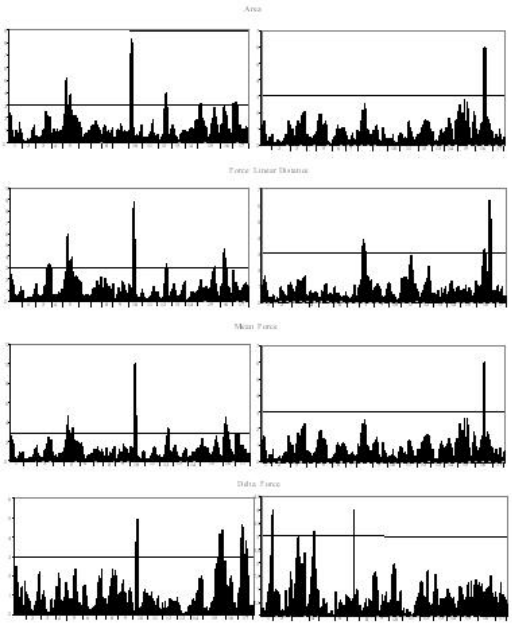

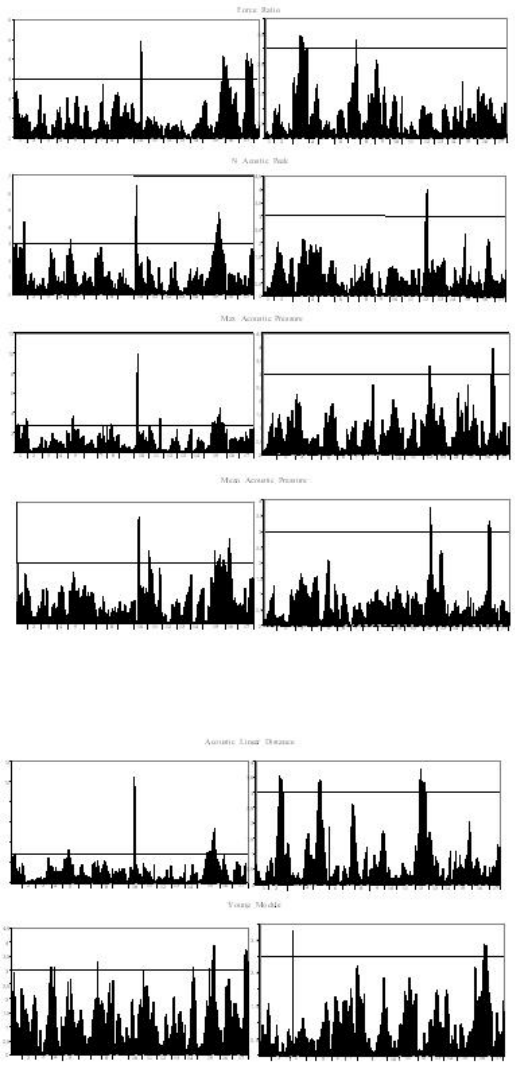

Figure 9.4: QTL profile overview computed with IM for the 14 parameters over the 17 chromosomes for both mapping populations. A general LOD threshold has been set at 3 after 1000 permutation. Y-axis: LOD value. X-axis: 17 chromosomes.

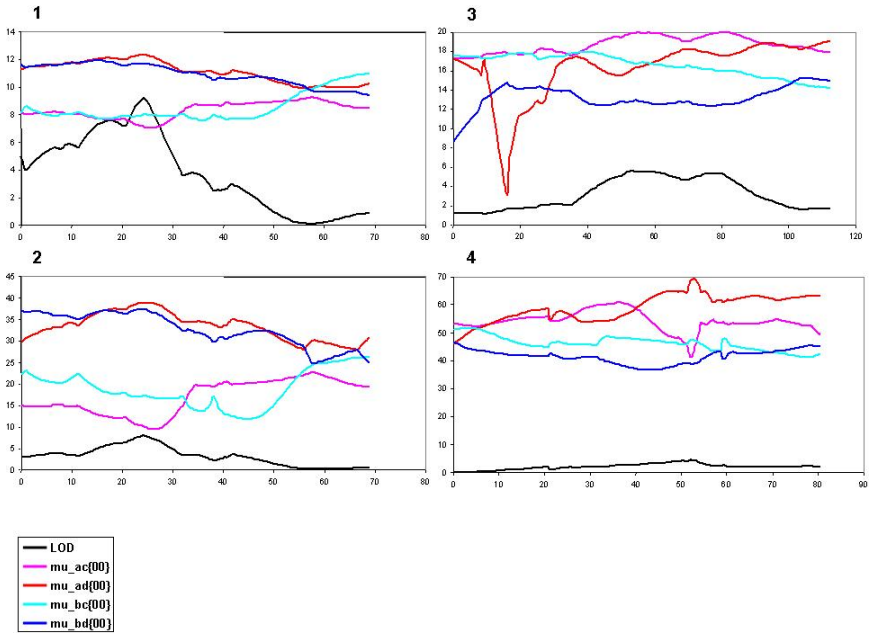

Figure 9.5: Estimated mean of the quantitative trait distribution associated with the genotypes. The four panels are: 1 Max Force in 'Fuji x Delearly' population; 2 Acoustic Peaks in 'Fuji x Delearly' population; 3 Max Force in 'Fuji x Pink Lady' population; 4 Acoustic Peaks in 'Fuji x Pink Lady' population. The alleles of Fuji are indicated with 'a' and 'b' for the two populations respectively, while 'c' and 'd' pointed the alleles of Delearly in panel 1 and 2, as well as the alleles of Pink Lady in panels 3 and 4.

	marker name	forward primer	reverse primer	LG	allele calling			fluorophore	tail
					FJ	PL	DEL		
triplet 1	CH02C02	CTTCAAGTTCAGCATCAAGACAA	TAGGGCACACTTGCTGGTC	2	141/-	129/-	129/-	FAM	
	CH03D10	CTCCCTTACCAAAAACACCAAA	GTGATTAAGAGAGTGATCGGGG	2	171/81	167/171	167/171	NED	
	Hi01D01	CTGAAATGGAAGGCTTGGAG	GTTTACCAATTAGGACTTAAAGCTG	9	195/220	199/222	195	VIC	
triplet 2	CH01H10	TGCAAAGATAGGTAGATATATGCCA	AGGAGGGATTGTTTGTGCAC	8	90/97	90/97	97/108	FAM	
	CH04G04	AGTGGCTGATGAGGATGAGG	GCTAGTTGCACCAAGTTCACA	12	173	173/181	171/173	NED	
	CH01C06	TTCCCCATCATCGATCTCTC	AAACTGAAGCCATGAGGGC	8	157/159	157/161	155/161	FAM	
triplet 3	Hi02A03	GACATGTGGTAGAACTCATCG	GTTTAGTGCGATTCATTTCCAAGG	5	175/185	175	169/173	NED	
	Hi01C04	GCTGCCGTTGACGTTAGAG	GTTTGTAGAAGTGGCGTTTGAGG	5	215/229	215	211/215	VIC	
	CH05E06	ACACGCACAGAGACAGAGACAT	GTTGAATAGCATCCCAAATGGT	5	146	146/158	146	FAM	
triplet 4	Hi05B02	GATGCGGTTTGACTTGCTTC	GTTTCTCCAGCTCCCATAGATTGC	10	124/132	163/178	178	FAM	
	Hi01A03	CGAATGAAATGTCTAAACAGGC	AAGCTACAGGCTTGTTGATAACG	10	167	167/191	167	NED	
	CH02C11	TGAAGGCAATCACTCTGTGC	TTCCGAGAATCCTCTTCGAC	10	229/233	208/233	217/233	VIC	
triplet 5	CH03A08	TTGGTTTGCTAGGAAAAGAAGG	AAGTTTATCGGGCCTACACG	13	185	185	185/191	NED	
	CH05C04	CCTTCGTTATCTTCCTTGCATT	GAGCTTAAGAATAAGAGAAGGGG	13	185/207	185/199	185/-	VIC	
	Hi03E04	CTTCACACCGTTTGGACCTC	GTTTCATATCCCACCACCACAGAAG	13	128/165	158	147/158	FAM	
triplet 6	Hi02D11	GCAATGTTGTGGGTGACAAG	GTTTGCAGAATCAAAACCAAGCAAG	14	246/261	237/245	245/257	VIC	
	Hi21E04	TGGAAACCTGTTGTGGGATT	TGCAGAGCGGATGTAAGTTG	4/14	129/133	131/133	133	FAM	
	CH01G05	CATCAGTCTCTTGCACTGGAAA	GACAGAGTAAGCTAGGGCTAGGG	14	138/143	136/138	138	NED	
triplet 7	CH05G08	CCAAGACCAAGGCAACATTT	CCCTTCACCTCATTCTCACC	1	177	177/182	159/171	NED	
	CH01F03b	GAGAAGCAAATGCAAAACCC	CTCCCCGGCTCCTATTCTAC	9	171/178	137/171	159/171	FAM	
	Hi01D01	CTGAAATGGAAGGCTTGGAG	GTTTACCAATTAGGACTTAAAGCTG	9	195/220	199/222	195	VIC	
triplet 8	CH03G07	AATAAGCATTCAAAGCAATCCG	TTTTTCCAAATCGAGTTTCGTT	3	116/123	126	116/126	FAM	
	Hi07D11	CCTTAGGGCCTTTGTGGTAAG	GTTTGAGCCGATTAGGGTTTAGGG	11	216/220	220	216/220	VIC	
	CH04D10	GAGGCATCTGTAGCTCCGAC	TGGTGAGTATCTGCTCGCTG	11	159/202	159/184	184	NED	
triplet 9	CH01H01	GAAAGACTTGCAGTGGGAGC	GGAGTGGGTTTGAGAAGGTT	17	116	112/118	118/120	FAM	
	Hi02B10	TGTCTCAAGAACACAGCTATCACC	GTTTCTTGGAGGCAGTAGTGCAG	1	201/221	201/251	201/217	VIC	
	CH03G12	GCGCTGAAAAAGGTCAGTTT	CAAGGATGCGCATGTATTTG	1/3	156/160	151/160	151/160	NED	
triplet 10	CH04G10	CAAAGATGTGGTGTGAAGAGGA	GGAGGCAAAAAGAGTGAACCT	15	141/-	132/-	132	FAM	
	CH04E05	AGGCTAACAGAAATGTGGTTTG	ATGGCTCCTATTGCCATCAT	7	175/202	175	175	NED	
	Hi22F06	CAATGGCGTCTGTGTCACTC	GTTTACGACGGGTAAGGTGATGTC	16	236/242	243	236/242	VIC	

single									
	CH01B12	CGCATGCTGACATGTTGAAT	CGGTGAGCCCTCTTATGTGA	4	176	150/176	152/176	FAM	
	CH02G09	TCAGACAGAAGAGGAACTGTATTTG	CAAACAAACCAGTACCGCAA	8	105/109		117/136	FAM	
	Hi02G06	AGATAGGTTTCACCGTCTCAGC	GACCTCTTTGGTGCGTCTG	15	161/163	161		FAM	
	CH02G02	AGATAGGTTTCACCGTCTCAGC	GACCTCTTTGGTGCGTCTG	15		105/109	117/136	FAM	
	CH02A04	GAAACAGGCGCCATTATTTG	AAAGGAGACGTTGCAAGTGG	2	105/107	95/97		FAM	
	CH02B10	CAAGGAAATCATCAAAGATTCAAG	CAAGTGGCTTCGGATAGTTG	2	129/131	119/123		FAM	
	AT000400	CTCCCTTTGCTCCCTCTCTT	AGGATGTCAGGGTTGTACGG	2	214/222	222/-	214/222	FAM	
	CH02F06	CCCTCTTCAGACCTGCATATG	ACTGTTTCCAAGCGATCAGG	2	136/157	142	149/157	FAM	
CG SSR									
	ACS 1	ATTTTCTCATGGGGATGCAA	GGTGATGATGAACCTTTCACG	15	223	219/223	219/223	VIC	M13
	AP2	ACACAAACGGGGTAAGATGG	TGTATCGTGGAAGAAAATTACAAA	10	208	206/219	208	VIC	M13
	CCR4	CAGGAAAGCCAACAGAGGAG	ACCCAGCAAAACCCAGAACT	8	194/212	196/200	200/208	VIC	M13
	EFE	ACATGGTGTGCCCTAGCTTC	CCCCCTATCGTTATCTTTTGG	13	185/197	197	187/197	VIC	M13
	tdr4 MADS	AGCCACTTGCCTACACTGGA	TGCTCTCCTTGGAGCTTCTC	14	241	229/241	229/241	VIC	M13
	PG LG 10	CTTGCTTAAACCGCATGCTT	AAATTGAGGCACGTGATGGT	10	169/188	171/188	169/188	VIC	M13
	PG LG5a	CCCCAAGGTTGTTTGTCCTA	AGACGATGATGCTCCTGCTT	5	207/209	202/220	203/207	VIC	M13
	Myb	TGGGCACAAGTTGTTTTCAA	AGCTTGTGGGAAAGGAGTGA	5	247		247/257	NED	SP6
	Myb c	TGTGAGGACTTGGCGTATGA	AGGGCCAACAGTTAATGTCC	10	266/268	268	268/268	NED	SP6
	PECT	GAATGTGCAAGGCACTGAGA	GATTCCCGTCAAAACCTGAA	14	211	201/205	201/211	NED	SP6
	Pect b	AAGACTTTTGGACCCCTTTTT	TGGATGTGTAGGTTGCCTTG	14	182	169/189	169/182	NED	SP6
	RIN	CCCTAAACACACAGCCTCCT	TGAGCAGCCCATTTCTTCTT	14	215/219	200/215	199/219	NED	SP6
	Wizz	AGCCGAAGGAGTCAGAATCA	CAAAGACTTCACCACCCACA	17	215/224	209	209	NED	SP6
	WRKY	CCCCAAAGAAAAGCAATCCT	CCCAAAATCTCTCCTCGACA	5	225/-	227/-		NED	SP6
	AAT6	ACGCTCGAGTGATGCAGAGT	GGCTGAAGTGCTTTGGAATG	2	218/222	218	218	FAM	T7
	AF527800	TGGAAAGGGTTGATTGACCT	AACAGCGGGTGGTAAATCTC	17	187	187/202	187	FAM	T7
	AJ0001681	CCTGAGGTTATTGACCCAAAA	CACTCAGTTGGAAAACCCTACA	17	187/241	207/209	187/207	FAM	T7
	AJ000761	CTGGGTGGATGCTTTGACTT	TCAATGACATTAATTCAACTTACAAAA	14	280/282	275/282	275/282	FAM	T7
	AJ25116	GATCAGAAAATTGCTAGGAAAAGG	AGAGAACGGTGAGCTCCTGA	2	185	185	185/187	FAM	T7
	NOR2	ATCAGCCCACTTTGCATGTT	CCCAGCTCATGGATCATTCT	5	218/220	202/210	218/220	FAM	T7
	PG 5B	CCCCAAGGTTGTTTGTCCTA	AGACGATGATGCTCCTGCTT	5	227	207	207/227	FAM	T7
	U78948	GATCGTCCGCCACCTTAAT	AGGGTTTTCATCATGCACATT	14	203/205	195/203	195/199	FAM	T7
	U78949	TTTGTCTACCTCTGATCTTAACCAA	CAGCATCGCAGAGAACTGAG	14	225/228	209/225	209/228	FAM	T7
	Md-XET	TACCAGCTGAGGCGGTCAT	GTCTCCCACCACACACACAC	9	242/244	244	242/256	FAM	T7
	Md-XET d	GTTGCAGAGGGTCCCAGATA	TCCTTTTCCCTCTCTCTATTCC	16	223/249	233/258	233/258	FAM	T7

Table 9.1: In the SSR table the different microsatellite markers are showed in three main sections. In the first are indicated all the primer assembled into triplex (multiplexing 3 primers pairs), in the second are listed all the SSR tested singularly and in the third category (indicated as CG-SSR) are listed all the SSR discovered in the candidate gene contigs. For each class are showed the marker name, the sequence of the forward and reverse primer, the linkage group and the size (allele calling). Only for the last category the sequence type used to link the tail at the 5' end of the forward primer is additionally reported

gene	forward primer	reverse primer
Md-PG1	ACCGGTGGGATAGCAACATC	ATTCCCTTTAGCTCCAAAAT
Md-PG5	GGGTCTCAAAGAGTTCAAGCCAG	CAAATACTCCTGAAACATGGTCTATT
Md-NOR	TCGCCTTATCAACAACACCA	CAAAACCCAATCATCAAGCC
Md-PECT	TACGCTATTGGAGGGAGTGC	CTGGTGCATCCTCATGTTTG
Md-ACO1	AACGACTCATTCATCAGCCC	TTCAAATCTTGGCTCCTTGG
Md-RIN	TTGCCAAAAGAAGAAATGGG	ATTCATAGAGCTTGCCACGG
Md-ACS1	GTCTTGGTCACGAACCCATC	ATCGCTAATGAGGTGGATGC
Md-XXT	AACCCTCACCCCTCTAAACG	AAGGTCGATCGGGAGAAACT
Md-Xet	AGCCAGCGGTTGCTCC	GGGTCCCTGCAATAGTCATATA
Md-XEG	AAGTGCCGGTTATCGATCTG	AAACCTCCATCCAAAAACCC
Md-Exp	CCCTGTCCTTCAGAGTCACG	TTCTTCCCGGTGAAAGTTTG

Table 9.3: List of forward and reverse primers for Real Time qPCR.

	SNP 1	SNP 2	SNP 3	SNP 4	SNP 5	SNP 6	SNP 7	SNP 8	SNP 9	SNP 10	SNP 11	SNP 12	SNP 13	SNP 14	SNP 15	SNP 16	SNP 17	SNP 18	SNP 19	SNP 20
Delearly	C C	T A	C C	T A	A G	T T	T T	C A	C C	T T	T T	A A	G G	T T	G G	A A	A A	A A	G G	C C
Fuji	C G	T A	C T	A A	A G	T G	C T	C A	C C	C T	T T	T A	A G	T A	A A	A G	A A	A G	A G	C T
Pink Lady	G G	A A	C C	A A	G G	G G	C C	C C	C T	C C	C T	T T	A A	n.a.	A A	G G	C A	G G	A A	T T

	SNP 21	SNP 22	SNP 23	SNP 24	SNP 25	SNP 26	SNP 27	SNP 28	SNP 29	SNP 30	SNP 31	SNP 32	SNP 33	SNP 34	SNP 35	SNP 36	SNP 37	SNP 38	SNP 39	SNP 40
Delearly	C C	A A	A A	C T	A A	A A	G G	G G	C C	A A	A G	T T	G G	T T	G G	C C	A A	C C	A A	A A
Fuji	C T	A G	A G	C T	T A	A G	G G	A G	C T	T A	A G	T T	A G	T T	n.a.	n.a.	A G	C T	A G	A G
Pink Lady	T T	G G	G G	C C	T T	G G	T G	A A	C C	A A	n.a.	n.a.	n.a.	n.a.	n.a.	n.a.	G G	T T	G G	G G

Table 9.6: SNP identification within the Md-XET gene among the three parental cultivars: 'Delearly', 'Fuji' and 'Pink Lady'.

CHAPTER 10

Supplementary material of chapter 5

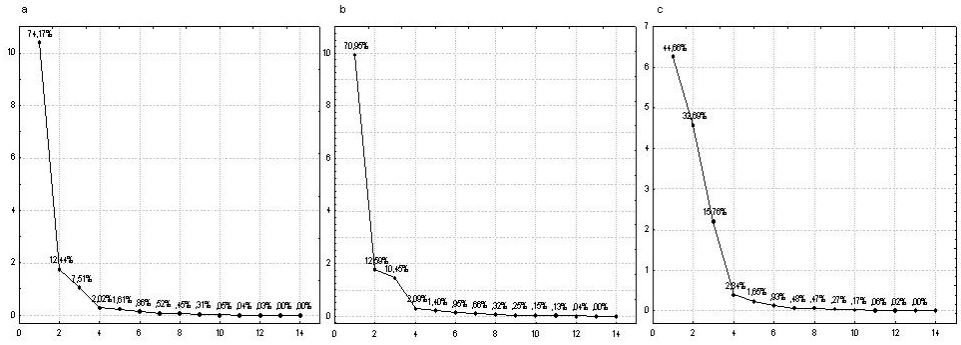

Figure 10.1: Eingene value for 2009 (a) and 2010 (b post harvest and c harvest)

Name	Forward	Reverse	LG
CH05G08	CCAAGACCAAGGCAACATTT	CCCTTCACCTCATTCTCACC	1
CH05E03	CGAATATTTTCACTCTGACTGGG	CAAGTTGTTGTACTGCTCCGAC	2
CH03G07	AATAAGCATTCAAAGCAATCCG	TTTTTCCAAATCGAGTTTCGTT	3
Hi23G02	TTTTCCAGGATATACTACCCTTCC	GTTTCTTCGAGGTCAGGGTTTG	4
CH04E03	TTGAAGATGTTTGGCTGTGC	TGCATGTCTGTCTCCTCCAT	5
CH03D12	GCCCAGAAGCAATAAGTAAACC	ATTGCTCCATGCATAAAGGG	6
Hi03A10	GGACCTGCTTCCCCTTATTC	CAGGGAACTTGTTTGATGG	7
CH01C06	TTCCCCATCATCGATCTCTC	AAACTGAAGCCATGAGGGC	8
CH01F03b	GAGAAGCAAATGCAAAACCC	CTCCCCGGCTCCTATTCTAC	9
CH02b03b	ATAAGGATACAAAAACCCTACACAG	GACATGTTTGGTTGAAAACTTG	10
CH02D08	TCCAAAATGGCGTACCTCTC	GCAGACACTCACTCACTATCTCTC	11
CH01G12	CCCACCAATCAAAAATCACC	TGAAGTATGGTGGTGCGTTC	12
CH05H05	ACATGTCACTCCTACGCGG	GTGCAGTGATTAGCATTGCTGT	13
CH01G05	CATCAGTCTCTTGCACTGGAAA	GACAGAGTAAGCTAGGGCTAGGG	14
NZ02B1	CCGTGATGACAAAGTGCATGA	ATGAGTTTGATGCCCTTGGA	15
CH04F10	GTAATGGAAATACAGTTTCACAA	TTAAATGCTTGGTGTGTTTTGC	16
GD96	CGGCGGAAAGCAATCACCT	GCCAGCCCTCTATGGTTCCAGA	17

Table 10.1: List of 17 SSR used to compute the population structure. For each marker the forward and reverse primer sequences and linkage group are provided.

	forward	reverse	Scale
CH01F12	CTCCTCCAAGCTTCAACCAC	GCAAAAACCACAGGCATAAC	macro-allelotyping
CH03D11	ACCCCACAGAAACCTTCTCC	CAACTGCAAGAATCGCAGAG	macro-allelotyping
Hi01B01	GCTACAGGCTTGTTGATAACGC	ACGAATGAAATGTCTAAACAGGC	macro-allelotyping
CH02b03b	ATAAGGATACAAAAACCCTACACAG	GACATGTTTGGTTGAAAACTTG	macro-allelotyping
PGSSR_3ku	CTTGCTTAAACCGCATGCTT	AAATTGAGGCACGTGATGGT	micro-allelotyping
PGSSR_10kd	TTTCTTCCTTGGGTTTTTGG	ACTCGTGCGCCAGATAGC	micro-allelotyping
PG_full	ACCTCAAGAGCCCAAGACGACACAAT	CTCGGGACTTCTTCCAACAATGTAGAAATGGTCG	gene-cloning
PG_1	AGGTCAACGCGCTTCATAGT	ACCACAAGAACCATAGCTCCA	micro-allelotyping
PG_2	GAAGGCAGCTTGTTCTTCCA	TGCACCTGTTGAAGGTCACA	micro-allelotyping
PG_3	ATGTGCAGGCTGTGACCTTC	CCGTCTTCTCCCAAGCTACC	micro-allelotyping
PG_4	AGAAAAGTGCGGGATGACTTT	TCTAGGGGAGACAACTCCTTTG	micro-allelotyping
PG_1ku	GTTGACAATCCAAAAATATCATCC	TGATGACAAAGAGAACGAACG	gene-cloning
PG_1ku2	GACATAGACCACTGGCTCATTA	AGACTAGGGTTGGAAATTACC	micro-allelotyping
PG_1kb_up_Gold	TATGGTTCTTGTGGTACCAAG	AGACTAGGGTTGGAAATTACC	micro-allelotyping
PG_1kd	CGACTAGCCTAACCCCAGC	CTTCTGCTGCTGTGTTGTGC	gene-cloning
MDC020950.238	CCTCTAACGTACATCGCATAGC	CTAGGAAACGGGAAACATAGC	macro-allelotyping
MDC009708.152	TGCAAAAAGCTCACCATTGC	TGGAGGTTTTTAGGTTGTTATTGG	macro-allelotyping
MDC022888.361	AAATGGGTAGTGACTGGTTGC	TCCTCCACATAATTTCCTGTCC	macro-allelotyping
MDC011778.144	TCTTTCTGCGTGTGTACTTCTCC	AACAACAATTGAGCTGCAACC	macro-allelotyping
MDC011413.171	TGCTGCGTTGCTTAGTATTCC	CCTGCTTATCATTTGCATCG	macro-allelotyping
MDC011435.443	ATTGGCAAAAGGAGCTTGC	AATGATCCTCGTGGTGATATGG	macro-allelotyping
MDC006342.275	ATGTCGTCTTCGTGGTGTGG	GAAAACATTCCCCATGATGC	macro-allelotyping
MDC006993.145	GGCAGGGTCCTCTTTTGG	GGGTTGCATCGACAACTAGG	macro-allelotyping
MDC001788.268	AGCAGTTTTCACAGCATGAGG	CTCCAAAATAGTGCTTCCTCTCC	macro-allelotyping
MDC011435.428	ATTGGCAAAAGGAGCTTGC	AATGATCCTCGTGGTGATATGG	macro-allelotyping
MDC006342.278	CATCTCCAATCAACAAAGAGAGG	AGGAACCCAAAAGAGCTTGC	macro-allelotyping
MDC022824.304	TTTTCTCCTCCAACACTTCTGG	GGAAGGAAGAATGAGCCTAACG	macro-allelotyping
MDC016688.112	AAATGGGTAGTGACTGGTTGC	AGGGGTGATGATTGTTCTCG	macro-allelotyping
MDC019740.197	GCAGCCATTGCTGATGG	CTTTTAGCTCAAACAATGCTTGAG	macro-allelotyping
MDC009365.281	GCCGAGCAACAATCAAGC	CCTCAAGGACGTTGTTACCC	macro-allelotyping
MDC006509.439	CCACCATTCCCAAGTTTTAGC	TCAGGAGGAACAGGAAGATAGC	macro-allelotyping
MDC009606.28	TTAGATTTGAAACGCACAACC	CCATCAGCATACCCACTAGC	macro-allelotyping
MDC007952.269	GCAATACCAAATGGGACCTAAAAAG	AATTAATCAGTTTCAACTATATGCACGG	macro-allelotyping
MDC007958.145	CATTGAGCAAGGCAATAATGG	AACTGGGCTCTTCTCCTTCC	macro-allelotyping
MDC022534.267	GAAGCACGTTCACTGTTTTCC	GCTATTCGTTTATCTTGAAGAGTGG	macro-allelotyping
MDC014096.132	TTGGGATTTCGATTCAGTGG	GAAAAATGGGATCAGCAAGC	macro-allelotyping
Xet_SSR	CCACCATTCCCAAGTTTTAGC	TCAGGAGGAACAGGAAGATAGC	macro-allelotyping
Xet_full	ATGCTCTCTCATCATCTATCTACACC	ATGATTTTGGCAAGTAATGACCC	micro-allelotyping
Xet_1	ATGGCTATCTTCCTGTTCCTCC	ATTCTTCCATCCCCACTTCC	micro-allelotyping
Xet_2	TGCCTGGTGAATTGATCAAATAGT	GGCCTTCAAACTAACATAATTGAGG	micro-allelotyping
Xet_3	CCTCAATTATGTTAGTTTGAAGGCC	TTAGCCCCAACACTCAGGTGT	micro-allelotyping

Table 10.2: List of markers used in the macro and micro allelotyping and cloning. For each marker forward and reverse primer sequences are provided.

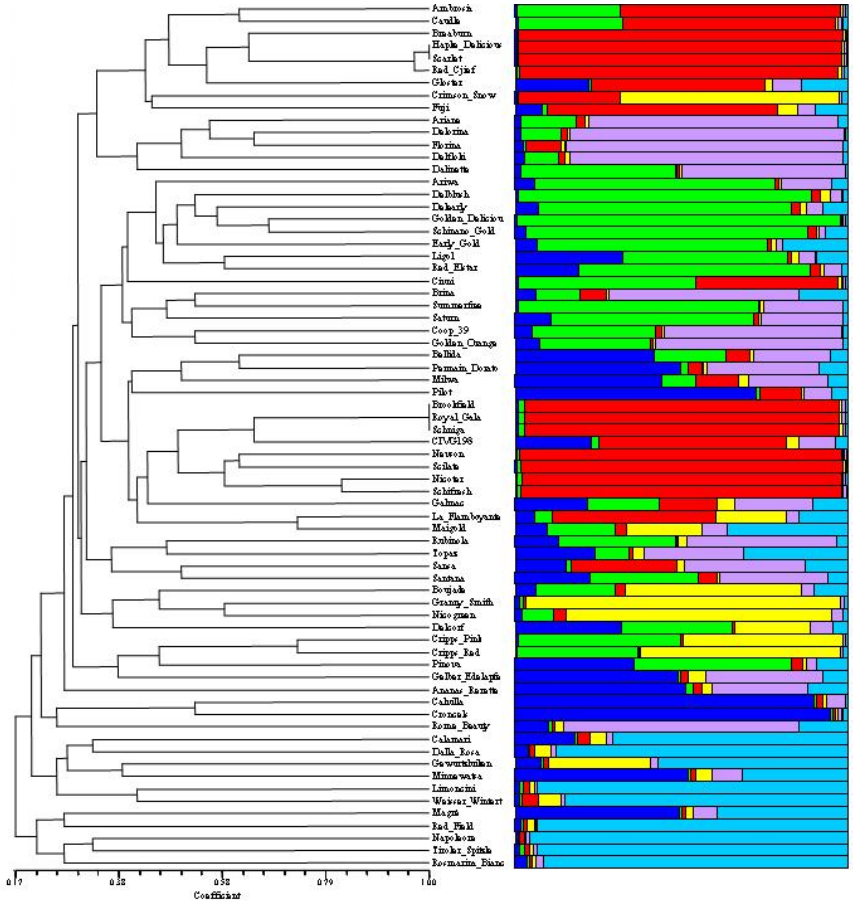

Figure 10.2: Similarity tree and population structure for the varieties phenotypically assessed in 2009 (K = 6).

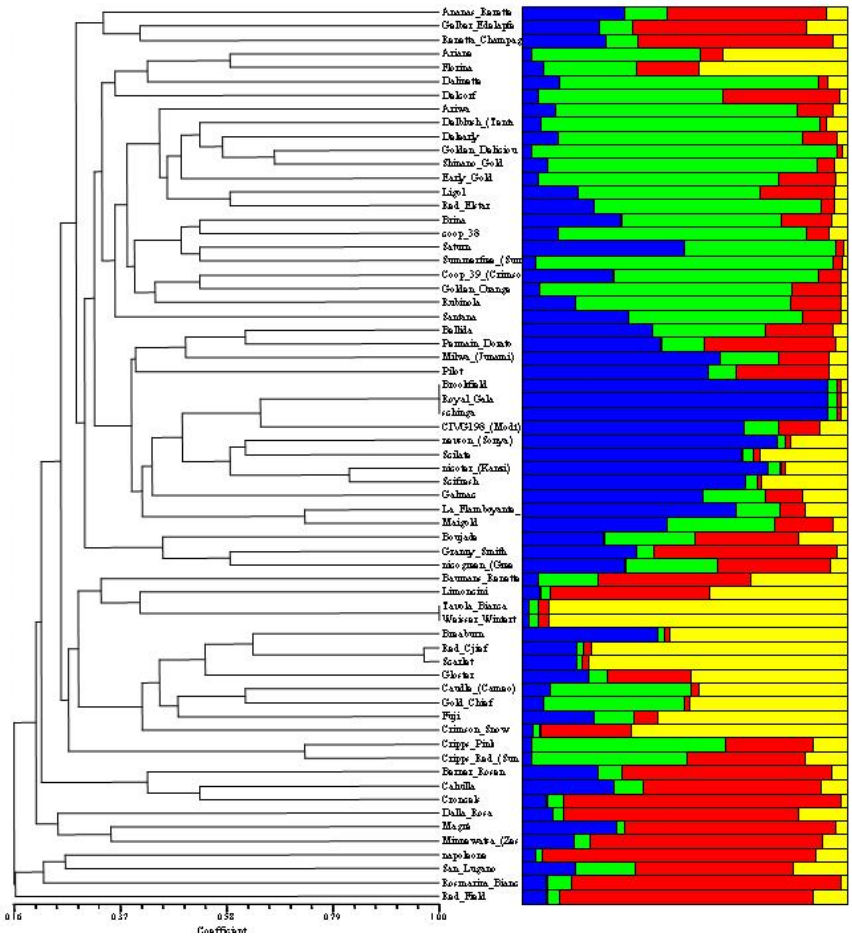

Figure 10.3: Similarity tree and population structure for the varieties phenotypically assessed in 2010 (K = 4).

Figure 10.4: *Md-PG1* aminoacid sequence derived by the predicted *Md-PG1* sequence.

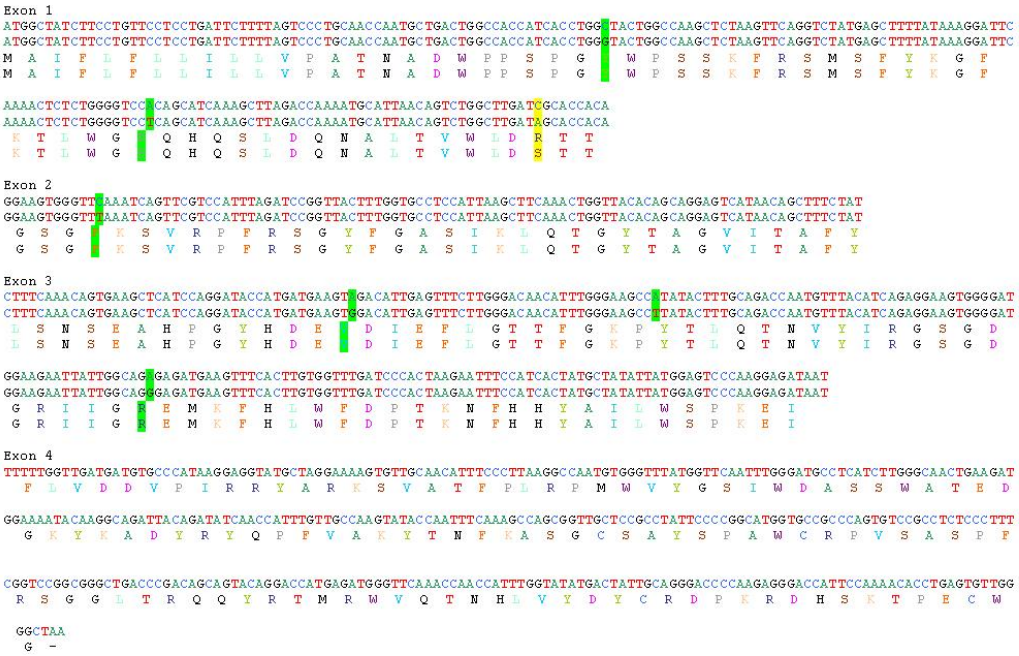

Figure 10.5: *Md-Xet* aminoacid sequence derived by the predicted *Md-Xet* sequence.

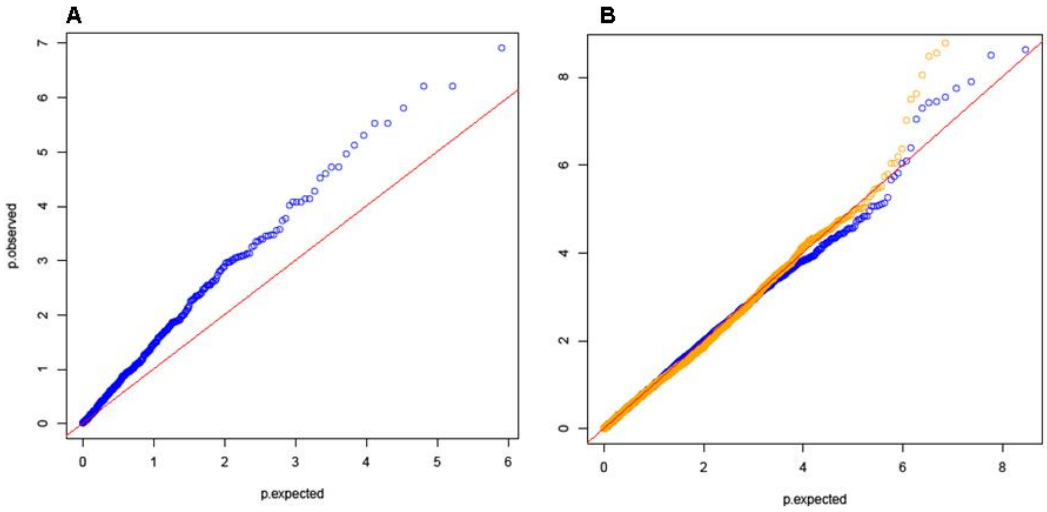

Figure 10.6: Q-Q plot of the P-value distribution.

	Force Peaks			Final Force			Yield Force			Mean Force			Max Force		
SNP	A	B	C	A	B	C	A	B	C	A	B	C	A	B	C
GD SNP02072	0,7822	0,5674	0,0462**	0,1329	0,0619	0,0018**	0,4496	0,1419	0,0021**	0,1419	0,0859	0,0011**	1	0,0219**	0,0016**
GD SNP02371	0,4276	1	0,4987	1	1	0,7760	1	1	0,9263	1	1	0,9405	1	1	0,9271
GD SNP01634	0,981	1	0,8131	1	1	0,6265	0,0299**	1	0,5177	0,0249**	1	0,3855	0,0089**	1	0,5840
PG full 01	0,6474	0,3247	0,0105**	0,0679	0,1079	0,0042**	0,6793	0,9361	0,0092**	0,2088	0,6134	0,0042**	0,2168	0,6134	0,0046**
PG full 04,07,14,22°	0,8751	0,9960	1	1	1	1	1	1	1	1	1	1	1	1	1
PG full 06	0,959	0,0499**	0,7133	0,6144	0,8631	0,1765	0,3197	0,8811	0,0632	0,2088	0,7143	0,1257	0,2787	0,9231	0,0992
PG full 10	0,5465	0,0149**	0,5412	0,2438	0,1988	0,5851	0,2827	0,3417	0,7508	0,1059	0,2677	0,688	0,1528	0,3706	0,8009
PG full 12	0,988	0,9880	0,1622	0,962	0,6404	0,0841	0,982	0,7892	0,1710	0,8671	0,6414	0,1083	1	0,5794	0,1237
PG full 15	0,7063	0,9920	0,0947	0,8881	1	0,4670	0,997	1	0,2686	0,9291	1	0,4425	0,956	1	0,4877
PG full 18	0,9121	0,0169**	0,0113**	0,8571	0,969	0,0069**	0,991	0,993	0,0066**	0,7303	0,996	0,0038**	0,9091	0,9960	0,0078**
PG full 19	1	0,8182	0,6906	0,994	0,7363	0,0413**	0,994	0,9081	0,0656	0,9361	0,7732	0,0378**	1	0,7023	0,0472**
PG full 20	1	0,5704	0,1670	1	1	0,0596	1	0,999	0,0389**	1	1	0,0534	1	1	0,0547
PG full 21	0,5944	0,0149**	0,5412	0,1968	0,2258	0,5851	0,2328	0,3786	0,7508	0,0839	0,3067	0,688	0,1349	0,4366	0,8009
23 3 'UTR	0,5654	0,2767	0,4160	0,5694	0,9451	0,4019	0,8012	1	0,5237	0,3337	0,997	0,509	0,4406	0,993	0,5733
PG 1kd 1	1	0,0459**	0,4126	1	1	0,7477	1	0,999	0,0670	1	0,999	0,0821	1	0,5275	0,1724
PG 1kd 7	0,8322	0,1528	0,1098	0,7123	0,6793	0,1523	0,989	0,8511	0,1116	0,7952	0,5095	0,0754	0,8831	1	0,1113
Md-PG1SSR 10kd 2	1	0,3057	0,7046	1	1	0,0768	1	1	0,0591	1	1	0,0711	1	1	0,0822
Md-PG1SSR 10kd 3	0,07393	0,3097	0,0684	0,0019**	0,0009**	0,0048**	0,0189**	0,0363**	0,006**	0,0049**	0,0289**	0,0074**	0,0039**	0,0199**	0,0065**

	Area			Acoustic Linear Distance			Max Acoustic Pressure			Mean Acoustic Pressure			Acoustic Peaks		
SNP	A	B	C	A	B	C	A	B	C	A	B	C	A	B	C
GD SNP02072	0,1658	0,0939	0,0012**	0,05495	0,0119**	0,0002**	0,0829	0,0069**	0,0016**	0,2647	0,1688	0,0083**	0,0419**	0,0079**	0,0004**
GD SNP02371	1	1	0,8878	0,03896**	1	0,4140	0,2178	1	0,6205	0,0399**	1	0,7420	0,0429**	1	0,3306
GD SNP01634	0,0379**	1	0,4283	1	1	0,4065	1	1	0,7260	1	1	0,9580	1	1	0,4414
PG full 01	0,2557	0,6893	0,0039**	0,05994	0,0119**	0,0031**	0,1169	0,0119**	0,0051**	0,1289	0,0349**	0,0125**	0,0809	0,0009**	0,0092**
PG full 04,07,14,22°	1	1	1	0,01399**	0,7413	1	0,0389**	1	1	0,0999	1	1	0,0119**	0,3746	1
PG full 06	0,2527	0,7273	0,0918	0,4825	0,0049**	0,0028**	0,5235	0,0079**	0,2541	1	0,0339**	0,2337	0,4276	0,0009**	0,3519
PG full 10	0,1189	0,2537	0,6811	0,03796**	0,7413	0,0019**	0,1269	0,0019**	0,9607	0,5894	0,0149**	0,6745	0,0489**	0,0009**	0,9300
PG full 12	1	0,7003	0,0722	0,6184	0,1369	0,0017**	0,3427	0,0349**	0,1580	1	0,3477	0,2039	0,4655	0,0169**	0,0685
PG full 15	0,9221	1	0,4579	0,02398**	0,7502	0,0245**	0,0219**	0,974	0,0223**	0,1029	1	0,0624	0,0139**	0,2448	0,0045**
PG full 18	0,7752	0,988	0,0048**	0,2937	0,0029**	0,0017**	0,8462	0,0029**	0,0026**	0,8851	0,0109**	0,0056**	0,3017	0,0009**	0,0025**
PG full 19	0,9461	0,7992	0,0326**	0,6913	0,0969	0,00317**	0,6643	0,0349**	0,0696	1	0,1728	0,2473	0,6004	0,0169**	0,0482**
PG full 20	1	1	0,0474**	1	0,1089	0,0367**	1	0,2448	0,0847	1	0,3287	0,0707	1	0,0329**	0,1763
PG full 21	0,1019	0,2877	0,6811	0,03497**	0,0019**	0,0019**	0,0869	0,0019**	0,9607	0,5335	0,0139**	0,6745	0,0509	0,0009**	0,9300
23 3 'UTR	0,4146	0,993	0,4994	0,01698**	0,0139**	0,0036**	0,0829	0,0719	0,3969	0,5824	0,1808	0,3128	0,0209**	0,0009**	0,8177
PG 1kd 1	1	0,999	0,1979	0,0550**	0,0479**	0,0699**	1	0,0339**	0,7090	1	0,2008	0,9600	1	0,0379**	0,3334
PG 1kd 7	0,8212	0,5435	0,0783	0,06094	0,0039**	0,0097**	0,1968	0,0029**	0,0246**	0,6983	0,0229**	0,0816	0,0549	0,0009**	0,0459**
$Md-PG1_{SSR}$_10kd_2	1	1	0,0674	1	0,1009	0,0143**	1	0,3277	0,3418	1	0,1818	0,3502	1	0,0419**	0,5950
$Md-PG1_{SSR}$_10kd_3	0,0029**	0,0409**	0,007**	0,0070**	0,0139**	0,0009**	0,0059**	0,0259**	0,0035**	0,1578	0,05794	0,0205**	0,0229**	0,0019**	0,0022**

Table 10.3: Association results between single SNP and texture sub-traits. For each parameter, A and B column refer to the two separate postharvest assessments carried out at 2009 and 2010 year, respectively. The column C is for the association performed with TASSEL and considering the LS mena of the two years implemented in the MLM model. **Statistically significance at P-value p<0.05. "°" with a MAF p<0.05.

haplotype 1	haplotype 3	haplotype 9	haplotype 10
Ambrosia	Ananas Renette	Brina	CIVg198
Bellida	Ariane	Gelber Edelapfel	Coop 39
Berner Rosen	Ariwa	Rome Beauty	Ligol
Breaburn	Caudle	Rubinola	Minnewatsa
Calamari	CIVg198	Topaz	
Croncels	Civni		
Dalla Rosa	Coop 39		
Delearly	Cripps Pink		
Delorina	Cripps Red		
Early gold	Delblush		
Gelber Edelapfel	Delcorf		
Gewurtzluiken	Fuji		
Gloster	Golden Delicious		
Golden Delicious	Granny Smith		
Golden Orange	Ligol		
Hapke Delicious	Milwa		
Limoncini	Nicogreen		
Magre	Pinova		
Maigold	Santana		
Napoleone	Schifresh		
Nevson	Schinano Gold		
Nicoter			
Permain Dorato			
Red Chief			
Red Elstar			
Red Field			
Rosmarina Bianca			
Royal Gala			
Sansa			
Scarlet			
Weisser Wintertaffen			
Tavola Bianca			
Renette Champagne			

Table 10.4: List of cultivars characterized by haplotypes 1, 3, 9 and 10.

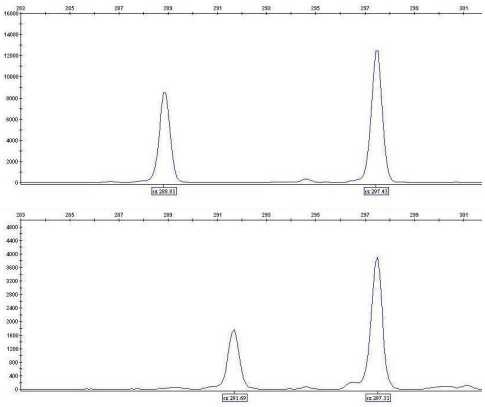

Figure 10.7: *Md-PG1SSR*_10Kd allelism. In the figure is illustrated the microsatellite allelic profile in two apple varieties, representing the three alleles detected within the assembled apple collection.

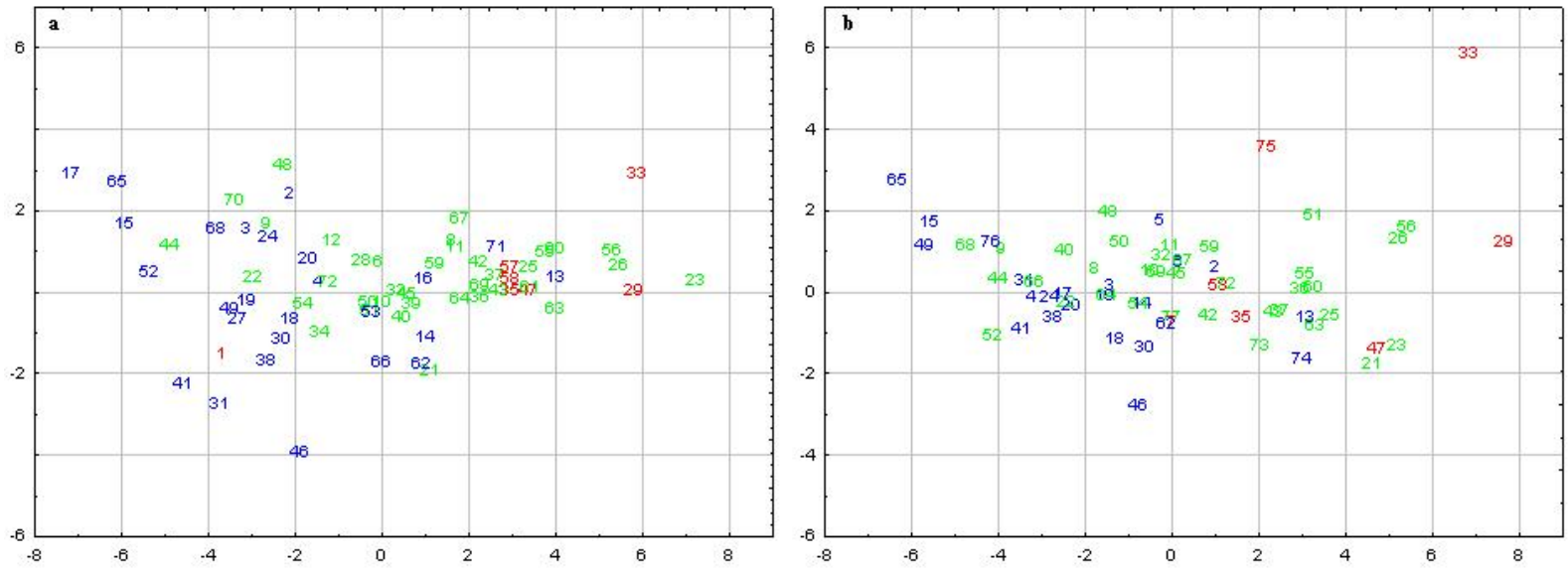

Figure 10.8: Two PCA distributions (a 2009 postharvest, b 2010 postharvest). Numbers correspond to the varieties as reported in Table 1. Colours means the allelic dosage for *Md-PG1*SSR 10kd 3, with blue used for cultivars characterized by the absence of the "3" allele, green for cultivar having this allele in heterozygous state and red for cultivars carrying this allele in a homozygous state (thus present two times).

Bibliography

[1] F. B. Abeles and C.L. Biles. Cellulase activity in developing apple fruits. *Scientia Horticulturae*, 47(1-2):77–87, 1991.

[2] F. B. Abeles and F. Takeda. Cellulase activity and ethylene in ripening strawberry and apple fruits. *Scientia Horticulturae*, 42(4):269–275, 1990.

[3] A. Aharoni, L. C. P. Keizer, H. J. Bouwmeester, Z. Sun, M. Alvarez-Huerta, H. A. Verhoeven, J. Blaas, A. M. M. L. van Houwelingen, R. C. H. De Vos, H. van der Voet, et al. Identification of the saat gene involved in strawberry flavor biogenesis by use of dna microarrays. *The Plant Cell Online*, 12(5):647, 2000.

[4] A. E. Ahmed and J. M. Labavitch. Cell Wall Metabolism in Ripening Fruit: I. cell wall changes in ripening barlett' pears. *Plant Physiology*, 65(5):1009, 1980.

[5] R. Alba, P. Payton, Z. J. Fei, R. McQuinn, P. Debbie, G. B. Martin, S. D. Tanksley, and J. J. Giovannoni. Transcriptome and selected metabolite analyses reveal multiple points of ethylene control during tomato fruit development. *Plant Cell*, 17(11):2954–2965, 2005.

[6] L. Alexander and D. Grierson. Ethylene biosynthesis and action in tomato: a model for climacteric fruit ripening. *Journal of Experimental Botany*, 53(377):2039, 2002.

[7] Z. Andani, S. R. Jaeger, I. Wakeling, and H. J. H. MacFie. Mealiness in apples: towards a multilingual consumer vocabulary. *Journal of food science*, 66(6):872–879, 2001.

[8] M. R. Anderberg. *Cluster analysis for application*. Academic press: New York, 1992.

[9] M. J. Asins. Present and future of quantitative trait locus analysis in plant breeding. *Plant Breeding*, 121(4):281–291, 2002.

[10] R. G. Atkinson. A cdna clone for endopolygalacturonase from apple. *Plant Molecular Biology*, 105(4):1437–1438, 1994.

[11] R. G. Atkinson and R. C. Gardner. A polygalacturonase gene from kiwifruit (actinidia-deliciosa). *Plant Molecular Biology*, 103(2):669–670, 1993.

[12] A. N. N. H. Barret, A. V. Cardello, L. L. Lesher, and I. A. Taub. Cellularity, mechanical failure, and textural perception of corn meal extrudates. *Journal of texture studies*, 25(1):77–95, 1994.

[13] J. C. Barrett, B. Fry, J. Maller, and Daly M. J. Haploview: analysis and visualization of ld and haplotype maps. *Bioinformatics*, 21(2):263–265, 2005.

[14] C. S. Barry and J. J. Giovannoni. Ethylene and fruit ripening. *Journal of Plant Growth Regulation*, 26(2):143–159, 2007.

[15] C. S. Barry, M. I. Llop-Tous, and D. Grierson. The regulation of 1-aminocyclopropane-1-carboxylic acid synthase gene expression during the transition from system-1 to system-2 ethylene synthesis in tomato. *Plant Physiology*, 123(3):979, 2000.

[16] G. E. Bartley and B. Ishida. Developmental gene regulation during tomato fruit ripening and in-vitro sepal morphogenesis. *BMC plant biology*, 3(1):4, 2003.

[17] C. Batisse, M. Buret, and P. J. Coulomb. Biochemical differences in cell wall of cherry fruit between soft and crisp fruit. *Journal of agricultural and food chemistry*, 44(2):453–457, 1996.

[18] C. Batisse, B. Fils-Lycaon, and M. Buret. Pectin changes in ripening cherry fruit. *Journal of food science*, 59(2):389–393, 1994.

[19] R. Ben-Arie, N. Kislev, and C. Frenkel. Ultrastructural changes in the cell walls of ripening apple and pear fruit. *Plant Physiology*, 64(2):197, 1979.

[20] C. R. Bird, C. J. S. Smith, J. A. Ray, P. Moureau, M. W. Bevan, A. S. Bird, S. Hughes, P. C. Morris, D. Grierson, and W. Schuch. The tomato polygalacturonase gene and ripening-specific expression in transgenic plants. *Plant Molecular Biology*, 11(5):651–662, 1988.

[21] S. M. Blankenship and J. M. Dole. 1-methylcyclopropene: a review. *Postharvest biology and technology*, 28(1):1–25, 2003.

[22] A. B. Bleecker and H. Kende. Ethylene: a gaseous signal molecule in plants. *Annual Review of Cell and Developmental Biology*, 16(1):1–18, 2000.

[23] C. Bonghi, L. Trainotti, A. Botton, A. Tadiello, A. Rasori, F. Ziliotto, V. Zaffalon, G. Casadoro, and A. Ramina. A microarray approach to identify genes involved in seed-pericarp cross-talk and development in peach. *BMC Plant Biology*, 11(1):107, 2011.

[24] A. Botton, G. Eccher, C. Forcato, A. Ferrarini, M. Begheldo, M. Zermiani, S. Moscatello, A. Battistelli, R. Velasco, B. Ruperti, and A. Ramina. Signaling pathways mediating the induction of apple fruitlet abscission. *Plant Physiology*, 155(1):185–208, 2011.

[25] M. C. Bourne. *Food texture and viscosity: concept and measurement.* Academic Press, San Diego, 2002.

[26] P. J. Bradbury, Z. Zhang, D. E. Kroon, T. M. Casstevens, Y. Ramdoss, and E. S. Buckler. Tassel: software for association mapping of complex traits in diverse samples. *Bioinformatics*, 23(19):2633–2635, 2007.

[27] P. L. Brookfield, S. Nicoll, F. A. Gunson, F. R. Harker, and M. Wohlers. Sensory evaluation by small postharvest teams and the relationship with instrumental measurements of apple texture. *Postharvest Biology and Technology*, 2010.

[28] D. A. Brummell. Cell wall disassembly in ripening fruit. *Functional Plant Biology*, 33(2):103–119, 2006.

[29] D. A. Brummell and M. H. Harpster. Cell wall metabolism in fruit softening and quality and its manipulation in transgenic plants. *Plant Molecular Biology*, 47(1):311–339, 2001.

[30] P. Campbell and J. Braam. Xyloglucan endotransglycosylases: diversity of genes, enzymes and potential wall-modifying functions. *Trends Plant Sci*, 4(9):361–366, 1999.

[31] L. Cappellin, F. Biasioli, E. Schuhfried, C. Soukoulis, T. D. Märk, and F. Gasperi. Extending the dynamics range of proton transfer reaction time-of-flight mass spectrometers by a novel dead time correction. *Rapid Communications in Mass Spectrometry*, 25(1):179–183, 2011.

[32] B. Cara and J. J. Giovannoni. Molecular biology of ethylene during tomato fruit development and maturation. *Plant Science*, 175(1-2):106–113, 2008.

[33] A. V. Cardello. 10 consumer expectations and their role in food acceptance. *Cereal Foods World*, 41:469–470, 1996.

[34] N. C. Carpita and D. M. Gibeaut. Structural models of primary cell walls in flowering plants: consistency of molecular structure with the physical properties of the walls during growth. *The Plant Journal*, 3(1):1–30, 1993.

[35] G. I. Cassab. Plant cell wall proteins. *Annual Review of Plant Biology*, 49(1):281–309, 1998.

[36] V. Cevik, C. D. Ryder, A. Popovich, K. Manning, G. J. King, and G. B. Seymour. A fruitfull-like gene is associated with genetic variation for fruit flesh firmness in apple (*Malus x domestica* borkh.). *Tree Genetics & Genomes*, 6(2):271–279, 2010.

[37] D. Chagné, K. Gasic, R. N. Crowhurst, Y. Han, H. C. Bassett, D. R. Bowatte, T. J. Lawrence, E. H. A. Rikkerink, S. E. Gardiner, and S. S. Korban. Development of a set of SNP markers present in expressed genes of the apple. *Genomics*, 92(5):353–358, 2008.

[38] M. A. Chauvin, C. F. Ross, M. Pitts, E. Kumpfermann, and B. Swanson. Relationship between instrumental and sensory determination of apple and pear texture. *Journal of Food Quality*, 33(2):181–198, 2010.

[39] M. A. Chauvin, F. Younce, C. Ross, and B. Swanson. Standard scales for crispness, crackliness and crunchiness in dry and wet foods: relationship with acoustical determinations. *Journal of Texture Studies*, 39(4):345–368, 2008.

[40] A. L. S. Chaves and P. C. de Mello-Farias. Ethylene and fruit ripening: from illumination gas to the control of gene expression, more than a century of discoveries. *Genet Mol Biol*, 29:508–515, 2006.

[41] C. M. Christensen and Z. M. Vickers. Relationships of chewing sounds to judgments of food crispness. *Journal of Food Science*, 46(2):574–578, 1981.

[42] N. O. I. Cogan, R. C. Ponting, A. C. Vecchies, M. C. Drayton, J. George, P. M. Dracatos, M. P. Dobrowolski, T. I. Sawbridge, K. F. Smith, G. C. Spangenberg, et al. Gene-associated single nucleotide polymorphism discovery in perennial ryegrass (Lolium perenne L.). *Molecular Genetics and Genomics*, 276(2):101–112, 2006.

[43] B. C. Y. Collard, M. Z. Z. Jahufer, J. B. Brouwer, and E. C. K. Pang. An introduction to markers, quantitative trait loci (qtl) mapping and marker-assisted selection for crop improvement: The basic concepts. *Euphytica*, 142(1-2):169–196, 2005. Times Cited: 92.

[44] D. J. Cosgrove. Loosening of plant cell walls by expansins. *Nature*, 407(6802):321–326, 2000.

[45] F. Costa, R. Alba, H. Schouten, V. Soglio, L. Gianfranceschi, S. Serra, S. Musacchi, S. Sansavini, G. Costa, Z. J. Fei, and J. Giovannoni. Use of homologous and heterologous gene expression profiling tools to characterize transcription dynamics during apple fruit maturation and ripening. *Bmc Plant Biology*, 10, 2010.

[46] F. Costa, L. Cappellin, S. Longhi, W. Guerra, P. Magnano, D. Porro, C. Soukoulis, S. Salvi, R. Velasco, F. Biasioli, and F. Gasperi. Assessment of apple (malus x domestica borkh.) fruit texture by a combined acoustic-mechanical profiling strategy. *Postharvest Biology and Technology*, 6:21–28, 2011.

[47] F. Costa, G. Costa, S. Sansavini, V. Soglio, L. Gianfranceschi, H. J. Schouten, R. Alba, and J. Giovannoni. Heterologous comparative genomics to identify candidate genes impacting fruit quality in apple (malus x domestica borkh.). *Acta Horticulturae*, 2(814):517–522, 2009.

[48] F. Costa, C. P. Peace, S. Stella, S. Serra, S. Musacchi, M. Bazzani, S. Sansavini, and W. E. Van de Weg. Qtl dynamics for fruit firmness and softening around an ethylene-dependent polygalacturonase gene in apple (malus x domestica borkh.). *Journal of Experimental Botany*, 61(11):3029–3039, 2010.

[49] F. Costa, S. Stella, W. E. Van de Weg, W. Guerra, M. Cecchinel, J. Dalla Via, B. Koller, and S. Sansavini. Role of the genes md-aco1 and md-acs1 in ethylene production and shelf life of apple (malus x domestica borkh). *Euphytica*, 141:181–190, 2005.

[50] F. Costa, W. E Van de Weg, S. Stella, L. Dondini, D. Pratesi, S. Musacchi, and S. Sansavini. Map position and functional diversity of md-exp7, a new putative expansin gene associated with fruit softening in apple (malus x domestica borkh.) and pear (pyrus communis). *Tree Genetics & Genomes*, 4:575–586, 2008.

[51] C. Dacremont. Spectral composition of eating sounds generated by crispy, crunchy and crackly foods. *Journal of texture studies*, 26(1):27–43, 1995.

[52] C. Dacremont and B. Colas. Contribution to the characterization of three french textural descriptors: croustillant (crispy), craquant (crackle) and croquant (crunchy) by acoustic and sensory studies. *PhD thesis*, 1992.

[53] B. Daillant-Spinnler, H. J. H. MacFie, P. K. Beyts, and D. Hedderley. elationship between perceived sensory properties and major preference directions of 12 varieties of apples from the southern hemisphere. *R. Food Qual. Prefer*, 7:113–126, 1996.

[54] V. Dal Cin, F. M. Rizzini, A. Botton, and P. Tonutti. The ethylene biosynthetic and signal transduction pathways are differently affected by 1-mcp in apple and peach fruit. *Post harvest biology and technology*, 42(2):125–133, 2006.

[55] V. Dal Cin, R. Velasco, and A. Ramina. Dominance induction of fruitlet shedding in malus x domestica (l. borkh): molecular changes associated with polar auxin transport. *Bmc Plant Biology*, 9, 2009.

[56] L. L. Dantec, D. Chagne, D. Pot, O. Cantin, P. Garnier-Gere, F. Bedon, J.M. Frigerio, P. Chaumeil, P. Leger, V. Garcia, et al. Automated SNP detection in expressed sequence tags: statistical considerations and application to maritime pine sequences. *Plant molecular biology*, 54(3):461–470, 2004.

[57] A. Darvasi and S. Shifman. The beauty of admixture. *Nature Genetics*, 37(2):118–119, 2005.

[58] M. W. Davey, K. Kenis, and J. Keulemans. Genetic control of fruit vitamin c contents. *Plant Physiology*, 142(1):343–351, 2006.

[59] N. De Belie, V. De Smedt, and J. De Baerdemaeker. Principal component analysis of chewing sounds to detect differences in apple crispness. *Postharvest biology and technology*, 18(2):109–119, 2000.

[60] N. De Belie, F. R. Harker, and J. De Baerdemaeker. PH–Postharvest Technology: Crispness Judgement of Royal Gala Apples Based on Chewing Sounds. *Biosystems engineering*, 81(3):297–303, 2002.

[61] R. Deshmukh, A. Singh, N. Jain, S. Anand, R. Gacche, K. Gaikwad, T. Sharma, T. Mohapatra, and N. Singh. Identification of candidate genes for grain number in rice (oryza sativa l.). *Functional & Integrative Genomics*, 10(3):339–347, 2010.

[62] A. Di Matteo, A. Sacco, M. Anacleria, M. Pezzotti, M. Delledonne, A. Ferrarini, L. Frusciante, and A. Barone. The ascorbic acid content in tomato fruits is associated with the expression of genes involved in pectin degradation. *BMC Plant Biology*, 10(1):163, 2010.

[63] R. W. Doerge. Mapping and analysis of quantitative trait loci in experimental populations. *Nature Reviews Genetics*, 3(1):43–52, 2002.

[64] J. G. Dong, J. C. Fernandez-Maculet, and S. F. Yang. Purification and characterization of 1-aminocyclopropane-1-carboxylate oxidase from apple fruit. *Proceedings of the National Academy of Sciences of the United States of America*, 89(20):9789, 1992.

[65] B. K. Drake. Food Crushing Sounds. An Introductory Studya, b. *Journal of Food Science*, 28(2):233–241, 1963.

[66] L. M. Duizer. A review of acoustic research for studying the sensory perception of crisp, crunchy and crackly textures. *Trends in food science & technology*, 12(1):17–24, 2001.

[67] L. M. Duizer, O. H. Campanella, and G. R. G. Barnes. Sensory, instrumental and acoustic characteristics of extruded snack food products. *Journal of texture studies*, 29(4):397–411, 1998.

[68] J. C. Dumville and S. C. Fry. Solubilisation of tomato fruit pectins by ascorbate: a possible non-enzymic mechanism of fruit softening. *Planta*, 217(6):951–961, 2003.

[69] F. Dunemann, D. Ulrich, L. Malysheva-Otto, W. E. Weber, S. Longhi, R. Velasco, and F. Costa. Functional allelic diversity of the apple alcohol acyl-transferase gene mdaat1 associated with fruit ester volatile contents in apple cultivars. *Molecular Breeding*, doi10.1007/s11032-011-9577-7:1–17, 2011.

[70] G. Echeverrìa, J. Graell, I. Lara, M. L. Lopez, and J. Puy. Panel consonance in the sensory evaluation of apple attributes: Influence of mealiness on sweetness perception. *Journal of Sensory Studies*, 23(5):656–670, 2008.

[71] J. A. Edmister and Z. M. Vickers. Instrumental acoustical measures of crispness in foods. *Journal of texture studies*, 16(2):153–167, 1985.

[72] I. M. Ehrenreich, Y. Hanzawa, L. Chou, J. L. Roe, P. X. Kover, and M. D. Purugganan. Candidate gene association mapping of arabidopsis flowering time. *Genetics*, 183(1):325–335, 2009.

[73] I. M. Ehrenreich, P. A. Stafford, and M. D. Purugganan. The genetic architecture of shoot branching in arabidopsis thaliana: A comparative assessment of candidate gene associations vs. quantitative trait locus mapping. *Genetics*, 176(2):1223–1236, 2007.

[74] F. Emanuelli, J. Battilana, L. Costantini, L. Le Cunff, J. M. Boursiquot, P. This, and M. S. Grando. A candidate gene association study on muscat flavor in grapevine (vitis vinifera l.). *Bmc Plant Biology*, 10, 2010.

[75] K. Esau. *Anatomy of seed plants.* Wiley-India, 2006.

[76] A. Fabris, F. Biasioli, P. M. Granitto, E. Aprea, L. Cappellin, E. Schuhfried, C. Soukoulis, T. D. Märk, F. Gasperi, and I. Endrizzi. Ptr-tof-ms and data-mining methods for rapid characterisation of agro-industrial samples: influence of milk storage conditions on the volatile compounds profile of

trentingrana cheese. *Journal of Mass Spectrometry*, 45(9):1065–1074, 2010.

[77] D. S. Falconer and T. F. C. Mackay. Introduction to quantitative genetics. *Genetics*, 167(4):389–409, 2004.

[78] D. Falush, M. Stephens, and J. K. Pritchard. Inference of population structure using multilocus genotype data: Linked loci and correlated allele frequencies. *Genetics*, 164(4):1567–1587, 2003.

[79] Z. Fei, X. Tang, R. Alba, and J. Giovannoni. Tomato expression database (ted): a suite of data presentation and analysis tools. *Nucleic Acids Research*, 34:D766–D770, 2006.

[80] L. Fillion and D. Kilcast. Concept and measurement of freshness of fruits and vegetables. *Leatherhead Food RA Research Reports*, 2000.

[81] L. Fillion and D. Kilcast. Consumer perception of crispness and crunchiness in fruits and vegetables. *Food quality and preference*, 13(1):23–29, 2002.

[82] S. A. Flint-Garcia, J. M. Thornsberry, and B. IV. Structure of linkage disequilibrium in plants. *Annual Review of Plant Biology*, 54(1):357–374, 2003.

[83] S. Fonseca, L. Hackler, Á. Zvara, S. Ferreira, A. Baldé, D. Dudits, M. S. Pais, and L. G. Puskás. Monitoring gene expression along pear fruit development, ripening and senescence using cdna microarrays. *Plant Sci*, 167(3):457–469, 2004.

[84] S. C. Fry. Oxidative scission of plant cell wall polysaccharides by ascorbate-induced hydroxyl radicals. *Biochemical Journal*, 332:507–515, 1998.

[85] J. Giovannoni. Molecular biology of fruit maturation and ripening. *Annual Review of Plant Physiology and Plant Molecular Biology*, 52:725, 2001.

[86] J. Giovannoni. Genetic regulation of fruit development and ripening. *Plant Cell*, 16:S170–S180, 2004.

[87] S. C. Gonzalez-Martinez, E. Ersoz, G. R. Brown, N. C. Wheeler, and D. B. Neale. Dna sequence variation and selection of tag single-nucleotide polymorphisms at candidate genes for drought-stress response in pinus taeda l. *Genetics*, 172(3):1915–1926, 2006.

[88] L. F. Goulao and C. M. Oliveira. Cell wall modifications during fruit ripening: when a fruit is not the fruit. *Trends in Food Science & Technology*, 19(1):4–25, 2008.

[89] L. F. Goulao, J. Santos, I. de Sousa, and C. M. Oliveira. Patterns of enzymatic activity of cell wall-modifying enzymes during growth and ripening of apples. *Postharvest biology and technology*, 43(3):307–318, 2007.

[90] K. C. Gross. Changes in free galactose, myo-inositol and other monosaccharides in normal and non-ripening mutant tomatoes. *Phytochemistry*, 22(5):1137–1139, 1983.

[91] K. C. Gross. Fractionation and partial characterization of cell walls from normal and non-ripening mutant tomato fruit. *Physiologia Plantarum*, 62(1):25–32, 1984.

[92] K. C. Gross and S. J. Wallner. Degradation of cell wall polysaccharides during tomato fruit ripening. *Plant Physiology*, 63(1):117, 1979.

[93] E. Guichoux, L. Lagache, S. Wagner, P. Chaumeil, P. Leger, O. Lepais, C. Lepoittevin, T. Malausa, E. Revardel, F. Salin, and et al. Current trends in microsatellite genotyping. *Molecular Ecology Resources*, 11(4):591–611, 2011.

[94] H. Guo and J. R. Ecker. Plant responses to ethylene gas are mediated by scfebf1/ebf2-dependent proteolysis of ein3 transcription factor. *Cell*, 115(6):667–677, 2003.

[95] P. K. Gupta, S. Rustgi, and P. L. Kulwal. Linkage disequilibrium and association studies in higher plants: present status and future prospects. *Plant Molecular Biology*, 57(4):461–485, 2005.

[96] L. N. Hall, G. A. Tucker, C. J. S. Smith, C. F. Watson, G. B. Seymour, Y. Bundick, J. M. Boniwell, J. D. Fletcher, J. A. Ray, W. Schuch, et al. Antisense inhibition of pectin esterase gene expression in transgenic tomatoes. *The Plant Journal*, 3(1):121–129, 1993.

[97] C. R. Hampson, H. A. Quamme, J. W. Hall, R. A. MacDonald, M. C. King, and M. A. Cliff. Sensory evaluation as a selection tool in apple breeding. *Euphytica*, 111(2):79–90, 2000.

[98] T. Harada, T. Sunako, Y. Wakasa, J. Soejima, T. Satoh, and M. Niizeki. An allele of the 1-aminocyclopropane-1-carboxylate synthase gene (md-acs1) accounts for the low level of ethylene production in climacteric fruits of some apple cultivars. *Theoretical and Applied Genetics*, 101(5-6):742–746, 2000.

[99] F. R. Harker, F. A. Gunson, and S. R. Jaeger. The case for fruit quality: an interpretive review of consumer attitudes, and preferences for apples. *Postharvest Biology and Technology*, 28(3):333–347, 2003.

[100] F. R. Harker, I. C. Hallett, S. H. Murray, and G. Carter. Food-mouth interactions: towards a better understanding of fruit texture. *Acta horticulturae*, 464:461–466, 1998.

[101] F. R. Harker, J. Maindonald, S. H. Murray, F. A. Gunson, I. C. Hallett, and S. B. Walker. Sensory interpretation of instrumental measurements 1: texture of apple fruit. *Postharvest Biology and Technology*, 24(3):225–239, 2002.

[102] F. R. Harker, A. White, F.A . Gunson, I. C. Hallett, and H. N. De Silva. Instrumental measurement of apple texture: A comparison of the single-edge notched bend test and the penetrometer. *Postharvest biology and technology*, 39(2):185–192, 2006.

[103] G. Haseneyer, S. Stracke, H. P. Piepho, S. Sauer, H. H. Geiger, and A. Graner. Dna polymorphisms and haplotype patterns of transcription factors involved in barley endosperm development are associated with key agronomic traits. *Bmc Plant Biology*, 10, 2010.

[104] K. Hiwasa, R. Nakano, A. Hashimoto, M. Matsuzaki, H. Murayama, A. Inaba, and Y. Kubo. European, chinese and japanese pear fruits exhibit differential softening characteristics during ripening. *Journal of Experimental Botany*, 55(406):2281–2290, 2004.

[105] J. B. Holland. Genetic architecture of complex traits in plants. *Current Opinion in Plant Biology*, 10(2):156–161, 2007.

[106] S. Holt. The satiety index: a new method to measure the filling powers of foods. *Food Australia*, 51(3):74–75, 1999.

[107] F. Hospital. Challenges for effective marker-assisted selection in plants. *Genetica*, 136(2):303–310, 2009.

[108] R. Hovav, N. Chehanovsky, M. Moy, R. Jetter, and A. A. Schaffer. The identification of a gene (Cwp1), silenced during Solanum evolution, which causes cuticle microfissuring and dehydration when expressed in tomato fruit. *The Plant Journal*, 52(4):627–639, 2007.

[109] J. Hua, C. Chang, Q. Sun, and E. M. Meyerowitz. Ethylene insensitivity conferred by arabidopsis ers gene. *Science*, 269(5231):1712, 1995.

[110] D. J. Huber and E. M. O'Donoghue. Polyuronides in avocado (Persea americana) and tomato (Lycopersicon esculentum) fruits exhibit markedly different patterns of molecular weight downshifts during ripening. *Plant Physiology*, 102(2):473, 1993.

[111] P. K. Ingvarsson and N. R. Street. Association genetics of complex traits in plants. *New Phytologist*, 189(4):909–922, 2011.

[112] Y. Ioannides, M. S. Howarth, C. Raithatha, M. Defernez, E. K. Kemsley, and A. C. Smith. Texture analysis of Red Delicious fruit: Towards multiple measurements on individual fruit. *Food quality and preference*, 18(6):825–833, 2007.

[113] S. R. Jaeger, Z. Andani, I. N. Wakeling, and H. J. H. MacFie. Consumer preferences for fresh and aged apples: a cross-cultural comparison. *Food quality and preference*, 9(5):355–366, 1998.

[114] B. J. Janssen, K. Thodey, R. J. Schaffer, R. Alba, L. Balakrishnan, R. Bishop, J. H. Bowen, R. N. Crowhurst, A. P. Gleave, S. Ledger, S. McArtney, F. B. Pichler, K. C. Snowden, and S. Ward. Global gene expression analysis of apple fruit development from the floral bud to ripe fruit. *Bmc Plant Biology*, 8, 2008.

[115] A. Jiménez-Bermúdez, G. Creissen, B. Kular, J. Firmin, S. Robinson, M. Verhoeyen, and P. Mullineaux. Changes in oxidative processes and components of the antioxidant system during tomato fruit ripening. *Planta*, 214(5):751–758, 2002.

[116] S. Jiménez-Bermúdez, J. Redondo-Nevado, J. Muñoz-Blanco, J.L. Caballero, J. M. López-Aranda, V. Valpuesta, F. Pliego-Alfaro, M. A. Quesada, and J. A. Mercado. Manipulation of strawberry fruit softening by antisense expression of a pectate lyase gene. *Plant Physiology*, 128(2):751, 2002.

[117] I. Jolliffe. Principal component analysis. *Encyclopedia of Statistics in Behavioral Science*, 2002.

[118] R. Karlova, F. M. Rosin, J. Busscher-Lange, V. Parapunova, P. T. Do, A. R. Fernie, P. D. Fraser, C. Baxter, G. C. Angenent, and R. A. de Maagd. Transcriptome and metabolite mrofiling show that apetala2a is a major regulator of tomato fruit ripening. *The Plant Cell Online*, 23(3):923, 2011.

[119] E. E. Katz and T. P. Labuza. Effect of water activity on the sensory crispness and mechanical deformation of snack food products. *Journal of Food Science*, 46(2):403–409, 1981.

[120] B. Keller. Structural cell wall proteins. *Plant physiology*, 101(4):1127, 1993.

[121] H. Kende. Ethylene biosynthesis. *Annual Review of Plant Biology*, 44(1):283–307, 1993.

[122] K. Kenis, J. Keulemans, and M.W. Davey. Identification and stability of qtls for fruit quality traits in apple. *Tree Genetics & Genomes*, 4(4):647–661, 2008.

[123] B. M. Kevany, M. G. Taylor, and H. J. Klee. Fruit-specific suppression of the ethylene receptor leetr4 results in early-ripening tomato fruit. *Plant biotechnology journal*, 6(3):295–300, 2008.

[124] D. Kilcast. Measuring consumer perceptions of texture: an overview. *Texture in food: volume 2: solid foods*, pages 3–32, 2004.

[125] C. Kimchi-Sarfaty, J. M. Oh, I. W. Kim, Z. E. Sauna, A. M. Calcagno, S. V. Ambudkar, and M. M. Gottesman. A "silent" polymorphism in the mdr1 gene changes substrate specificity. *Science*, 315(5811):525, 2007.

[126] G. J. King, J. R. Lynn, C.J. Dover, K. M. Evans, and G.B. Seymour. Resolution of quantitative trait loci for mechanical measures accounting for genetic variation in fruit texture of apple (malus pumila mill.). *Theoretical and Applied Genetics*, pages 1227–1235, 2001.

[127] G. J. King, C. Maliepaard, J. R. Lynn, F. H. Alston, C. E. Durel, K. M. Evans, B. Griffon, F. Laurens, A. G. Manganaris, T. Schrevens, S. Tartarini, and J. Verhaegh. Quantitative genetic analysis and comparison of physical and sensory descriptors relating to fruit flesh firmness in apple (malus pumila mill.). *Theoretical and Applied Genetics*, 100(7):1074–1084, 2000.

[128] M. Knee. Changes in structural polysaccharides of apples ripening during storage. In *International Colloquium CNRS Facteurs et Régulation de la Maturation des Fruits*, volume 238, pages 341–345, 1974.

[129] J. M. Kolkman, A. J. Berry, S. T. Leon, M. B. Slabaugh, S. Tang, W. Gao, D. K. Shintani, J. M. Burke, and S. J. Knapp. Single nucleotide polymorphisms and linkage disequilibrium in sunflower. *Genetics*, 177(1):457–468, 2007.

[130] A. B. Kouassi, C. E. Durel, F. Costa, S. Tartarini, E. van de Weg, K. Evans, F. Fernandez-Fernandez, C. Govan, A. Boudichevskaja, F. Dunemann, A. Antofie, M. Lateur, M. Stankiewicz-Kosyl, A. Soska, K. Tomala, M. Lewandowski, K. Rutkovski, E. Zurawicz, W. Guerra, and F. Laurens. Estimation of genetic parameters and prediction of breeding values for apple fruit-quality traits using pedigreed plant material in europe. *Tree Genetics & Genomes*, 5(4):659–672, 2009.

[131] C. Kulheim, S. Yeoh, J. Maintz, W. J. Foley, G. F. Moran, and S. H. Yeoh. Comparative snp diversity among four eucalyptus species for genes from secondary metabolite biosynthetic pathways. *BMC Genomics*, 10(452), 2009.

[132] D. T. A. Lamport. *Hydroxyproline-O-glycosidic linkage of the plant cell wall glycoprotein extensin*. Nature Publishing Group, 1967.

[133] C. C. Lashbrook, C. Gonzalez-Bosch, and A. B. Bennett. Two divergent endo-[beta]-1, 4-glucanase genes exhibit overlapping expression in ripening fruit and abscising flowers. *The Plant Cell Online*, 6(10):1485, 1994.

[134] Y. P. Lee, G. H. Yu, Y. S. Seo, S. E. Han, Y. O. Choi, D. Kim, I. G. Mok, W. T. Kim, and S. K. Sung. Microarray analysis of apple gene expression engaged in early fruit development. *Plant cell reports*, 26(7):917–926, 2007.

[135] J. G. Li and R. C. Yuan. Naa and ethylene regulate expression of genes related to ethylene biosynthesis, perception, and cell wall degradation during fruit abscission and ripening in 'delicious' apples. *Journal of Plant Growth Regulation*, 27(3):283–295, 2008.

[136] L. Li, B. Zhu, P. Yang, D. Fu, Y. Zhu, and Y. Luo. The regulation mode of rin transcription factor involved in ethylene biosynthesis in tomato fruit. *Journal of the Science of Food and Agriculture*, 2011.

[137] R. Liebhard, L. Gianfranceschi, B. Koller, C. D. Ryder, R. Tarchini, E. Van de Weg, and C. Gessler. Development and characterisation of 140 new microsatellites in apple (*Malus x domestica* borkh.). *Molecular Breeding*, 10(4):217–241, 2002.

[138] R. Liebhard, B. Koller, L. Gianfranceschi, and C. Gessler. Creating a saturated reference map for the apple (*Malus x domestica* borkh.) genome. *Theoretical and Applied Genetics*, 106(8):1497–1508, 2003.

[139] D. Lijavetzky, J.A. Cabezas, A. Ibáñez, V. Rodríguez, and J.M. Martínez-Zapater. High throughput SNP discovery and genotyping in grapevine(Vitis vinifera L.) by combining a re-sequencing approach and SNPlex technology. *BMC genomics*, 8(1):424, 2007.

[140] Z. Lin, S. Zhong, and D. Grierson. Recent advances in ethylene research. *Journal of experimental botany*, 60(12):3311, 2009.

[141] W. Lindinger, A. Hansel, and A. Jordan. On-line monitoring of volatile organic compounds at pptv levels by means of proton-transfer-reaction mass spectrometry (ptr-ms) medical applications, food control and environmental research. *International Journal of Mass Spectrometry and Ion Processes*, 173(3):191–241, 1998.

[142] X. Liu, S. Shiomi, A. Nakatsuka, Y. Kubo, R. Nakamura, and A. Inaba. Characterization of ethylene biosynthesis associated with ripening in banana fruit. *Plant physiology*, 121(4):1257, 1999.

[143] S. Longhi, M. Moretto, R. Viola, R. Velasco, and F. Costa. Comprehensive qtl mapping survey dissects the complex fruit texture physiology in apple (*Malus x domestica* borkh.). *Journal of Experimental Botany*, doi 10.1093/jxb/err326, 2011.

[144] H. Luyten, Plijter J.J, and T. Van Vliet. Crispy/crunchy crusts of cellular solid foods: A literature review with discussion. *Journal of texture studies*, 35(5):445–492, 2004.

[145] T. F. C. Mackay, E. A. Stone, and J. F. Ayroles. The genetics of quantitative traits: challenges and prospects. *Nature Reviews Genetics*, 10(8):565–577, 2009.

[146] G. Maclachlan and C. Brady. Endo-1, 4-[beta]-glucanase, xyloglucanase, and xyloglucan endo-transglycosylase activities versus potential substrates in ripening tomatoes. *Plant Physiology*, 105(3):965, 1994.

[147] C. Maliepaard, F. H. Alston, G. van Arkel, L. M. Brown, E. Chevreau, F. Dunemann, K. M. Evans, S. Gardiner, P. Guilford, A. W. van Heusden, J. Janse, F. Laurens, J. R. Lynn, A. G. Manganaris, A. P. M. den Nijs, N. Periam, E. Rikkerink, P. Roche, C. Ryder, S. Sansavini, H. Schmidt, S. Tartarini, J. J. Verhaegh, M. Vrielink-van Ginkel, and G. J. King. Aligning male and female linkage maps of apple (malus pumila mill.) using multi-allelic markers. *Theoretical and Applied Genetics*, 97(1-2):60–73, 1998.

[148] C. Maliepaard, M. J. Sillanpaa, J. W. van Ooijen, R. C. Jansen, and E. Arjas. Bayesian versus frequentist analysis of multiple quantitative trait loci with an application to an outbred apple cross. *Theoretical and Applied Genetics*, 103(8):1243–1253, 2001.

[149] M. C. Marìn-Rodrìguez, D. L. Smith, K. Manning, J. Orchard, and G. B. Seymour. Pectate lyase gene expression and enzyme activity in ripening banana fruit. *Plant Molecular Biology*, 51(6):851–857, 2003.

[150] H. Martens and T. Naes. *Multivariate calibration*. John Wiley & Sons Inc, 1992.

[151] P. Massiot, A. Baron, and J. F. Drilleau. Effect of storage of apple on the enzymatic hydrolysis of cell wall polysaccharides. *Carbohydrate polymers*, 29(4):301–307, 1996.

[152] A. J. Matas, N. E. Gapper, M. Y. Chung, J. J. Giovannoni, and J. K. C. Rose. Biology and genetic engineering of fruit maturation for enhanced quality and shelf-life. *Current Opinion in Biotechnology*, 20(2):197–203, 2009.

[153] R. Mauricio. Mapping quantitative trait loci in plants: Uses and caveats for evolutionary biology. *Nature Reviews Genetics*, 2(5):370–381, 2001.

[154] M. McCann and J. Rose. Blueprints for building plant cell walls. *Plant Physiology*, 153(2):365–365, 2010.

[155] M. C. McCann and K. Roberts. Architecture of the primary cell wall. *The cytoskeletal basis of plant growth and form. Academic Press, London*, pages 109–129, 1991.

[156] F. McKee. East of Eden: a brief history of fruit and vegetable consumption. *British Food Journal*, 97(7):5–9, 1995.

[157] E. J. McMurchie, W. B. McGlasson, and I. L. Eaks. Treatment of fruit with propylene gives information about the biogenesis of ethylene. *Nature*, 237:235–236, 1972.

[158] S. McQueen-Mason, D. M. Durachko, and D. J. Cosgrove. Two endogenous proteins that induce cell wall extension in plants. *The Plant Cell Online*, 4(11):1425, 1992.

[159] E. Mehinagic, G. Royer, R. Symoneaux, D. Bertrand, and F. Jourjon. Prediction of the sensory quality of apples by physical measurements. *Postharvest biology and technology*, 34(3):257–269, 2004.

[160] D. Micheletti, M. Troggio, A. Zharkikh, F. Costa, M. Malnoy, R. Velasco, and S. Salvi. Genetic diversity of the genus malus and implications for linkage mapping. *Tree Genetics & Genomes*, DOI 10.1007 s11295-011-0380-8, 2011.

[161] S. Moore, P. Payton, M. Wright, S. Tanksley, and J. Giovannoni. Utilization of tomato microarrays for comparative gene expression analysis in the solanaceae. *Journal of Experimental Botany*, 56(421):2885–2895, 2005.

[162] S. Moore, J. Vrebalov, P. Payton, and J. Giovannoni. Use of genomics tools to isolate key ripening genes and analyse fruit maturation in tomato. *Journal of Experimental Botany*, 53(377):2023–2030, 2002.

[163] S. P. Moose and R. H. Mumm. Molecular plant breeding as the foundation for 21st century crop improvement. *Plant Physiology*, 147(3):969–977, 2008.

[164] D. Mousdale and M. Knee. Indolyl-3-acetic acid and ethylene levels in ripening apple fruits. *Journal of Experimental Botany*, 32(4):753, 1981.

[165] S. Myles, J. Peiffer, P. J. Brown, E. S. Ersoz, Z. W. Zhang, D. E. Costich, and E. S. Buckler. Association mapping: Critical considerations shift from genotyping to experimental design. *Plant Cell*, 21(8):2194–2202, 2009.

[166] R. Nakano, E. Ogura, Y. Kubo, and A. Inaba. Ethylene biosynthesis in detached young persimmon fruit is initiated in calyx and modulated by water loss from the fruit. *Plant physiology*, 131(1):276, 2003.

[167] K. J. Niklas. *Plant biomechanics: an engineering approach to plant form and function*. University of Chicago press, 1992.

[168] K. J. Nunan, C. Davies, S. P. Robinson, and G. B. Fincher. Expression patterns of cell wall-modifying enzymes during grape berry development. *Planta*, 214(2):257–264, 2001.

[169] JC Oliveros. Venny. an interactive tool for comparing lists with venn diagrams, 2007.

[170] R. C. O'Malley, F. I. Rodriguez, J.J. Esch, B.M. Binder, P. O'Donnell, H. J. Klee, and A.B. Bleecker. Ethylene-binding activity, gene expression levels, and receptor system output for ethylene receptor family members from arabidopsis and tomato. *The Plant Journal*, 41(5):651–659, 2005.

[171] Van Ooijen. Joinmap®4, software for the calculation of genetic linkage mapes in experimental populations. *Kyazma, B.V, Wageningen*, 2006.

[172] Van Ooijen. Mapqtl®6, software for the mapping of quantitative trait loci in experimental populations of diploid species. *Kyazma B.V Wageningen*, 2009.

[173] N. Oraguzie, P. Alspach, R. Volz, C. Whitworth, C. Ranatunga, R. Weskett, and R. Harker. Postharvest assessment of fruit quality parameters in apple using both instruments and an expert panel. *Postharvest Biology and Technology*, 52(3):279–287, 2009.

[174] B. V. Pamies, G. Roudaut, C. Dacremont, M. L. Meste, and J. R. Mitchell. Understanding the texture of low moisture cereal products: mechanical and sensory measurements of crispness. *Journal of the Science of Food and Agriculture*, 80(11):1679–1685, 2000.

[175] A. Patocchi, F. Fernandez-Fernandez, K. Evans, D. Gobbin, F. Rezzonico, A. Boudichevskaia, F. Dunemann, M. Stankiewicz-Kosyl, F. Mathis-Jeanneteau, C. E. Durel, L. Gianfranceschi, F. Costa, C. Toller, V. Cova, D. Mott, M. Komjanc, E. Barbaro, L. Kodde, E. Rikkerink, C. Gessler, and W. E. van de Weg. Development and test of 21 multiplex pcrs composed of ssrs spanning most of the apple genome. *Tree Genetics & Genomes*, 5(1):211–223, 2009.

[176] M. Pindo, S. Vezzulli, G. Coppola, D. A. Cartwright, A. Zharkikh, R. Velasco, and M. Troggio. Snp high-throughput screening in grapevine using the snplextm genotyping system. *BMC Plant Biology*, 8(12), 2008.

[177] V. Prasanna, TN Prabha, and RN Tharanathan. Fruit ripening phenomena–an overview. *Critical reviews in food science and nutrition*, 47(1):1–19, 2007.

[178] J. K. Pritchard and P. Donnelly. Inference of population structure using multilocus genotype data. *Genetics*, 155(2):945–959, 2000.

[179] S. Purcell, B. Neale, K. Todd-Brown, L. Thomas, M. A. R. Ferreira, D. Bender, J. Maller, P. Sklar, P. I. W. de Bakker, Daly M. J., and et al. A tool set for whole-genome association and population-based linkage analyses. *American Journal of Human Genetics*, 81(3):559–575, 2007.

[180] X. Qu, B. Hall, Z. Gao, and G. E. Schaller. A strong constitutive ethylene-response phenotype conferred on arabidopsis plants containing null mutations in the ethylene receptors etr1 and ers1. *BMC Plant Biology*, 7(1):3, 2007.

[181] A. Rafalski. Applications of single nucleotide polymorphisms in crop genetics. *Current Opinion in Plant Biology*, 5(2):94–100, 2002.

[182] J. A. Rafalski. Association genetics in crop improvement. *Current Opinion in Plant Biology*, 13(2):174–180, 2010.

[183] R. J. Redgwell and S. C. Fry. Xyloglucan endotransglycosylase activity increases during kiwifruit (actinidia deliciosa) ripening (implications for fruit softening). *Plant Physiology*, 103(4):1399, 1993.

[184] R. M. Reeve. Relationship of historical structure to texture of fresh processed fruit and vegetables. *J. Text. Stud*, 1:247, 1970.

[185] K. Roberts and C. Domingo Carrasco. Pectin degrading enzymes, 1999. WO Patent WO/1999/007,857.

[186] H. Rohm. Consumer awareness of food texture in austria. *Journal of Texture Studies*, 21(3):363–373, 1990.

[187] J. K. C. Rose and A. B. Bennett. Cooperative disassembly of the cellulose-xyloglucan network of plant cell walls: parallels between cell expansion and fruit ripening. *Trends in Plant Science*, 4(5):176–183, 1999.

[188] J. K. C. Rose, H. H. Lee, and A. B. Bennett. Expression of a divergent expansin gene is fruit-specific and ripening-regulated. *Proceedings of the National Academy of Sciences*, 94(11):5955, 1997.

[189] A. J. Rosenthal. *Food texture: measurement and perception*. Springer Us, 1999.

[190] G. Roudaut, C. Dacremont, B. Vallčs Pāmies, B. Colas, and M. Le Meste. Crispness: a critical review on sensory and material science approaches. *Trends in food science & technology*, 13(6-7):217–227, 2002.

[191] J. M. Rouillard, M. Zuker, and E. Gulari. Oligoarray 2.0: design of oligonucleotide probes for dna microarrays using a thermodynamics approach. *Nucleic acids research*, 31(12):3057, 2003.

[192] B. Ruperti, C. Bonghi, A. Rasori, A. Ramina, and P. Tonutti. Characterization and expression of two members of the peach 1-aminocyclopropane-1-carboxylate oxidase gene family. *Physiologia Plantarum*, 111(3):336–344, 2001.

[193] AI Saeed, V. Sharov, J. White, J. Li, W. Liang, N. Bhagabati, J. Braisted, M. Klapa, T. Currier, M. Thiagarajan, et al. Tm4: a free, open-source system for microarray data management and analysis. *Biotechniques*, 34(2):374, 2003.

[194] M. Saladie, A. J. Matas, T. Isaacson, M. A. Jenks, S. M. Goodwin, K. J. Niklas, X. L. Ren, J. M. Labavitch, K. A. Shackel, A. R. Fernie, A. Lytovchenko, M. A. O'Neill, C. B. Watkins, and J. K. C. Rose. A reevaluation of the key factors that influence tomato fruit softening and integrity. *Plant Physiology*, 144(2):1012–1028, 2007.

[195] M. Saladie, J. K. C. Rose, D. J. Cosgrove, and C. Catala. Characterization of a new xyloglucan endotransglucosylase/hydrolase (xth) from ripening tomato fruit and implications for the diverse modes of enzymic action. *The Plant Journal*, 47:282–295, 2006.

[196] J. Sanzol. Dating and functional characterization of duplicated genes in the apple (*Malus x domestica* borkh.) by analyzing est data. *Bmc Plant Biology*, 10, 2010.

[197] R.J . Schaffer, E. N. Friel, E. J. F. Souleyre, K. Bolitho, K. Thodey, S. Ledger, J. H. Bowen, J. H. Ma, B. Nain, D. Cohen, et al. A genomics approach reveals that aroma production in apple is controlled by ethylene predominantly at the final step in each biosynthetic pathway. *Plant Physiology*, 144(4):1899, 2007.

[198] P. Scheet and M. Stephens. A fast and flexible statistical model for large-scale population genotype data: Applications to inferring missing genotypes and haplotypic phase. *American Journal of Human Genetics*, 78(4):629–644, 2006.

[199] M. Schuelke. An economic method for the fluorescent labeling of pcr fragments. *Nature Biotechnology*, 18(2):233–234, 2000.

[200] G. B. Seymour, C. D. Ryder, C. Cevik, A. Hammond, J. P. ans Popovich, G. J. King, J. Vrebalov, J. J. Giovannoni, and K. Manning. A sepallata gene is involved in the development and ripening of strawberry (fragariax-ananassa duch.) fruit, a non-climacteric tissue. *Journal of Experimental Botany*, 63(2):1179–1188, 2011.

[201] R. E. Sheehy, M. Kramer, and W. R. Hiatt. Reduction of polygalacturonase activity in tomato fruit by antisense rna. *Proceedings of the National Academy of Sciences*, 85(23):8805, 1988.

[202] E. Silfverberg-Dilworth, C. L. Matasci, W. E. van de Weg, M. P. W. van Kaauwen, M. Walzer, L. P. Kodde, V. Soglio, L. Gianfranceschi, C. E. Durel, F. Costa, T. Yamamoto, B. Koller, C. Gessler, and A. Patocchi. Microsatellite markers spanning the apple (*Malus x domestica* borkh.) genome. *Tree Genetics & Genomes*, 2:202–224, 2006.

[203] I. Simko. Development of est-ssr markers for the study of population structure in lettuce (lactuca sativa l.). *Journal of Heredity*, 100(2):256, 2009.

[204] Y. Sitrit and A. B. Bennett. Regulation of tomato fruit polygalacturonase mRNA accumulation by ethylene: a re-examination. *Plant Physiology*, 116(3):1145, 1998.

[205] C. J. S. Smith, C. F. Watson, J. Ray, C. R. Bird, P. C. Morris, W. Schuch, and D. Grierson. *Antisense RNA inhibition of polygalacturonase gene expression in transgenic tomatoes*. Nature Publishing Group, 1988.

[206] V. Soglio, F. Costa, J. W. Molthoff, W. M. J. Weemen-Hendriks, H. J. Schouten, and L. Gianfranceschi. Transcription analysis of apple fruit development using cdna microarrays. *Tree Genetics & Genomes*, 5:685–698, 2009.

[207] C. Soukoulis, E. Aprea, F. Biasioli, L. Cappellin, E. Schuhfried, T. D. Märk, and F. Gasperi. Proton transfer reaction time-of-flight mass spectrometry monitoring of the evolution of volatile compounds during lactic acid fermentation of milk. *Rapid Communications in Mass Spectrometry*, 24(14):2127–2134, 2010.

[208] R. Stevens, M. Buret, P. Duffe, C. Garchery, P. Baldet, C. Rothan, and M. Causse. Candidate genes and quantitative trait loci affecting fruit ascorbic acid content in three tomato populations. *Plant Physiology*, 143(4):1943–1953, 2007.

[209] A. S. Szczesniak. The meanong of textural characteristics-crispness. *Journal of Texture Studies*, 19(1):51–59, 1988.

[210] A. S. Szczesniak. Texture is a sensory property. *Food Quality and Preference*, 13(4):215–225, 2002.

[211] A.S. Szczesniak, M.A. Brandt, and H.H. Friedman. Development of standard rating scales for mechanical parameters of texture and correlation between the objective and the sensory methods of texture evaluation. *Journal of Food Science*, 28(4):397–403, 1963.

[212] M. Taniwaki, T. Hanada, Tohro M., and N. Sakurai. Non-destructive determination of the optimum eating ripeness of pears and their texture measurements using acoustical vibration techniques. *Postharvest Biology and Technology*, 51(1):305–310, 2009.

[213] M. Taniwaki, T. Hanada, and N. Sakurai. Device for acoustic measurement of food texture using a piezoelectric sensor. *Food research international*, 39(10):1099–1105, 2006.

[214] M. Taniwaki, T. Hanada, and N. Sakurai. Postharvest quality evaluation of "fuyu" and "taishuu" persimmons using a nondestructive vibrational method and an acoustic vibration technique. *Postharvest Biology and Technology*, 51(1):80–85, 2009.

[215] M. Taniwaki and N. Sakurai. Texture measurement of cabbages using an acoustical vibration method. *Postharvest Biology and Technology*, 50(2-3):176–181, 2008.

[216] M. Tatsuki, A. Endo, and H. Ohkawa. Influence of time from harvest to 1-mcp treatment on apple fruit quality and expression of genes for ethylene biosynthesis enzymes and ethylene receptors. *Post harvest biology and technology*, 43(1):28–35, 2007.

[217] T. R. Thomas, K. A. Shackel, and M. A. Matthews. Mesocarp cell turgor in vitis vinifera l. berries throughout development and its relation to firmness, growth, and the onset of ripening. *Planta*, 228(6):1067–1076, 2008.

[218] J. E. Thompson and S. C. Fry. Evidence for covalent linkage between xyloglucan and acidic pectins in suspension-cultured rose cells. *Planta*, 211(2):275–286, 2000.

[219] K. Tiwari and G. Paliyath. Microarray analysis of ripening-regulated gene expression and its modulation by 1-mcp and hexanal. *Plant Physiology and Biochemistry*, 2011.

[220] L. Trainotti, C. Bonghi, F. Ziliotto, D. Zanin, A. Rasori, G. Casadoro, A. Ramina, and P. Tonutti. The use of microarray [mu] peach1. 0 to investigate transcriptome changes during transition from pre-climacteric to climacteric phase in peach fruit. *Plant Science*, 170(3):606–613, 2006.

[221] J. Vandesompele, K. De Preter, F. Pattyn, B. Poppe, N. Van Roy, A. De Paepe, and F. Speleman. Accurate normalization of real-time quantitative rt-pcr data by geometric averaging of multiple internal control genes. *Genome Biology*, 3(7), 2002.

[222] P. Varela, J. Chen, S. Fiszman, and M. J. W. Povey. Crispness assessment of roasted almonds by an integrated approach to texture description: Texture, acoustics, sensory and structure. *Journal of chemometrics*, 20(6-7):311–320, 2006.

[223] R. Velasco, A. Zharkikh, J. Affourtit, A. Dhingra, A. Cestaro, A. Kalyanaraman, P. Fontana, S. K. Bhatnagar, M. Troggio, D. Pruss, S. Salvi, M. Pindo, P. Baldi, S. Castelletti, M. Cavaiuolo, G. Coppola, F. Costa, V. Cova, A. Dal Ri, V. Goremykin, M. Komjanc, S. Longhi, P. Magnago, G. Malacarne, M. Malnoy, D. Micheletti, M. Moretto, M. Perazzolli, A. Si-Ammour, S. Vezzulli, E. Zini, G. Eldredge, L. M. Fitzgerald, N. Gutin, J. Lanchbury, T. Macalma, J. T. Mitchell, J. Reid, B. Wardell, C. Kodira, Z. Chen, B. Desany, F. Niazi, M. Palmer, T. Koepke, D. Jiwan, S. Schaeffer, V. Krishnan, C. Wu, V. T. Chu, S. T. King, J. Vick, Q. Tao, A. Mraz, A. Stormo, K. Stormo, R. Bogden, D. Ederle, A. Stella, A. Vecchietti, M. M. Kater, S. Masiero, P. Lasserre, Y. Lespinasse, A. C. Allan, V. Bus, D. Chagne, R. N. Crowhurst, A. P. Gleave, E. Lavezzo, J. A. Fawcett, S. Proost, P. Rouze, L. Sterck, S. Toppo, B. Lazzari, R. P. Hellens, C. E. Durel, A. Gutin, R. E. Bumgarner, S. E. Gardiner, M. Skolnick, M. Egholm, Y. Van de Peer, F. Salamini, and R. Viola. The genome of the domesticated apple (*Malus x domestica* borkh.). *Nature Genetics*, 42(10):833–839, 2010.

[224] Z. M. Vickers. Crispness and crunchiness-a difference in pitch? *Journal of texture studies*, 15(2):157–163, 1984.

[225] Z. M. Vickers. Sensory, Acoustical, and Force-Deformation Measurements of Potato Chip Crispness. *Journal of Food Science*, 52(1):138–140, 1987.

[226] Z. M. Vickers. Instrumental measures of crispness and their correlation with sensory assessment. *Journal of texture studies*, 19(1):1–14, 1988.

[227] Z.M. Vickers and M. C. Bourne. A psychoacoustical theory of crispness. *Journal of Food Science*, 41(5):1158–1164, 1976.

[228] J. F. V. Vincent. The quantification of crispness. *Journal of the Science of Food and Agriculture*, 78(2):162–168, 1998.

[229] J. Vrebalov, D. Ruezinsky, V. Padmanabhan, R. White, D. Medrano, R. Drake, W. Schuch, and J. Giovannoni. A mads-box gene necessary for fruit ripening at the tomato ripening-inhibitor (rin) locus. *Science*, 296(5566):343–346, 2002.

[230] A. Wagner. The fate of duplicated genes: loss or new function? *BioEssays*, 20(10):785–788, 1998.

[231] Y. Wakasa, H. Kudo, R. Ishikawa, S. Akada, M. Senda, M. Niizeki, and T. Harada. Low expression of an endopolygalacturonase gene in apple fruit with long-term storage potential. *Postharvest Biology and Technology*, 39(2):193–198, 2006.

[232] K. W. Waldron, M. L. Parker, and A. C. Smith. Plant cell walls and food quality. *Comprehensive Reviews in Food Science and Food Safety*, 2(4):2 (4) 101–119, 2003.

[233] K. W. Waldron, A. C. Smith, A. J. Parr, A. Ng, and M. L. Parker. New approaches to understanding and controlling cell separation in relation to fruit and vegetable texture. *Trends in Food Science & Technology*, 8(7):213–221, 1997.

[234] A. Wang, J. Yamakake, H. Kudo, Y. Wakasa, Y. Hatsuyama, M. Igarashi, A. Kasai, T. Li, and T. Harada. Null mutation of the mdacs3 gene, coding for a ripening-specific 1-aminocyclopropane-1-carboxylate synthase, leads to long shelf life in apple fruit. *Plant physiology*, 151(1):391, 2009.

[235] C. B. Watkins. The use of 1-methylcyclopropene (1-mcp) on fruits and vegetables. *Biotechnology Advances*, 24(4):389–409, 2006.

[236] C. B. Watkins. Overview of 1-methylcyclopropene trials and uses for edible horticultural crops. *HortScience*, 43(1):86–94, 2008.

[237] P. J. White. Recent advances in fruit development and ripening: an overview. *Journal of Experimental Botany*, 53(377):1995–2000, 2002.

[238] D. J. Whittaker, G. S. Smith, and R. C. Gardner. Expression of ethylene biosynthetic genes in Actinidia chinensis fruit. *Plant molecular biology*, 34(1):45–55, 1997.

[239] L. M. Wilson, S. R. Whitt, A. M. Ibanez, T. R. Rocheford, M. M. Goodman, and E. S. Buckler. Dissection of maize kernel composition and starch production by candidate gene association. *The Plant Cell Online*, 16(10):2719, 2004.

[240] M. Yamamoto, T. Miki, Y. Ishiki, K. Fujinami, Y. Yanagisawa, H. Nakagawa, N. Ogura, T. Hirabayashi, and T. Sato. The synthesis of ethylene in melon fruit during the early stage of ripening. *Plant and cell physiology*, 36(4):591, 1995.

[241] Z. H. Ye and J. E. Varner. Tissue specific expression of cell wall proteins in developing soybean tissues. *The Plant Cell Online*, 3(1):23, 1991.

[242] S. D. Yoo, Y. Cho, and J. Sheen. Emerging connections in the ethylene signaling network. *Trends in plant science*, 14(5):270–279, 2009.

[243] S. Yoshikawa, S. Nishimaru, T. Tashiro, and M. Yoshida. Collection and classification of words for description of food texture. *Journal of Texture Studies*, 1(4):443–451, 1970.

[244] J. M. Yu, G. Pressoir, W. H. Briggs, IV Bi, M. Yamasaki, J. F. Doebley, M. D. McMullen, B. S. Gaut, D. M. Nielsen, J. B. Holland, and et al. A unified mixed-model method for association mapping that accounts for multiple levels of relatedness. *Nature Genetics*, 38(2):203–208, 2006.

[245] A. Zdunek, D. Konopaka, and K. Jesionkowska. Crispness and crunchiness judgment of apples based on contact acoustic emission. *Journal of Texture Studies*, 41(1):75–91, 2010.

[246] S. Zenoni, A. Ferrarini, E. Giacomelli, L. Xumerle, M. Fasoli, G. Malerba, D. Bellin, M. Pezzotti, and M. Delledonne. Characterization of transcriptional complexity during berry development in vitis vinifera using rna-seq. *Plant physiology*, 152(4):1787, 2010.

[247] Y. M. Zhu and B. H. Barritt. Md-acs1 and md-aco1 genotyping of apple (*Malus x domestica* borkh.) breeding parents and suitability for marker-assisted selection. *Tree Genetics & Genomes*, 4(3):555–562, 2008.

[248] F. Ziliotto, M. Begheldo, A. Rasori, C. Bonghi, and P. Tonutti. Transcriptome profiling of ripening nectarine (prunus persica l. batsch) fruit treated with 1-mcp. *Journal of experimental botany*, 59(10):2781, 2008.

[249] V. Ziosi, M. Noferini, G. Fiori, A. Tadiello, L. Trainotti, G. Casadoro, and G. Costa. A new index based on vis spectroscopy to characterize the progression of ripening in peach fruit. *Postharvest Biology and Technology*, 49(3):319–329, 2008.